CRYSTAL COULOMB ENERGIES:

I. ORGANIC DONOR-ACCEPTOR COMPLEXES--A REVIEW

II. CLASSICAL EWALD CALCULATIONS OF THE COULOMB BINDING ENERGY OF FOUR DONOR-ACCEPTOR CRYSTALS AND WURSTER'S BLUE PERCHLORATE

III. A RAPID-CONVERGENCE QUANTUM-MECHANICAL FORMALISM FOR CRYSTAL ELECTRONIC ENERGIES

Thesis by

Robert Melville Metzger

In Partial Fulfillment of the Requirements

For the Degree of

Doctor of Philosophy

California Institute of Technology

Pasadena, California

1969

(Submitted October 24, 1968)

Szüleimnek

ACKNOWLEDGMENTS

It is a pleasant duty to record here my debt of gratitude to my advisor, Professor Harden Marsden McConnell, who inspired, stimulated and assisted my first efforts, then with great forbearance granted me the freedom of developing my abilities, yet went to bat for me many times when my contributions were only a promise; to Professor Willard Frank Libby, who first showed me the vast panorama of science and made my graduate career possible; to Professor Paul Gravis Simpson for his encouragement, patience, and friendship in difficult times; to my parents for their love, encouragement, and sacrifices.

Graduate school has been a pleasant experience: my thanks to the California Institute of Technology and to Stanford University for their long hospitality; my thanks also to the fellow students whose friendship, advice, and open sharing of knowledge have been so important to me: Mr. J. W. Becker, Dr. J. C. A. Boeyens, Dr. S. H. Brown, Dr. F. R. Gamble, Prof. O. H. Griffith, Dr. D. W. Halford, Prof. B. M. Hoffman, Dr. R. C. Hughes, Dr. M. S. Itzkowitz, Dr. D. E. Lundquist, Dr. A. W. Merkl, Dr. P.-L. Nordio, Dr. S. Ogawa, Dr. D. J. Silverman, Prof. H. J. Silverstone, Dr. I. C. Smith, Prof. Z. G. Soos, Prof. T. J. Stone, Mrs. R. Frost Swanson, and last but not least my "fidus Achates", Dr. R. H. Young. Life was made enjoyable by the friends of Mosher-Jorgensen Graduate House and of Kingsley Club in Palo Alto.

Mrs. Dorothy Colbert deserves much praise for a beautiful typing job.

Finally, I wish to acknowledge my indebtedness to the United States of America for granting me citizenship; to the Woodrow Wilson Foundation for a graduate fellowship (1962-63); to the National Science Foundation for a summer fellowship (1963); to the National Institutes of Health for three fellowships (1963-1966); to the Center for Materials Research, Stanford University for almost two years of support (1966-68); to my parents for support as this thesis was completed (Summer 1968).

It is proper and fitting to remember here Luigi Maria Pittarelli and Ákos Kovács, whom the Grim Reaper took from us before they could show their full promise.

To the reader an apology for the inordinate length of this thesis: its over-detailed and uneven style bears witness to the struggles of an experimentalist who strove belatedly to delve into theoretical problems.

七転八起

ABSTRACT

CHAPTER I

Theories for organic donor-acceptor (DA) complexes in solution and in the solid state are reviewed, and compared with the available experimental data. As shown by McConnell *et al.* (Proc. Natl. Acad. Sci. U.S., 53, 46-50 (1965)), the DA crystals fall into two classes, the holoionic class with a fully or almost fully ionic ground state, and the nonionic class with little or no ionic character. If the total lattice binding energy $2\epsilon_1$ (per DA pair) gained in ionizing a DA lattice exceeds the cost $2\epsilon_0$ of ionizing each DA pair, $\epsilon_1 + \epsilon_0 < 0$, then the lattice is holoionic. The charge-transfer (CT) band in crystals and in solution can be explained, following Mulliken, by a second-order mixing of states, or by any theory that makes the CT transition strongly allowed, and yet due to a small change in the ground state of the non-interacting components D and A (or D^+ and A^-). The magnetic properties of the DA crystals are discussed.

CHAPTER II

A computer program, EWALD, was written to calculate by the Ewald fast-convergence method the crystal Coulomb binding energy E_C due to classical monopole-monopole interactions for crystals of any symmetry. The precision of E_C values obtained is high:

the uncertainties, estimated by the effect on E_C of changing the Ewald convergence parameter η, ranged from ± 0.00002 eV to ± 0.01 eV in the worst case. The charge distribution for organic ions was idealized as fractional point charges localized at the crystallographic atomic positions: these charges were chosen from available theoretical and experimental estimates. The uncertainty in E_C due to different charge distribution models is typically ± 0.1 eV (± 3%): thus, even the simple Hückel model can give decent results.

E_C for Wurster's Blue Perchlorate is -4.1 eV/molecule: the crystal is stable under the binding provided by direct Coulomb interactions. E_C for N-Methylphenazinium Tetracyanoquinodimethanide is 0.1 eV: exchange Coulomb interactions, which cannot be estimated classically, must provide the necessary binding.

EWALD was also used to test the McConnell classification of DA crystals. For the holoionic (1:1)-(N,N,N',N'-Tetramethyl-para-phenylenediamine:7,7,8,8-Tetracyanoquinodimethan) $E_C = -4.0$ eV while $2\epsilon_o = 4.6_5$ eV: clearly, exchange forces must provide the balance. For the holoionic (1:1)-(N,N,N',N'-Tetramethyl-para-phenylenediamine:para-Chloranil) $E_C = -4.4$ eV, while $2\epsilon_o = 5.0$ eV: again E_C falls short of $2\epsilon_1$. As a Gedankenexperiment, two nonionic crystals were assumed to be ionized: for (1:1)-(Hexamethylbenzene:para-Chloranil) $E_C = -4.5$ eV, $2\epsilon_o = 6.6$ eV; for (1:1)-(Naphthalene:Tetracyanoethylene) $E_C = -4.3$ eV, $2\epsilon_o = 6.5$ eV. Thus, exchange energies in these nonionic crystals must not exceed 1 eV.

CHAPTER III

A rapid-convergence quantum-mechanical formalism is derived to calculate the electronic energy of an arbitrary molecular (or molecular-ion) crystal: this provides estimates of crystal binding energies which include the exchange Coulomb interactions. Previously obtained LCAO-MO wavefunctions for the isolated molecule(s) ("unit cell spin-orbitals") provide the starting-point. Bloch's theorem is used to construct "crystal spin-orbitals". Overlap between the unit cell orbitals localized in different unit cells is neglected, or is eliminated by Löwdin orthogonalization. Then simple formulas for the total kinetic energy Q_{λ}^{XT}, nuclear attraction $[\lambda|\lambda]^{XT}$, direct Coulomb $[\lambda\lambda|\lambda'\lambda']^{XT}$, and exchange Coulomb $[\lambda\lambda'|\lambda'\lambda]^{XT}$ integrals are obtained, and direct-space brute-force expansions in atomic wavefunctions are given. Fourier series are obtained for $[\lambda|\lambda]^{XT}$, $[\lambda\lambda|\lambda'\lambda']^{XT}$, and $[\lambda\lambda'|\lambda'\lambda]^{XT}$ with the help of the convolution theorem; the Fourier coefficients require the evaluation of Silverstone's two-center Fourier transform integrals. If the short-range interactions are calculated by brute-force integrations in direct space, and the long-range effects are summed in Fourier space, then rapid convergence is possible for $[\lambda|\lambda]^{XT}$, $[\lambda\lambda|\lambda'\lambda']^{XT}$, and $[\lambda\lambda'|\lambda'\lambda]^{XT}$. This is achieved, as in the Ewald method, by modifying each atomic wavefunction by a "Gaussian convergence acceleration factor", and evaluating separately in direct and in Fourier space appropriate portions of $[\lambda|\lambda]^{XT}$, etc., where some of the portions contain the Gaussian factor.

TABLE OF CONTENTS

Gallia est omnis divisa in partes tres

CHAPTER I

ORGANIC DONOR-ACCEPTOR COMPLEXES

> ἀνθρώποισι γὰρ
> τοῖς πᾶσι κοινόν ἐστι τοὐξαμαρτάνειν·
> ἐπεὶ δ᾽ ἁμάρτῃ, κεῖνος οὐκέτ᾽ ἔστ᾽ ἀνὴρ
> ἄβουλος οὐδ᾽ ἄνολβος ὅστις ἐς κακὸν
> πεσὼν ἀκεῖται μηδ᾽ ἀκίνητος πέλει.
>
> Sophocles, Antigone 1023-1028

A. Introduction and Literature Survey

Certain organic molecules are known as "good donors" (D) because their ionization potential I_D is comparatively low:

$$(101) \qquad D \longrightarrow D^+ + e^- \qquad\qquad I_D \cong 6 \text{ to } 8 \text{ eV};$$

other organic molecules are known as "good acceptors" (A) because their electron affinity A_A is fairly large:

$$(102) \qquad A^- \longrightarrow A + e^- \qquad\qquad A_A \cong +(1 \text{ to } 2) \text{ eV}.$$

When D and A are separately dissolved in suitable organic solvents, (or, rarely, water) they usually yield faintly colored or colorless solutions; when these solutions are mixed, an intense coloration appears, and a "molecular complex" is assumed to be formed. Under suitable conditions a precipitate is obtained with a color similar to that of the complex in solution.

These "donor-acceptor" (DA) or "pi" or "intermolecular charge-transfer" (CT) complexes have been studied extensively both in solution and in the solid state, and are of interest also in inorganic chemistry. A complete survey of the literature is out of the question here; rather, we refer the reader to recent review articles by Mulliken et al. (1), McConnell (2), Nordio et al. (3), and to books by Briegleb (4) and Andrews and Keefer (5); the review articles by Kommandeur (6) and LeBlanc (7) are also of pedagogic value. Instead, we aim to give here a brief account of the experimental evidence and the theoretical arguments pertinent to the ground state of the solid 1:1 organic pi complexes such as (1:1)-(Hexamethylbenzene:para-Chloranil) and (1:1)-(para-Phenylenediamine:para-Chloranil).

The salient feature of these DA complexes in solution is their intense color; their optical absorption spectrum consists of a superposition of the spectra of the neutral donor D and of the neutral acceptor A, plus a very strongly allowed absorption band that is responsible for the coloration, but cannot be attributed to D, D^+, A, A^-, or to the solvent; this band, which (anticipating slightly) we call "charge-transfer" band, peaks at a frequency ν^*_{CT} which is empirically related to $I_D - A_A$ as follows:

$$h\nu^*_{CT} = I_D - A_A + C, \tag{103}$$

where h is Planck's constant, and C is a constant of the order of magnitude of 3 eV. If $I_D - A_A$ is relatively small ($\lesssim$ 6 eV) and if the solution is sufficiently polar, then the complex, if ever formed, breaks up rather rapidly into the separately solvated radical ions D^+ and A^-, and the CT band disappears. The complexes in solution possess an electric dipole moment even when neither D nor A alone have measurable moments. Furthermore, the heat of formation ΔH_{CT} of these complexes is relatively small, about 0.2 eV/pair,[*] which is insufficient for a true chemical bond but resembles hydrogen-bond energies. In Appendix I we summarize in two tables some of the data available in charge-transfer literature; the purpose is two-fold: to provide a framework for the ensuing discussion on theoretical models, and to place the crystal Coulomb calculations of Chapter II in an appropriate experimental perspective. In Table I we collect experimental and semi-empirical ionization potentials and electron affinities for a selected group of aromatic donors and acceptors. The experimental ionization potentials are from gaseous photoionization (I_{exp}) and crystal surface photoionization (I_{exp}^{surf}); the experimental electron affinities (A_{exp}) are from calorimetry and electron capture; the semi-empirical ionization potentials (I_{CT}) and electron affinities (A_{CT}) are obtained from Briegleb's correlations (8,9) of solution CT spectra. A discussion of the reliability of I_{CT} and A_{CT} is deferred to the end of Chapter II. In Table I we also tabulate the differences I_{CT} - A_{CT} for comparison with the data in Table II. Table II contains most of the experimental information

---

[*] Throughout this thesis, we assume that 1 mole of DA complex consists of N_o (Avogadro's number) donors D and N_o acceptors A; energy quantities are also quoted as eV/pair, or eV/DA pair, i.e. electron volts per one D molecule and one A molecule.

presently available for the 1:1 complexes formed by the above-mentioned donors and acceptors, namely: (i) solution data: charge-transfer bands $E^{*} = h\nu^{*}_{CT}$ and their molar absorptivities ϵ^{*}, dipole moments μ^{*} and high-pressure effects; (ii) crystal data: charge-transfer bands E, their molar absorptivities ϵ, characteristics of infrared (IR) and visible-ultra-violet (VUV) absorption spectra, room-temperature electrical resistivities ρ, activation energies for electrical conduction e_c, concentration of paramagnetic species at room-temperature (EPR), activation energies for paramagnetism at high and low temperatures e_s^H and e_s^L, characteristics of nuclear electrical quadrupole resonance spectra (NQR), charge-transfer bands in gases E^{gas}, and effects of pressure on E, ϵ, ρ, EPR, whenever available; crystal-structure data are also given: The D and A molecules are planar and the 1:1 DA complexes invariably crystallize as linear arrays of overlapping alternating donor and acceptor molecules DADADA...; the intermolecular distances along the stacking axis are equal, i.e. there is no distance alternation, but the D and A planes are often not perpendicular to the stacking axis: accordingly we give the space group, the D-A interplanar separation along the stacking axis, and the perpendicular distance from D to the nearest A, as well as an indication as to whether the molecular structure of the crystal is known. In order to reduce the clutter, Tables I and II are relegated to Appendix I.

B. Theories of DA Complexes in the Gaseous State and in Solution

Enough was known about DA complexes in the nineteen thirties to puzzle the chemists who sought theoretical explanations for them (see Ref. (4) pages 26-28 for a historical review). In 1942 Weiss (10) suggested that the CT absorption was due to a transition $DA \rightarrow D^{+}A^{-}$, but there is at least one strong objection against this interpretation: the transitions $D \rightarrow D^{+}$, $A \rightarrow A^{-}$ are severally forbidden, and hence, if D and A are separate molecules with small electron overlap, the $DA \rightarrow D^{+}A^{-}$ transition is also forbidden, whereas the CT transition is strongly allowed experimentally.

To get around this problem, Mulliken (11) proposed in 1950 that the ground-state wavefunction of the CT complex in the gaseous state or in solution, ψ_N, is a linear combination of the normalized wavefunctions $\psi_0 \equiv |DA\rangle$ and $\psi_1 \equiv |D^{+}A^{-}\rangle$. This is a resonance between two valence-bond states or a configuration interaction in the molecular orbital formalism.* $|DA\rangle$ is taken to describe the complex formed by a small overlap between the neutral donor molecule and the neutral acceptor molecule at an equilibrium perpendicular distance of 3.2 to 3.5 Å, i.e. close to a van der Waals distance; this complex is bound by all the electronic effects of the approach of D to A, plus electrical

---

*For a translation of Mulliken's theory into molecular-orbital language, cf. Dewar & Lepley (12).

dipole-dipole, London induced dipole-induced dipole, charge-dipole and charge-induced dipole, and hydrogen-bond forces. $|D^+A^-\rangle$ describes the complex formed by a small overlap between the donor monocation D^+ and the acceptor monoanion A^-; the binding forces are the same as for $|DA\rangle$, plus the fairly large ion-ion and ion-multipole forces. So, to first order, Mulliken writes for the ground-state wavefunction of the DA complex:

$$\psi_N = a_N|DA\rangle + b_N|D^+A^-\rangle, \tag{104}$$

and assumes $a_N >> b_N$. For the "charge-transfer excited state" of the DA complex Mulliken defines the wavefunction (again to first order in the perturbation expansion):

$$\psi_E = a_E|D^+A^-\rangle - b_E|DA\rangle, \tag{105}$$

where $a_E >> b_E$ and moreover $a_N \approx a_E$, $b_N \approx b_E$. After defining the matrix elements:

$$H_{00} \equiv \langle DA|\hat{\mathcal{H}}|DA\rangle, \tag{106a}$$

$$H_{11} \equiv \langle D^+A^-|\hat{\mathcal{H}}|D^+A^-\rangle, \tag{106b}$$

$$H_{01} \equiv \langle DA|\hat{\mathcal{H}}|D^+A^-\rangle, \tag{106c}$$

where $\hat{\mathcal{H}}$ is the "appropriate" Hamiltonian, and the overlap integral:

$$\mathcal{S} \equiv \langle DA|D^+A^-\rangle, \tag{107}$$

we can write:

$$\text{(108a)} \qquad h\nu^{*}_{CT} = H_{11} + R_{E} - H_{00} - R_{N} \equiv$$

$$\text{(108b)} \qquad \equiv I_{D} - A_{A} + \{E_{\mathcal{S}} + R_{E} - H_{00} - R_{N}\},$$

where E_S is the binding energy of $|D^{+}A^{-}\rangle$ relative to D^{+} and A^{-} at infinite separation, and R_N, R_E are valence-bond "resonance energies". This explains the attribution of $h\nu^{*}_{CT}$ to a "charge-transfer" transition. By second-order perturbation theory we can obtain estimates for R_N, R_E as follows:

$$\text{(109a)} \qquad R_{N} \cong - \frac{(H_{01} - \mathcal{S}H_{00})^{2}}{H_{11} - H_{00}},$$

$$\text{(109b)} \qquad R_{E} \cong \frac{(H_{01} - \mathcal{S}H_{11})^{2}}{H_{11} - H_{00}},$$

whence we get for the second-order splitting:

$$\text{(109c)} \qquad R_{E} - R_{N} \cong \frac{2H_{01}^{2} + \mathcal{S}^{2}(H_{00}^{2} + H_{11}^{2}) - 2\mathcal{S}H_{01}(H_{00} + H_{11})}{H_{11} - H_{00}},$$

and for the total splitting:

$$\text{(110a)} \qquad h\nu^{*}_{CT} = H_{11} - H_{00} + \frac{2H_{01}^{2} + \mathcal{S}^{2}(H_{00}^{2} + H_{11}^{2}) - 2\mathcal{S}H_{01}(H_{00} + H_{01})}{H_{11} - H_{00}},$$

or:

$$\text{(110b)} \qquad h\nu^{*}_{CT} = I_{D} - A_{A} + \left\{[E_{\mathcal{S}} - H_{00}] + \frac{[2H_{01}^{2} + \mathcal{S}^{2}(H_{00}^{2} + H_{11}^{2}) - 2\mathcal{S}H_{01}(H_{00} + H_{11})]}{I_{D} - A_{A} + [E_{S} - H_{00}]}\right\}.$$

Here we see that the linear relationship between $h\nu^{*}_{CT}$ and I_D-A_A in Eq. (103) follows if the term in braces in Eq. (110b) is approximately the same for all complexes, and that a parabolic relationship obtains if only the quantities in square brackets in Eq. (110b) are constant for all complexes. These conditions seem to be satisfied to the extent that linear and parabolic least-squares correlations of CT spectra have yielded reasonable values for I_{CT} and A_{CT}, but this situation must be considered as a "lucky," fortuitous consequence of the Mulliken formalism since it has no a-priori theoretical justification and does not reinforce the correctness of Mulliken's theory. Rather, Mulliken's real and fundamental contribution is to have made the $\psi_N \longrightarrow \psi_E$ transition theoretically strongly allowed, so that reasonable extinction coefficients can be estimated. After assuming, without loss of generality, that ψ_N, ψ_E are orthonormalized, one may calculate a_N, b_N, a_E, b_E from electrical dipole moment data, or from heats of formation ΔH_{CT} and $h\nu^{*}_{CT}$, or, finally, from ϵ^{*}. In Fig. I we give a schematic energy level diagram for a 1:1 DA complex in solution, together with numerical estimates of the quantities mentioned above, calculated by Briegleb (4) for (1:1)-(Hexamethylbenzene:para-Chloranil) and (1:1)-(Naphthalene:para-Chloranil) [(1:1)-(HMB:pChl) and (1:1)-(Naphth:TCNE)]. Note that $|DA\rangle$ and $|D^{+}A^{-}\rangle$ could have chosen to be orthogonal. Let us define $|DA\rangle_{\perp}$ and $|D^{+}A^{-}\rangle_{\perp}$ so that:

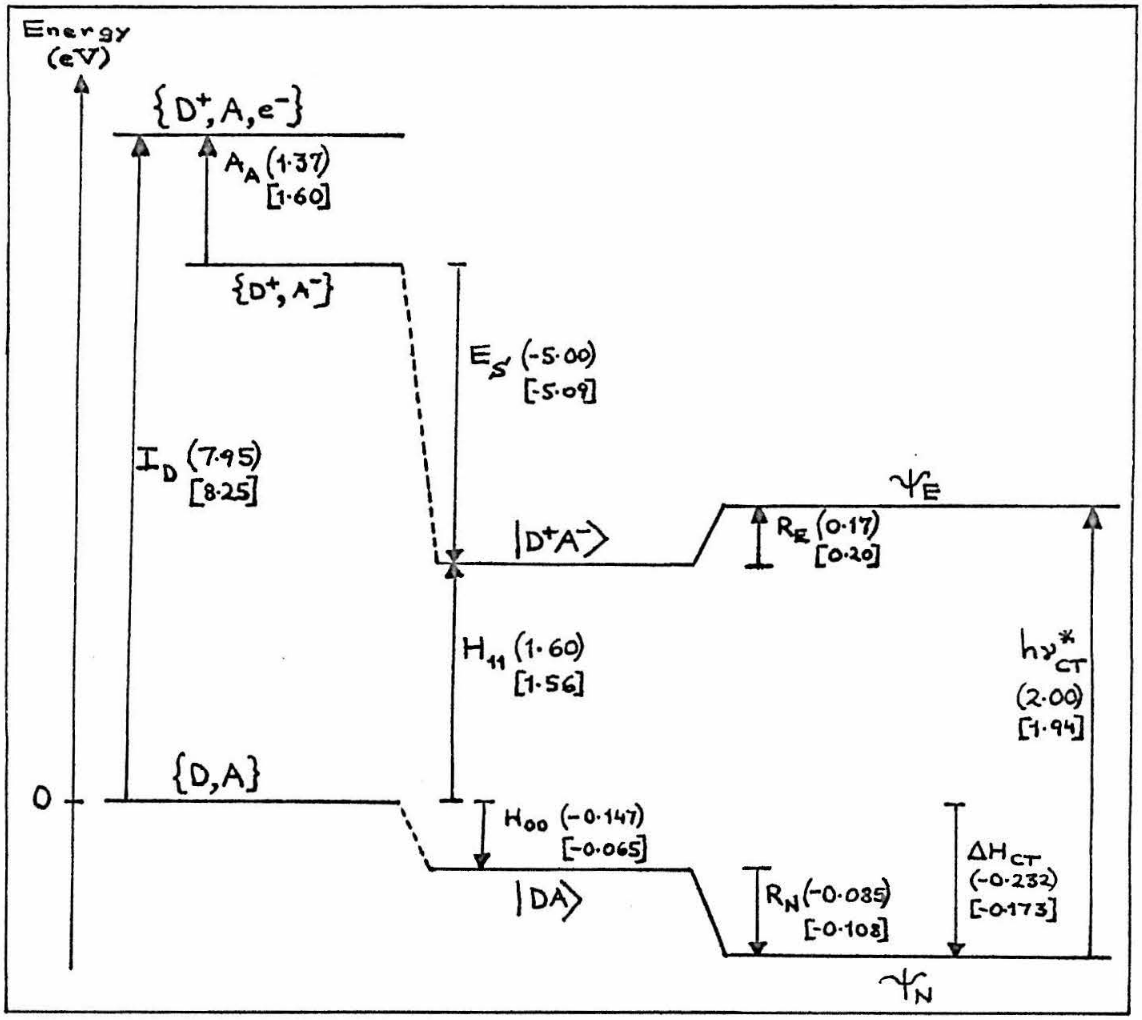

Fig. I

Schematic energy-level diagram for 1:1 DA complex in gaseous state or solution, according to Mulliken (not to scale). $\{D,A\}$ means "D and A at infinite mutual separation". (In parentheses) [in square brackets] the energy values in eV calculated by Briegleb (4) (for (1:1)-(HMB:pChl)) [for (1:1)-(Naphth:TCNE)]; the values for $h\nu^*_{CT}$ are the mirror points between CT absorption and fluorescent emission energies at 83°K; thus vibrational effects are accounted for. For (1:1)-(HMB:pChl) Briegleb calculates $a_N = 0.957$, $b_N = 0.209$ (whence 4.4% CT), $a_E = 0.983$, $b_E = 0.306$, $S = 0.0985$, $H_{01} = -0.391$ eV; for (1:1)-(Naphth:TCNE) he gets $a_N = 0.945$, $b_N = 0.245$ (6.3% CT), $a_E = 0.973$, $b_E = 0.341$, $S = 0.091$, $H_{01} = -0.427$ eV. Note: % CT is $100 \times b_N^2/(a_N^2 + b_N^2)$.

(111) $$\left(|DA\rangle_{\perp}\right)^{\dagger}|D^{+}A^{-}\rangle_{\perp} = 0,$$

where $\dagger$ denotes Hermitian conjugation. Then $a_N^{\perp}$, $b_N^{\perp}$, $a_E^{\perp}$, $b_E^{\perp}$, $H_{oo}^{\perp}$, $H_{11}^{\perp}$, $H_{01}^{\perp}$, $R_E^{\perp} = -R_N^{\perp}$, and $E_S^{\perp}$ replace a_N, b_N, a_E, b_E, H_{oo}, H_{11}, H_{01}, R_N, R_E, and E_S respectively. Then:

(112) $$R_N^{\perp} = \frac{-(H_{01}^{\perp})^2}{H_{11}^{\perp} - H_{00}^{\perp}} = -R_E^{\perp},$$

and:

(113a) $$h\nu_{CT}^{*} = H_{11}^{\perp} - H_{00}^{\perp} + 2R_E^{\perp} =$$

(113b) $$= I_D - A_A + \left\{[E_S^{\perp} - H_{00}^{\perp}] + \frac{2[(H_{01}^{\perp})^2]}{I_D - A_A + [E_S - H_{00}^{\perp}]}\right\}$$

replace Eqs. (109, 110) and, if the overlap S was small to begin with, then $a_N^{\perp} = a_E^{\perp}$, $b_N^{\perp} = b_E^{\perp}$ will differ slightly from a_N, a_E, b_N, b_E. The numerical values quoted in Fig. I for (HMB:pChl) change somewhat upon orthogonalization, and are given in Fig. II. H_{oo} expresses the binding due to the London induced-dipole-induced-dipole attraction forces and is relatively small. E_S is large: it consists of a direct Coulomb part H, an exchange Coulomb contribution E_{xs}, and a London-type term E_{ℓ}:

(114) $$E_S = H + E_{xs}$$

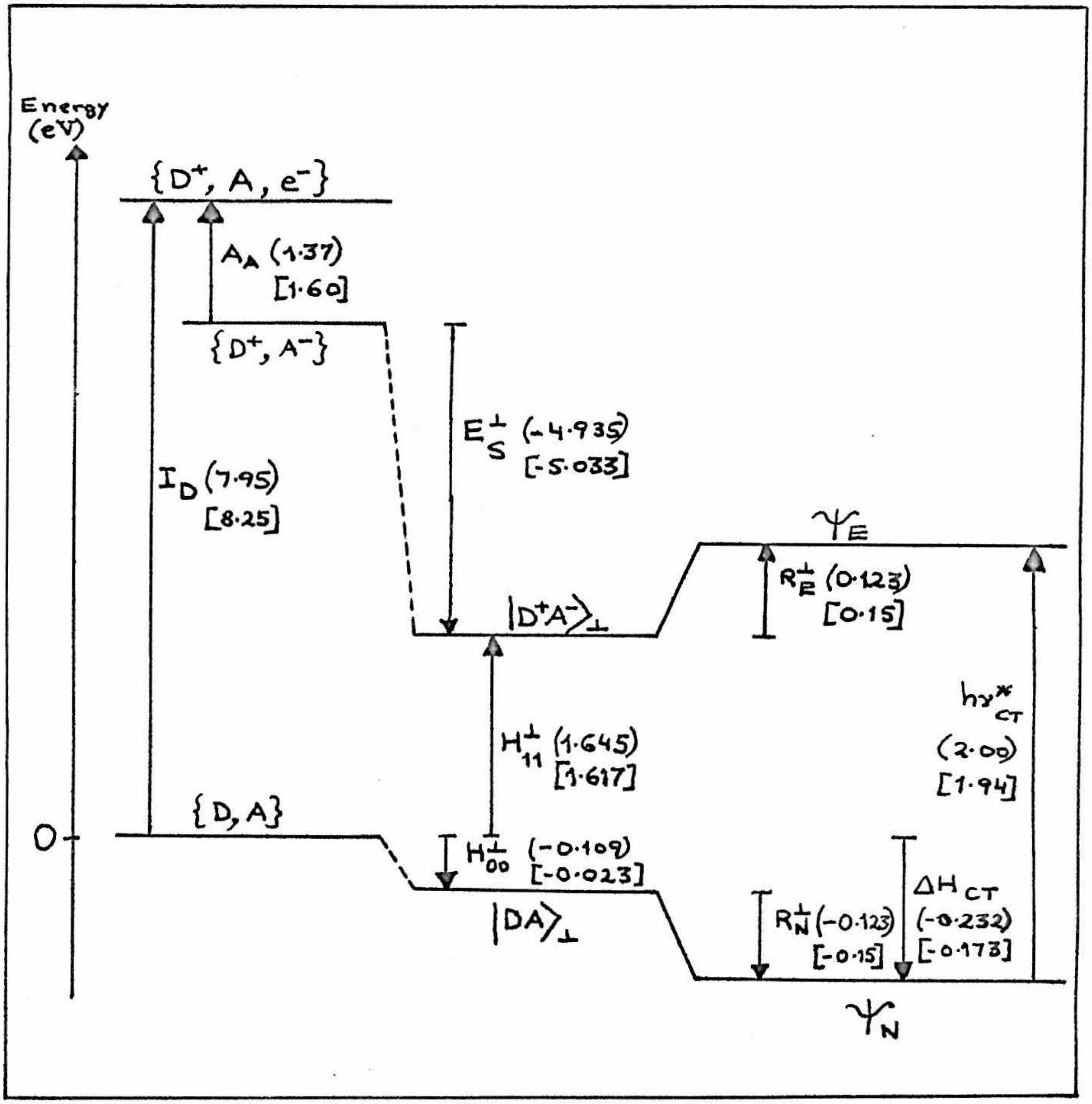

Fig. II

Schematic energy-level diagram for 1:1 DA complex in gaseous state or solution according to Mulliken's theory modified so that $|DA\rangle_{\perp}$ and $|D^+A^-\rangle_{\perp}$ are orthogonal. For (1:1)-(HMB:pChl) $a_N^{\perp} \equiv a_E^{\perp} = 0.967$, $b_N^{\perp} \equiv b_E^{\perp} = 0.256$ (6.54% CT), $S^{\perp} \equiv 0$, $H_{01}^{\perp} = -0.464$ eV; for (1:1)-(Naphth:TCNE) $a_N^{\perp} \equiv a_E^{\perp} = 0.957$, $b_N^{\perp} \equiv b_E^{\perp} = 0.289$ (8.36% CT) $S^{\perp} \equiv 0$, $H_{01}^{\perp} = -0.496$ eV. Note: % CT is $100\,(b_N^{\perp})^2/[(a_N^{\perp})^2 + (b_N^{\perp})^2]$.

In Chapter II we see from estimates of H that $E_{xs} + E_{\ell}$ must be about as large as H if the values of E_S quoted in Figs. I and II are to be obtained; E_{ℓ} is probably of the order of magnitude of H_{00}, i.e. negligible compared to E_S. Thus exchange forces must be very important in the CT excited state.

C. Theories for DA Crystals

It would seem that Mulliken's theory allows *a priori* for almost *any* relative admixture of states in ψ_E and ψ_N, except that if $a_N \cong b_N$ and $a_E \cong b_E$ obtain, then second-order perturbation schemes can no longer be used to calculate R_N, R_E.* The possibility of observing almost any "percentage of charge transfer" within the spectrum of all organic DA complexes underlay much of the intuitive chemical thinking in the 1950's, but received a severe jolt by the accumulating experimental data and by the theories on DA crystals presented by McConnell *et al*. (13): they proposed that at 0°K** 1:1 organic DA crystals fall into two distinct classes: one consists, to first order, of formally neutral D and A molecules (we shall call this the "nonionic" class), the other consists, to first order, of donor monocations

---

*This seems to be the case for (1:1)-(Pyridine:Iodine) complex (25% CT according to Ref. (4), p. 22) but we are not concerned with Iodine complexes in this Thesis.

**Experimental results described in this Thesis suggest that this classification is valid to about 400°K; at this temperature, even 100°K below the melting point, EPR suggests irreversible changes in the crystals.

D^{+} and acceptor monoanions A^{-} (we shall call this the "holoionic" class). This classification was partly suggested by experimental data, and partly by a previous theoretical study by Krugler, Montgomery, and McConnell (14). The spectrum of charge excitations in a neutral lattice and its mirror equivalent of neutral excitations in an ionic lattice had been obtained by Krugler _et al._ _via_ second quantization techniques within the framework of the Hartree or "molecular-field" approximation. A CT Hamiltonian $\hat{\mathcal{H}}_{CT}$ for a one-dimensional cyclic linear chain of N_o equidistant D and N_o A molecules was diagonalized; the energies involved in the creation of a concentration of charged singlet excitations of the type:*

$$|DA\ldots DADADA\ldots DA\rangle \longrightarrow |DA\ldots DAD^{+}_{\uparrow}\,A^{-}_{\downarrow}\,DA\ldots DA\rangle \quad \text{or}$$
$$\longrightarrow |DA\ldots D^{+}_{\uparrow}\,ADADA^{-}_{\downarrow}\ldots DA\rangle$$

are: (i) the energy $I_D - A_A \equiv 2\varepsilon_o$ required to ionize a DA pair, (ii) the ionic crystal binding energy $2N_o\varepsilon_1$ gained if all the N_o D molecules and the N_o A molecules are converted to their ions D^{+} and A^{-}, (iii) the so-called "Mulliken resonance integral"** γ:

---

* $\uparrow$ denotes α spin, $\downarrow$ β spin. The sign convention for ε_1 (and for ε_1' below) is that of Ref. (14), and not Ref. (13). Also we use Avogadro's number N_o throughout. Spin excitations are not considered at this point, so total spin zero must be conserved. Spin labels will be specified below only when necessary.

** γ corresponds to $H_{01}^{\perp}$, and is equal to it but for London dispersion forces and charge-induced dipole interactions. For convenience, orthonormalization of the pure state $|DA\ldots DA\ldots DA\rangle$ (N_o D's and N_o A's at the equilibrium distances within the

(115) $$\gamma \equiv \left\langle DA\ldots DADADA\ldots DA \middle| \hat{\mathcal{H}}_{CT} \middle| DA\ldots DA\, D^{+}_{\uparrow} A^{-}_{\downarrow}\, DA\ldots DA \right\rangle ,$$

an off-diagonal matrix element which allows second-order mixing of ionic states in the nonionic crystal ground state, and of nonionic states in the holoionic crystal ground state. In terms of Fermion excitation creation operators $\hat{f}_n^{+}$ and annihilation operators $\hat{f}_n$ ($\hat{f}_n^{+}$ creates D^{+} from D if n is even, A^{-} from A if n is odd) the excitation density ρ is the expectation value of the number operator:

(116) $$\rho = \frac{1}{2N_0} \sum_{n=1}^{2N_0} \langle \hat{f}_n^{+} \hat{f}_n \rangle ,$$

and the Hamiltonian becomes:

(117) $$\hat{\mathcal{H}}_{CT} = \sum_{n=1}^{2N_0} \epsilon_0 \hat{f}_n^{+} \hat{f}_n + \gamma \sum_{n=1}^{2N_0-1} \left(\hat{f}_n^{+} \hat{f}_{n-1}^{+} + \hat{f}_{n+1} \hat{f}_n \right) -$$
$$- \gamma \left(\hat{f}_{2N_0}^{+} \hat{f}_1^{+} + \hat{f}_1 \hat{f}_{2N_0} \right) + \left\{ \sum_{n=1}^{2N_0} \epsilon_1 \rho \hat{f}_n^{+} \hat{f}_n \right\} .$$

---

crystal) with respect to $|D^{+}A^{-}\ldots D^{+}A^{-}\ldots D^{+}A^{-}\rangle$ (N_o D^{+}'s and N_o A^{-}'s) is tacitly assumed, even if difficult to do exactly (cf. Chapter III). In reality γ depends on the overlap between adjacent D's and A's in the crystal. We write $\{D,A,\ldots, D,A,\ldots, D,A\}$ to depict N_o free D and N_o free A molecules, all at infinite distances from each other; we attach similar meanings to $\{D^{+},A,e^{-},\ldots,D^{+},A\ ,e^{-},\ldots D^{+},A,e^{-}\}$ and write $\{D,A,\ldots,D,A,D^{+},A^{-}, D,A,\ldots,D,A\}$ to depict N_o-1 free D molecules, N_o-1 free A molecules, one D^{+} ion, and one A^{-} ion. $\{D,A,\ldots,D,A,D,A,D,A,\ldots,D,A\}$ is identically $\{D,A,\ldots,D,A,\ldots,D,A\}$.

The term in braces approximates the excitation-excitation interaction: it is the Hartree direct-Coulomb interaction operator. Exchange Coulomb, multipole field, and multiple ionization effects are formally neglected in this treatment. One may, however, lump into ϵ_1 that fraction of the exchange Coulomb and the multipole field energies that is proportional to ρ in the same way as the Madelung energy. Similarly, another part of these energies can be lumped into ϵ_0 (see below p. (17)). The diagonal elements of $\hat{\mathcal{H}}_{CT}$ give the crystal energy:

$$E = 2N_0\left(\epsilon_0\rho + \epsilon_1\rho^2\right), \tag{118}$$

and, if $|\gamma/\epsilon_0|$, $|\gamma/\epsilon_1|$ are small, E will determine the ground state of the crystal. Thus if $\epsilon_0 + \epsilon_1 > 0$ then the crystal is nonionic $(\rho = 0)$, and if $\epsilon_0 + \epsilon_1 < 0$ then the crystal is holoionic $(\rho = 1)$, to first order. In the (rare) case $\epsilon_0 + \epsilon_1 \cong 0$ two separate crystal forms, nonionic and holoionic, or else the coexistence in the same crystal of domains of one and the other form are conceivable. The γ-perturbation will function as $H_{01}^{\perp}$ in Mulliken's theory to create a <u>few</u> D^+A^- pairs in the nonionic lattice (a <u>few</u> DA pairs in the holoionic lattice) or, equivalently, γ will perturb uniformly the neutral (holoionic) lattice by admixing a <u>small</u> amount of ionic (neutral) character in the ground state of each DA (D^+A^-) pair in the crystal. Intense intermolecular optical absorption bands are predicted to be due to the charge-transfer transition $h\nu_{CT}$ (back charge-transfer transition (BCT) $h\nu_{BCT}$) in the nonionic (holoionic) crystal.

The arguments of McConnell et al. can be understood qualitatively by stating that a cooperative effect* (which is made possible by the long range of the direct Coulomb interaction) will favor the formation of a holoionic DA crystal from neutral donors and acceptors if and only if the binding energy gained by ionizing the lattice exceeds the energy required to ionize each DA pair, and by further declaring that charge-transfer mixing in the ground state of these crystals is relatively small (less than ten percent?).

Assume that the pure normalized state $|DA\ldots DA\ldots DA\rangle$, orthogonal to $|D^+A^-\ldots D^+A^-\ldots D^+A^-\rangle$, is stabilized with respect to the state $\{D,A\ldots,D,A,\ldots,D,A\}$ by an energy E_p which consists mainly of van der Waals forces. E_p is probably close to $H_{oo}^{\perp}$ because of the extremely short range of van der Waals forces. The molar crystal interionic energy $2\epsilon_1$ per DA pair is the energy difference between the states $|D^+A^-\ldots D^+A^-\ldots D^+A^-\rangle$ and $\{D^+,A^-,\ldots,D^+,A^-,\ldots,D^+,A^-\}$ and consists of the Madelung energy E_C (due to direct Coulomb interactions between all the D^+ and all the A^- ions in the holoionic crystal, cf. Chapter II), of the energy E_x due to the Madelung-type contribution of the exchange Coulomb interactions, and of the energy E_m due to the Madelung-type multipole interactions:

---

*The ionization of a DA pair in $|DA\ldots DAD^+A^-DA\ldots DA\rangle$ will increase the probability of ionizing the nearest-neighbor pairs, etc.

$$2\epsilon_1 \equiv E_C + E_x + E_m . \qquad (119)$$

The part of the exchange and multipole interactions which involves adjacent D^+ and A^- can also be lumped into $2\epsilon_o$ as an additional term (presumably negative) E_{corr}:

$$2\epsilon_o \equiv I_D - A_A + E_{corr} . \qquad (120)$$

E_C, E_x, and E_m are all expected to be negative (i.e. binding), and a good first guess for E_m is $E_m \cong E_p$ and if $E_p \cong H^{\perp}_{oo}$ then we may assume $E_m \ll 2\epsilon_1$. E_C is expected to be the dominant term, but our Madelung calculations (cf. Chapter II) show that the neglect of E_x is a dangerous oversimplification. The creation of a state $|DA\ldots DAD^+_{\uparrow} A^-_{\downarrow} DA\ldots DA\rangle$ from the state $|DA\ldots DADADA\ldots DA\rangle$ costs $2\epsilon_o - E_p$ for ionization, plus a binding energy $\epsilon_1' < 0$, where:

$$\epsilon_1' \equiv H + E_x' + E_m' ; \qquad (121)$$

as before, H is the direct Coulomb attraction between D^+ and its nearest neighbor A^-, E_x' is the interionic exchange Coulomb energy, similar in magnitude to E_x, and E_m' is the multipole term, presumably small. Thus the energy of $|DA\ldots DAD^+A^-DA\ldots DA\rangle$ lies:

$$e_{in} \equiv 2\epsilon_o + \epsilon_1' - E_p \qquad (122)$$

above the energy of $|DA\ldots DA\ldots DA\rangle$. The energy of the state $|D^+A^-\ldots D^+A^-DAD^+A^-\ldots D^+A^-\rangle$ is e_{ni} above the energy of the state $|D^+A^-\ldots D^+A^-\ldots D^+A^-\rangle$, where:

(123) $$e_{ni} = -4\epsilon_1 + \epsilon_1' - 2\epsilon_0 .$$

Consider the nonionic DA crystal, $\epsilon_0 + \epsilon_1 > 0$, whose energy level diagram is depicted in Fig. III. The resonance stabilization energy for the ground state is (in eV/pair):

(124a) $$R_{N,DA} = \frac{-\gamma^2}{2\epsilon_0 + 2\epsilon_1} ,$$

and the destabilization for the CT excited state is:

(124b) $$R_{E,DA} = \frac{\gamma^2}{2\epsilon_0 + 2\epsilon_1} .$$

The ground state wavefunction is:

(125a) $$\psi_{N,DA} = a_{N,DA} |DA \ldots DA \ldots DA\rangle + b_{N,DA} |D^+A^- \ldots D^+A^- \ldots D^+A^-\rangle ,$$

where $a_{N,DA} >> b_{N,DA}$, and the CT excited state wavefunction is:

(125b) $$\psi_{E,DA} = a_{E,DA} |D^+A^- \ldots D^+A^- \ldots D^+A^-\rangle - b_{E,DA} |DA \ldots DA \ldots DA\rangle ,$$

and since $\langle DA\ldots DA\ldots DA | D^+A^-\ldots D^+A^-\ldots D^+A^-\rangle = 0$ by construction, therefore $a_{E,DA} = a_{N,DA}$ and $b_{E,DA} = b_{N,DA}$. Next, consider the holoionic DA crystal, $\epsilon_0 + \epsilon_1 < 0$ (Fig. IV). The resonance energies are:

(126a) $$R_{N,D^+A^-} = \frac{-\gamma^2}{2\epsilon_0 + 2\epsilon_1} =$$

(126b) $$= - R_{E,D^+A^-} ;$$

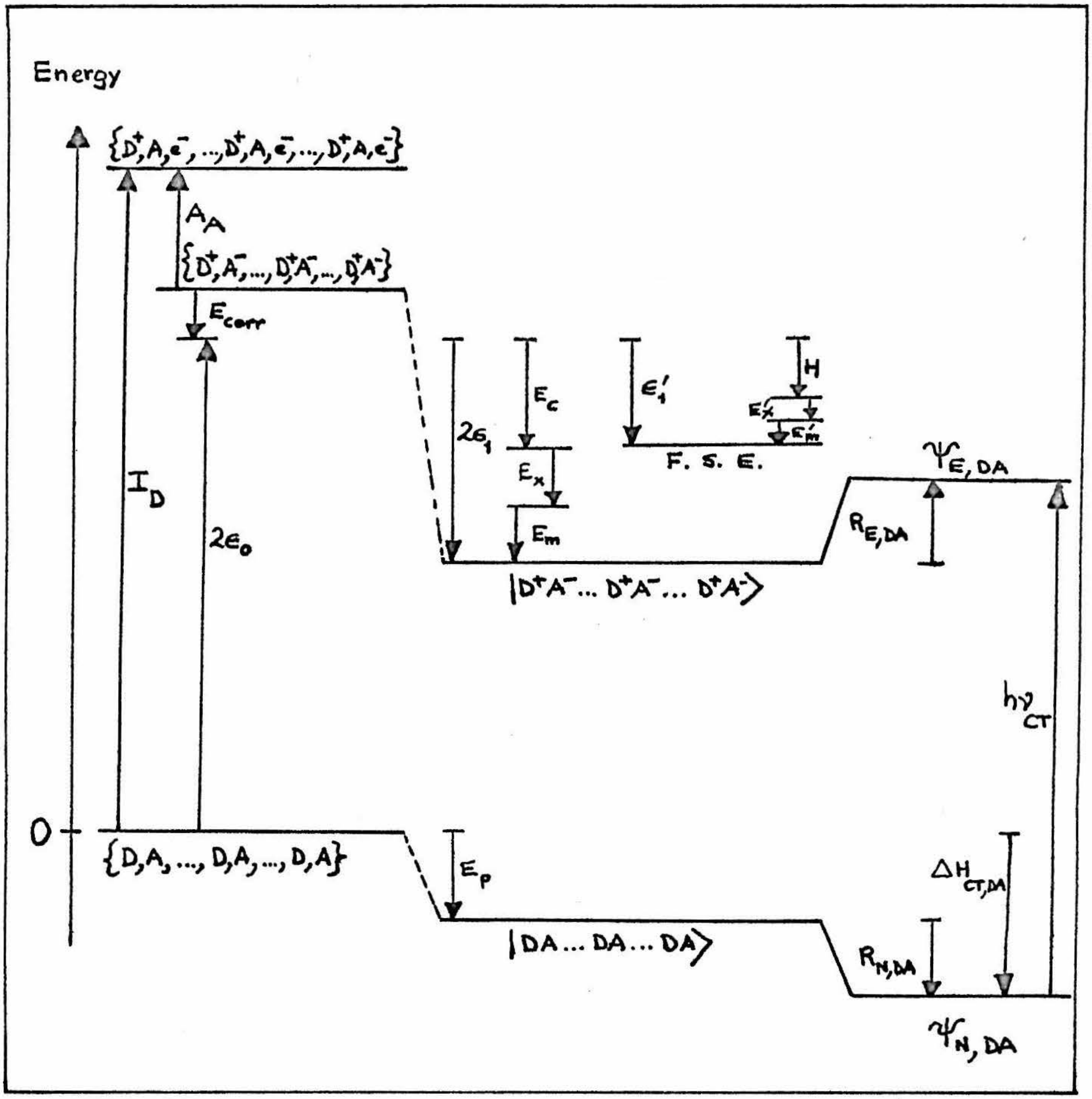

Fig. III

Schematic energy-level diagram for nonionic DA crystal, $\epsilon_0 + \epsilon_1 > 0$. The signs of E_m, E_p, E_m', E_x, E_x', E_{corr} are conjectural. F.S.E. = energy level for Frenkel spin exciton $|DA\ldots DAD^{+}_{\uparrow}\ A^{-}_{\uparrow}\ DA\ldots DA\rangle$, which is very close to the state $|DA\ldots DAD^{+}_{\uparrow}A^{-}_{\downarrow}DA\ldots DA\rangle$.

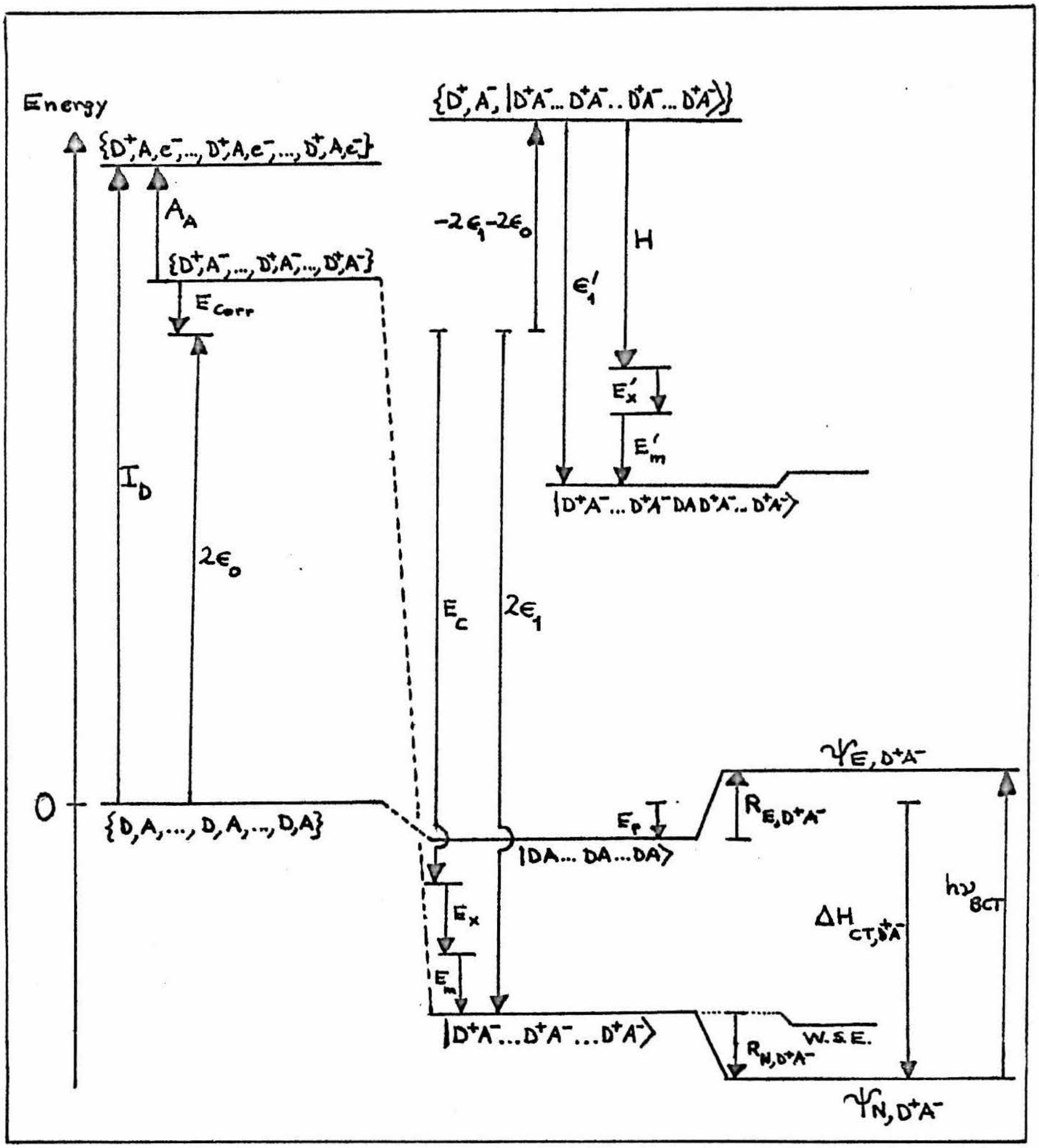

Fig. IV

Schematic energy level diagram for holoionic DA crystal, $\epsilon_0 + \epsilon_1 < 0$. W.S.E. = energy level for Wannier spin exciton, $|^{0}D^{+}_{\uparrow}\,A^{-}_{\downarrow}\ldots D^{+}_{\uparrow}\,A^{-}_{\downarrow}\;D^{+}_{\uparrow}\,A^{-}_{\uparrow}\;D^{+}_{\uparrow}\,A^{-}_{\downarrow}\ldots D^{+}_{\uparrow}\,A^{-}_{\downarrow}\rangle$.

the ground state wavefunction is

$$(127a)\qquad \psi_{N,D^+A^-} = a_{N,D^+A^-}\left|D^+A^-\ldots D^+A^-\ldots D^+A^-\right\rangle + b_{N,D^+A^-}\left|DA\ldots DA\ldots DA\right\rangle,$$

where $a_{N,D^+A^-} \gg b_{N,D^+A^-}$, and the BCT excited-state wavefunction is:

$$(127b)\qquad \psi_{E,D^+A^-} = a_{E,D^+A^-}\left|DA\ldots DA\ldots DA\right\rangle - b_{E,D^+A^-}\left|D^+A^-\ldots D^+A^-\ldots D^+A^-\right\rangle,$$

and again $a_{E,D^+A^-} = a_{N,D^+A^-}$, $b_{E,D^+A^-} = b_{N,D^+A^-}$ because of the convenient orthogonalization.

By order-of-magnitude estimates of the energies involved, McConnell et al. (13) showed that the γ-perturbation is indeed small enough to justify the above classification. The experimental data presented in Table II support strongly these arguments, but we defer their discussion until after we dispose of the theories of Kommandeur, and after we mention the alternate theories for solution and gaseous CT bands by Hanna and Boeyens.

Kommandeur and Pott (15,16) have advanced theories which are exactly opposite to those of McConnell et al.: they propose the existence of "molionic" crystals, in which the species D^+, A^-, D, A, D^{++}, A^{--} coexist simultaneously. They first proposed (15) that the charge-induced dipole interactions between the charges on the ions and the induced dipoles on the neutral species in a molionic lattice might make the molionic lattice more stable (lower in energy) than either the nonionic or the holoionic lattice. Their calculation of the electric fields in a highly idealized NaCl-type molionic lattice (by Evjen techniques?) are suggestive but hardly convincing; in Proposition I of this thesis we present Ewald-type electric field calculations on real DA crystals which, if reasonable experimental values for molecular polarizabilities can be found and digital computing funds are made available, could prove or (more likely) disprove Kommandeur's contentions about the relative importance of such effects. In an experimental paper on crystals of (1:1)-(Tetramethyl-para-phenylenediamine:para-Chloranil) [(TMPD:pChl)] evidence is presented by Pott and Kommandeur (16) for the presence of $TMPD^{++}$ and $pChl^{--}$ ions and of TMPD and pChl neutral molecules in the ground state. Their EPR "identification" of the paramagnetic species as $pChl^{-}$ excited states by the comparison of g-values for crystals of (TMPD:pChl) with the g-value of $pChl^{-}$ in solution is untenable (one could be convinced if the g-value for say, Li^{+} $pChl^{-}$ crystal had been obtained, but then the extreme narrowing of the (TMPD:pChl) resonance would be difficult to explain). Their optical absorption spectrum assignments are erroneous, and have been correctly assigned to $TMPD^{+}$ and $pChl^{-}$ in a single-crystal polarized optical absorption spectrum study by Amano, Kuroda, and Akamatu (17). The X-ray evidence (bond distances and angles) which was published later by de Boer and Vos (18) seems to argue for the presence of TMPD and of neutral chloranil and is more difficult to dismiss forthwith; it is considered in greater detail in Proposition II. Suffice it to say here that this would not be the first known example of a refinement of a molecular structure which proves to be chemically unrealistic. It is remotely possible that DA crystals for which $\varepsilon_o + \varepsilon_1 \cong 0$ could be molionic, but none of the DA crystals studied to date can be safely assigned to such a category.

We turn now to a more disturbing thought: is there really CT in DA complexes in solutions, gases and solids? Mulliken and McConnell's theories jointly show that the CT mixing of states is a relatively small effect in all DA complexes, i.e. a "less than ten per cent" effect. Given the present state of sophistication of quantum chemistry, many a theoretical effect could conceivably be "adjusted" to account for some of the experimental aspects of DA complexes. The dependence of $h\nu^*_{CT}$ on I_D-A_A is not a strong proof of Mulliken's theory, especially since Scheibe noticed (19) that the energy of the lowest excited singlet state of isolated aromatic hydrocarbons is proportional to I_D; Kollaard and Colpa (20) have accounted for this by Hartree-Fock self-consistent field calculations. In a tour-de-force, Boeyens (21) used parametrized electron-in-the-box calculations to account for CT bands. In a more serious effort, Hanna (22) has recently calculated the interaction between the electrical field due to the non-zero electrical quadrupole moment of benzene, estimated theoretically, and the experimental field-induced polarizabilities of Cl_2, Br_2, I_2, and ICl: by these means Hanna calculates reasonable values for ΔH_{CT} and for the dipole moment of the complex, μ^*, and argues that CT need not be invoked in the stabilization of the ground state of these benzene-halogen complexes. The CT optical transition is not discussed by Hanna, and the tantalizing questions are: (i) what would the intermolecular excited state ψ_E be in Hanna's theory, (ii) can the experimental intensities of the "CT transition" be accounted for by quadrupole effects, (iii) can the polarization of the CT band in the solid (see below) be accounted for? This writer does not feel qualified to take a position on these questions, and eagerly awaits further developments. In any case McConnell's classification of solid DA complexes would survive in its essentials.

D. Comparison of Theory and Experiment

At this point, comparisons may be drawn between Mulliken's theory for DA complexes in gases and solutions, McConnell's theory for DA crystals, and the representative experimental data collected in Table II.

The CT optical absorptions of the so-called "weak" DA complexes in solution (e.g. benzene through perylene, I_D = 9.24 to 7.0 eV, with all acceptors) are mildly solvent-dependent, and occur at the same energies as the solid CT optical absorptions to within 0.1 eV, i.e. a vibrational overtone or so, and solution and solid CT bands have the *same* intensities. *Thus the same theoretical explanation must account for both the solution and solid CT bands*; this is accomplished by the complementary theories of Mulliken and McConnell. Also, the relative geometrical configuration of D and A must be very similar in solution and in the crystal.

The optical absorption spectrum of solutions of "strong" DA complexes (donors: Phenothiazine (PTZ), para-Phenylenediamine (pPD), and TMPD, I_D = 6 to 7 eV; with acceptors: 2,3-Dichloro-5,6-dicyano-1,4-benzoquinone (DDQ), 7,7,8,8-Tetracyanoquinodimethan (TCNQ) through pChl, A_A = 1 to 2 eV) is difficult to obtain experimentally, because of the rapid formation of the separately solvated radical ions D^+ and A^-: this is especially true in polar solvents. It has *not* been definitely established whether the CT band is accompanied by the absorption of the neutral D and A or by bands due to D^+ and A^-. Of the two possible mechanisms:

(i) [D in solvent cage (SC)] + [A in SC] $\xrightarrow{\text{very fast}}$ [DA complex in SC, ground state mostly $|DA\rangle$, $a_N \gg b_N$, with $h\nu^*_{CT}$ absorption] $\xrightarrow{\text{fast}}$ [D^+ in SC] + [A^- in SC],

(ii) [D in SC] + [A in SC] $\xrightarrow{\text{very fast}}$ [DA complex in SC, ground state mostly $|D^+A^-\rangle$, $a_N \lll b_N$, with $h\nu^*_{BCT}$ absorption] $\xrightarrow{\text{fast}}$ [D^+ in SC] + [A^- in SC],

the former seems to be favored by the evidence presented by Foster *et al.* (23,24,25,60), but there remains a great need for definitive kinetic studies using fast-reaction techniques. The optical absorption and reflection spectra of crystals of "strong" DA complexes consist unequivocally (17) of the spectra of D^+, A^-, plus an intermolecular band that in light of McConnell's theory must be a BCT band, $h\nu_{BCT}$. The crystal BCT band occurs at 1 to 1.2 eV, and seems to be 0.3 to 0.5 eV to the red of the solution intermolecular band (see also Ref. (123)). If the solution band is indeed due to CT and not BCT, it is surprising that $h\nu^*_{CT}$ and $h\nu_{BCT}$ should be so close!

Polarized optical absorption studies of DA crystals, coupled with X-ray molecular structure determinations, have established conclusively that the CT (and BCT) absorption is highest when the electric vector of the absorbed radiation is parallel to the line connecting the center of D (D^+) with the center of the nearest-neighbor A (A^-), as is expected from Mulliken's theory. It is also clear that multiple CT bands must be due to a contribution of several molecular orbitals of D (less probably of A) to the CT configuration interaction. Detailed solvent, temperature, and pressure effects on $h\nu^*_{CT}$, ϵ^*, $h\nu_{CT}$, $h\nu_{BCT}$, ϵ will not be discussed here.

The relative geometries of D and A in the solid state deserve a few comments. Some complexes partially disordered, sometimes hopelessly so [(1:1)-(Anthracene:sym-Trinitrobenzene); (1:1)-(PTZ:TCNQ); (1:1)-(10-Methyl-PTZ:TCNQ) (26); (1:1)-(2,3,5,6-Tetramethyl-1,4-diaminobenzene:pChl) (27)]. Most DA crystals exhibit D and A molecules that lie in parallel planes and either overlap completely

((TMPD:pChl)) or, more often, partially; the perpendicular intermolecular distance $\underset{\sim}{r}_{DA}$ is close to the van der Waals interplanar separation in graphite (3.40 Å), but there seems to be no correlation between $\underset{\sim}{r}_{DA}$ and I_D-A_A, or between I_D-A_A and the angle of tilt of $\underset{\sim}{r}_{DA}$ with respect to the stacking axis.

The solid DA complexes are semiconductors. The holoionic crystals are much more conductive than the nonionic ones; in fact, some holoionic crystals are among the most conductive organic compounds known. The mechanism of conduction is unknown in either class, and attempts to link the activation energies for conduction, e_c, with $h\nu_{CT}$ or $h\nu_{BCT}$ have failed. The low level of reproducibility, especially of data obtained from crystalline powders, suggests very strongly that the conductivity is often affected, or even dominated, by the impurities present in the crystals.

The detection of ionic contributions to the ground state of DA crystals has interested many investigators.* Nuclear electrical quadrupole resonance (NQR) techniques have met very limited success (28,29,244). An upper limit of 10% CT was estimated for (1:1)-(HMB:pChl) by Douglass (28) in accord with the

---

*It is interesting to quote here the cautious remarks of Salem (Ref. (30), page 463): "In the intermolecular case, the existence of a donor-acceptor complex itself is not conclusive evidence of charge transfer in the ground state. Although part of the stability can be attributed to the depression of the ground state through admixture of a small percentage of CT state, there may be other stabilizing effects, such as back-coordination involving the interaction between filled orbitals of A and empty orbitals of D, so that one should not take too literally the name CT complex."

data of Figs. I and II. The extreme susceptibility of the NQR signal to chemical impurities and to lattice defects seems to have defeated the efforts of Hughes (31) to extend the work of Douglass to other pChl and DDQ complexes. Methods of detecting percent CT which seem highly questionable include: (i) estimates from calculations of the X-ray structure factor F_{000} (32,33); (ii) estimates obtained (34) from comparing and superimposing optical absorption spectra of KBr pellets of solid DA complexes (where D is 1,6-Diaminopyrene (DAP)[*]) on the spectra of the presumed components D, A, D^{+} and A^{-}; (iii) estimates from shifts of IR absorption bands which are attributed to the effect of "partial" formal charge (35,94). Possibly realistic estimates of partial CT may have been obtained with DA complexes with NO_2 as a paramagnetic acceptor from the size of the N^{15} hyperfine splitting of EPR lines (36).

Temperature-dependent paramagnetism is present in holoionic complexes but not in nonionic complexes.[**] McConnell _et al_. explained this by proposing that whereas in nonionic crystals the lowest possible paramagnetic state is a triplet (Frenkel) exciton $|DA\ldots DAD^{+}_{\uparrow}\, A^{-}_{\uparrow}\, DA\ldots DA\rangle$, which exists only at relatively high energies above the ground state $\Psi_{N,DA}$, on the other hand in

---

[*] Much of the work on crystals of the DAP complexes may have to be repeated in order to clarify the conflicting data reported in the literature.

[**] Except for impurities already present in the badly purified D or A, or for lattice defects introduced during the crystallization.

holoionic crystals the thermally accessible paramagnetic state $|D^+_\uparrow A^-_\downarrow \ldots D^+_\uparrow A^-_\downarrow D^+_\uparrow A^-_\uparrow D^+_\uparrow A^-_\downarrow \ldots D^+_\uparrow A^-_\downarrow\rangle$ is degenerate with the pure state $|D^+_\uparrow A^-_\downarrow \ldots D^+_\uparrow A^-_\downarrow D^+_\uparrow A^-_\downarrow D^+_\uparrow A^-_\downarrow \ldots D^+_\uparrow A^-_\downarrow\rangle$ in the first approximation, and ends up slightly above the crystal ground state ψ_{N,D^+A^-} when the latter is lowered in virtue of the second-order CT mixing of states. The energy of the triplet Frenkel exciton in nonionic crystals lies $e_{in} = 2\varepsilon_o + \varepsilon_1'$ eV above $\psi_{N,DA}$. This exciton has not yet been observed experimentally, but may be accessible by optical pumping and detectable by EPR if it is a sufficiently long-lived state. In holoionic crystals the state $|D^+A^- \ldots D^+A^- D^+_\uparrow A^-_\uparrow D^+A^- \ldots D^+A^-\rangle$ is a spin excitation of an antiferromagnetic linear chain of spin-1/2 entities, governed by a spin Hamiltonian:

$$\hat{\mathcal{H}}_{spin} = \sum_i J\, \hat{\underset{\sim}{S}}_i \cdot \hat{\underset{\sim}{S}}_{i+1}, \tag{128}$$

where by second-order perturbation theory[*] one estimates:

$$J = \frac{\gamma^2}{\Delta E}\,; \tag{129}$$

γ is given by Eq. (115) above; ΔE could be either $2\varepsilon_o + 2\varepsilon_1$ or rather, if we assume that the first-order states involved in the γ-perturbation are $|D^+A^- \ldots D^+A^- \ldots D^+A^-\rangle$ and $|D^+A^- \ldots D^+A^- DAD^+A^- \ldots D^+A^-\rangle$ then:

---

[*] There is an erroneous factor of 4 in the numerator of Eq. (10) of Ref. (13). J corresponds to e_S^H in Table II.

$$\Delta E = e_{ni} = -4\epsilon_1 + \epsilon_1' - 2\epsilon_0 - E_p . \tag{130}$$

The state $\left| D^+_\uparrow A^-_\downarrow \ldots D^+_\uparrow A^-_\downarrow D^+_\uparrow A^-_\uparrow D^+_\uparrow A^-_\downarrow \ldots D^+_\uparrow A^-_\downarrow \right\rangle$ is a triplet state, but since all D^+ to A^- distances along the linear chain are equal, it is susceptible to spin exchange, aided by the interionic Coulomb attraction;* hence the spin excitation is rapidly delocalized over the chain and becomes a spin wave with no detectable fine-structure splitting, or, as Soos calls it (37), a "Wannier spin exciton." The rapid delocalization of this thermally produced Wannier spin exciton is sufficient to not only eliminate the fine-structure splitting characteristic of localized triplet states and Frenkel triplet spin excitons, but also wipe out all or almost all the hyperfine structure from the EPR spectrum, so that one observes an extremely narrow line, with line-width less than 1 Oersted and a g-tensor whose diagonal values are all close to 2.0 and are a complicated function of the g-tensors of D^+ and A^-. Soos and Hughes (38) have studied the α-form of (pPD:pChl) in great detail, and have shown theoretically and experimentally that for the Wannier spin exciton the spin-exchange activation energy J and the EPR line-width are, to first order, independent of the concentrations of spin excitons, and

---

*On the other hand, interionic Coulomb repulsion and the alternation of interionic distances preserves the "local" Frenkel character of the triplet spin excitons for the linear chains of D^+ in Wurster's blue perchlorate (212) and the linear chains of A^- in (Triphenylmethylphosphonium$^+$)$(TCNQ)_2^-$ (92).

hence are relatively insensitive to temperature and pressure changes. They tentatively attributed the low-temperature EPR spectra (with lower spin concentration activation energies e_S^L) to chain-termination effects, but a report of a phase transition (18) in (TMPD:pChl) at low temperatures places some uncertainty on this interpretation (see Proposition II). Soos also attributed (39) a line-narrowing and g-factor anisotropy decrease with increasing temperature at $\gtrsim$ 315°K to dipole-coupled delocalization of the Wannier exciton over all the magnetically inequivalent chains, i.e. he believes the Wannier spin exciton is "three-dimensional" above 315°K;* Soos's theory must yet be buttressed by X-ray crystallographic proof that the effect is <u>not</u> due to a phase transition (see Proposition II).

Holoionic complexes exhibit irreversible changes in EPR signals above about 350°K (38) and in their conductivities above about 350°K at 1 bar, or at about 300°K above 200 kilobars (40); these changes indicate some subtle breakdown of the holoionic lattice far below its melting point (or, rather, diffuse decomposition point) at about 450°K.

In Chapter II of this thesis we perform classical calculations of E_C and H for two nonionic (HMB:pChl and Naphth:TCNE) and two holoionic ($TMPD^+pChl^-$ and $TMPD^+TCNQ^-$) DA crystals in an attempt to estimate ϵ_1 and ϵ_1', and to confirm the McConnell classification.

---

*In this case there might be a measurable Hall effect! It should be noted that the efforts of several investigators to measure a Hall effect in DA crystals have been unsuccessful (41).

APPENDIX I

TABLE I

Ionization Potential and Electron Affinities from Direct Experiment (I_{exp}, A_{exp}), Charge-transfer Spectra (I_{CT}, A_{CT}), Differences ($I_{CT} - A_{CT}$) and Crystal Surface Photoionization Potentials (I_{exp}^{surf}), all in eV/Molecule

		ACCEPTOR		DDQ[a]	TCNQ[b]	TCNE[c]	pBro[d]	pChl[e]	*s*-TNB[f]
		A_{exp} →			3.7			2.48	
		(Ref) →			(42)			(43)	
		A_{CT} →		1.9_5	1.7	1.6	1.3_7	1.37	0.7
		(Ref) →		(9)	(9)	(9)	(9)	(9)	(9)
DONOR	I_{exp}^{surf} (Ref)	I_{exp} (Ref)	I_{CT} (Ref)	$I_{CT} - A_{CT}$					
Benzene		9.24 (44) 9.40 (45)	9.24 (‡)	7.3	7.5_5	7.6_5	7.9	7.9	8.5_5
Naphth[g]	6.75 (46)	8.12 (44) 8.15 (51) 8.26 (50)	8.08 (49)	6.1	6.4	6.5	6.7	6.7	7.4
HMB[h]			7.95 (8)	6.0	6.2	6.3	6.6	6.6	7.2_5

TABLE I--Continued

Aniline		7.70 (44) 8.04 (45)	7.85 (8)	5.9	6.1_5	6.2_5	6.5	6.5	7.1_5
Pyrene	5.6 to 5.8 (53)	7.72 (50)	7.5 (8) 7.48 (49)	5.5_5	5.8	5.9	6.1	6.1	6.8
Anthr^i	5.65 (46)	7.3 (44) 7.42 (53) 7.55 (50) 7.66 (52)	7.40 (8)	5.5	5.7	5.8	6.0	6.0	6.7
DMA^j		7.51 (45)	7.3 (8)	5.3_5	5.6	5.7	5.9	5.9	6.6
Perylene	5.40 (53)	6.92 (53)	7.15 (8) 7.06 (49)	5.2	5.4_5	5.5_5	5.8	5.8	6.4_5
PTZ^k	4.99 (54)	(6.7) (†) $<$ 7.0 (53)	7.28 (49)	5.3	5.6	5.7	5.9	5.9	6.6
DAP^l	4.71 (47)								
MPNZ^m									
pPD^n			7.15 (8)	5.2	5.4_5	5.5_5	5.8	5.8	6.4_5
TMPD^o	4.63 (53)	$\leqslant$6.25 (53) $\leqslant$7.00 (53)	6.35 (8) 6.6 (8) 6.55 (48) 6.5 (4) 6.7 (8)	4.4	4.6_5	4.7_5	5.0	5.0	5.6_5

Footnotes to Table I

a: DDQ = 2,3-Dichloro-5,6-dicyano-para-quinone or 2,3-Dichloro-5,6-dicyano-1,4-cyclohexadiene-1,4-dione

b: TCNQ = 7,7,8,8-Tetracyanoquinodimethan or 2,5-Cyclohexadiene-$\Delta^{1,\alpha;4,\alpha'}$-dimalononitrile

c: TCNE = 1,1,2,2-Tetracyanoethylene or Ethene-1,1,2,2-tetracarbonitrile

d: pBro = para-Bromanil or 2,3,5,6-Tetrabromo-1,4-cyclohexadienedione

e: pChl = para-Chloranil or 2,3,5,6-Tetrachloro-1,4-cyclohexadienedione

f: s-TNB = sym-Trinitrobenzene or 1,3,5-Trinitrobenzene

g: Naphth = Naphthalene

h: HMB = Hexamethylbenzene

i: Anthr = Anthracene

j: DMA = N,N-Dimethylaniline

k: PTZ = Phenothiazine. Note that neutral phenothiazine is known to be non-planar (55,56) but its monocation is predicted to be planar; see discussion below, Proposition II.

l: DAP = 3,8-Diaminopyrene or 1,6-Diaminopyrene

m: MPNZ = N-Methylphenazine or 5-Methylphenazine

n: pPD = para-Phenylenediamine or 1,4-Diaminobenzene

o: TMPD = N,N,N',N'-Tetramethyl-para-phenylenediamine

‡: Assumed value for the evaluation of all other I_{CT} from CT spectra, Ref. (8).

†: Value extrapolated from I^{surf}_{exp}, Ref. (46).

TABLE II

Summary of Experimental Data for Selected 1:1 DA Complexes

	DDQ	TCNQ	TCNE	pBro	pChl	s-TNB
Benzene	$E^* = 2.90^g$ ϵ^* :$[3.40^g]$		$E^* = 3.51^b$ to 3.24^j ϵ^* :$[3.36^j]$		$E^* = 3.64^h$ to 3.60^j ϵ^* :$[3.37^j]$	$E^* = 4.36^g$ to 4.42^l ϵ^* :$[3.59^j]$
						$\left\{ \begin{matrix} ??\\ 3.30\text{Å},\\ ??\ ,\\ \text{none} \end{matrix} \right\}$
Naphth	$E^{1*} = 1.98^g$ $E^{2*} = 2.64^g$ ϵ^{1*} :$[3.05^g]$ ϵ^{2*} :$[3.13^g]$	$E^* = 2.22^g$	$E^{1*} = 2.64^{dd}$ to 2.26^j $E^{2*} = 2.88^e$ to 2.91^j ϵ^{1*} :$[3.20^e]$ ϵ^{2*} :$[3.22^e]$ μ^* :$[1.28^j]$	$E^* = 2.59^g$ to 2.55^j ϵ^* : $[2.91^g]$	$E^{1*} = 2.75^f$ to 2.57^j $E^{2*} = 3.22^j$ ϵ^{1*} :$[2.97^j]$ ϵ^{2*} :$[2.98^j]$ μ^* :$[0.90^j]$	$E^* = 3.40^g$ to 3.35^j ϵ^* :$[3.16^j]$ μ^* :$[0.69^j]$
			$E^1 = 2.17^\dagger$ $E^2 = 3.18^\dagger$ ρ :$[3.2 \times 10^{15}]$ $e_c = 1.24$ EPR :[none]			$E = 3.31^t$

TABLE II--Continued

.	DDQ	TCNQ	TCNE	pBro	pChl	s-TNB
Naphth (cont'd)			{$C\ 2/m$ 3.60 Å, 3.30 Å, M}			{$P\ 2_1/c$ 3.49 Å, 3.45 Å, none}
HMB	E^* = 2.10[b] to 2.00[k] ϵ^* : [3.51[e]]	E^* = 2.08[g] to 2.06[k]	E^* = 2.38[b] to 2.36[l] ϵ^* :[3.64[e]] μ^* :[1.35[j]]	E^* = 2.36[j] to 2.34[k] ϵ^* : [3.30[j]]	E^* = 2.49[c] to 2.39[j] ϵ^* : [3.40[j]] μ^* : [1.0[j]]	E^* = 3.32[b] to 3.28[l] ϵ^* :[3.33[j]] μ^* :[0.87[j]]
			E = 2.06[t] IR :[DA] ρ :[4 x 10^{13}] e_c = 0.58 EPR :[yes] $E^{gas} \cong 2.4$	IR : [DA]	E = 2.40† IR : [DA] ρ : [10^{11}] NQR: [DA] {$P\ 2_1/c$, 3.65 Å, 3.51 Å, M}	IR :[DA]

TABLE II--Continued

	DDQ	TCNQ	TCNE	pBro	pChl	s-TNB
Aniline		$E^{*} = 1.96^{d}$		$E^{*} = 2.21^{j}$	$E^{*} = 2.29^{f}$ to 2.33^{j} ϵ^{*} :[3.07^{g}]	$E^{*} = 3.14^{d}$ to 3.18^{h} ϵ^{*} :[3.23^{j}]
				ρ :[10^{9}] $e_c = 0.23$	ρ :[10^{9}] $e_c = 0.24$	$E = 2.82^{t}$ VUV :[DA] ρ :[10^{17}] $e_c = 1.27$
Pyrene	$E^{1*} = 1.55^{e}$ $E^{2*} = 2.26^{e}$ to 2.30^{g} ϵ^{1*} :[3.18^{e}] ϵ^{2*} :[3.08^{e}]	$E^{1*} = 1.62^{g}$ $E^{2*} = 2.50^{g}$	$E^{1*} = 1.98^{dd}$ to 1.70^{j} $E^{2*} = 2.50^{e}$ to 2.47^{j} $E^{3*} = 3.20^{e}$ ϵ^{1*} :[3.05^{e}] ϵ^{2*} :[2.93^{e}] μ^{*} :[2.0^{j}]	$E^{*} = 2.03^{e}$ to 2.04^{j} ϵ^{*} :[2.91^{g}]	$E^{1*} = 2.04^{e}$ to 2.02^{j} $E^{2*} = 2.86^{j}$ ϵ^{1*}:[2.94^{j}] ϵ^{2*}:[2.84^{j}]	$E^{*} = 2.95^{f}$ to 2.79^{j}
			$E^{1} = 1.57^{\dagger}$ $E^{2} = 2.48^{\dagger}$ $E^{3} = 3.62^{\dagger}$	$E = 1.96^{\dagger}$	$E = 2.05^{v}$ $1.94^{\dagger}$	$E^{1} = 2.72^{\dagger}$ $E^{2} = 3.60^{\dagger}$

TABLE II--Continued

	DDQ	TCNQ	TCNE	pBro	pChl	s-TNB
Pyrene (cont'd)	IR :[DA] ρ :[10^{13}] e_c = 0.9 EPR:[none]	ρ :[10^{12}]	ρ :[4.5 x 10^{15}] e_c = 0.85 EPR :[none] $\left\{ \begin{matrix} P2_1/a, \\ 4.04\ \text{Å}, \\ 3.32\ \text{Å}, \\ M \end{matrix} \right\}$	ρ :[2 x 10^{15}] e_c = 1.95 EPR :[none]	IR :[DA] ρ :[10^{15}] e_c = 1.0 EPR :[~~yes~~]	ϵ :[$\geqslant 2.84^t$] IR :[DA] ρ :[10^{20}] e_c = 1.10
Anthr		$E^{1*} = 1.52^g$ $E^{2*} = 2.69^g$	$E^{1*} = 1.67^j$ $E^{2*} = 2.66^j$	$E^* = 1.94^g$ to 1.97^j ϵ^* :[2.71^g]	$E^* = 1.97^g$ to 1.93^j ϵ^* :[2.66^j]	$E^* = 2.85^f$ to 2.72^j ϵ^* :[3.18^j]
		IR :[DA] EPR :[none]		$E = 1.92^{\dagger}$	$E = 1.90^{\dagger}$	$E^1 = 2.50^{\dagger}$ $E^2 = 3.66^{\dagger}$ ϵ^1 :[$3.30^{\dagger}$] VUV :[DA] ρ :[9 x 10^{17}]

TABLE II--Continued

	DDQ	TCNQ	TCNE	pBro	pChl	s-TNB
Anthr (cont'd)						e_c = 0.9 {C2/c, 3.30 Å, 3.28 Å, M}
DMA		E^* = 1.41^{g}		E^* = 1.87^{ff} to 1.89^{j}	E^* = 1.86^{g} to 1.96^{k} ϵ^* :[3.32^{g}] μ^* :[2.64^{j}]	E^* = 2.73^{f} to 2.66^{l} ϵ^* :[3.13^{j}]
				IR :[DA] ρ :[10^9] e_c = 0.45 EPR :[~~yes~~]	E = $1.90^{\dagger}$ IR :[DA] ρ :[10^9] e_c = 0.45 EPR :[~~yes~~] {??, 3.40 Å 3.40 Å none}	E = 2.43^{t} IR :[DA] VUV :[DA] ρ :[10^{16}] e_c = 1.04

TABLE II--Continued

	DDQ	TCNQ	TCNE	pBro	pChl	s-TNB
Perylene		$E^{*} = 1.30^{g}$	$E^{*} = 1.38^{e}$ to 1.39^{j}	$E^{*} = 1.68^{j}$	$E^{*} = 1.64^{g}$ to 1.68^{j}	$E^{*} = 2.58^{g}$ to 2.43^{j}
	IR :[DA] ρ :[3×10^{6}] $e_c = 0.45$ EPR :[none]		$E^{1} = 1.30^{\dagger}$ $E^{2} = 2.99^{\dagger}$ ρ :[2.4×10^{12}] $e_c = 0.72$ EPR :[none] $\left\{\begin{matrix} P2_1/a \\ 4.09\text{Å} \\ ? \\ \text{none} \end{matrix}\right\}$	$E = 1.49^{t}$ EPR :[none]	$E = 1.53^{t}$ IR :[DA] ρ :[2.8×10^{11}]	$E^{1} = 2.30^{\dagger}$ $E^{2} = 4.10^{\dagger}$ ε^{1} :[$\geqslant 2.84^{t}$] VUV :[DA] ρ :[10^{19}] $e_c = 0.83$
PTZ			$E^{*} = 1.45^{b}$	$E^{*} = 1.57^{b}$	$E^{*} = 1.57^{b}$ to 1.54^{g}	$E^{*} = 2.50^{b}$ to 2.38^{f}
	IR :[$D^{+}A^{-}$]	EPR :[yes]				

TABLE II--Continued

	DDQ	TCNQ	TCNE	pBro	pChl	s-TNB
PTZ (cont'd)		$\left\{\begin{array}{c}\text{monoclinic}\\ 3.5\ \text{Å},\\ ??,\\ \text{none}\end{array}\right\}$				$\left\{\begin{array}{c}Pbcn,\\ ??,\\ ??,\\ \text{none}\end{array}\right\}$
DAP	IR : $[D^+A^-]$ ρ : $[10^2]$	IR : $[D^+A^-]$ VUV : $[D^+A^-]$ ρ : $[0.5]$ $e_c = 0.14$		IR : [??] ρ : $[10^3]$ $e_c = 0.15$	Three Allomorphs α, β, γ IR :[??]$\alpha\beta\gamma$ VUV:[??]$\alpha\beta\gamma$ ρ :$[10^7]\alpha$ ρ :$[10^5]\beta$ ρ :$[<10]\gamma$ $e_c = 0.15$	
MPNZ		ρ : $[0.007^{‡}]$ $\left\{\begin{array}{c}P\bar{1},\\ 8.2\text{Å},\\ 3.51\text{Å},\\ M\end{array}\right\}$				

TABLE II--Continued

	DDQ	TCNQ	TCNE	pBro	pChl	s-TNB
pPD					$E^* = 1.72^k$	$E^* = 2.36^f$ to 2.48^j
	IR : $[D^+A^-]$ ρ : $[10^6]$ $e_c = 0.37$ EPR:[yes]	ρ: $[3\times10^3]$ $e_c = 0.28$ EPR :[0.1%]	no solvent occlusion ρ:$[2\times10^{15}$??] $e_c = 0.78$?? EPR :[yes]	solvent occlusion: Two allomorphs α,β IR : $[D^+A^-]$ ρ : $[10^{10}]$ EPR: [yes]	solvent occlusion: Three allomorphs α,β,γ $E = 1.2^{\dagger}\beta$ IR :$[D^+A^-]$ VUV :$[D^+A^-]$ ρ:$[10^7]\alpha\beta$ $e_c = 0.43$ EPR :[0.1%] β? $e_s^H = 0.13\alpha,^{\ddagger}$ $0.16\beta^{\ddagger}$ $e_s^L = 0.015\alpha$ $\left\{\begin{matrix}P\,2_1/n,\\ 3.40\ \text{Å},\\ 3.4\ \text{Å},\\ \text{none}\end{matrix}\right\}\beta$	$E = 2.48^t$ IR :[DA] VUV :[DA] ρ: $[8\times10^{16}]$ $e_c = 1.02$

TABLE II--Continued

	DDQ	TCNQ	TCNE	pBro	pChl	s-TNB
pPD (cont'd)					$\left\{\begin{array}{l}P\ \bar{3}m1\ (?)\\ 3.31\ \text{Å},\\ 3.3\ \text{Å},\\ \text{none}\end{array}\right\}$	
TMPD		$E^{*} = 1.06^{g}$	$E^{*} = 1.27^{g}$	$E^{*} = 1.41^{k}$	$E^{*} = 1.34^{b}$ to 1.43^{k}	$E^{*} = 2.12^{b}$ to 2.00^{l} ϵ^{*} :[3.14^{l}]
	VUV:[$D^{+}A^{-}$]	IR :[$D^{+}A^{-}$] VUV:[$D^{+}A^{-}$] ρ :[$\sim 10^{7}$] EPR:[17%] $e_{\zeta}^{H} = 0.075$	VUV:[$D^{+}A^{-}$]	$E = 1.06^{t}$ IR :[$D^{+}A^{-}$] VUV:[$D^{+}A^{-}$] ρ :[10^{5}] $e_{c} = 0.28$ EPR:[7%]	$E = 1.02^{\dagger}$ IR :[$D^{+}A^{-}$] VUV:[$D^{+}A^{-}$] ρ :[10^{4}] $e_{c} = 0.27$ EPR:[5%] $e_{\zeta}^{H} = 0.13\alpha^{\ddagger}$ $0.16\beta^{\ddagger}$ $e_{\zeta}^{L} = 0.010\alpha^{\ddagger}$ $0.007\beta^{\ddagger}$	$E = 1.90^{t}$ IR :[DA] VUV:[DA]

TABLE II--Continued

	DDQ	TCNQ	TCNE	pBro	pChl	s-TNB
TMPD (cont'd)		C2/m 3.86 Å, 3.27 Å, M		C 2/m, 3.31 Å, 3.31 Å, none	C 2/m, 3.28 Å, 3.28 Å, M αβ	

Footnotes to Table II: Explanation of Symbols

†	:	The solid charge-transfer absorption of a single crystal of the complex is highest for plane-polarized light with electric vector parallel to a line connecting the center of the D molecule with the center of the A molecule (57);
††	:	ditto for single crystal specular reflectance spectroscopy;
( )	:	Literature reference;
‡	:	Single-crystal measurement (except for X-ray diffraction and measurements denoted by † or ††);
*	:	Solution measurement;
§	:	Fluorescent emission measurement;
Q:[[↑]]	:	Quantity Q increases with application of hydrostatic pressure;
Q:[[↓]]	:	Quantity Q decreases with application of hydrostatic pressure;
$P\ 2_1/c$	: Crystal structure data:	Space group
3.50 Å,		D-A distance along "stacking axis" (Å)
3.50 Å,		D-A perpendicular separation $\underset{\sim}{r}_{DA}$ (Å)
M		M: Molecular structure is known; else "none"

All data at room temperature unless otherwise noted;

$E^{1*}, E^{2*}, E^{3*}, E^{\star}$	:	First, second, third, and only charge-transfer band maximum in solution (in eV/DA pair)
E^1, E^2, E^3, E	:	ditto for crystals
e_c	:	activation energy for electrical conduction (eV) expressed as $\rho = \rho_o \exp(e_c/kT)$
e_s^H (and e_s^L)	:	activation energy for paramagnetism at high (and low) temperature (eV) expressed as $\sigma^H = \sigma_o^H \exp(e_s^H/kT)$

μ^* : [dipole moment, Debye units] in solution

ϵ^* : [decimal logarithm of the molar absorptivity or extinction coefficient (expressed in liter mole^{-1} cm^{-1}), i.e. $\log_{10}\epsilon$] in solution

ϵ : [ditto] for crystals

ρ : [room-temperature resistivity, ohm cm] for crystals

IR:[DA] : "the infrared absorption spectrum of the solid complex shows it to be neutral inasmuch as it is the superposition of the separate infrared spectra of the neutral donor and of the neutral acceptor, and no bands due to ionic forms can be detected" at room temperature

VUV:[DA] : "ditto for visible-ultraviolet absorption spectra" at R.T.

NQR:[DA] : "the nuclear electrical quadrupole resonance spectrum of the complex does not show the presence of D^+ or A^- ions or a clear effect due to partial charge-transfer"

IR:[D^+A^-] : "the infrared absorption spectrum of the solid complex shows it to be holoionic inasmuch as the spectrum is the superposition of the separate spectra for the donor monocation and for the acceptor monoanion, and no trace of the spectra of neutral donor or acceptor can be detected" at room temperature

VUV:[D^+A^-]: "ditto for visible-ultraviolet absorption spectra"

EPR:[yes] : "paramagnetism is detectable at room temperature"

EPR:[none]: "no paramagnetism is detected at room temperature"

EPR:[5%] : "the paramagnetic species at room temperature comprise 5% of the total (species)"

/ or [/] : "unreliable result"

E^{gas} : charge-transfer band in gas phase (eV/DA pair)

a : Solvent is Water (dielectric constant ε' = 78.54 at 25°C)
b : " " Acetonitrile (ε' = 37.5 at 20°C)
c : " " Methanol (ε' = 32.63 at 20°C)
d : " " Ethanol (ε' = 24.3 at 25°C)
dd : " " Acetone (ε' = 20.7 at 25°C)
ddd: " " Cyclohexanone (ε' = 18.3, Ref. (58))
e : " " Dichloromethane (ε' = 9.08 at 20°C)
ee : " " Ethyl acetate (ε' = 6.02,Ref. (58))
f : " " Tetrahydrofuran (ε' = 7.3 at 20°C Ref. (59))
ff : " " Dimethylaniline (ε' = 4.91,Ref. (60))
g : " " Chloroform (ε' = 4.806 at 20°C)
h : " " Butyl ether (ε' = 3.06 at 25°C)
i : " " Benzene (ε' = 2.284 at 20°C)
j : " " Carbon tetrachloride (ε' = 2.238 at 20°C)
k : " " Cyclohexane (ε' = 2.023 at 20°C)
l : " " n-Heptane (ε' = 1.924 at 20°C)

All dielectric constant data, except when noted otherwise, are from Ref. (61).

m : (3:1) - (Propyl ether: iso-Pentane) glass
n : (4:1) - (Propyl ether: Methylcyclohexane) glass
o : at -40°C
p : at -65°C
q : at -160°C
r : at -190°C
s : in Cellulose Acetate polymer matrix
t : crystal dispersed in KBr pellet
u : crystal dispersed in NaCl pellet
v : crystalline film
w : Nujol mull
x : crystal, measured by diffuse reflectance spectroscopy

<u>Footnotes to Table II (cont'd):</u>
<u>Further Data and Literature References</u>

[Benzene:DDQ]:

$$E^* = 2.90^g(62)$$
$$\varepsilon^* = [3.40^g(62)]$$

[Benzene:TCNE]:

$E^* = 3.51^b(63), 3.23^e(64), 3.22^e(63), 3.20^e(65), 3.22^g(66),$ ~~3.16^g~~$^g(63), 3.24^j(67)$

ϵ^* = [3.55^e(64), 3.07^e(241), 3.36^j(67)]
E^* : [[$\downarrow$](241)]
ϵ^* : [[$\uparrow$](241)]
μ^* : [1.35^j(4)]

[Benzene:pChl]:
E^* = 3.22^g(68), 3.65^h(69), 3.60^j(71), 3.57^j(67), 3.58^k(70)
ϵ^* = [3.34^h(69), 3.37^j(67)]
μ^* : [1.0^j(4)]

[Benzene:s-TNB]:
E^* = 4.36^g(75), 4.40^j(71), 4.38^j(72,76), 4.43^k(76), 4.42^l (77)
ϵ^* : [3.99^g(75), 3.77^j(72), 3.59^j(76), 3.59^k(76)]
μ^* : [0.87^j(4)]
Crystal structure:(78)
Molecular structure: none

[Naphth:DDQ]:
E^{1*} = 1.98^g(62)
E^{2*} = 2.64^g(62)
ϵ^{1*} : [3.05^g(62)]
ϵ^{2*} : [3.13^g(62)]

[Naphth:TCNQ]:
E^* = 2.22^g(79)

[Naphth:TCNE]:
E^{1*} = ~2.64^{dd}(58), 2.26^e(64,83), 2.24^e(58), 2.22^e(80), 2.48^{ee}(58), 2.22^g(58), 2.21^g(66), 2.28^i(58), 2.26^j (58,67,81), 2.30^k(58), 2.33^l(82), 2.38^s(83)
E^{2*} = 2.88^e(58,80,83), 3.06^{ee}(58), 2.86^g(58), 2.91^j(58), 2.90^j(67,81), 2.96^k(58), 2.98^l(82), 2.95^s(83)
ϵ^{1*} : [3.09^e(64), 3.20^j(67)]
ϵ^{2*} : [3.22^j(67)]
E^* : [[$\downarrow$](241)]

ϵ^{*} : [[$\uparrow$](241)]
E^{p*} : [[$\downarrow$](83)]
μ^{*} : [1.28^{j}(4)]
E^{1} = $2.17^{\dagger}$(81), 2.30^{v}(82), 2.27^{u}(82), 2.18^{t}(80)
E^{2} = $3.04^{\dagger}$(81), 2.89^{v}(82), 3.04^{u}(82), 3.18^{t}(80)
E : [[$\downarrow$](82,83)]
ϵ : [[$\uparrow$](82)]
ρ : [3.2×10^{15}(80)]
e_c = 1.24 (80)
EPR : [none (80)]
Crystal structure:(85,86)
Molecular structure:(85)

[Naphth:pBro]:
E^{*} = 2.59^{g}(87), 2.55^{j}(49)
ϵ^{*} : [2.99^{g}(87)]

[Naphth:pChl]:
E^{1*} = 2.75^{f}(79), 2.64^{g}(87), 2.50^{g}(79), 2.69^{h}(69), 2.60^{i}(68), 2.63^{j}(71), 2.59^{j}(67), 2.57^{j}(8), $2.56^{m,r}$(74), $1.93^{m,r\S}$(74)
E^{2*} = 3.22^{j}(67)
ϵ^{1*} : [2.85^{g}(87), 2.91^{h}(69), 2.97^{j}(67)]
ϵ^{2*} : [2.98^{j}(67)]
μ^{*} : [0.90^{j}(4)]

[Naphth:s-TNB]
E^{*} = 3.40^{g}(75), 3.35^{i}(88), 3.40^{j}(89), 3.35^{j}(71,72), 3.40 to 3.45^{k}(89), 3.40 to 3.50^{l}(89), $3.28^{m,r}$(74), $2.42^{m,r\S}$(74)
ϵ^{*} : [3.13^{g} (75), 3.16^{j}(72), 3.11^{j}(89)]
μ^{*} : [0.69^{j}(4)]
E = 3.31^{t}(90), 3.41^{x}(239), $2.38^{x\S}$(239), $2.34^{t\S}$(90)
Crystal structure:(78,91)
Molecular structure: none

[HMB:DDQ]:

E^* = 2.10^b(243), 2.12^d(243), 1.98^e(246), 1.97^j(112), 2.00^k(84)

ϵ^* : [3.51^e(246)]

[HMB:TCNQ]:

E^* = 2.08^g(79), 2.06^k(84)

[HMB:TCNE]:

E^* = 2.38^b(63), 2.42^{dd}(58), 2.48^{ddd}(58), 2.29^e(63), 2.28^e(58,64,80,83), 2.42^{ee}(58), 2.30^g(58), 2.28^g(63), 2.30^i(58), 2.33^j(67), 2.32^j(58), 2.34^k(58), 2.30^k(84), 2.41^l(58), 2.36^l(82), $2.23^{n,r}$(93), 2.34^s(83)

ϵ^* : [3.68^j(67), 3.64^e(64), $4.0^{n,r}$(93)]

E^* : [[↑](241)]

ϵ^* : [[↑](241)]

E^{p*} : [[↑](83)]

μ^* : [1.35^j(4)]

E = 2.06^t(80), 2.26^u(82)

E : [[↑](82)]

ϵ : [[↑](94)]

IR : [DA‡(94)]

ρ : [4×10^{13}(80), 10^{11}(95)]

e_c = 0.58(80)

EPR : [~~0.005%~~(80)]

$E^{gas} \cong 2.4$ (quoted in Ref. (58))

A 2:1 complex is known (96)

[HMB:pBro]:

E^* = 2.36^j(97), 2.34^k(84)

ϵ^* : [3.30^j(97)

E^{p*} : [[↓](98)]

ϵ^{p*} : [[↑](98)]

IR : [DA(99)]

[HMB:pChl]:

E^* = 2.48^{b}(243), 2.46^{b}(100), 2.49^{c}(100), 2.51^{d}(243), 2.50^{d}(100), 2.42^{dd}(58), 2.38^{e}(100), 2.28^{e}(58), 2.40^{g}(79,100), 2.30^{g}(58), 2.46^{h}(69), 2.30^{i}(58), 2.40^{j}(100), 2.39^{j}(97), 2.46^{k}(70), 2.43^{k}(84,100), 2.34^{k}(58), $2.46^{m,r}$(73), $1.67^{m,r\S}$(73)

ϵ^* : [3.46^{h}(69), 3.40^{j}(97)]

E^{p*} : [[$\downarrow$](98)]

ϵ^{p*} : [[$\uparrow$](98)]

μ^* : [1.0^{j}(4)]

E = $2.40^{\dagger}$(101,102)

E : [[$\downarrow$](102)]

ϵ : [[$\uparrow$](102)]

IR : [DA(99)]

ρ : [10^{11}(95)]

NQR : [DA(28)]

Crystal structure:(78,103)

Molecular structure: (103,104,105)

[HMB:s-TNB]:

E^* = 3.32^{b}(100), 3.18^{e}(242), 3.19^{g}(76), 3.18^{g}(100,106), 3.16^{j}(76), 3.14^{j}(72,100,106), $3.19^{j,q}$(93), 3.20^{k}(76,84,100), 3.18^{k}(245), 3.22^{l}(76), $3.10^{n,r}$(93)

ϵ^* : [3.42^{g}(106), 3.37^{g}(76), 3.41^{j}(76), 3.40^{j}(106), 3.33^{j}(72), 3.38^{k}(76), 3.35^{l}(76), $3.20^{n,r}$(93)]

μ^* : [0.87^{j}(4)]

IR : [DA(99)]

[Aniline:TCNQ]:

E^* = 1.96^{g}(79)

[Aniline:pBro]:

E^* = 2.21^j(49)

ρ : [10^9(95), 9×10^7 or 1.5×10^9(107)]

e_c = 0.27(95), 0.23(107)

[Aniline:pChl]:

E^* = 2.29^f(79), 2.34^g(79,108), 2.33^j(71)

ϵ^* : [3.07^g(108)]

ρ : [10^9(95), 5×10^7 or 8.1×10^8(107)]

e_c = 0.27(95), 0.24(107)

[Aniline:s-TNB]:

E^* = 3.14^d(88), 3.10^g(75), 3.14^i(88), 3.10^j(71,109), 2.94^j(240), 3.18^k(110)

ϵ^* : [3.16^g(75), 3.23^j(110)]

E = 2.82^t(109)

VUV : [DA(109)]

ρ : [10^{17}(109)]

e_c = 1.27(109)

[Pyrene:DDQ]:

E^{1*} = ~1.55^e(111), 1.51^e(112)

E^{2*} = ~2.26^e(111), 2.30^g(62)

ϵ^{1*} : [3.18^e(111)]

ϵ^{2*} : [3.08^e(111), 3.09^g(62)]

IR : [DA(113)]

ρ : [10^{13}(113)]

e_c = 0.9(113)

EPR : [none(113)]

[Pyrene:TCNQ]:

E^{1*} = 1.62^g(79)

E^{2*} = 2.50^g(79)

ρ : [10^{12}(114,115), 2×10^{12}(116)]

[Pyrene:TCNE]:

E^{1*} = 1.98^{dd}(58), ~ 1.77^{e}(111), 1.72^{e}(58), 1.71^{e}(64), 1.70^{e}(80), 1.92^{ee}(58), 1.72^{g}(66), 1.70^{g}(58), 1.74^{i}(58), 1.74^{j}(58,67), 1.70^{j}(81,117,118), 1.79^{k}(58)

E^{2*} = 2.50^{e}(58,64), 2.48^{e}(80), 2.69^{ee}(58), 2.48^{g}(58), 2.54^{j}(67), 2.52^{j}(58), 2.47^{j}(81,118), 2.44^{j}(117), 2.58^{k}(58), 2.59^{l}(82), 2.62^{s}(83)

E^{3*} = 3.20^{j}(67)

ϵ^{1*} : [3.05^{e}(64,111)]

ϵ^{2*} : [2.93^{e}(64)]

μ^{*} : [2.0^{j}(81)]

E^{1} = $1.57^{\dagger}$(81,117,118,119), 1.49^{t}(80,120), plus vibrational overtones (117)

E^{2} = $2.48^{\dagger}$(81,117,118,119), 2.43^{t}(80,120), 2.49^{u}(82), 2.48^{v}(82)

E^{3} = $3.62^{\dagger}$(118), $3.52^{\dagger}$(117), plus vibrational overtones (117)

E^{1}, E^{2}, E^{3}: [[↓](82)]

$\epsilon^{1}, \epsilon^{2}, \epsilon^{3}$: [[↑](82)]

ρ : [4.5×10^{15}(80), 10^{8} or 10^{10}(95)]

e_c = 0.85 (80)

EPR : [none(80)]

Crystal structure:(86,119,121) unusual crystal habit (stacking axis is not longest, "needle," axis)

Molecular structure: (121)

[Pyrene:pBro]:

E^{*} = 2.03^{e}(112), 2.01^{g}(87), 2.04^{j}(49), 2.00^{j}(87)

ϵ^{*} : [2.92^{g}(87)]

E^{P*} : [[↓](98)]

ϵ^{P*} : [[↑](98)]

E = 1.91^{t}(49), 1.86^{t}(120), 2.03^{v}(123), $1.96^{\dagger}$(250)

ρ : [2×10^{15}(123)]

e_c = 0.94(123)

EPR : [none(49), ~~1.0%~~(123)]

[Pyrene:pChl]:

E^{1*} = $2.22^{c}(79)$, $2.24^{dd}(79)$, $2.04^{e}(64,79)$, $2.03^{e}(112)$, $2.20^{ee}(79)$, $2.17^{f}(79)$, $2.07^{g}(124)$, $2.03^{g}(87)$, $2.01^{g}(79)$, $2.08^{i}(68,79)$, $2.06^{j}(67)$, $2.04^{j}(79)$, $2.02^{j}(87)$

E^{2*} = $2.86^{j}(67)$

ϵ^{1*} : [$2.94^{e}(64)$, $2.94^{g}(87)$, $2.94^{j}(67)$]

ϵ^{2*} : [$2.84^{j}(67)$]

E^{p*} : [[$\downarrow$](98)]

ϵ^{p*} : [[$\uparrow$](98)]

E = $2.05^{v}(123)$, $1.94^{\dagger}(250)$

IR : [DA(125)]

ρ : [$10^{15}(123)$, $10^{11}(95)$, $10^{10}(125)$]

e_c = 1.0(123)

EPR : [~~0.001%~~(123)]

[Pyrene:s-TNB]:

E^{*} = $2.95^{f}(79)$, $2.79^{g}(79)$, $2.78^{g}(124)$, $2.79^{j}(109,118)$

E^{1} = $2.72^{\dagger}(118)$, $2.78^{t}(12)$, $2.70^{t}(90)$, $2.68^{t}(109,120)$, $2.21^{t\S}$ (90), $2.86^{x}(126)$

E^{2} = $3.60^{\dagger}$ (118)

ϵ : [$\geqslant 2.84^{t}(12)$]

IR : [DA(109)]

ρ : [$10^{20}(109)$]

e_c = 1.10(109)

[Anthr:TCNQ]:

E^{1*} = $1.52^{g}(79)$

E^{2*} = $2.69^{g}(79)$

IR : [DA(53)]

ρ : [$2 \times 10^{11}(116)$, $10^{11}(114,115)$]

EPR : [none(53)]
Crystal structure: (127)
Molecular structure: (127)

[Anthr:TCNE]:

E^{1*} = 1.67^{j}(67)
E^{2*} = 2.67^{j}(67)

[Anthr:pBro]:

E^{*} = 1.94^{g}(87), 1.97^{j}(49), 1.94^{j}(87)
ϵ^{*} = [2.71^{g}(87)] ; $E^{\dagger}$ = 1.92 (250)

[Anthr:pChl]:

E^{*} = 2.17^{f}(79), 1.97^{g}(79,87), 2.04^{h}(69), 2.05^{i}(68), 1.98^{j}(67), 1.95^{j}(87), 1.93^{j}(8)
ϵ^{*} : [2.70^{g}(87), 2.51^{h}(69), 2.66^{j}(67)]; E = $1.90^{\dagger}$(250)

[Anthr:s-TNB]:

E^{*} = 2.85^{f}(79), 2.74^{g}(124), 2.69^{g}(75,79), 2.75^{i}(88), 2.79^{j}(109), 2.73^{j}(71), $2.68^{m,r}$(74), $2.66^{n,r}$(93), $2.04^{m,r\,\S}$(74)
ϵ^{*} : [3.18^{g}(75), $3.25^{n,r}$(93)]
E^{1} = lowest vibrational 0-0 band ($^{1}A \longrightarrow {}^{1}A$) (128): $2.50^{\dagger}$(128), $2.48^{\dagger}$(249), 2.53^{t}(109)

first vibrationally excited band: $2.68^{\dagger}$(128), $2.72^{\dagger}$(247), 2.70^{t}(12), 2.68^{t}(90,109), 2.74^{x}(239), $2.08^{\dagger\S}$(248), $2.34^{\dagger\S\,r}$(248), $2.18^{t\,\S}$(90), $2.11^{x\,\S}$(239)

second vibrationally excited band: $2.82^{\dagger}$(128), 2.80^{t}(109)

E^{2} = $3.66^{\dagger}$(247), $3.48^{\dagger}$(249)
E^{3} = $4.60^{\dagger}$(249)
ϵ : [$\geq 3.30^{t}$(12), $3.30^{\dagger}$(128,129)]

E : [[↓](130)]
VUV : [DA(109)]
ρ : [9×10^{17} (109)]
e_c = 0.9(109)
Crystal structure: (78,131)
Molecular structure: (131): partial disorder

[DMA:TCNQ]:
E^* = 1.46^g(79)

[DMA:pBro]:
E^* = 1.87^{ff}(60), 1.89^j(49)
IR : [DA(99)]
ρ : [10^9(95)]
e_c = 0.45(95)
EPR : [~~5%, g= 2.0071±0.0005(132~~)]

[DMA:pChl]:
E^* = 1.86^g(79), 1.84^g(108), 1.91^j(17,110,133), 1.96^k (134)
ϵ^* : [3.32^g(108)]
E : $1.90^{\dagger}$ (17), $2.02^{\dagger\dagger}$ (100), $2.15^{\dagger\dagger}$ ((100) probably vibrational overtone)
IR : [DA(99)]
ρ : [10^9(95), 10^{10}(95)]
e_c = 0.45(95)
EPR : [~~0.01%, g = 2.0003±0.0004(132); $g_{\parallel}$= 2.0004, $g_{\perp}$= 2.0076(135~~)]
Crystal structure: (78)
Molecular structure: none

[DMA:s-TNB]:

E^{*} = 2.73^{f}(79), 2.55^{g}(110), 2.54^{g}(75), 2.52^{g}(79), 2.60^{j} (71,109), 2.56^{j}(110), 2.62^{k}(110), 2.66^{l}(110)
ϵ^{*} : [3.17^{g}(75), 3.05^{g}(110), 3.13^{j}(110), 3.11^{k}(110), 3.07^{l}(110)]
E = 2.43^{t}(109)
IR : [DA(109)]
VUV : [DA(109)]
ρ : [10^{16}(109), 10^{8} or 10^{11}(95)]
e_c = 1.04(109)

[Perylene:DDQ]:

IR : [DA(113)]
ρ : [3×10^{6}(113)]
e_c = 0.45(113)
EPR : [none(113)]

[Perylene:TCNQ]:

E^{*} = 1.30^{g}(79)

[Perylene:TCNE]:

E^{*} = 1.38^{e}(80), 1.43^{e}((80)) vibrational overtone), 1.35^{g} (66), 1.39^{j}(79)
E^{1} = $1.30^{\dagger}$ (118) with vibrational structure), 1.28^{t}(80), 1.46^{t} ((80) vibrational overtone)
E^{2} = $2.99^{\dagger}$((118) with vibrational structure)
ρ : [2.4×10^{12}(80), 10^{8} or 10^{11}(95)]
e_c = 0.72(80)
ρ : [[↓](40)]
EPR : [< 0.005%(80)]
Crystal structure: (86,118)
Molecular structure: none

[Perylene:pBro]:

E^{*} = 1.68^{j}(49)

E = 1.49^{t}(136), 1.62^{t}((136) probably vibrational overtone), 1.64^{t}(49)

IR : [DA(136)]

EPR : [none(49)]

[Perylene:pChl]:

E^{*} = 1.64^{g}(79), 1.68^{j}(8), 1.72^{j}(67)

E = 1.53^{t}(136), 1.65^{t}((136) probably vibrational overtone)

IR : [DA(136)]

ρ : [2.8×10^{11}(137), 10^{8}(95,139)]

ρ : [[$\downarrow$](137)]

[Perylene:s-TNB]:

E^{*} = 2.58^{g}(79), 2.43^{j}(109)

E^{1} = 2.30^{+}(118), 2.53^{t}(12), 2.23^{t}(109)

E^{2} = 4.10^{+}(118)

ϵ^{1} : [$\geqslant 2.84^{t}$(12)]

VUV : [DA(109)]

ρ : [10^{19}(109)]

e_{c} = 0.83(109)

[PTZ:DDQ]:

IR : [$D^{+}A^{-}$(35)]

[PTZ:TCNQ]:

EPR : [yes(139)]

Crystal structure: (139) partial disorder

Molecular structure: none

[PTZ:TCNE]:

E^{*} = 1.45^{b}(24)

[PTZ:pBro]:

E^{1*} = 1.57^b(24), < 1.55^j(49)
E^{2*} = 1.86^j(49)

[PTZ:pChl]:

E^* = 1.57^b(24), 1.61^f(79), 1.54^g(79)

[PTZ:s-TNB]:

E^* = 2.50^b(24), 2.38^f(79), 2.38^g(79)
Crystal structure: (140)
Molecular structure: none

[DAP:DDQ]:

VUV : [D^+A^-((38) reinterpreted)]
IR : [D^+A^-(125)]
ρ : [10^2(34)]

[DAP:TCNQ]:

VUV : [D^+A^-((141) reinterpreted)]
IR : [D^+A^-(141)]
ρ : [0.5(141)]
e_c = 0.14(141)

[DAP:pBro]:

VUV : [D^+A^-((34) reinterpreted)]
IR : [DA(95)]
ρ : [10^3(95)]
e_c = 0.15(138)
ρ : [[$\downarrow$](40)]

[DAP:pChl]:

"Three allomorphs: α recrystallized from Chloroform (green)
β recrystallized from Benzene (brown)
γ recrystallized from Benzene and compressed" (142)

VUV : [D^+A^-(34), DA(142) for α,β,γ]

IR : [DA(125,142) for α,β,γ]

cf. also Ref. (53)

ρ : [4×10^3(143), 1.2×10^4(137), 10^4(95), 10^5‡ to 10^9‡ (137), 10^7(142)] for allomorph α

ρ : [10^5(142)] for allomorph β

ρ : [a few (142)] for allomorph γ

e_c = 0.15(138) for allomorph α

ρ : [[$\downarrow$](40)]

[MPNZ:TCNQ]:

Strictly speaking, not a D^+A^- crystal because of negligible overlap between D^+ and A^-, as against large overlap of D^+ with D^+, and of A^- with A^- (cf. end of Chapter II)

ρ : [0.007‡ along needle axis, 0.5 powder (144)]

Crystal structure: (145)
Molecular structure: (145)

[pPD:DDQ]:

IR : [D^+A^-(113)]
ρ : [10^6(113)]
e_c = 0.37(113)
EPR : [yes(113)]

[pPD:TCNQ]:

ρ : [8×10^5(116), 3×10^3(114,115)]
e_c = 0.28 (114,115)
EPR : [0.1%(115)]

[pPD:TCNE]:

no solvent occlusion (146)
E = ~~2.26^{t}(146~~) probably is pPD$^+$ absorption band
ρ : [~~2 x 10^{15}~~(146)]
e_c = ~~0.78~~(146)
EPR : [yes(146)]

[pPD:pBro]:

"Two allomorphs: α solvent-free, by co-grinding,
β 1/6 molecule of Benzene per DA pair" (147)
IR : [D$^+$A$^-$(35)]
ρ : [10^{10}(95), 2 x 10^{10}(40)] for allomorph β
ρ : [[↓](40)] for allomorph β
EPR : ["0.3 intensity in arbitrary units at 77°K," g = 2.0095, 2.0050 (148,149)]

[pPD:pChl]:

E^* = 1.72^k(25)
"Three allomorphs: α solvent-free, by co-grinding (150) or by co-sublimation (38),
β 1/2 molecule Benzene per DA pair (137,150)
γ 1/3 molecule Dichloromethane per DA pair (150)"
E = 1.2†(17) allomorph β
VUV : [D$^+$A$^-$(17)] allomorph β
IR : [D$^+$A$^-$(35,113)]
ρ and e_c are independent of allomorph (150)
ρ : [10^7 (95,138,150), 1.5 x 10^7 (146), 10^9(151), 4.3 x 10^6(137)]
e_c = 0.66(138), 0.58(95,151), 0.57(152), 0.46(146), 0.43(150)
ρ : [[↓](40,137)] allomorph β

EPR : ["0.2 intensity in arbitrary units at 77°K," g = ~~2.002 ± 0.001~~(148,149); g = ~~$2.003, 2.005$~~ (153); g = 2.0026, 2.0058(154); $g_{\parallel}$ = 2.0023 ± 0.00015, $g_{\perp}$ = 2.0053 ± 0.00015 at 9 and 35 GHz for allomorph β (?) (155); 0.1%(151); $g_{\parallel}$ = ~~2.0068 ± 0.0005~~‡, $g_{\perp}$ = ~~2.0047 ± 0.0005~~‡ allomorph β (151); $g_{\parallel}$ = 2.0021 ± 0.0001‡, $g_{\perp}$ = 2.0052 ± 0.0001‡ allomorph β (156); $g_{\parallel}$= 2.0024 ± 0.0002‡, $g_{\perp}$= 2.0054 ±0.0002‡ allomorph α at 9 and 35 GHz(38)]

hence g-values are independent of allomorph

e_s^H = 0.13 allomorph β (150), 0.175 ± 0.005‡ allomorph β (151), 0.16‡ allomorph β (156), 0.13 ± 0.01‡ allomorph α (38)

e_s^L = ~~0.08~~‡ allomorph β (156), 0.015 ± 0.005‡ allomorph α (38)

EPR : [[↓](38)] allomorph α

Crystal structure: (156) allomorph β; (38,157) allomorph α

Molecular structure: none

[pPD:s-TNB]:

E^* = 2.37^f(79), 2.48^g(75,79), 2.48^j(109), 2.50^k(25)

E = 2.44^t(158), 2.14^t(109)

IR : [DA(99)]

VUV : [DA(109)]

ρ : [8×10^{16}(109)]

e_c = 1.02(109)

[TMPD:DDQ]:

VUV: [D^+A^-(84)]

[TMPD:TCNQ]:

E^* = 1.06^g(23)

Crystals prepared by disproportionation from $TMPD^+ClO_4^-$ and Li^+TCNQ^- as well as from TMPD and TCNQ (159)

IR : [D^+A^-(53,159)]

VUV : [D^+A^-(53,84, 115 reinterpreted)

ρ : [10^6 to 10^8(114,115)]

EPR : [17% at 23°C, $g = 2.0032 \pm 0.0001$(159)]

e_s^H = 0.075(159), 0.07(38), 0.067(53)

e_s^L = ~~0.10~~(53) ???

Crystal structure: (160)

Molecular structure: (160)

A 1:2 triclinic complex is known by EPR data (161) and its crystal and molecular structure (162)

[TMPD:TCNE]:

E^* = $1.28^?$(163), 1.27^g(23)

VUV : [D^+A^-(84)]

[TMPD:pBro]:

E^* = $1.45^{b,o}$(23), 1.41^k(23)

E = 1.06^t(158)

IR : [D^+A^-(99)]

VUV : [D^+A^-(84)]

ρ : [4.2×10^4 or 1.3×10^5(107)]

e_c = 0.28(107)

ρ : [[↓](140)]

EPR: ["2.0 intensity in arbitrary units at 77°K" (149); 7%(132); $g = 2.0043 \pm 0.001$(132,154)]

Crystal structure: (78,91)

Molecular structure: none

[TMPD:pChl]:

E^* = 1.34^b(60), $1.47^{b,o}$(23), 1.47^k(25), 1.43^k(23,164)
E = $1.02^{\dagger}$(17), $< 1.2^{\dagger\dagger}$(164), 0.99^t(158)
IR : [D^+A^-(99)]
VUV : [D^+A^-(17,84,158)]
ρ : [10^9(95), 1.3×10^4 or 2.0×10^4(107)]
e_c = 0.27(107)
EPR : ["0.2 intensity in arbitrary units at 77°K,"
$g = 2.0023$(148,149); 5%, $g = 2.0036 \pm 0.0004$(132);
$g_{xx} = 2.0062 \pm 0.0002$, $g_{yy} = 2.0021 \pm 0.0002$,
$g_{zz} = 2.0072 \pm 0.0002$(16)]
e_s^H = $0.134 \pm 0.002^{\ddagger}$(16) for allomorph α, $0.165 \pm 0.004^{\ddagger}$(16) for allomorph β
e_s^L = $0.010^{\ddagger}$(16) for allomorph α, $0.007^{\ddagger}$(16) for allomorph β
Crystal structure: (18,78,91) allomorphs α, β are indistinguishable
Molecular structure: (18,91)
There is a phase transition at 250°K, monoclinic to triclinic?(18)

[TMPD:s-TNB]:

E^* = 2.12^b(23), 1.98^d(242), 2.20^f(79), 2.02^g(165), 2.23^j(71), 2.07^k(110), 2.02^k(23,25), 2.01^k(245), 2.00^l(166)
ϵ : [2.93^g(165), 3.14^l(166)]
E : 1.91^t(158), 1.91^w(82)
IR : [DA(99)]
VUV : [DA(84)]

CHAPTER II

CLASSICAL EWALD CALCULATIONS OF THE COULOMB BINDING ENERGY OF SOME ORGANIC DONOR-ACCEPTOR CRYSTALS AND WURSTER'S BLUE PERCHLORATE

Per aspera

A. Introduction

The molar interionic Coulomb energies, or Madelung energies, E_C, of selected organic crystals have been calculated classically to a high degree of precision by the Ewald method in order to answer two unrelated questions:

(i) whether the ion-radical salt, Wurster's Blue Perchlorate* with its amazing linear stacks of positive N,N,N',N'-Tetramethyl-para-phenylenediamine radical ions (TMPD$^{\underset{\cdot}{+}}$), packed sandwich-style and separated by perchlorate anions acting as "glue" between the stacks, can be stable as a crystalline solid under the influence of Coulomb-law forces alone, or whether inter-cationic electron-exchange interactions, or, less likely, van der Waals interactions must be invoked to account for the stability of these bluish-

---

*Named after Casimir Wurster (1854-1913), German chemist; cf. obituary in Chem. Ber., 47, 1 (1914).

black crystals. This question was very relevant to McConnell and Soos' (167,168) interpretation of spin-exchange line-broadening effects in the paramagnetic resonance spectra of this crystal.

(ii) whether the organic donor-acceptor complexes previously described as "exhibiting very strong polarization bonding" can be "holoionic", i.e. have an ionic ground state $|D^+A^-\ldots D^+A^-\ldots D^+A^-\rangle$ as proposed by McConnell et al. (13), and conversely, whether the "weak complexes" are "nonionic," i.e. on the whole, molecular crystals $|DA\ldots DA\ldots DA\rangle$. The quantity E_C^T, minus all intraionic terms, is expected to be the largest component of $2N_o\epsilon_1$, and the energy $N_o(I_D - A_A)$ required to ionize N_o DA ion pairs, is the preponderant term of $2N_o\epsilon_o$ (cf. Chapter I), and the theory of McConnell et al. predicts a holoionic crystal if $\epsilon_o + \epsilon_1 < 0$, and a nonionic crystal if $\epsilon_o + \epsilon_1 > 0$.

The Madelung energies of several inorganic crystals were also calculated in order to test and verify the correctness of our numerical approach.

The classical molar Coulomb energy, E_C^T, of an ionic crystal can be defined as the binding energy due to the Coulomb interactions between the ions, or as the work done reversibly by an external agent on the ions in order to bring them in from infinity to their respective equilibrium positions in the crystal lattice. This energy is by convention negative for those ionic crystals which are stable under the influence of interionic Coulomb-law interactions.

The organic crystals studied here consist of large molecular free-radical ions. The charge distribution in the organic crystal is approximated as being localized at the atomic positions $\underset{\sim}{r}_i^{o}$ determined from crystal-structure data;[*] the charges $\zeta_i |\epsilon|$ on these "charged atoms" are chosen from spin-density data, simple Hueckel theory, or results of other theoretical calculations on these ions, whenever available in the literature, or even from naive chemical guesswork; $-|\epsilon|$ is the charge of the electron.

The quantity of interest here is the INTERionic Coulomb E_C; the TOTAL Coulomb energy E_C^T, which we call the Madelung energy:

$$E_C^T = \frac{Q}{2} \sum_{\substack{i=1 \\ i \neq j}}^{M\frac{N_a}{Z}} \sum_{j=1}^{M\frac{N_a}{Z}} \frac{\zeta_i \zeta_j |\epsilon|^2}{|\underset{\sim}{r}_i^{o} - \underset{\sim}{r}_j^{o}|} \tag{201}$$

includes also the undesired "intraionic" repulsions between the fractional charges $\zeta_i |\epsilon|$ on the SAME ion; it is convenient, however, to first calculate E_C^T, and then subtract from E_C^T the

---

[*] This approximation might seem crude, but is justified by the results obtained (see page 144).

repulsion term Δ:

(202) $$E_c \equiv E_c^T - \Delta \equiv E_c^T - (\Delta_1 + \Delta_2),$$

where for the v anions:

(203a) $$\Delta_1 \equiv \frac{QN_o}{2} \sum_{\ell=1}^{v} \sum_{m_\ell=1}^{v_\ell} \sum_{\substack{n_\ell=1 \\ m_\ell \neq n_\ell}}^{v_\ell} \frac{\zeta_{m_\ell} \zeta_{n_\ell} |\epsilon|^2}{|\underset{\sim}{r}^o_{m_\ell} - \underset{\sim}{r}^o_{n_\ell}|},$$

and for the w cations:

(203b) $$\Delta_2 \equiv \frac{QN_o}{2} \sum_{\ell'=1}^{w} \sum_{m_{\ell'}=1}^{w_{\ell'}} \sum_{\substack{n_{\ell'}=1 \\ m_{\ell'} \neq n_{\ell'}}}^{w_{\ell'}} \frac{\zeta_{m_{\ell'}} \zeta_{n_{\ell'}} |\epsilon|^2}{|\underset{\sim}{r}^o_{m_{\ell'}} - \underset{\sim}{r}^o_{n_{\ell'}}|}.$$

N_o is Avogadro's number; there are Z molecules and M charged atoms per crystallographic unit cell; there are v anions and w cations per molecule; Q is the appropriate energy unit conversion factor (see Table IX for units chosen in the present calculations); the vectors r_i^o are arranged so that:

$$|\underset{\sim}{r}^o_1| \leq |\underset{\sim}{r}^o_2| \leq \ldots \leq |\underset{\sim}{r}^o_i| \leq \ldots |\underset{\sim}{r}^o_{M\frac{N_o}{Z}}|.$$

In order to relate our results with the known Madelung (176) constants, and to obtain estimates for ϵ_1' (see Chapter I) we found it useful to compute H (eta), the molar Coulomb energy of attraction between the v nearest-neighbor anions and the w nearest-neighbor cations:

$$(204) \qquad H \equiv Q N_0 \sum_{\ell=1}^{v} \sum_{m_\ell=1}^{v_\ell} \sum_{\ell'=1}^{w} \sum_{n_{\ell'}=1}^{w_{\ell'}} \frac{\zeta_{m_\ell} \zeta_{n_{\ell'}} |e|^2}{|\underset{\sim}{r}^{\circ}_{m_\ell} - \underset{\sim}{r}^{\circ}_{n_{\ell'}}|},$$

and also, to define a "generalized Madelung constant" ω by:

$$(205) \qquad \omega \equiv \frac{E_c}{H};$$

ω does not depend on the concept of sublattices, (inopportune for our organic crystals) but reduces to the ordinary Madelung constant α for the inorganic crystals (where $\Delta_1 = \Delta_2 = 0$ and sublattices are used routinely).

The Madelung energy can be evaluated exactly if the ionic point charges and the interionic distances in the crystal are known, but a brute-force summation of the interionic Coulomb attractions and repulsions is impossibly lengthy because of the long range of the Coulomb interaction and the extremely slow convergence of the summation over reciprocal distances.

There is, however, quite a choice of time-proven transform methods. Since the organic ions considered here are not monoatomic, an application of the Madelung (176) or the Evjen (177) techniques would be rather unwieldy; the Fourier transform method introduced by F. Bertaut (169) is acknowledged by Templeton et al. (178) to be of inferior precision as compared to the two-series method discovered by P. P. Ewald (179). The Ewald series can be made to converge very rapidly and give extremely precise results, provided that good values of the error function, erf(x), are available.

Therefore, a general computer program, EWALD, was written in Burroughs Extended Algol for use on the Burroughs B-5500 digital computer,[*] for the purpose of calculating the crystal Coulomb energy of a crystal of arbitrary symmetry, atomic arrangement and charge distribution. A preliminary program, CELLMAP, digests the crystallographic information and the assumed charge distribution and prepares the data input to EWALD.

For the sake of didactic completeness, an account of the Ewald method follows; unabashed use is made of the collective wisdom of Bertaut (169), Leibfried (170), Kittel (171), Born and Huang (172) and Ziman (173); experts may take due note of Eqs. (232, 233) and skip to page 93.

B. Ewald's Method: Three Interpretations

We define the self-potential of the i-th charge atom, as the electrostatic potential, evaluated at $\underset{\sim}{r}_i^{o}$, due to all the <u>other</u> charges in the crystal $\zeta_j |\epsilon|$, to wit:

$$\overline{\Psi}_i\left(\underset{\sim}{r}_i^{o}\right) \equiv \sum_{\substack{j=1 \\ j \neq i}}^{M \frac{N_0}{Z}} \frac{\zeta_j |\epsilon|}{\left|\underset{\sim}{r}_i^{o} - \underset{\sim}{r}_j^{o}\right|} \; ; \qquad (206)$$

---

[*] At Stanford University (1965-1967), at the Stanford Research Institute (1968).

then Eq. (201) becomes:

$$(207)\qquad E_C^T = \frac{Q}{2}\sum_{i=1}^{M\frac{N_0}{Z}} \zeta_i\,|\epsilon|\,\overline{\Psi}_i(\underset{\sim}{r}_i^{\circ}),$$

and, if end effects are neglected, we can utilize the periodicity of the lattice (the period is the unit cell, of volume V) and write:

$$(208)\qquad E_C^T = \frac{Q N_0 |\epsilon|}{2Z}\sum_{n=1}^{M} \zeta_n\,\overline{\Psi}_n(\underset{\sim}{r}_n^{\circ}).$$

Furthermore, the following expression will prove useful:

$$(209)\qquad \overline{\Psi}_n(\underset{\sim}{r}_n^{\circ}) = \lim_{\underset{\sim}{r}\to\underset{\sim}{r}_n^{\circ}}\left[\psi(\underset{\sim}{r}) - \frac{\zeta_n|\epsilon|}{|\underset{\sim}{r}-\underset{\sim}{r}_n^{\circ}|}\right],$$

where the total potential $\psi(r)$ is defined, for a charge density function $\rho(\underset{\sim}{r}')$, as:

$$(210)\qquad \psi(\underset{\sim}{r}) \equiv \iiint_{\substack{\text{WHOLE}\\ \text{CRYSTAL}}} d\sigma(\underset{\sim}{r}')\,\frac{\rho(\underset{\sim}{r}')}{|\underset{\sim}{r}-\underset{\sim}{r}'|};$$

obviously, $\psi(\underset{\sim}{r})$ includes the singularity at $\underset{\sim}{r} = \underset{\sim}{r}'$. In our crystals of point-charges the charge density function can be written, using the three-dimensional Dirac delta function:

(211) $$\rho(\underset{\sim}{r}) = \sum_{j=1}^{M\frac{N_0}{Z}} \zeta_j \,|\epsilon|\, \delta(\underset{\sim}{r} - \underset{\sim}{r}_j^{\circ}).$$

Since the charge density function is periodic (crystal edge effects being again neglected), therefore:

(212) $$\underset{\substack{\frac{N_0 V}{Z} \\ \text{WHOLE} \\ \text{CRYSTAL}}}{\iiint} dv(\underset{\sim}{r})\,\rho(\underset{\sim}{r}) = \frac{N_0}{Z} \underset{\substack{V \\ \text{ONE} \\ \text{UNIT} \\ \text{CELL}}}{\iiint} dv(\underset{\sim}{r})\,\rho(\underset{\sim}{r}),$$

and furthermore, $\rho(\underset{\sim}{r})$ may be expanded in a Fourier series:

(213) $$\rho(\underset{\sim}{r}) = \frac{1}{V} \sum_{h=-\infty}^{\infty} \sum_{k=-\infty}^{\infty} {\sum_{\ell=-\infty}^{\infty}}' P(\underset{\sim}{\not{d}}_{hk\ell}) \exp(i\, \underset{\sim}{\not{d}}_{hk\ell} \cdot \underset{\sim}{r}),$$

where $\underset{\sim}{\not{d}}_{hkl}$ is the reciprocal lattice vector multiplied by 2π (*):

(214) $$\underset{\sim}{\not{d}}_{hk\ell} \equiv \frac{2\pi}{V} \left\{ h[\underset{\sim}{b} \wedge \underset{\sim}{c}] + k[\underset{\sim}{c} \wedge \underset{\sim}{a}] + \ell[\underset{\sim}{a} \wedge \underset{\sim}{b}] \right\},$$

and $\underset{\sim}{a}$, $\underset{\sim}{b}$, $\underset{\sim}{c}$ are the edges of the direct lattice unit cell, and (hkl) are the Miller indices. The Fourier coefficients of Eq. (213) are:

---

[*] Quantities containing a vertical crossbar or slash have an explicit factor of 2π. (This is in analogy to $\hbar \equiv h/2\pi$). Read: "d slash."

$$\text{(215a)} \qquad \mathrm{P}(\underset{\sim}{\text{đ}}_{hkl}) \equiv \iiint\limits_{V} dv(\underset{\sim}{r})\,\rho(\underset{\sim}{r})\,\exp(-i\underset{\sim}{\text{đ}}_{hkl}\cdot\underset{\sim}{r}) =$$

$$\text{(215b)} \qquad = \sum_{m=1}^{M} \zeta_m\,|\epsilon|\,\exp(-i\underset{\sim}{\text{đ}}_{hkl}\cdot\underset{\sim}{r}_m^{\circ}),$$

and are the complex conjugates of what crystallographers call "structure factors" * . Since the unit cell is electrically neutral, therefore:

$$\text{(216)} \qquad \mathrm{P}(\underset{\sim}{\text{đ}}_{000}) = \mathrm{P}(0) = \sum_{m=1}^{M} \zeta_m\,|\epsilon| = 0;$$

We shall avoid including the term (000) in the Fourier expansion of $\rho(\underset{\sim}{r})$: this is denoted by the prime in Eq. (213). Finally,

$$\text{(217)} \qquad \rho(\underset{\sim}{r}) = \frac{1}{V}\sum_{h=-\infty}^{\infty}\sum_{k=-\infty}^{\infty}\sum_{l=-\infty}^{\infty}{}' \sum_{m=1}^{M} \zeta_m\,|\epsilon|\,\exp\{i\underset{\sim}{\text{đ}}_{hkl}\cdot(\underset{\sim}{r}-\underset{\sim}{r}_m^{\circ})\}.$$

Substituting Eq. (211) into Eq. (210) we get:

$$\text{(218)} \qquad \Psi(\underset{\sim}{r}) = \sum_{j=1}^{M\frac{N_0}{Z}} \frac{\zeta_j\,|\epsilon|}{|\underset{\sim}{r}-\underset{\sim}{r}_j^{\circ}|}.$$

---

[*] Note that Bertaut (169) defines his Fourier series with opposite signs.

The Ewald technique consists of two shrewd manipulations of Eq. (218). First, the identity:

$$(219) \qquad \frac{1}{|\underset{\sim}{r}-\underset{\sim}{r}_j^\circ|} = \frac{2}{\sqrt{\pi}}\int_0^\infty dt\, \exp\left(-|\underset{\sim}{r}-\underset{\sim}{r}_j^\circ|^2 t^2\right),$$

which holds also for $\underset{\sim}{r} = \underset{\sim}{r}_j^\circ$, is rewritten as:

$$(220a) \qquad \frac{1}{|\underset{\sim}{r}-\underset{\sim}{r}_j^\circ|} = \frac{2}{\sqrt{\pi}}\int_0^{\frac{\sqrt{\eta}}{V^{1/3}}} dt\, \exp\left(-|\underset{\sim}{r}-\underset{\sim}{r}_j^\circ|^2 t^2\right) + $$

$$+ \frac{2}{\sqrt{\pi}}\int_{\frac{\sqrt{\eta}}{V^{1/3}}}^\infty dt\, \exp\left(-|\underset{\sim}{r}-\underset{\sim}{r}_j^\circ|^2 t^2\right),$$

where V is, as before, the direct unit cell volume and η is called the Ewald convergence parameter. By utilizing the definition of Gauss' error function:

$$(220b) \qquad \mathrm{erf}\,(bx) \equiv \frac{2b}{\sqrt{\pi}}\int_0^x dt\, \exp\left(-b^2 t^2\right),$$

and remembering the improper integral:

$$(220c) \qquad \int_0^\infty dt\, \exp\left(-b^2 t^2\right) = \frac{\sqrt{\pi}}{2b},$$

we can rewrite Eq. (220a) and, substituting the result in Eq. (218) and interchanging a summation and an integration, we get:

$$(221)\quad \psi(\underset{\sim}{r}) = \int_0^{\frac{\sqrt{\eta}}{V^{1/3}}} dt \sum_{j=1}^{M\frac{N_0}{Z}} \frac{2\zeta_j|\epsilon|}{\sqrt{\pi}} \exp\left(-|\underset{\sim}{r}-\underset{\sim}{r}_j^{\circ}|^2 t^2\right) + \sum_{j=1}^{M\frac{N_0}{Z}} \frac{\zeta_j|\epsilon|}{|\underset{\sim}{r}-\underset{\sim}{r}_j^{\circ}|}\left\{1-\mathrm{erf}\left(\frac{\sqrt{\eta}}{V^{1/3}}|\underset{\sim}{r}-\underset{\sim}{r}_j^{\circ}|\right)\right\}.$$

The second trick of Ewald's consists in using the Jacobi theta-function transformation to rewrite the integrand in Eq. (221). We shall rederive this transformation, following Ziman (173). The function:

$$(222)\quad f(\underset{\sim}{r},t) \equiv \frac{2|\epsilon|}{\sqrt{\pi}} \sum_{j=1}^{M\frac{N_0}{Z}} \zeta_j \exp\left(-|\underset{\sim}{r}-\underset{\sim}{r}_j^{\circ}|^2 t^2\right)$$

is periodic in $\underset{\sim}{r}$, and the unit cell of volume V is the "repeat volume." This statement becomes obvious if one considers that, whereas the summation in Eq. (221) is ordered so that $|\underset{\sim}{r}_j^{o}| \leqslant |\underset{\sim}{r}^{o}_{j+1}|$ $(j = 1, \ldots, (\frac{M}{Z}N_o - 1))$, the only effect of increasing $\underset{\sim}{r}$ to, say, $\underset{\sim}{r} + n\underset{\sim}{a}$ (where n is an integer) is to merely rearrange the order of summation so that $|\underset{\sim}{r}_{\ell} - n\underset{\sim}{a}| \leqslant |\underset{\sim}{r}_{\ell+1} - n\underset{\sim}{a}|$ $(\ell = 1, \ldots, (\frac{M}{Z}N_o - 1))$. Hence we may expand $f(\underset{\sim}{r},t)$ in a Fourier series; we omit the (000) term, as is explained below:

$$(223)\qquad f(\underset{\sim}{\mathbf{r}},t)=\sum_{h=-\infty}^{\infty}\sum_{k=-\infty}^{\infty}{\sum_{l=-\infty}^{\infty}}' F(\underset{\sim}{\mathfrak{h}}_{hkl})\exp(i\,\underset{\sim}{\mathfrak{h}}_{hkl}\cdot\underset{\sim}{\mathbf{r}});$$

the Fourier coefficients are given by:

$$(224)\qquad F(\underset{\sim}{\mathfrak{h}}_{hkl})\equiv\frac{1}{V}\iiint_{V}dv(\underset{\sim}{\mathbf{r}})\,\frac{2|\epsilon|}{\sqrt{\pi}}\sum_{j=1}^{M\frac{N_0}{Z}}\zeta_j\,\times$$
$$\times\,\exp\left[-|\underset{\sim}{\mathbf{r}}-\underset{\sim}{\mathbf{r}}_j^{o}|^2t^2-i\,\underset{\sim}{\mathfrak{h}}_{hkl}\cdot\underset{\sim}{\mathbf{r}}\right].$$

We may interchange summation and integration, and multiply and divide the integrand by $\exp(+i\underset{\sim}{\mathfrak{h}}_{hkl}\cdot\underset{\sim}{\mathbf{r}}_j^{o})$; furthermore, by the considerations which justify Eq. (212) we may integrate over the whole crystal:

$$(225)\qquad F(\underset{\sim}{\mathfrak{h}}_{hkl})=\frac{2|\epsilon|}{V\sqrt{\pi}}\frac{Z}{N_0}\sum_{j=1}^{M\frac{N_0}{Z}}\zeta_j\exp(-i\,\underset{\sim}{\mathfrak{h}}_{hkl}\cdot\underset{\sim}{\mathbf{r}}_j^{o})\times$$

$$\times\iiint_{\frac{N_0V}{Z}}dv(\underset{\sim}{\mathbf{r}}-\underset{\sim}{\mathbf{r}}_j^{o})\exp\left[-|\underset{\sim}{\mathbf{r}}-\underset{\sim}{\mathbf{r}}_j^{o}|^2t^2-i\,\underset{\sim}{\mathfrak{h}}_{hkl}\cdot(\underset{\sim}{\mathbf{r}}-\underset{\sim}{\mathbf{r}}_j^{o})\right].$$

The integral in the above formula, which happens to be also the Fourier transform of the square-integrable function $\exp[-|\underset{\sim}{\mathbf{r}}-\underset{\sim}{\mathbf{r}}_j^{o}|^2t^2]$ is evaluated in a spherical polar coordinate system, with $\underset{\sim}{\mathfrak{h}}_{hkl}$ as the polar axis:

$$\iiint\limits_{\frac{N_0 V}{Z}} dv(\underset{\sim}{r}-\underset{\sim}{r}_j^0)\exp[-|\underset{\sim}{r}-\underset{\sim}{r}_j^0|^2t^2 - i\,\underset{\sim}{d}_{hkl}\cdot(\underset{\sim}{r}-\underset{\sim}{r}_j)] =$$

(226a)

$$= 2\pi\int_0^\infty dq\, q^2\int_0^\pi d\vartheta \sin\vartheta \exp[-t^2q^2 - i|\underset{\sim}{d}_{hkl}|\,q\cos\vartheta] =$$

(226b)

$$= \left(\frac{\pi}{t^2}\right)^{3/2} \exp\left(-\frac{d_{hkl}^2}{4t^2}\right);$$

since the remaining sum over j in Eq. (225) has the periodicity of $\rho(\underset{\sim}{r})$, therefore we get:

$$F(\underset{\sim}{d}_{hkl}) = \frac{1}{V}\,\frac{2\pi|\epsilon|}{t^3}\exp\left(-\frac{d_{hkl}^2}{4t^2}\right)\times$$

(227)

$$\times\sum_{m=1}^{M}\zeta_m \exp(-i\,\underset{\sim}{d}_{hkl}\cdot\underset{\sim}{r}_m^0).$$

Furthermore, $F(\underset{\sim}{d}_{000}) = 0$ because $\sum_{m=1}^{M}\zeta_m = 0$; thus we finally write our theta-function transformation:

$$\frac{2|\epsilon|}{\sqrt{\pi}}\sum_{j=1}^{M\frac{N_0}{Z}}\zeta_j\exp(-|\underset{\sim}{r}-\underset{\sim}{r}_j^0|^2t^2) =$$

(228)

$$= \frac{1}{V}\,\frac{2\pi|\epsilon|}{t^3}\sum_{h=-\infty}^{\infty}\sum_{k=-\infty}^{\infty}{\sum_{l=-\infty}^{\infty}}'\exp\left(-\frac{d_{hkl}^2}{4t^2}\right)\sum_{m=1}^{M}\zeta_m\exp[i\,\underset{\sim}{d}_{hkl}\cdot(\underset{\sim}{r}-\underset{\sim}{r}_m^0)].$$

Substitution of the right-hand side of Eq. (228) into Eq. (221) and integration over t yield the total potential:

$$\psi(\underset{\sim}{r}) = \frac{4\pi|\epsilon|}{V}\sum_{h=-\infty}^{\infty}\sum_{k=-\infty}^{\infty}{\sum_{l=-\infty}^{\infty}}' \frac{\exp\left(-\frac{d_{hkl}^{2}V^{2/3}}{4\eta}\right)}{d_{hkl}^{2}}\sum_{m=1}^{M}\zeta_m \exp\left[i\underset{\sim}{d}_{hkl}\cdot(\underset{\sim}{r}-\underset{\sim}{r}_m^{\circ})\right] +$$

(229)

$$+\ |\epsilon|\sum_{j=1}^{M\frac{N_0}{2}}\frac{\zeta_j}{|\underset{\sim}{r}-\underset{\sim}{r}_j^{\circ}|}\left\{1-\operatorname{erf}\left(\frac{\sqrt{\eta}}{V^{1/3}}\,|\underset{\sim}{r}-\underset{\sim}{r}_j^{\circ}|\right)\right\},$$

In the application of Eq. (209) to Eq. (229) the following limit is established:

$$\lim_{\underset{\sim}{r}\to\underset{\sim}{r}_n^{\circ}}\left[-\frac{\zeta_n|\epsilon|}{|\underset{\sim}{r}-\underset{\sim}{r}_n^{\circ}|}+\frac{\zeta_n|\epsilon|}{|\underset{\sim}{r}-\underset{\sim}{r}_n^{\circ}|}\left\{1-\operatorname{erf}\left(\frac{\sqrt{\eta}}{V^{1/3}}|\underset{\sim}{r}-\underset{\sim}{r}_n^{\circ}|\right)\right\}\right]=$$

(230a)

$$= -\zeta_n|\epsilon|\lim_{q\to 0}\left[\frac{\frac{2}{\sqrt{\pi}}\int_0^{\frac{\sqrt{\eta}\,q}{V^{1/3}}}dt\,\exp(-t^2)}{q}\right]=$$

(230b) $$= -\frac{2}{\sqrt{\pi}}\zeta_n|\epsilon|\lim_{q\to 0}\left[\frac{\left[\frac{d}{ds}\int_0^{s}dw\,\exp\left(-\frac{\eta w^2}{V^{2/3}}\right)\right]_{s=q}\frac{\sqrt{\eta}}{V^{1/3}}}{\left[\frac{d}{ds}\,s\right]_{s=q}}\right]=$$

(230c) $$= -\frac{2}{\sqrt{\pi}}\zeta_n|\epsilon|\frac{\sqrt{\eta}}{V^{1/3}}$$

So we can finally write the self-potential:

(231a) $$\Psi_n(\underset{\sim}{r}_n^{\circ}) \equiv A_n + B_n + \Gamma_n$$

where:

(231b) $$A_n = -\frac{2\,|\epsilon|\sqrt{\eta}}{\sqrt{\pi}\;V^{1/3}}\,\zeta_n\,,$$

(231c) $$B_n = \frac{4\pi|\epsilon|}{V}\sum_{h=-\infty}^{\infty}\sum_{k=-\infty}^{\infty}{\sum_{\ell=-\infty}^{\infty}}{}' \frac{\exp\left(-\frac{\mathfrak{d}_{hk\ell}^{2}V^{2/3}}{4\eta}\right)}{\mathfrak{d}_{hk\ell}^{2}}\sum_{m=1}^{M}\zeta_m \exp\left[i\,\underset{\sim}{\mathfrak{d}}_{hk\ell}\cdot\left(\underset{\sim}{r}_n^{\circ}-\underset{\sim}{r}_m^{\circ}\right)\right],$$

(231d) $$\Gamma_n = |\epsilon|\sum_{\substack{j=1\\ j\neq n}}^{M\frac{N_0}{Z}} \frac{\zeta_j}{|\underset{\sim}{r}_n^{\circ}-\underset{\sim}{r}_j^{\circ}|}\left\{1-\mathrm{erf}\left(\frac{\sqrt{\eta}}{V^{1/3}}\,|\underset{\sim}{r}_n^{\circ}-\underset{\sim}{r}_j^{\circ}|\right)\right\}.$$

And the Ewald expansion for the total crystal Coulomb energy is then:

(232) $$E_c^{T} \equiv A + B + \Gamma$$

where:

(233a) $$A = \left(-\frac{Q\,N_0\,|\epsilon|^2}{\sqrt{\pi}}\right)\frac{\sqrt{\eta}}{Z\,V^{1/3}}\sum_{n=1}^{M}\zeta_n^2\,,$$

(233b) $$B = \left(2\pi Q\,N_0|\epsilon|^2\right)\frac{1}{Z\,V}\sum_{h=-\infty}^{\infty}\sum_{k=-\infty}^{\infty}{\sum_{\ell=-\infty}^{\infty}}{}' \frac{\exp\left(-\frac{\mathfrak{d}_{hk\ell}^{2}V^{2/3}}{4\eta}\right)}{\mathfrak{d}_{hk\ell}^{2}}\;\times$$
$$\times\sum_{n=1}^{M}\sum_{m=1}^{M}\zeta_m\zeta_n\exp\left[i\,\underset{\sim}{\mathfrak{d}}_{hk\ell}\cdot\left(\underset{\sim}{r}_n^{\circ}-\underset{\sim}{r}_m^{\circ}\right)\right],$$

(233c) $$\Gamma = \left(\frac{Q\,N_0|\epsilon|^2}{2}\right)\frac{1}{Z}\sum_{\substack{j=1\\ j\neq n}}^{M\frac{N_0}{Z}}\sum_{n=1}^{M}\frac{\zeta_j\zeta_n}{|\underset{\sim}{r}_n^{\circ}-\underset{\sim}{r}_j^{\circ}|}\left\{1-\mathrm{erf}\left(\frac{\sqrt{\eta}}{V^{1/3}}\,|\underset{\sim}{r}_n^{\circ}-\underset{\sim}{r}_j^{\circ}|\right)\right\}.$$

Last but not least, the value obtained for E_C^T must, of course, be independent of η ; a repetition of the calculation with a different value of η serves as an excellent check on the precision and convergence qualities of the calculation.

Bertaut (169) and Shockley (171) have presented interesting physical interpretations and generalizations of Ewald's method.

Let us define a "self-excluded charge density function," $\bar{\rho}(n,\underset{\sim}{r})$ which takes into account all charges in the crystal except the one at $\underset{\sim}{r}_n^o$:

$$(234) \qquad \bar{\rho}(n, \underset{\sim}{r}) \equiv \rho(\underset{\sim}{r}) - \zeta_n |e| \delta(\underset{\sim}{r} - \underset{\sim}{r}_n^o) = \sum_{\substack{j=1 \\ j\neq n}}^{M\frac{N_0}{Z}} \zeta_j |e| \delta(\underset{\sim}{r} - \underset{\sim}{r}_j^o);$$

by using $\bar{\rho}(n,\underset{\sim}{r})$, the singularity at $\underset{\sim}{r}_n^o$ is avoided easily in the calculation of the self-potential:

$$(235) \qquad \overline{\Psi}_n(\underset{\sim}{r}_n^o) = \iiint_{\frac{N_0 V}{Z}} dv(\underset{\sim}{r}') \frac{\bar{\rho}(n,\underset{\sim}{r}')}{|\underset{\sim}{r}' - \underset{\sim}{r}_n^o|}.$$

Shockley asserts that the three contributions A_n, B_n, Γ_n to Ewald's self-potential could be obtained by superposing on the real point charges at each lattice point a fictitious spherically symmetric Gaussian charge distribution, and then subtracting it out again, and calculating the self-potential due to each term;

in fact, he defines:

$$\bar{\rho}\left(n, \underset{\sim}{r}\right) \equiv \bar{\rho}_1\left(n, \left|\underset{\sim}{r} - \underset{\sim}{r}^{\circ}_{n}\right|\right) + \bar{\rho}_2\left(\left|\underset{\sim}{r}\right|\right) + \bar{\rho}_3\left(n, \left|\underset{\sim}{r}\right|\right), \tag{236a}$$

where:

$$\bar{\rho}_1\left(n, \left|\underset{\sim}{r} - \underset{\sim}{r}^{\circ}_{n}\right|\right) = \zeta_n |\epsilon| \left\{ - \frac{1}{V}\left(\frac{\eta}{\pi}\right)^{3/2} \exp\left(-\frac{\eta}{V^{2/3}}\left|\underset{\sim}{r} - \underset{\sim}{r}^{\circ}_{n}\right|^2\right)\right\}, \tag{236b}$$

$$\bar{\rho}_2\left(\left|\underset{\sim}{r}\right|\right) = \sum_{j=1}^{M\frac{N_0}{Z}} \zeta_j |\epsilon| \left\{ + \frac{1}{V}\left(\frac{\eta}{\pi}\right)^{3/2} \exp\left(-\frac{\eta}{V^{2/3}}\left|\underset{\sim}{r} - \underset{\sim}{r}^{\circ}_{j}\right|^2\right)\right\}, \tag{236c}$$

$$\bar{\rho}_3\left(n, \left|\underset{\sim}{r}\right|\right) = \sum_{\substack{j=1 \\ j \neq n}}^{M\frac{N_0}{Z}} \zeta_j |\epsilon| \left\{ \delta\left(\underset{\sim}{r} - \underset{\sim}{r}^{\circ}_{j}\right) - \frac{1}{V}\left(\frac{\eta}{\pi}\right)^{3/2} \exp\left(-\frac{\eta}{V^{2/3}}\left|\underset{\sim}{r} - \underset{\sim}{r}^{\circ}_{j}\right|^2\right)\right\}; \tag{236d}$$

and further:

$$\overline{\Psi}_n\left(\underset{\sim}{r}^{\circ}_{n}\right) \equiv \sum_{p=1}^{3} \overline{\Psi}_{np}\left(\underset{\sim}{r}^{\circ}_{n}\right), \tag{237a}$$

where:

$$\overline{\Psi}_{n1}\left(\underset{\sim}{r}^{\circ}_{n}\right) \equiv \iiint_{\frac{N_0 V}{Z}} dv\left(\underset{\sim}{r}' - \underset{\sim}{r}^{\circ}_{n}\right) \frac{\bar{\rho}_1\left(n, \left|\underset{\sim}{r}' - \underset{\sim}{r}^{\circ}_{n}\right|\right)}{\left|\underset{\sim}{r}' - \underset{\sim}{r}^{\circ}_{n}\right|}, \tag{237b}$$

$$\overline{\Psi}_{n2}\left(\underset{\sim}{r}^{\circ}_{n}\right) \equiv \iiint_{\frac{N_0 V}{Z}} dv\left(\underset{\sim}{r}'\right) \frac{\bar{\rho}_2\left(\left|\underset{\sim}{r}'\right|\right)}{\left|\underset{\sim}{r}' - \underset{\sim}{r}^{\circ}_{n}\right|}, \tag{237c}$$

(237d) $$\overline{\Psi_{n3}}(\underset{\sim}{r}_n^o) \equiv \iiint\limits_{\frac{N_0V}{Z}} dv(\underset{\sim}{r}')\,\frac{\overline{\rho_3}(n,\underset{\sim}{r}')}{|\underset{\sim}{r}'-\underset{\sim}{r}_n^o|}.$$

By substituting Eq. (236b) into Eq. (237b) he gets at once:

(238) $$\overline{\Psi_{n1}}(\underset{\sim}{r}_n^o) = A_n.$$

Next, by noticing that $\overline{\Psi_{n2}}(\underset{\sim}{r}_n^o)$ as well as $\overline{\rho}_2(|\underset{\sim}{r}_n^o|)$ must be expansible in Fourier series, and by invoking Poisson's equation to obtain the relationship between the respective Fourier transforms, Shockley gets:

(239) $$\overline{\Psi_{n2}}(\underset{\sim}{r}_n^o) = \frac{1}{V}\sum_{h=-\infty}^{\infty}\sum_{k=-\infty}^{\infty}\sum_{\ell=-\infty}^{\infty}{}' \frac{4\pi}{\underset{\sim}{d}_{hk\ell}^2}\exp(i\underset{\sim}{d}_{hk\ell}\cdot\underset{\sim}{r}_n^o)\iiint\limits_{\frac{N_0V}{Z}}\sum_{j=1}^{M\frac{N_0}{Z}} dv(\underset{\sim}{r}-\underset{\sim}{r}_j^o)\times$$
$$\times\,\zeta_j|\epsilon|\left\{\frac{1}{V}\left(\frac{\eta}{\pi}\right)^{3/2}\exp\left(-\frac{\eta}{V^{2/3}}|\underset{\sim}{r}-\underset{\sim}{r}_j^o|^2\right)\right\}\exp(-i\underset{\sim}{d}_{hk\ell}\cdot\underset{\sim}{r}),$$

which, after manipulations resembling those used to obtain Eq. (227), reduces to:

(240) $$\overline{\Psi_{n2}}(\underset{\sim}{r}_n^o) = B_n.$$

Finally, in order to evaluate $\overline{\Psi_{n3}}(\underset{\sim}{r}_n^o)$, Shockley uses the following Lemma, valid for spherically symmetric charge density functions $\rho'(\underset{\sim}{r}) = \rho'(|\underset{\sim}{r}|)$:

$$(241a)\qquad \Psi(\underset{\sim}{r}_0) \equiv \underset{\text{ALL SPACE}}{\iiint} dv(\underset{\sim}{r})\, \frac{\rho'(|\underset{\sim}{r}|)}{|\underset{\sim}{r}-\underset{\sim}{r}_0|} =$$

$$(241b)\qquad = \frac{1}{|\underset{\sim}{r}_0|}\int_0^{|\underset{\sim}{r}_0|} dr\, 4\pi r^2 \rho'(|\underset{\sim}{r}|) + \int_{|\underset{\sim}{r}_0|}^{\infty} dr\, 4\pi r^2 \frac{\rho'(|\underset{\sim}{r}|)}{r}\,.$$

Then, after interchanging the summation over j in Eq. (236d) and the integration in Eq. (237d), he applies the above decomposition to the integral about each lattice point, uses the definition of the error function and obtains at last:

$$(242)\qquad \overline{\Psi}_{n3}(\underset{\sim}{r}_n^{\,o}) = \Gamma_n\,.$$

Therefore, the charge distribution $\bar{\rho}(n,\underset{\sim}{r})$ does indeed give the Ewald self-potential $\overline{\Psi}_n(\underset{\sim}{r}_n^{\,o})$, as claimed.

On the other hand, Bertaut (169) presents a generalized treatment of the problem, based on the following theorem of electrostatics:

"If one replaces a system of point charges $\zeta_j|\epsilon|$ localized at crystal lattice sites $\underset{\sim}{r}_j^{\,o}$:

$$(211)\qquad \rho(\underset{\sim}{r}) = \sum_{j=1}^{M\frac{N_o}{Z}} \zeta_j |\epsilon|\, \delta(\underset{\sim}{r}-\underset{\sim}{r}_j^{\,o})$$

by a system of spatially diffuse charges:

$$(243)\qquad \rho'(\underset{\sim}{r}) = \sum_{j=1}^{M\frac{N_o}{Z}} \zeta_j |\epsilon|\, \vartheta(\underset{\sim}{r}-\underset{\sim}{r}_j^{\,o})$$

where:

$$\iiint\limits_{\frac{N_o V}{Z}} dv(\underset{\sim}{r}-\underset{\sim}{r}_j^{\circ})\,\vartheta(\underset{\sim}{r}-\underset{\sim}{r}_j^{\circ}) = 1 \tag{244}$$

then the Coulomb interaction energy E_C^T remains unchanged provided that:

(a) the functions ϑ are spherically symmetric, and

(b) the functions ϑ do not overlap."

Bertaut also uses repeatedly the convolution theorem for Fourier transforms:

> "If the square-integrable (or periodic) functions $f(\underset{\sim}{r})$ and $g(\underset{\sim}{r})$ have Fourier transforms $F(\underset{\sim}{\mathfrak{d}}_{hkl})$ and $G(\underset{\sim}{\mathfrak{d}}_{hkl})^{\dagger}$ respectively, then their convolutions:
>
> $$f \star g \equiv \iiint dv(\underset{\sim}{r})\, f(\underset{\sim}{R}-\underset{\sim}{r})\, g(\underset{\sim}{r}) \ , \tag{245a}$$
>
> $$f \star\star\, g \equiv \iiint dv(\underset{\sim}{r})\, f(\underset{\sim}{R}+\underset{\sim}{r})\, g^{*}(\underset{\sim}{r}) \tag{245b}$$
>
> (where each integral is over the volume of periodicity V of the function $g(\underset{\sim}{r})$ if $g(\underset{\sim}{r})$ is periodic, but is over all space if $g(\underset{\sim}{r})$ is merely square-integrable) have Fourier transforms $F(\underset{\sim}{\mathfrak{d}}_{hkl})G(\underset{\sim}{\mathfrak{d}}_{hkl})$ and $F(\underset{\sim}{\mathfrak{d}}_{hkl})G^{*}(\underset{\sim}{\mathfrak{d}}_{hkl})$ respectively (where * denotes complex conjugation)."

The Fourier transform of $\rho(\underset{\sim}{r})$ is $P(\underset{\sim}{\mathfrak{d}}_{hkl})$ (see Eq. (215)). Assume $\vartheta(\underset{\sim}{r})$ to be expansible in a Fourier series (i.e. $\vartheta(\underset{\sim}{r})$ is of Lebesgue class L^2); then the transform of $\vartheta(\underset{\sim}{r})$ is:

[†] If f,g are not periodic, then the argument of F,G is $\underset{\sim}{\mathfrak{K}} = 2\pi\underset{\sim}{k}$.

(246a) $$\Theta(\underset{\sim}{k}) \equiv \iiint\limits_{\frac{N_0 V}{Z}} dv(\underset{\sim}{r})\,\vartheta(r)\exp(-i\,\underset{\sim}{k}\cdot\underset{\sim}{r}) =$$

(246b) $$= \frac{4\pi}{|\underset{\sim}{k}|}\int_0^\infty dx\; x\,\vartheta(x)\sin(|\underset{\sim}{k}|x),$$

and its convolution:

(247a) $$p(\underset{\sim}{r}) \equiv \iiint\limits_{\frac{N_0 V}{Z}} dv(\underset{\sim}{r}')\,\vartheta(\underset{\sim}{r}'+\underset{\sim}{r})\,\vartheta(\underset{\sim}{r}')$$

has Fourier transform:

(247b) $$\iiint\limits_{\frac{N_0 V}{Z}} dv(\underset{\sim}{r})\,p(\underset{\sim}{r})\exp(-i\,\underset{\sim}{k}\cdot\underset{\sim}{r}) = \left|\Theta(\underset{\sim}{k})\right|^2;$$

$p(\underset{\sim}{r})$ is spherically symmetric because $\vartheta(\underset{\sim}{r})$ is. Notice also that because of the delta-function character of $\rho(\underset{\sim}{r})$ we may write:

$$\iiint\limits_{\frac{N_0 V}{Z}} dv(\underset{\sim}{r}')\,\rho(r-\underset{\sim}{r}')\,\vartheta(\underset{\sim}{r}') =$$

(248a) $$= \sum_{j=1}^{M\frac{N_0}{Z}} \zeta_j\,|e| \iiint\limits_{\frac{N_0 V}{Z}} dv(\underset{\sim}{r}')\,\delta(\underset{\sim}{r}-\underset{\sim}{r}_j^0-\underset{\sim}{r}')\,\vartheta(\underset{\sim}{r}') =$$

(248b) $$= \rho'(\underset{\sim}{r}),$$

whence by the convolution theorem:

(249) $$\rho'(\underset{\sim}{r}) = \frac{1}{V}\sum_{h=-\infty}^{\infty}\sum_{k=-\infty}^{\infty}{\sum_{l=-\infty}^{\infty}}' P(\underset{\sim}{\mathfrak{H}}_{hkl})\,\Theta(\underset{\sim}{\mathfrak{H}}_{hkl})\exp(i\underset{\sim}{\mathfrak{H}}_{hkl}\cdot\underset{\sim}{r}).$$

Again the requirement that each unit cell be electrically neutral gives $P(0)\Theta(0) = 0$, whence we avoid the term $h = k = l = 0$ and denote this precaution by a prime in Eq. (249). Note that the argument of $\Theta(\underset{\sim}{\mathfrak{H}}_{hkl})$ is discrete in Eq. (249) though it was continuous in Eq. (246). Next, Bertaut finds it convenient to define a "grand-total electrostatic energy" E_C^{GT}:

(250) $$E_c^{GT} \equiv \frac{Q}{2}\iiint_{\frac{N_0V}{Z}} \frac{dv(\underset{\sim}{r}')}{|\underset{\sim}{r}'|}\iiint_{\frac{N_0V}{Z}} dv(\underset{\sim}{r})\,\rho(\underset{\sim}{r}+\underset{\sim}{r}')\,\rho(\underset{\sim}{r}),$$

which however contains the infinite self-energy term E_{self}, as can be seen by direct substitution of Eq. (211) into Eq. (250):

(251a) $$E_c^{GT} = \frac{Q|e|^2}{2}\sum_{i=1}^{M\frac{N_0}{Z}}\sum_{j=1}^{M\frac{N_0}{Z}}\frac{\zeta_i\zeta_j}{|\underset{\sim}{r}_i^0-\underset{\sim}{r}_j^0|} =$$

(251b) $$= E_C^T + \left\{ \frac{Q N_0 |e|^2}{2Z} \sum_{n=1}^{M} \zeta_n^2 \iiint_{\frac{N_0 V}{Z}} dv(\underset{\sim}{r}') \, \frac{\delta(\underset{\sim}{r}')}{|\underset{\sim}{r}'|} \right\} \equiv$$

(251c) $$\equiv E_C^T + \left\{ E_{self} \right\}.$$

This equation is obviously inconvenient for the calculation of E_C^T, since both E_C^{GT} and E_{self} are infinite and hence intractable. But there is a way out: if, in Eq. (250), the equivalent charge distribution function $\rho'(\underset{\sim}{r})$ is used instead of the real point-charge distribution $\rho(\underset{\sim}{r})$, then, of course, different values, $E_C^{GT'}$ and E'_{self}, will be obtained for the grand-total electrostatic energy and the self-energy, but $\rho'(\underset{\sim}{r})$ is so chosen that both $E_C^{GT'}$ and E'_{self} are finite. Furthermore Bertaut argues that the total electrostatic energy remains unchanged:

(252a,b) $$E_C^T = E_C^{GT} - E_{self} = E_C^{GT'} - E'_{self}$$

provided that the $\vartheta(\underset{\sim}{r})$ have been so chosen that they do not overlap:

(252c) $$\iiint_{\frac{N_0 V}{Z}} dv(\underset{\sim}{r}) \, \vartheta(\underset{\sim}{r} - \underset{\sim}{r}_i^0) \, \vartheta(\underset{\sim}{r} - \underset{\sim}{r}_j^0) = \delta_{ij}$$

or else provided that the effect of $\vartheta(\underset{\sim}{r})$ overlaps can be accounted for separately. In fact, using the convolution theorem and

Eq. (249)(*) he gets:

$$(253a)\quad E_C^{GT'} \equiv \frac{Q}{2}\iiint_{\frac{N_0V}{Z}} \frac{dv(\mathbf{r}')}{|\mathbf{r}'|}\iiint_{\frac{N_0V}{Z}} dv(\mathbf{r})\,\rho'(\mathbf{r}+\mathbf{r}')\,\rho'(\mathbf{r}) =$$

$$(253b)\quad = \frac{Q}{2}\iiint_{\frac{N_0V}{Z}} \frac{dv(\mathbf{r}')}{|\mathbf{r}'|}\,\frac{N_0}{VZ}\sum_{h=-\infty}^{\infty}\sum_{k=-\infty}^{\infty}{\sum_{l=-\infty}^{\infty}}' |P(\mathbf{h}_{hkl})|^2\,|\Theta(\mathbf{h}_{hkl})|^2 \exp(i\mathbf{h}_{hkl}\cdot\mathbf{r}') =$$

$$(253c)\quad = \frac{2\pi Q N_0}{ZV}\sum_{h=-\infty}^{\infty}\sum_{k=-\infty}^{\infty}{\sum_{l=-\infty}^{\infty}}' \frac{|P(\mathbf{h}_{hkl})|^2\,|\Theta(\mathbf{h}_{hkl})|^2}{h_{hkl}^2}.$$

Note that the Fourier expansion for E_C^{GT} would read:

$$(254a)\quad E_C^{GT} = \frac{2\pi Q N_0}{ZV}\sum_{h=-\infty}^{\infty}\sum_{k=-\infty}^{\infty}{\sum_{l=-\infty}^{\infty}}' \frac{|P(\mathbf{h}_{hkl})|^2}{h_{hkl}^2} =$$

$$(254b)\quad = \frac{QN_0}{2Z}\sum_{m=1}^{M}\sum_{n=1}^{M} Z_m Z_n \times$$

$$\times\left\{\frac{4\pi}{V}\sum_{h=-\infty}^{\infty}\sum_{k=-\infty}^{\infty}{\sum_{l=-\infty}^{\infty}}' \frac{\exp[i\mathbf{h}_{hkl}\cdot(\mathbf{r}_m^0-\mathbf{r}_n^0)]}{h_{hkl}^2}\right\},$$

---

[*] The integral over r' is evaluated in spherical polar coordinates with $\mathbf{h}_{hkl}$ as the polar axis and a trick:

$$(255a)\quad \iiint_{\frac{N_0V}{Z}} dv(\mathbf{r}')\,\frac{\exp(\pm i\mathbf{h}_{hkl}\cdot\mathbf{r}')}{|\mathbf{r}'|} =$$

$$= \lim_{\alpha\to 0}\left[\int_0^{\infty} dt\, 2\pi t\exp(-\alpha t)\int_0^{\pi} d\vartheta \sin\vartheta \exp\left(i|\mathbf{h}_{hkl}|\,t\cos\vartheta\right)\right] =$$

$$(255b)\quad = \frac{4\pi}{h_{hkl}^2}.$$

which diverges for physical reasons because the infinite self-energy terms i=j in Eq. (251) are included in the definition of E_C^{GT}, and for mathematical reasons because the quantity in braces reduces* to $|\underset{\sim}{r}_m^o - \underset{\sim}{r}_n^o|^{-1}$, which is infinite if m=n. $E_C^{GT'}$ does not, however, diverge, thanks to the extra factor $|\Theta(\underset{\sim}{\alpha}_{hkl})|^2$, or, in direct space, because

$$\sum_{i=1}^{M\frac{N_0}{Z}} \zeta_i^2 |\epsilon|^2 \iiint_{\frac{N_0V}{Z}} dv(\underset{\sim}{r})\, \frac{\mathfrak{p}(\underset{\sim}{r})}{|\underset{\sim}{r}|}$$

is made to be finite.

Bertaut then evaluates $E_C^{GT'}$ by a different route: from Eq. (243) and Eq. (247) we note that:

$$\iiint_{\frac{N_0V}{Z}} dv(\underset{\sim}{r})\,\rho'(\underset{\sim}{r}+\underset{\sim}{r}')\,\rho'(\underset{\sim}{r}) = |\epsilon|^2 \sum_{i=1}^{M\frac{N_0}{Z}} \sum_{\substack{j=1\\ i\neq j}}^{M\frac{N_0}{Z}} \zeta_i \zeta_j\, \mathfrak{p}(\underset{\sim}{r}'+\underset{\sim}{r}_j^o-\underset{\sim}{r}_i^o) + $$

$$(256) \qquad + |\epsilon|^2 \frac{N_0}{Z} \sum_{n=1}^{M} \zeta_n^2\, \mathfrak{p}(\underset{\sim}{r}').$$

Before substituting Eq. (256) into Eq. (253a) we must evaluate the integral over $\underset{\sim}{r}'$ of $|\underset{\sim}{r}'|^{-1}\mathfrak{p}(\underset{\sim}{r}' - (\underset{\sim}{r}_i^o - \underset{\sim}{r}_j^o))$: choose spherical polar coordinates, with $(\underset{\sim}{r}_i^o - \underset{\sim}{r}_j^o)$ as the polar axis and $t \equiv |\underset{\sim}{r}' - (\underset{\sim}{r}_i^o - \underset{\sim}{r}_j^o)|$ as the radial coordinate; next, use Eq. (241) and remember that $\mathfrak{p}(\underset{\sim}{r})$ is a spherically symmetric

---

*Ref. (171), page 5, Eq. (24).

normalized function*:

$$\text{(257a)}\quad \iiint_{\frac{N_0V}{Z}} dv(\mathbf{r}')\,\frac{p(\mathbf{r}'-(\mathbf{r}_i^\circ-\mathbf{r}_j^\circ))}{|\mathbf{r}'|} = \frac{4\pi}{|\mathbf{r}_i^\circ-\mathbf{r}_j^\circ|}\int_0^{|\mathbf{r}_i^\circ-\mathbf{r}_j^\circ|} dt\, t^2 p(t) + 4\pi\int_{|\mathbf{r}_i^\circ-\mathbf{r}_j^\circ|}^{\infty} dt\, t\, p(t) =$$

$$\text{(257b)}\quad = \frac{1}{|\mathbf{r}_i^\circ-\mathbf{r}_j^\circ|} - \frac{4\pi}{|\mathbf{r}_i^\circ-\mathbf{r}_j^\circ|}\int_{|\mathbf{r}_i^\circ-\mathbf{r}_j^\circ|}^{\infty} dt\left(t^2 - t|\mathbf{r}_i^\circ-\mathbf{r}_j^\circ|\right)p(t).$$

Finally, from Eqs. (253a), (256), and (257b) Bertaut gets:

$$\text{(258a)}\quad E_c^{GT'} = \left\{\frac{Q|\epsilon|^2}{2}\sum_{\substack{i=1\\ i\neq j}}^{M\frac{N_0}{Z}}\sum_{j=1}^{M\frac{N_0}{Z}}\frac{\zeta_i\zeta_j}{|\mathbf{r}_i^\circ-\mathbf{r}_j^\circ|}\right\} + \left[2\pi Q|\epsilon|^2\sum_{\substack{i=1\\ i\neq j}}^{M\frac{N_0}{Z}}\sum_{j=1}^{M\frac{N_0}{Z}}\frac{(-1)\zeta_i\zeta_j}{|\mathbf{r}_i^\circ-\mathbf{r}_j^\circ|}\times \times\int_{|\mathbf{r}_i^\circ-\mathbf{r}_j^\circ|}^{\infty} dt\left(t^2 - t|\mathbf{r}_i^\circ-\mathbf{r}_j^\circ|\right)p(t)\right] + \frac{2\pi Q N_0|\epsilon|^2}{Z}\sum_{n=1}^{M}\zeta_n^2\int_0^{\infty} dt\, t\, p(t) \equiv$$

$$\text{(258b)}\quad \equiv\left\{E_c^T\right\} + \left[E'_{overlap}\right] + E'_{self} =$$

$$\text{(258c)}\quad = E_c^{T'} + E'_{self},$$

---

*because:

$$\text{(257c)}\quad \iiint_{\frac{N_0V}{Z}} p(\mathbf{r})\,dv(\mathbf{r}) = 4\pi\int_0^{\infty} dt\, t^2 p(t) = \left[\iiint_{\frac{N_0V}{Z}} dv(\mathbf{r}')\,\vartheta(\mathbf{r}')\right]^2 = 1.$$

and since $\rho(\underset{\sim}{r})$ vanishes for $|\underset{\sim}{r}| > |\underset{\sim}{r}_i^o - \underset{\sim}{r}_j^o|$ whenever the functions ϑ do not overlap, therefore if Eq. (252b) holds then:

$$E'_{overlap} = 0 \ , \quad \text{and} \quad E_c^{T'} = E_c^T , \tag{258d,e}$$

which proves the first theorem invoked by Bertaut, Q.E.D.

Thus, for a general, spherically symmetric, equivalent charge distribution Bertaut has shown that:

$$E_c^T = E_c^{GT'} - E'_{self} - E'_{overlap} , \tag{259a}$$

where:

$$E_c^{GT'} = \frac{2\pi Q N_o |\epsilon|^2}{Z V} \sum_{m=1}^{M} \sum_{n=1}^{M} \zeta_m \zeta_n \times \tag{259b}$$

$$\times \sum_{h=-\infty}^{\infty} \sum_{k=-\infty}^{\infty} {\sum_{l=-\infty}^{\infty}}' \frac{|\Theta(\underset{\sim}{\mathbf{h}}_{hkl})|^2 \exp[i\,\underset{\sim}{\mathbf{h}}_{hkl} \cdot (\underset{\sim}{r}_m^o - \underset{\sim}{r}_n^o)]}{\mathbf{h}_{hkl}^2} ,$$

$$E'_{self} = \frac{2\pi Q N_o |\epsilon|^2}{Z} \sum_{n=1}^{M} \zeta_n^2 \int_0^\infty dt\, t\, \rho(t) , \tag{259c}$$

$$E'_{overlap} = 2\pi Q |\epsilon|^2 \sum_{\substack{i=1 \\ i \neq j}}^{M\frac{N_o}{Z}} \sum_{j=1}^{M\frac{N_o}{Z}} \frac{(-1)\zeta_i \zeta_j}{|\underset{\sim}{r}_i^o - \underset{\sim}{r}_j^o|} \int_{|\underset{\sim}{r}_i^o - \underset{\sim}{r}_j^o|}^{\infty} dt\, t(t - |\underset{\sim}{r}_i^o - \underset{\sim}{r}_j^o|)\rho(t) \tag{259d}$$

From this generalized expression of E_C^T, Bertaut shows that Ewald's series can be obtained as a special case if for $\vartheta(\underset{\sim}{r})$ one chooses a Gaussian charge distribution (with overlap). In fact, if one sets:*

(260) $$\vartheta(\underset{\sim}{r} - \underset{\sim}{r}_j^\circ) \equiv \frac{1}{V}\left(\frac{2\eta}{\pi}\right)^{3/2} \exp\left\{-\frac{2\eta}{V^{2/3}}\,|\underset{\sim}{r} - \underset{\sim}{r}_j^\circ|^2\right\},$$

then: (a) from Eq. (247) one gets:

(261a) $$p(\underset{\sim}{t}) = \frac{1}{V}\left(\frac{\eta}{\pi}\right)^{3/2} \exp\left\{-\frac{\eta}{V^{2/3}}\,t^2\right\};$$

(b) from Eqs. (246), (260) and (233b):

(261b) $$\Theta\left(\underset{\sim}{\mathbb{H}}_{hkl}\right) = \exp\left\{-\frac{\mathbb{H}_{hkl}^2\, V^{2/3}}{8\eta}\right\} \implies E_C^{GT'} = B;$$

(c) from Eqs. (261a) and (233a):

(261c) $$\int_0^\infty dt\; t\, p(t) = +\frac{1}{2\pi^{3/2}}\,\frac{\sqrt{\eta}}{V^{1/3}} \implies E'_{self} = -A;$$

---

[*] Notice the factor of two. Eq. (260) and Eq. (236) do <u>not</u> say the same thing. So Bertaut's treatment is not a reinterpretation of Shockley's observations!

(d) from Eqs. (220b) and (233c) and (261a):

$$\int_{|\underset{\sim}{r}_i^o-\underset{\sim}{r}_j^o|}^{\infty} dt\, p(t)\left(t^2 - t|\underset{\sim}{r}_i^o - \underset{\sim}{r}_j^o|\right) = \frac{1-\mathrm{erf}\left(\frac{\sqrt{\epsilon}}{V^{1/3}}|\underset{\sim}{r}_i^o-\underset{\sim}{r}_j^o|\right)}{4\pi} \tag{261d}$$

$$\Longrightarrow E'_{\text{overlap}} = -\Gamma.$$

C. Description of Computer Programs EWALD and CELLMAP

The adaption of Eqs. (202, 232, 233) to digital computer methods deserves some further comment.

The atom positions $\left\{\underset{\sim}{r}_m^o;\ m = 1, 2, \ldots, M\right\}$ and the direct lattice unit cell sides $\underset{\sim}{a}$, $\underset{\sim}{b}$, $\underset{\sim}{c}$ and angles α, β, γ required in our computations were derived from known crystal and molecular structures, as determined by X-ray crystallographic techniques. Some manipulation of these data was necessary, however, and a preliminary program CELLMAP, was written to provide, as output, punched IBM cards suitable as input for the main program, EWALD.

CELLMAP generates, for a crystal of any given symmetry, the Cartesian coordinates $\left\{r_m^x,\ r_m^y,\ r_m^z;\ m = 1, 2, \ldots, M\right\}$ of all the atoms within the same unit cell, which we will call the ZEROTH CELL. The input data are the usual crystallographic parameters (cell sides $\underset{\sim}{a}$, $\underset{\sim}{b}$, $\underset{\sim}{c}$; cell angles α, β, γ; atom coordinates of the "asymmetric unit", and the "coordinates for the symmetry-equivalent positions"*). The Cartesian axes used

---

*As listed in the International Tables for X-ray crystallography (174).

in CELLMAP are defined as follows:

$$(262a)\quad \vec{e}_x \equiv \left(\frac{1}{\sin\gamma}\right)\vec{e}_a - \left(\frac{\cos\gamma}{\sin\gamma}\right)\vec{e}_b,$$

$$(262b)\quad \vec{e}_y \equiv \vec{e}_b,$$

$$(262c)\quad \vec{e}_z \equiv \frac{[\vec{e}_a \wedge \vec{e}_b]}{\sin\gamma} = \left(\frac{\cos\gamma\cos\alpha - \cos\beta}{\sin\gamma\sqrt{}}\right)\vec{e}_a + \left(\frac{\cos\beta\cos\gamma - \cos\alpha}{\sin\gamma\sqrt{}}\right)\vec{e}_b + \left(\frac{\sin\gamma}{\sqrt{}}\right)\vec{e}_c,$$

where $\vec{e}_a \equiv \underset{\sim}{a}|\underset{\sim}{a}|^{-1}$, and so on, and $\sqrt{}$ stands for $[1 - \cos^2\alpha - \cos^2\beta - \cos^2\gamma + 2\cos\alpha\cos\beta\cos\gamma]^{1/2}$. In this coordinate system the reciprocal lattice vector $\underset{\sim}{d}_{hkl}$ is written:

$$(263)\quad \underset{\sim}{d}_{hkl} = d^x_{hkl}\,\vec{e}_x + d^y_{hkl}\,\vec{e}_y + d^z_{hkl}\,\vec{e}_z,$$

where:

$$(264a)\quad d^x_{hkl} \equiv 2\pi\left\{h\left[\frac{1}{|\underset{\sim}{a}|\sin\gamma}\right] + k\left[\frac{-\cos\gamma}{|\underset{\sim}{b}|\sin\gamma}\right]\right\},$$

$$(264b)\quad d^y_{hkl} \equiv 2\pi\left\{k\left[\frac{1}{|\underset{\sim}{b}|}\right]\right\},$$

$$(264c)\quad d^z_{hkl} \equiv 2\pi\left\{h\left[\frac{\cos\gamma\cos\alpha - \cos\beta}{|\underset{\sim}{a}|\sin\gamma\sqrt{}}\right] + k\left[\frac{\cos\beta\cos\gamma - \cos\alpha}{|\underset{\sim}{b}|\sin\gamma\sqrt{}}\right] + l\left[\frac{\sin\gamma}{|\underset{\sim}{c}|\sqrt{}}\right]\right\}.$$

The values in square brackets in Eq. (264) are calculated and punched onto cards by CELLMAP for later use by EWALD.

Furthermore, if we label all the unit cells in the crystal by the triad of integers (d,f,g), the zeroth cell being the (0,0,0) cell, then we may rewrite the general direct lattice vector $\underset{\sim}{r}_j^o$ by using the appropriate $\underset{\sim}{r}_m^o$:

$$\text{(265a)} \quad \underset{\sim}{r}_j^o \equiv \underset{\sim}{r}_m^o + \underset{\sim}{r}_{dfg} = \underset{\sim}{r}_m^o + d\underset{\sim}{a} + f\underset{\sim}{b} + g\underset{\sim}{c} =$$

$$\text{(265b)} \quad = (r_m^x + r_{dfg}^x)\vec{e}_x + (r_m^y + r_{dfg}^y)\vec{e}_y + (r_m^z + r_{dfg}^z)\vec{e}_z,$$

$$\left\{ j = 1,2,\ldots, M\frac{N_o}{Z}\ ;\ m = 1,2,\ldots, M\ ;\ -\frac{1}{2}\left[\left(\frac{N_o}{Z}\right)^{1/3} - 1\right] \leq d,f,g \leq \frac{1}{2}\left[\left(\frac{N_o}{Z}\right)^{1/3} - 1\right] \right\},$$

where:

$$\text{(266a)} \quad r_{dfg}^x = d a_x + g c_x = d\left[|\underset{\sim}{a}| \sin\gamma\right] + g\left[|\underset{\sim}{c}| \frac{\cos\beta - \cos\gamma \cos\alpha}{\sin\gamma}\right],$$

$$\text{(266b)} \quad r_{dfg}^y = d a_y + f b_y + g c_y = d\left[|\underset{\sim}{a}| \cos\gamma\right] + f\left[|\underset{\sim}{b}|\right] + g\left[|\underset{\sim}{c}| \cos\alpha\right],$$

$$\text{(266c)} \quad r_{dfg}^z = g c_z = g\left[|\underset{\sim}{c}| \frac{\sqrt{\quad}}{\sin\gamma}\right];$$

again the values in square brackets are put out on punched cards by CELLMAP. Similar relations to Eq. (266) hold, of course, for r_m^x, r_m^y, r_m^z in terms of the "atom coordinates in the asymmetric unit", r_m^a, r_m^b, r_m^c:

$$\text{(267a)} \quad \underset{\sim}{r}_m^o = r_m^x \vec{e}_x + r_m^y \vec{e}_y + r_m^z \vec{e}_z \equiv r_m^a \underset{\sim}{a} + r_m^b \underset{\sim}{b} + r_m^c \underset{\sim}{c},$$

where:

$$\text{(267b)} \quad r_m^x = r_m^a\left[|\underset{\sim}{a}| \sin\gamma\right] + r_m^c\left[|\underset{\sim}{c}| \frac{\cos\beta - \cos\gamma \cos\alpha}{\sin\gamma}\right],$$

$$(267c)\quad r_m^y = r_m^a\left[\,|\underset{\sim}{a}|\cos\gamma\right] + r_m^b\left[\,|\underset{\sim}{b}|\,\right] + r_m^c\left[\,|\underset{\sim}{c}|\cos\alpha\right],$$

$$(267d)\quad r_m^z = r_m^c\left[\,|\underset{\sim}{c}|\,\frac{\sqrt{\quad}}{\sin\gamma}\right].$$

CELLMAP also avoids placing any atom on the sides, faces, or corners of the zeroth cell, by translating all atomic coordinates by a preset amount, i.e., by establishing the origin of the Cartesian coordinate system according to the option of the programmer; if this precaution is not taken, the Ewald series would become meaningless (cf. Eq. (233c) for $j \neq n$ but when $\underset{\sim}{r}_j^o = \underset{\sim}{r}_n^o$).

The point charges $\{\zeta_m;\ m = 1, 2, \ldots, M\}$ on the various atoms were assigned on the basis of previous published theoretical or experimental data, since we wished to merely establish the sensitivity of our results to the variations in charge assignments, and to avoid the labor of <u>ab initio</u> single-molecule calculations, or searches for the "ultimate" ideal charge assignment. These charge assignments are discussed further in Section D below. EWALD accepts any number s of different charge assignments for each atom, $\{\zeta_m(e=1), \zeta_m(e=2), \ldots, \zeta_m(e=s);\ m = 1, 2, \ldots, M\}$: all energies are calculated separately for each charge assignment at very little additional cost in computation time, because EWALD is organized so that it obtains all the time-consuming intermediate numerical results only once, and then multiplies them very rapidly by all the appropriate ζ_m to give the final results.

EWALD computes and prints out A, B, Γ, Δ_1, Δ_2, Δ, H, E_C^T, and E_C in various units, as well as a summary of the input data for purposes of reference (and to make sure the data cards were read in correctly!). Valuable time is saved by avoiding the print-out of all intermediate results of the computation, because the Burroughs B-5500 at Stanford University prints out everything "on-line". Since the calculations of the error function are extremely time-consuming, and B-5500 is notoriously slow at evaluating trigonometric functions, EWALD was designed to minimize computation time insofar as possible without affecting its general applicability to the arbitrary crystal.

The term A is obviously trivial to compute. A few remarks are needed for the term B (Eq. (233b)), which, after due note is taken of Eq. (264) and (266), is rewritten as:

$$B = \frac{2\pi N_o Q |e|^2}{Z V} \sum_{h=-\infty}^{\infty} \sum_{k=-\infty}^{\infty} \sum_{\ell=-\infty}^{\infty}{}' \frac{\exp\left[-\frac{\mathfrak{d}_{hk\ell}^2 V^{2/3}}{4\eta}\right]}{\mathfrak{d}_{hk\ell}^2} \times$$

(268a)

$$\times \sum_{m=1}^{M} \sum_{n=1}^{M} \zeta_m \zeta_n \exp\left\{i\left[\mathfrak{d}_{hk\ell}^x (r_m^x - r_n^x) + \mathfrak{d}_{hk\ell}^y (r_m^y - r_n^y) + \mathfrak{d}_{hk\ell}^z \left(r_m^z - r_n^z\right)\right]\right\}.$$

Because of the symmetry of the sum over m, n, the imaginary term vanishes and we are left with:

(268b)

$$B = \frac{2\pi N_0 Q|\epsilon|^2}{ZV} \sum_{h=-\infty}^{\infty} \sum_{k=-\infty}^{\infty} {\sum_{l=-\infty}^{\infty}}' \frac{\exp\left[-\frac{\mathbb{d}^2_{hkl} V^{2/3}}{4\eta}\right]}{\mathbb{d}^2_{hkl}} \left\{ \sum_{m=1}^{M} \zeta_m^2 + \right.$$

$$\left. + 2 \sum_{m=2}^{M} \sum_{n=1}^{m-1} \zeta_m \zeta_n \cos\left[\mathbb{d}^x_{hkl}(r^x_n - r^x_m) + \mathbb{d}^y_{hkl}(r^y_n - r^y_m) + \mathbb{d}^z_{hkl}(r^z_n - r^z_m)\right]\right\}.$$

The above is the "simplest-looking" formula for B, but in fact it hides a two-fold redundancy. This is because cos (x) is an even function and because even in the most general triclinic crystal $\mathbb{d}^2_{hkl} = \mathbb{d}^2_{-h-k-l}$. We may therefore appeal to the following identity, which holds if and only if F(p,q,r) = F(-p,-q,-r):

(269)

$$I \equiv \sum_{p=-P}^{P} \sum_{q=-Q}^{Q} \sum_{r=-R}^{R} F(p,q,r) = 2 \sum_{p=0}^{P} \sum_{q=0}^{Q} \sum_{r=0}^{R} \left[\left(1 - \frac{\delta_{p0}}{2}\right)\left(1 - \frac{\delta_{q0}}{2}\right) \times \right.$$

$$\left. \times \left(1 - \frac{\delta_{r0}}{2}\right)\right] \left[F(p,q,r) + F(p,q,-r) + F(p,-q,r) + F(-p,q,r)\right],$$

where δ_{p0} is the Kronecker delta: $\delta_{p0} = 1$ if p = 0, $\delta_{p0} = 0$ otherwise. The identity can be rewritten more conveniently if we define two auxiliary functions:

(270a) $e(\lambda) \equiv 1$ for $\{\lambda = 1, 2\}$ and $e(\lambda) \equiv -1$ for $\{\lambda = 3, 4\}$,

(270b) $s(\lambda) \equiv 1$ for $\{\lambda = 1, 3\}$ and $s(\lambda) \equiv -1$ for $\{\lambda = 2, 4\}$;

then

$$(271)\qquad I = 2\sum_{p=0}^{P}\sum_{q=0}^{Q}\sum_{r=0}^{R}\left[\left(1-\frac{\delta_{p0}}{2}\right)\left(1-\frac{\delta_{q0}}{2}\right)\left(1-\frac{\delta_{r0}}{2}\right)\right]\sum_{\lambda=1}^{4}F(p,qe(\lambda),rs(\lambda)).$$

We may then use this identity to rewrite B in the fastest possible form for automatic computation:

$$(272)\qquad \begin{aligned} B = {} & \frac{4\pi N_0 Q|e|^2}{ZV}\sum_{h=0}^{\infty}\sum_{k=0}^{\infty}{\sum_{l=0}^{\infty}}'\left[\left(1-\frac{\delta_{h0}}{2}\right)\left(1-\frac{\delta_{k0}}{2}\right)\left(1-\frac{\delta_{l0}}{2}\right)\right]\times \\ & \times\sum_{\lambda=1}^{4}\left[\mathfrak{H}_{h,e(\lambda)k,s(\lambda)l}\right]^{-2}\exp\left[-\frac{V^{2/3}}{4\eta}\left(\mathfrak{H}_{h,e(\lambda)k,s(\lambda)l}\right)^2\right]\left\{\sum_{m=1}^{M}\zeta_m^2 + \right. \\ & +2\sum_{m=2}^{M}\sum_{n=1}^{m-1}\zeta_m\zeta_n\cos\left[\mathfrak{H}^x_{h,e(\lambda)k,s(\lambda)l}\left(r_n^x-r_m^x\right)+\mathfrak{H}^y_{h,e(\lambda)k,s(\lambda)l}\times\right. \\ & \left.\left.\times\left(r_n^y-r_m^y\right)+\mathfrak{H}^z_{h,e(\lambda)k,s(\lambda)l}\left(r_n^z-r_m^z\right)\right]\right\}. \end{aligned}$$

The above is a perfectly general formula.

Further simplifications are possible, however, if the crystal is of orthorhombic or higher symmetry: in that case we note that:

1) the general expression for $\mathfrak{H}^2_{hkl}$, which is:

(273) $$\mathbb{d}^2_{hk\ell} = \frac{4\pi^2}{(\sqrt{\ })^2}\left\{\frac{h^2}{a^2}\sin^2\alpha + \frac{k^2}{b^2}\sin^2\beta + \frac{\ell^2}{c^2}\sin^2\gamma + \right.$$
$$+ \frac{2hk}{|\underset{\sim}{a}||\underset{\sim}{b}|}(\cos\alpha\cos\beta - \cos\gamma) + \frac{2k\ell}{|\underset{\sim}{b}||\underset{\sim}{c}|}(\cos\beta\cos\gamma - \cos\alpha) +$$
$$\left. + \frac{2\ell h}{|\underset{\sim}{c}||\underset{\sim}{a}|}(\cos\gamma\cos\alpha - \cos\beta)\right\}$$

can be simplified so that for $\alpha = \beta = \gamma = 90°$ one obtains $\mathbb{d}^2_{hkl} = \mathbb{d}^2_{hk-l} = \mathbb{d}^2_{h-kl} = \mathbb{d}^2_{-hkl}$;

(2) the following identity can be utilized:

(274) $$\cos(\alpha_1+\alpha_2+\alpha_3) + \cos(\alpha_1+\alpha_2-\alpha_3) + \cos(\alpha_1-\alpha_2+\alpha_3) +$$
$$+ \cos(\alpha_1-\alpha_2-\alpha_3) = 4\cos\alpha_1\cos\alpha_2\cos\alpha_3 ,$$

whence we finally get, for crystals of orthorhombic or higher symmetry:

$$B = \frac{32\pi N_0 Q|\epsilon|^2}{zV}\sum_{h=0}^{\infty}\sum_{k=0}^{\infty}{\sum_{\ell=0}^{\infty}}'\left[\left(1-\frac{\delta_{h0}}{2}\right)\left(1-\frac{\delta_{k0}}{2}\right)\left(1-\frac{\delta_{\ell 0}}{2}\right)\right] \times$$

(275) $$\times\ \mathbb{d}^{-2}_{hk\ell}\exp\left(-\frac{V^{2/3}\,\mathbb{d}^2_{hk\ell}}{4\eta}\right)\left\{\sum_{m=1}^{M}\zeta_m^2 + 2\sum_{m=2}^{M}\sum_{n=1}^{m-1}\zeta_m\zeta_n \times\right.$$

$$\left.\times \cos\left[\mathbb{d}^x_{hk\ell}(r^x_m - r^x_n)\right]\cos\left[\mathbb{d}^y_{hk\ell}(r^y_m - r^y_n)\right]\cos\left[\mathbb{d}^z_{hk\ell}(r^z_m - r^z_n)\right]\right\}.$$

The computer program EWALD, version ZZ, computes B_{CALC}, a suitably truncated version of Eq. (272):

$$B_{CALC} = \frac{4\pi Q N_0 |e|^2}{Z V} \sum_{h=0}^{p} \sum_{k=0}^{q} {\sum_{\ell=0}^{r}}' \left(1 - \frac{\delta_{h0}}{2}\right)\left(1 - \frac{\delta_{h0}}{2}\right)\left(1 - \frac{\delta_{\ell 0}}{2}\right) \times$$

$$\times \sum_{\lambda=1}^{4} \left[\text{đ}_{h,e(\lambda)k,s(\lambda)\ell}\right]^{-2} \exp\left[-\frac{V^{2/3}}{4\eta}\left(\text{đ}_{h,e(\lambda)k,s(\lambda)\ell}\right)^{2}\right] \times \tag{276}$$

$$\times \left\{ \sum_{m=1}^{M} \zeta_m^2 + 2 \sum_{m=2}^{M} \sum_{n=1}^{m-1} \zeta_m \zeta_n \cos\left[\text{đ}^{x}_{h,e(\lambda)k,s(\lambda)\ell}\left(r_m^x - r_n^x\right) + \right.\right.$$

$$\left.\left. + \text{đ}^{y}_{h,e(\lambda)k,s(\lambda)\ell}\left(r_m^y - r_n^y\right) + \text{đ}^{z}_{h,e(\lambda)k,s(\lambda)\ell}\left(r_m^z - r_n^z\right)\right]\right\}.$$

If η was judiciously chosen, then the three positive integers p, q, r can be set to be as small as 3 or 4. At the programmer's option, EWALD will (1) further compute the addition to B_{CALC} obtained by increasing p, q, and r to p + 1, q + 1, r + 1 respectively, and call this addition B', (2) compute the ratio B'/B_{CALC}, and (3) return to compute a new addition B" by increasing the limits of h, k, l to p + 2, q + 2, r + 2, and so on, and continue to loop until the ratio: $B^{''\ldots'} \times (B_{CALC} + B' + B'' + \ldots + B^{'\ldots'} + B^{''\ldots'})^{-1}$ is less than a certain small infinitesimal preset by the programmer. EWALD prints out $B^{''\ldots'}$ along with $(B_{CALC} + B' + B'' + \ldots + B^{'\ldots'} + B^{''\ldots'})$ to give an estimate of the rate of convergence.

Last but not least is the term Γ. Combining Eqs. (233c) and (265) we get:

$$\Gamma = \frac{Q N_0 |\epsilon|^2}{2Z} \sum_{d=-t}^{t} \sum_{f=-u}^{u} \sum_{g=-v}^{v} \sum_{m=1}^{M} \sum_{\substack{n=1 \\ \text{if } d=f=g=0 \text{ then } m \neq n}}^{M} \zeta_m \zeta_n \times$$

$$\times \left[(r_m^x - r_n^x + r_{dfg}^x)^2 + (r_m^y - r_n^y + r_{dfg}^y)^2 + (r_m^z - r_n^z + r_{dfg}^z)^2 \right]^{-1/2} \times \tag{277}$$

$$\times \left\{ 1 - \mathrm{erf}\left(\frac{\sqrt{\eta}}{V^{1/3}} \left[(r_m^x - r_n^x + r_{dfg}^x)^2 + (r_m^y - r_n^y + r_{dfg}^y)^2 + \right.\right.\right.$$

$$\left.\left.\left. + (r_m^z - r_n^z + r_{dfg}^z)^2 \right]^{1/2} \right) \right\},$$

where t, u, v are integers so chosen that $M \frac{N_o}{Z}$ unit cells are included (and for all intents we may assume t, u, v to be infinite). In practice, EWALD gives sufficiently good results if t, u, v are all set equal to 1 (which means that 27 unit cells are considered in the calculation). Formally, Eq. (277) requires the evaluation of $\left\{ M^2(2t+1)(2u+1)(2v+1)-M \right\}$ error functions. The algorithm used to obtain values of erf(x) is a subroutine obtained from the Stanford Computation Center Program Library (175), which calculates erf(x) as the sum of k Taylor's series expansions for erf(a_k), $0 < a_k < x$, and obtains in $(8 + 20x + x^2)$ milliseconds a value of erf(x) which agrees to more than 7 significant figures with tabulations available in the literature. If $x > 5$, then erf(x) is set equal to 1 directly. It is obviously desirable to minimize the number of error functions which must be evaluated. If an enormous magnetic memory core were available, a table of "error functions already evaluated" should be constructed, and at each step when a new erf(x) would be required, a quick search through the table would avoid a redundant calculation. Unfortunately, the Burroughs B-5500 has only a 16,384 48-bit word memory, and in the early stages of this project it did not have a magnetic disk file. The approach of generating and storing and retrieving a table of erf(x) from magnetic tape or disk was judged not to be more economical in time and money than generating a new erf(x) when required during the computation.

Mathematical manipulation of Eq. (277) does reduce the number of evaluations of erf(x) slightly, to wit, $\frac{M(M-1)}{Z}$ iterations are avoided by treating separately the case $\left\{d=f=g=0,\ m \neq n,\ \text{where} \left|\underset{\sim}{r}^{o}_{m} - \underset{\sim}{r}^{o}_{n}\right| = \left|\underset{\sim}{r}^{o}_{n} - \underset{\sim}{r}^{o}_{m}\right|\right\}$, and $\left\{[(2t+1)(2u+1)(2v+1) - 1] \times M - [(t+1)(2u+1)(2v+1) - 1]\right\}$ iterations are eliminated by avoiding redundancies in the case $\left\{m=n,\ d,f,g \text{ not all zero, where, e.g. } (r^{x}_{dfg})^2 = (r^{x}_{-d-f-g})^2\right\}$; the final equation is:

$$\begin{aligned}
\Gamma_{CALC} = \frac{QN_0|\epsilon|^2}{2Z}\Bigg\{ & 2\sum_{m=2}^{M}\sum_{n=1}^{m-1} \zeta_m \zeta_n \Big[(r^x_m - r^x_n)^2 + (r^y_m - r^y_n)^2 + \\
& + (r^z_m - r^z_n)^2\Big]^{-1/2} \Bigg\{1 - \operatorname{erf}\left(\frac{\sqrt{\eta}}{V^{1/3}}\Big[(r^x_m - r^x_n)^2 + (r^y_m - r^y_n)^2 + \right. \\
& \left. + (r^z_m - r^z_n)^2\Big]^{1/2}\right)\Bigg\} + 2\sum_{m=1}^{M} \zeta_m^2 \underset{\text{If } d=0 \text{ then } f,g \neq 0}{\sum_{d=0}^{t}\sum_{f=-u}^{u}\sum_{g=-v}^{v}} \left(1 - \frac{\delta_{d0}}{2}\right) \times \\
& \times \Big[(r^x_{dfg})^2 + (r^y_{dfg})^2 + (r^z_{dfg})^2\Big]^{-1/2} \Bigg\{1 - \operatorname{erf}\left(\frac{\sqrt{\eta}}{V^{1/3}}\Big[(r^x_{dfg})^2 + (r^y_{dfg})^2 + (r^z_{dfg})^2\Big]^{1/2}\right)\Bigg\} +
\end{aligned} \tag{278}$$

$$+ \sum_{\substack{d=-t \\ \text{If } d=0 \text{ then } f,g\neq 0}}^{t} \sum_{f=-u}^{u} \sum_{g=-v}^{v} \sum_{\substack{m=1 \\ m\neq n}}^{M} \sum_{n=1}^{M} \zeta_m \zeta_n \Big[(r_m^x - r_n^x + r_{dfg}^x)^2 +$$

$$+ (r_m^y - r_n^y + r_{dfg}^y)^2 + (r_m^z - r_n^z + r_{dfg}^z)^2 \Big]^{-1/2} \Big\{ 1 - \mathrm{erf}\Big(\frac{\sqrt{\pi}}{V^{1/3}} \Big[(r_m^x - r_n^x + r_{dfg}^x)^2 +$$

$$+ (r_m^y - r_n^y + r_{dfg}^y)^2 + (r_m^z - r_n^z + r_{dfg}^z)^2 \Big]^{1/2} \Big) \Big\} \Big\},$$

which requires $\left\{(2u+1)(2v+1)[(2t+1)(M^2-M) + (t+1)] - \frac{1}{2}(M^2-M+2)\right\}$ values of erf(x)

It was found most convenient to set (t=1, u=1, v=1) in most EWALD runs: this meant including 27 unit cells in the computation of Γ. Also, to give some realistic estimate of the convergence of Γ, the contribution to Γ due to the unit cell (d=t+1, f=0, g=0) was calculated as Γ_{TEST}; a good guess for the series termination error in Γ might be $< 10(\Gamma_{TEST})$.

EWALD computes Δ_1, Δ_2 and H by using Eqs. (203a, 203b, 204). Since, however, it rarely happens that all the atoms of the same anion and all the atoms of the same cation can be fit into the zeroth unit cell without drastically affecting the choice of unit cell sides and angles, therefore for each atom EWALD is given a triad of integers d_m^{patch}, f_m^{patch}, g_m^{patch} (each of which can assume the values +1, 0, or -1) which, with Eqs. (265, 266) can displace $\underset{\sim}{r}_m^o$ to $\left(\underset{\sim}{r}_m^o + \underset{\sim}{r}_{d_m^{patch},\ f_m^{patch},\ g_m^{patch}}\right)$ into a neighboring unit cell, as required.

The dependence of A, B, Γ, and E_C^T on η deserves some comment. Eq. (233) implies the following: (i) if $\eta=0$, then A=0, B=0, and $\Gamma = E_C^T$; (ii) if $\eta = \infty$, then $A=-E_{self} = -\infty$, $B = E_C^{GT} = \infty$, and $\Gamma = 0$; (iii) for increasing η, A is strictly negative and decreases monotonically, whence $(B+\Gamma)$ must increase monotonically; (iv) because $\zeta_i \zeta_j$ and cos(x) can be positive or negative, no statements can be made *a-priori* about the η-dependence of B, Γ, $|B|$ or $|\Gamma|$; (v) the absolute value of each *term* of Γ decreases, and the absolute value of each η-dependent *term* of B increases with increasing η; (vi) if E_C^T is *a-posteriori* positive then $(B+\Gamma)$ must be positive. Anticipating slightly, we found empirically that (vii) for fast computation η should be of the order of magnitude of $V^{1/3}$ (expressed in Å): (viii) the smaller $|B|$, $|\Gamma|$ are, the faster they converge: hence, if a good guess of a negative value for E_C^T is available, then fastest possible convergence is predicted if η is so chosen ($\eta \cong \eta_{opt}$) that $A \cong E_C^T$ (and B and Γ are both small); (ix) within the range $\eta \cong V^{1/3}$, B was found always positive and increasing with increasing η regardless of the sign of E_C^T: this is rather surprising, and hints to a monotonic increase with increasing η; (x) within the range $\eta \cong V^{1/3}$ and provided $E_C^T > 0$, Γ is positive and decreasing with increasing η; (xi) within the range $\eta \cong V^{1/3}$, for the case $E_C^T < 0$, Γ negative and increasing with increasing η was found if $E_C^T < A$, whereas if $0 > E_C^T > A$ we found three cases, $\Gamma < 0$ and $\Gamma\uparrow$, $\Gamma > 0$ and $\Gamma\uparrow$, and

$\Gamma > 0$ and $\Gamma\downarrow$: this hints to an increase of Γ from the negative value E_C^T at $\eta = 0$ to a maximum positive value for η slightly larger than η_{opt},* and then to a positive decreasing Γ for $\eta \rightarrow \infty$. These hints (vii-x) are to be taken only as "rules-of-thumb" and are presented in this section as mere trends of our data.

Finally, EWALD was improved so that at the outset it would search for all possible "degeneracies" in the vector differences $\left\{ \underset{\sim}{r}_m^o - \underset{\sim}{r}_n^o;\ m, n = 1, 2, \ldots, M \right\}$ for the crystal at hand, and then it would sequence its calculations so as to avoid and yet compensate for all repetitive calculations due to such degeneracies. A reduction in computer run times of about 40% was obtained for a small monoclinic test crystal, but this improvement was developed too late to benefit the lengthy organic crystal runs reported below. A further improvement of 120% was obtained (i) by using the 4 μsec cycle-time SRI B-5500 after the 6 μsec Stanford B-5500 had been sold; (ii) by using a machine-language intrinsic erf(x) program developed by the Burroughs Corp. in place of the subroutine described above.

D. Results - General

The crystals whose Madelung energies E_C^T (along with Δ_1, Δ_2, H, ω) were determined are:

---

*The turning-point seems to be when $A \cong -1.7 \left| E_C^T \right|$.

(i) Sodium chloride, a cubic test crystal

(ii) Yttrium chloride, a monoclinic test crystal

(iii) Dimagnesium trihydroxy monochloride tetrahydrate, a triclinic test crystal

(iv) the ion-radical salt Wurster's blue perchlorate ($TMPD^{\dot{+}}$ ClO_4^- or WBP)

(v) (1:1)-(N,N,N',N'-Tetramethyl-para-phenylenediamine: 7,7,8,8-Tetracyanoquinodimethan) ($TMPD^{\dot{+}}$ $TCNQ^{\dot{-}}$), a holoionic DA crystal

(vi) (1:1)-(N,N,N',N'-Tetramethyl-para-phenylenediamine: para-Chloranil) ($TMPD^{\dot{+}}$ $pChl^{\dot{-}}$), a holoionic DA crystal

(vii) (1:1)-(Hexamethylbenzene: para-Chloranil) (HMB: pChl), a nonionic DA crystal*

(viii) (1:1)-(Naphthalene: Tetracyanoethylene) (Naphth:TCNE), a nonionic DA crystal*

(ix) the ion-radical salt N-Methylphenazinium 7,7,8,8-Tetracyanoquinodimethanide ($MPNZ^{\dot{+}}$ $TCNQ^{\dot{-}}$)

(x) Bismuth trifluoride**

(xi) Yttrium trifluoride**

Fig. I shows the numbering scheme for the atoms of the eight larger ions involved in our calculations. For these same

---

*In a sort of "Gedankenexperiment" these crystals were considered ionic for the purpose of determining their Madelung energies.

**For Dr. D. Cubicciotti of Stanford Research Institute, in exchange for computer time; these compounds are discussed in Appendix I.

ions, Tables I through VIII list the available theoretical and experimental estimates of point-charge distributions. These estimates come from various sources:

(i) chemical "reasoning"

(ii) pure guesswork

(iii) valence-bond (VB) arguments

(iv) experimental spin densities from the electron paramagnetic resonance (EPR) determination of hyperfine coupling constants, plus semiempirical estimates of the relevant McConnell constant Q

(v) theoretical spin densities[*] from simple Hückel molecular orbital theory (SHMO)

(vi) theoretical spin densities from Hückel MO theory with McLachlan self-consistent configuration interaction procedure (HMO-McL)

(vii) theoretical spin densities from Roothaan-type closed-shell Hartree-Fock self-consistent field molecular orbital theory, with approximations suggested by Pariser, Parr, and Pople (R-SCF-PPP)

(viii) theoretical charge[**] densities from R-SCF-PPP

---

[*] Squares of the real atomic coefficients of the highest occupied pi molecular orbital of neutral molecule D if spin densities are for the monocation D^+, or if the lowest unoccupied molecular orbital of A if spin densities are for monoanion A^-.

[**] Sum of squares of atomic coefficients of all occupied pi molecular orbitals (multiplied by 2 if orbital is doubly occupied).

(ix) theoretical spin or charge densities from Roothaan-type open shell Hartree-Fock self-consistent field MO theory, with approximations of Pariser, Parr and Pople (R-OS-SCF-PPP)

(x) same as (ix), but with approximations of Mataga (R-OS-SCF-M)

(xi) same as (ix), but with added reminimization procedure (180) devised by Hoyland and Goodman (R-OS-SCF-PPP-HG)

(xii) theoretical spin or charge densities from unrestricted Hartree-Fock theory due to Amos and Snyder (181) (UHF)

In Tables I to VIII, the "Charge Assignment Label" (CAL) is a column heading used later in Tables XII to XVII to refer to the charge distributions chosen; "Species" refers to the molecule for which the calculations or the experiment was done.

Table IX lists the fundamental constants used in the EWALD programs.

Tables X through XVII describe in detail the results of EWALD runs for all crystals (except $Mg_2(OH)_3Cl \cdot 4H_2O$, YF_3, and BiF_3). The crystal and molecular structure data are taken from the literature, except that for $TMPD^+pChl^-$ and for $TMPD^+ClO_4^-$ unpublished reports had to be used: for the sake of completeness, Tables XVIII and XIX record the relevant crystallographic data for these two crystals.

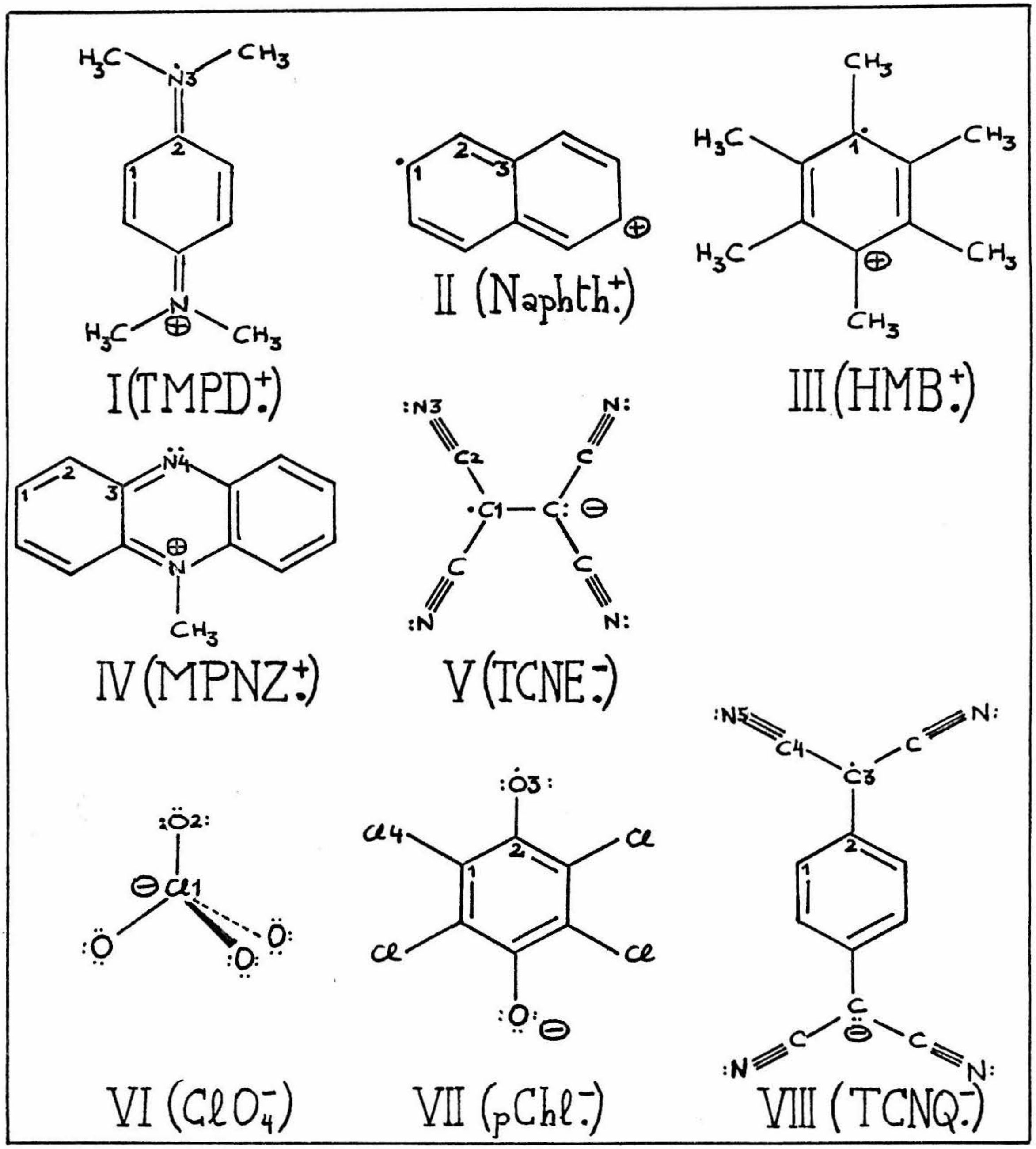

Fig. I

Structures of the molecular ions considered, with the atom-numbering schemes used in the Tables below.

TABLE I

Atom Charge Assignments for the TMPD$^{+\cdot}$ Cation, in Units of the Electronic Charge $|\varepsilon|$

Charge Assignment Label (CAL):	Ia	Ib	--	Ic‡	Id	--
Species:	TMPD	TMPD	TMPD	TMPD$^{+\cdot}$	pPD	pPD$^{+\cdot}$
Method:	Theory SHMO	Theory R-SCF-PPP	Theory R-SCF-PPP	Exp. EPR	Theory R-SCF-PPP	Exp. EPR
Density:	spin	spin	charge	spin	spin	spin
Footnote:	(a)	(b)	(c)	(d)	(e)	(f)
Atom I-1:	0.068	0.056	0.087	0.07(g)	0.071529	0.076(g)
Atom I-2:	0.034	0.109	0.032	0.09(h)	0.162699	0.122(h)
Atom I-3:	0.330	0.278	0.297	0.27(i)	0.194234	0.236(j)
I_D (k) :	--	8.06 eV	8.06 eV	--	9.88 eV	--

‡ CAL Ic' has charge 0.085 for Atom I-2 (by mistake)

(a) from McLachlan, Ref. (182); this result for 9 pi electrons can also be used for the pChl$^-$ anion (cf. Table VII)

(b) from Monkhorst and Kommandeur, Table I, No. 2 of Ref. (183)

(c) from Monkhorst and Kommandeur, Fig. 2 and 3 of Ref. (183)

(d) from Bolton, Carrington, and dos Santos-Veiga, Ref. (184)

(e) from Giacometti, Nordio, and Rigatti, Ref. (185) Tabella III, entries for -9.882 eV; the para-Phenylenediamine (pPD) study naturally omits the effects of methyl group hyperconjugation in TMPD

(f) from Melchior and Maki, Ref. (186)

(g) if McConnell's constant Q_{CH} = -28 Oersted

(h) by difference, assuming there are no negative spin densities

(i) if McConnell's constant Q_{N-Me} = 25 Oersted

(j) if McConnell's constant Q_{NH} = -25 Oersted

(k) ionization potentials obtained by Koopman's theorem; these can be too high by 2 to 4 eV according to Hoyland and Goodman, Ref. (187)

TABLE II

Atom Charge Assignments for the Naphth$^{\dot{+}}$ Cation, in Units of the Electronic Charge $|\epsilon|$

Charge Assignment Label (CAL):	--	--	IIa	--
Species:	Naphth$^{\dot{+}}$	Naphth$^{\dot{+}}$	Naphth$^{\dot{+}}$	Naphth$^{\dot{+}}$
Method:	Theory ROS-SCF-PPP-HG	Theory ROS-SCF-PPP-HG	Theory UHF	Theory UHF
Density:	spin	charge	spin	charge
Footnote:	(a)	(b)	(c)	(d)
Atom II-1:	0.0640	0.1076	0.026	0.098
Atom II-2:	0.1860	0.1694(e)	0.262	0.184
Atom II-3:	0.0	-0.0536	-0.076	-0.063

(a) from Hoyland and Goodman, Ref. (180), Table I, entries for q_1, q_2, and q_9 for Ψ_5

(b) from Hoyland and Goodman, Ref. (180), Table I, 1.0 minus entries for total charge density, and also Ref. (187) Table III

(c) from Amos and Snyder, Ref. (181), Table IV, Column 5

(d) from Amos and Snyder, Ref. (181), 1.0 minus entry in Column 6

(e) there is a discrepancy in the last digit between Ref. (180) and Ref. (187)

TABLE III

Atom Charge Assignments for the $\mathrm{HMB}^{\overset{+}{\cdot}}$ Cation, in Units of the Electronic Charge $|\varepsilon|$

Charge Assignment Label (CAL):	IIIa
Species:	$\mathrm{HMB}^{\overset{+}{\cdot}}$
Method:	Theory SHMO assuming D_{6h} symmetry
Density:	spin or charge
Atom III-1:	0.166666

TABLE IV

Atom Charge Assignments for the $\mathrm{MPNZ}^{\overset{+}{\cdot}}$ Cation, in Units of the Electronic Charge $|\varepsilon|$

Charge Assignment Label (CAL):	IVa[‡]	--
Species:	MPNZ	$\mathrm{MPNZ}^{\overset{+}{\cdot}}$
Method	Theory SHMO	Experiment EPR
Density:	spin	spin
Footnote:	(a)	(a)
Atom IV-1:	0.052	0.071
Atom IV-2:	0.044	0.024
Atom IV-3:	0.060	--
Atom IV-4:	0.189	--

[‡] CAL IVa' has charge 0.188 for Atom IV-4

(a) from Bolton, Carrington, and dos Santos-Veiga, Ref. (188)

TABLE V

Atom Charge Assignments for the TCNE$^{\bar{\cdot}}$ Anion, in Units of the Electronic Charge |ε|

Charge Assignment Label (CAL):	Va	--
Species:	TCNE	TCNE
Method:	Theory SHMO	Theory HMO-McL
Density:	spin	spin
Footnote:	(a)	(a)
Atom V-1:	-0.2814	-0.3056
Atom V-2:	-0.0348	-0.0211
Atom V-3:	-0.0745	-0.0765

(a) from Rieger and Fraenkel, Ref. (189)

TABLE VI

Atom Charge Assignments for the Perchlorate Anion, in Units of the Electronic Charge $|\epsilon|$

Charge Assignment Label (CAL):	VIa	VIb	VIc	VId	VIe
Species:	ClO_4^-	ClO_4^-	ClO_4^-	ClO_4^-	ClO_4^-
Method:	Theory VB	Theory guess 1	Theory guess 2	Theory guess 3	Theory guess 4
Density	charge	charge	charge	charge	charge
Footnote:	(a)	(b)	(c)	(d)	(e)
Atom VI-1:	-0.90	-1.0	3.0	-0.2	0.0
Atom VI-2:	-0.025	0.0	-1.0	-0.2	-0.25

(a) from Pauling, Ref. (190), page 321; but Pauling does not believe this result, <u>ibid</u>., p. 322

(b) valid if ion (with point-group symmetry C_{3v}) tumbles or rotates freely and approximates spherical symmetry, or if statistical disorder in the crystal gives a spherically symmetric average configuration

(c) naive "valence state" assignment of Monkhorst and Kommandeur, Ref. (191), rather unrealistic

(d) "perfect democracy"

(e) "tyranny of the majority": the oxygens (Pauling electronegativity 3.5) gang up on chlorine (Pauling electronegativity 3.0) and rob it of all its net charge

TABLE VII

Atom Charge Assignments for the pChl$^{\dot{-}}$ Anion, in Units of the Electronic Charge $|\epsilon|$

Charge Assignment Label (CAL):	VIIa	VIIb	VIIc	VIId
Species:	TMPD	pChl	pChl	pChl
Method:	Theory SHMO	Theory SHMO	Theory HMO-McL	Theory R-SCF-PPP
Density:	spin	spin	spin	spin
Footnote:	(a)	(b)	(c)	(d)
Atom VII-1:	-0.068	-0.1129	-0.1025	-0.103903
Atom VII-2:	-0.034	-0.0496	-0.0918	-0.118956
Atom VII-3:	-0.330	-0.2244	-0.2031	-0.153343
Atom VII-4:	0.0	0.0	0.0	-0.009944
A_A(e):	--	--	--	3.29 eV

(a) from McLachlan, Ref. (182) with signs changed: the nine pi electrons in pChl$^{\dot{-}}$ are equivalent, in this approximation, to the 9 pi electrons in TMPD$^{\dot{+}}$ or pPD$^{\dot{+}}$

(b) from Broze, Luz, and Silver, Ref. (192)

(c) from Broze, Luz, and Silver, Ref. (192)

(d) from Giacometti, Nordio, and Rigatti, Ref. (185) Tabella II, squares of entries for -3.289 eV

(e) electron affinity of pChl, from Koopman's theorem; it is expected to be too large by 2 eV

TABLE VIII

Atom Charge Assignments for the TCNQ$^{\cdot -}$ Anion, in Units of the Electronic Charge $|\epsilon|$

Charge Assignment Label (CAL):	VIIIa	VIIIb[‡]	VIIIc	VIIId	VIIIe	VIIIf	VIIIg
Species:	TCNQ$^{\cdot -}$	TCNQ	TCNQ	TCNQ	TCNQ$^{\cdot -}$	TCNQ	TCNQ$^{\cdot -}$
Method:	Theory ROS-SCF -PPP	Theory SHMO	Theory HMO-McL	Theory SHMO	Theory ROS-SCF -M	Theory R-SCF-PPP	Theory UHF
Density:	spin	spin	spin	spin	spin	spin	spin
Footnote:	(a)	(b)	(c)	(d)	(e)	(f)	(g)
Atom VIII-1:	-0.067	-0.054	-0.043	-0.047	-0.058	-0.065	-0.045
Atom VIII-2:	-0.072	-0.050	-0.010	-0.073	-0.070	-0.071	-0.056
Atom VIII-3:	-0.206	-0.225	-0.297	-0.133	-0.201	-0.199	-0.225
Atom VIII-4:	-0.007	-0.013	0.0	-0.033	-0.012	-0.006	0.0
Atom VIII-5:	-0.037	-0.047	-0.054	-0.071	-0.045	-0.044	-0.067

‡ CAL VIIIb' has charge -0.054 for Atom VIII-5 (by mistake)

(a) from Lowitz, Ref. (193), Table VI, Set 3

(b) from Rieger and Fraenkel, Ref. (189)

(c) from Rieger and Fraenkel, Ref. (189); we ignored the small negative spin density at Atom VII-4 and reset it to zero

(d) from Menefee and Pao, Ref. (194)

(e) from Lowitz, Ref. (193), Table VI, Set 7

(f) from Lowitz, Ref. (193), Table VI, Set 1

(g) from Lowitz, Ref. (193), Table VI, Set 10; again the small negative spin density at Atom VIII-4 was reset to zero

TABLE IX

Fundamental Physical Constants Used in EWALD Programs

(see Ref. (195))

Electronic charge: $|\varepsilon| = 4.80298 \times 10^{-10}$ statcoulomb

Avogadro's number: $N_o = 6.02252 \times 10^{+23}$

Conversion factor $= 4.185$ joule calorie^{-1}

whence:

$QN_o|\varepsilon|^2 = 331.974192584$ kcal Å mole^{-1}

$N_o|\varepsilon|^2 = 1.389312065 \times 10^{13}$ erg Å mole^{-1}

Conversion factor $= 23.05540$ kcal mole^{-1} eV^{-1} molecule

---

TABLE X

Crystal Coulomb Energy of Sodium Chloride (NaCl)

Crystal structure data of : T. Batuecas (196)
CELLMAP run identifier : D24
Space group : Fm3m (197)
Number of molecules per unit cell, Z = 4
Number of charged atoms per unit cell, M = 8
Cube root of unit cell volume, $V^{1/3}$ = 5.63978 Å (at 298°K)
Shortest interionic distance = 2.81989 Å (a)

INPUT PARAMETERS:

EWALD Run :	BZB7	ZZ01	BZB5A
η =	5.0	5.0	9.0
Sum limits to B term (initial): p,q,r =	3,3,3	1,1,1	3,3,3
Sum limits to Γ term: t,u,v =	1,1,1	1,1,1	1,1,1

CONVERGENCE ESTIMATES:

Final sum limits to B: p,q,r =	4,4,4	2,2,2	4,4,4
"Last" contrib. to B: (kcal/mole) =	$< 1.0 \times 10^{-10}$	$< 1.0 \times 10^{-10}$	$< 1.0 \times 10^{-10}$
"Test" contrib. to Γ (kcal/mole) =	0.0000227	0.0000227	0.0000005

B5500 COMPUTER RUN TIMES:

Compiler =	46 seconds	71 seconds	45 seconds
Processor =	121 seconds	222 seconds	118 seconds
I/O time =	7 seconds	91 seconds	7 seconds

INPUT CHARGE ASSIGNMENT: Sodium cation = +1, Chloride anion = -1

TABLE X--Continued

Data Col. No.	:	X-1	X-2	X-3
EWALD No.	:	BZB7	ZZ01	BZB5A
Cation Charge	:	1	1	1
Anion Charge	:	-1	-1	-1
η	=	5.0	5.0	9.0
RESULTS (kcal/mole):				
A	=	-148.519066	-148.519066	-199.259236
B	=	1.071426	1.071426	14.894793
Γ	=	- 58.285975	- 58.285975	- 21.369240
E_C^T	=	-205.733615	-205.733615	-205.733684
$-\Delta$	=	0.0	0.0	0.0
E_C	=	-205.733615	-205.733615	-205.733684
RESULTS (eV/molecule):				
Cation Δ_2	=	0.0	0.0	0.0
Anion Δ_1	=	0.0	0.0	0.0
Δ	=	0.0	0.0	0.0
H	=	- 5.106222	- 5.106222	- 5.106222
E_C	=	- 8.923446	- 8.923446	- 8.923449
MADELUNG CONSTANT, ω	=	1.747564	1.747564	1.747564

(a) Note that Johnson and Templeton (198) use 2.813840 Å and get ω = 1.74756.

TABLE XI

Crystal Coulomb Energy of Yttrium (Tri)chloride (YCl_3)

Crystal structure data of : Templeton & Carter(199)
CELLMAP run identifier : B21
Space group : C2/m
Number of Molecules per unit cell, Z = 4
Number of charged atoms per unit cell, M = 16
Cube root of unit cell volume, $V^{1/3}$ = 7.919833 Å
Shortest interionic distance = 2.5845506 Å

INPUT PARAMETERS:

EWALD Run :	PX7	PX1	PX6	PX8,ZZ04 (a)
=	3.0	5.0	8.0	14.2
Sum limits to B term (initial): p,q,r =	3,3,3	3,3,3	3,3,3	3,3,3
Sum limits to Γ term: t,u,v =	1,1,1	1,1,1	1,1,1	1,1,1
CONVERGENCE ESTIMATES:				
Final sum limits to B: p,q,r =	4,4,4	4,4,4	5,5,5	6,6,6
"Last" contrib. to B (kcal/mole) =	3.0×10^{-9}	1.6×10^{-5}	2.5×10^{-6}	3.29×10^{-4}
"Test" contrib. to Γ: (kcal/mole) =	-0.432366	-0.038092	-0.001043	-7.9×10^{-7}
B5500 COMPUTER RUN TIMES:				
Compiler =	337 seconds	47 seconds	49 seconds	49 seconds (70)
Processor =	760 seconds	607 seconds	744 seconds	766 seconds (653)
I/O time =	68 seconds	61 seconds	64 seconds	70 seconds (92)

INPUT CHARGE ASSIGNMENTS: Yttrium cation = +3, Chloride anion = -1

TABLE XI--Continued

Data Col. No. :	XI-1	XI-2	XI-3	XI-4
EWALD No. :	PX7	PX1	PX6	PX8, ZZ04
Cation Charge :	3.0	3.0	3.0	3.0
Anion Charge :	-1.0	-1.0	-1.0	-1.0
η =	3.0	5.0	8.0	14.2
RESULTS (kcal/mole):				
A =	-491.535896	-634.570114	-802.674757	-1069.396564
B =	1.114277	11.787606	46.866222	153.064590
Γ =	-575.290176	-444.767471	-311.913885	- 151.395956
E_C^T =	-1065.711791	-1067.549977	-1067.722420	-1067.727929
$-\Delta$ =	-272.010458	-272.010458	-272.010458	- 272.010458
E_C =	-1337.722249	-1339.560435	-1339.732878	-1339.738387
RESULTS (eV/molecule) :				
Cation Δ_2 =	0.0	0.0	0.0	0.0
Anion Δ_1 =	11.798125	11.798125	11.798125	11.798125
Δ =	11.798125	11.798125	11.798125	11.798125
H =	- 49.841485	- 49.841485	- 49.841485	- 49.841485
E_C =	- 58.022079	- 58.101808	- 58.109288	- 58.109526
MADELUNG CONSTANT, ω =	1.163734	1.165732	1.165882	1.165887
Johnson-Templeton constant, $A(R_o)$ =	8.296826	8.311137	8.312478	8.312522

(a) Runs PX8 and ZZ04 differed in programming details, but were given the same input parameters and yielded results which were identical in all aspects; computer run times were different, and those for ZZ04 are given in parentheses.

TABLE XII

Crystal Coulomb Energy of Wurster's Blue Perchlorate ($TMPD^{\dot{+}}\ ClO_4^-$)

Crystal structure data of : Turner & Albrecht (200) (see Table XVIII)
CELLMAP Run Identifier : A13
Space group : Pn2n (?)
Number of molecules per unit cell, Z = 2
Number of charged atoms per unit cell, M = 26
Cube root of unit cell volume, $V^{1/3}$ = 8.5480592 Å

INPUT PARAMETERS:			
EWALD Run Identifier	:	ZZ09	ZZ03
Convergence parameter, η	=	7.0	9.0
Initial sum limits to B term: p,q,r	=	3,4,4	3,4,4
Sum limits to Γ term: t,u,v	=	1,1,1	1,1,1
Charge assignments: see below for CAL (Charge Assignment Label)			
CONVERGENCE ESTIMATES:			
Final sum limits to B term: p,q,r	=	4,5,5	4,5,5
"Last" contribution to B term, for e = 1, (kcal/mole)	=	+0.0000000001	+0.0000000229
"Test" contribution to Γ term, Γ_{test} for e = 1, due to (d = t+1, f = 0, g = 0) cell (kcal/mole)	=	+0.0000283667	+0.0000422864
B-5500 COMPUTER RUN TIMES:			
Compiler time	=	70 seconds	95 seconds
Processor time	=	3556 seconds	3323 seconds
Input/Output time	=	100 seconds	102 seconds

TABLE XII--Continued

Data Col. No. :	XII-1	XII-2	XII-3	XII-4
EWALD No. :	ZZ09 (e = 1)	ZZ03 (e = 1)	ZZ09 (e = 3)	ZZ03 (e = 3)
Cation CAL :	Ia	Ia	Ib	Ib
Anion CAL :	VIb	VIb	VIb	VIb
η =	7.0	9.0	7.0	9.0
RESULTS (kcal/mole):				
A =	-71.803358	-81.417355	-69.036170	-78.279659
B =	13.607681	22.208471	14.208432	23.071330
Γ =	5.155473	6.166234	11.463668	11.841760
E_C^T =	-53.040203	-53.042650	-43.364070	-43.366569
$-\Delta$ =	-42.232897	-42.232897	-51.724968	-51.724968
E_C =	-95.273100	-95.275547	-95.089038	-95.091537
RESULTS (eV/molecule):				
Cation Δ_2 =	1.831801	1.831801	2.243508	2.243508
Anion Δ_1 =	0.0	0.0	0.0	0.0
Δ =	1.831801	1.831801	2.243508	2.243508
H =	- 2.767859	- 2.767859	- 2.770803	- 2.770803
E_C =	- 4.132355	- 4.132461	- 4.124372	- 4.124480
MADELUNG CONSTANT, ω =	1.492979	1.493017	1.488511	1.488550

Data Col. No. :	XII-5	XII-6	XII-7	XII-8
EWALD No. :	ZZ09 (e = 11)	ZZ03 (e = 11)	ZZ09 (e = 10)	ZZ03 (e = 10)
Cation CAL :	Ib	Ib	Ib	Ib
Anion CAL :	VIa	VIa	VId	VId
η =	7.0	9.0	7.0	9.0
RESULTS (kcal/mole):				
A =	-58.166605	-65.954731	-22.659361	-25.693300
B =	13.722173	22.228868	10.644860	16.987968
Γ =	21.802492	21.084433	37.916887	34.614653
E_C^T =	-22.641941	-22.641430	25.902386	25.909320
$-\Delta$ =	-72.389679	-72.389679	-120.465438	-120.465438
E_C =	-95.031620	-95.031109	-94.563052	-94.556118
RESULTS (eV/molecule):				
Cation Δ_2 =	2.243508	2.243508	2.243508	2.243508
Anion Δ_1 =	0.896307	0.896307	2.981534	2.981534
Δ =	3.139815	3.139815	5.225042	5.225042
H =	- 2.770674	- 2.770674	- 2.769766	- 2.769766
E_C =	- 4.121881	- 4.121860	- 4.101558	- 4.101257
MADELUNG CONSTANT, ω =	1.487681	1.487674	1.480723	1.480832

TABLE XII--Continued

Data Col. No.	:	XII-9	XII-10	XII-11	XII-12
EWALD No.	:	ZZ09 (e = 9)	ZZ03 (e = 9)	ZZ09 (e = 5)	ZZ03 (e = 5)
Cation CAL	:	Ib	Ib	Ib	Ib
Anion CAL	:	VIe	VIe	VIc	VIc
η	=	7.0	9.0	7.0	9.0
RESULTS (kcal/mole):					
A	=	-25.557912	-28.979948	-764.688302	-867.075034
B	=	9.870574	15.701534	3.853363	7.656566
Γ	=	24.438274	22.033413	-1142.152999	-1043.859363
E_C^T	=	18.750936	18.755000	-1902.987938	-1093.277831
$-\Delta$	=	-103.158694	-103.158694	1812.051839	1812.051839
E_C	=	-94.407758	-94.403694	-90.936099	-91.225992
RESULTS (eV/molecule):					
Cation Δ_2	=	2.243508	2.243508	2.243508	2.243508
Anion Δ_1	=	2.230875	2.230875	-80.839058	-80.839058
Δ	=	4.474383	4.474383	-78.595550	-78.595550
H	=	- 2.769507	- 2.769507	- 2.765618	- 2.765618
E_C	=	- 4.094822	- 4.094646	- 3.944243	- 3.956817
MADELUNG CONSTANT, ω	=	1.478538	1.478475	1.426170	1.430717

Data Col. No.	:	XII-13	XII-14	XII-15	XII-16
EWALD No.	:	ZZ09 (e = 2)	ZZ03 (e = 2)	ZZ09 (e = 6)	ZZ03 (e = 6)
Cation CAL	:	Ic	Ic	Ic	Ic
Anion CAL	:	VIb	VIb	VIa	VIa
η	=	7.0	9.0	7.0	9.0
RESULTS (kcal/mole):					
A	=	-68.498546	-77.670051	-57.628982	-65.345124
B	=	14.182570	23.019607	13.696023	22.176317
Γ	=	11.182421	11.514482	21.518390	20.754839
E_C^T	=	-43.133556	-43.135962	-22.414569	-22.413968
$-\Delta$	=	-52.275518	-52.275518	-72.940228	-72.940228
E_C	=	-95.409074	-95.411480	-95.354797	-95.354196
RESULTS (eV/molecule):					
Cation Δ_2	=	2.267387	2.267387	2.267387	2.267387
Anion Δ_1	=	0.0	0.0	0.896307	0.896307
Δ	=	2.267387	2.267387	3.163694	3.163694
H	=	- 2.772759	- 2.772759	- 2.772658	- 2.772658
E_C	=	- 4.138253	- 4.138357	- 4.135899	- 4.135873
MADELUNG CONSTANT, ω	=	1.492468	1.492506	1.491673	1.491644

TABLE XII--Continued

Data Col. No. :	XII-17	XII-18	XII-19	XII-20
EWALD No. :	ZZ09 (e = 8)	ZZ03 (e = 8)	ZZ09 (e = 7)	ZZ03 (e = 7)
Cation CAL :	Ic	Ic	Ic	Ic
Anion CAL :	VId	VId	VIe	VIe
η =	7.0	9.0	7.0	9.0
RESULTS (kcal/mole):				
A =	-22.121738	-25.083693	-25.020288	-28.370340
B =	10.616692	16.929626	9.841828	15.641538
Γ =	37.612802	34.268840	24.128480	21.682967
E_C^T =	26.107757	26.114773	18.950019	18.954164
$-\Delta$ =	-121.015988	-121.015988	-103.709243	-103.709243
E_C =	-94.908231	-94.901215	-94.759224	-94.755079
RESULTS (eV/molecule):				
Cation Δ_2 =	2.267387	2.267387	2.267387	2.267387
Anion Δ_1 =	2.981534	2.981534	2.230875	2.230875
Δ =	5.248921	5.248921	4.498262	4.498262
H =	- 2.771954	- 2.771954	- 2.771753	- 2.771753
E_C =	- 4.116529	- 4.116225	- 4.110066	- 4.109887
MADELUNG CONSTANT, ω =	1.485064	1.484954	1.482840	1.482775

Data Col. No. :	XII-21	XII-22	XII-23	XII-24
EWALD No. :	ZZ09 (e = 4)	ZZ03 (e = 4)	ZZ09 (e = 13)	ZZ03 (e = 13)
Cation CAL :	Id	Id	Id	Id
Anion CAL :	VIb	VIb	VId	VId
η =	7.0	9.0	7.0	9.0
RESULTS (kcal/mole):				
A =	-66.600646	-75.518034	-20.223837	-22.931676
B =	14.977405	24.179964	11.338461	18.000543
Γ =	16.540403	16.252931	42.993806	39.046572
E_C^T =	-35.082838	-35.085140	34.108430	34.115440
$-\Delta$ =	-60.678699	-60.678699	-129.419169	-129.419169
E_C =	-95.761537	-95.763839	-95.310739	-95.303729
RESULTS (eV/molecule):				
Cation Δ_2 =	2.631865	2.631865	2.631865	2.631865
Anion Δ_1 =	0.0	0.0	2.981534	2.981534
Δ =	2.631865	2.631865	5.613399	5.613399
H =	- 2.779211	- 2.779211	- 2.779326	- 2.779326
E_C =	- 4.153540	- 4.153640	- 4.133988	- 4.133684
MADELUNG CONSTANT, ω =	1.494503	1.494539	1.487407	1.487297

TABLE XII--Continued

Data Col. No.	:	XII-25	XII-26
EWALD No.	:	ZZ09 (e = 12)	ZZ03 (e = 12)
Cation CAL	:	Id	Id
Anion CAL	:	VIe	VIe
η	=	7.0	9.0
RESULTS (kcal/mole):			
A	=	-23.122388	-26.218323
B	=	10.545331	16.690095
Γ	=	29.515239	26.470521
E_C^T	=	16.938182	16.942292
$-\Delta$	=	-112.112424	-112.112424
E_C	=	-95.174242	-95.170132
RESULTS (eV/molecule):			
Cation Δ_2	=	2.631865	2.631865
Anion Δ_1	=	2.230875	2.230875
Δ	=	4.862740	4.862740
H	=	- 2.779355	- 2.779355
E_C	=	- 4.128067	- 4.127889
MADELUNG CONSTANT, ω	=	1.485261	1.485197

TABLE XIII

Crystal Coulomb Energy of (1:1)-(N,N,N',N'-Tetramethyl-para-phenylenediamine:7,7,8,8-Tetracyanoquinodimethan)
($TMPD^{\dagger}$ $TCNQ^{\overline{\cdot}}$)

Crystal structure data : A. W. Hanson (160)
CELLMAP Run Identifier : A19
Space group : $\underline{C2}/\underline{m}$
Number of molecules per unit cell, Z = 2
Number of charged atoms per unit cell, M = 48
Cube root of unit cell volume, $V^{1/3}$ = 9.869961 Å

INPUT PARAMETERS:

EWALD Run Identifier	:	ZZ12	ZZ06
Convergence parameter, η	=	10.0	15.0
Initial sum limits to B term: p,q,r	=	3,3,3	3,3,3
Sum limits to Γ term: t,u,v	=	1,1,1	1,1,1
Charge assignments: see below for CAL (Charge Assignment Label)			

CONVERGENCE ESTIMATES:

Final sum limits to B term: p,q,r	=	4,4,4	4,4,4
"Last" contribution to B term, for e = 1, (kcal/mole)	=	0.0000192847	0.0008132633
"Test" contribution to Γ term, Γ_{test} for e = 1, due to (d = t+1, f = 0, g = 0) cell (kcal/mole)	=	-0.0000000468	$< 1.0 \times 10^{-10}$

B-5500 COMPUTER RUN TIMES:

Compiler time	=	85 seconds	70 seconds
Processor time	=	8837 seconds	7526 seconds
Input/Output time	=	107 seconds	110 seconds

TABLE XIII--Continued

Data Col. No. :	XIII-1	XIII-2	XIII-3	XIII-4
EWALD No. :	ZZ12 (e = 1)	ZZ06 (e = 1)	ZZ12 (e = 2)	ZZ06 (e = 2)
Cation CAL :	Ic'	Ic'	Ic'	Ic'
Anion CAL :	VIIIa	VIIIa	VIIIb'	VIIIb'
η =	10.0	15.0	10.0	15.0
RESULTS (kcal/mole):				
A =	-17.925667	-21.954369	-18.608925	-22.791186
B =	6.118647	12.509434	6.042233	12.400679
Γ_T =	20.495305	18.132954	19.255440	-17.072519
E_C =	8.688285	8.688020	6.688747	6.682011
$-\Delta$ =	-100.616085	-100.616085	-99.476207	-99.476207
E_C =	-91.927800	-91.928065	-92.787460	-92.794196
RESULTS (eV/molecule):				
Cation Δ_2 =	2.204701	2.204701	2.204701	2.204701
Anion Δ_1 =	2.159400	2.159400	2.109959	2.109959
Δ =	4.364101	4.364101	4.314660	4.314660
H =	- 3.081412	- 3.081412	- 3.119223	- 3.119223
E_C =	- 3.987257	- 3.987268	- 4.024543	- 4.024836
MADELUNG CONSTANT, ω =	1.293971	1.293974	1.290239	1.290333

Data Col. No. :	XIII-5	XIII-6	XIII-7	XIII-8
EWALD No. :	ZZ12 (e = 3)	ZZ06 (e = 3)	ZZ12 (e = 4)	ZZ06 (e = 4)
Cation CAL :	Ic'	Ic'	Ic'	Ic'
Anion CAL :	VIIIc	VIIIc	VIIId	VIIId
η =	10.0	15.0	10.0	15.0
RESULTS (kcal/mole):				
A =	-22.534933	-27.599543	-15.556765	-19.053069
B =	5.966947	12.343346	5.776354	11.780638
Γ_T =	13.921365	12.609139	20.806178	18.295914
E_C =	- 2.646621	- 2.647058	11.025766	11.023483
$-\Delta$ =	-86.842786	-86.842786	-100.431013	-100.431013
E_C =	-89.489407	-89.489844	-89.405247	-89.407530
RESULTS (eV/molecule):				
Cation Δ_2 =	2.204701	2.204701	2.204701	2.204701
Anion Δ_1 =	1.562000	1.562000	2.151373	2.151373
Δ =	3.766701	3.766701	4.356074	4.356074
H =	- 3.005797	- 3.005797	- 3.008714	- 3.008714
E_C =	- 3.881494	- 3.881513	- 3.877844	- 3.877943
MADELUNG CONSTANT, ω =	1.291336	1.291342	1.288871	1.288904

TABLE XIII--Continued

Data Col. No.	:	XIII-9	XIII-10	XIII-11	XIII-12
EWALD No.	:	ZZ12 (e = 5)	ZZ06 (e = 5)	ZZ12 (e = 6)	ZZ06 (e = 6)
Cation CAL	:	Ic'	Ic'	Ic'	Ic'
Anion CAL	:	VIIIe	VIIIe	VIIIf	VIIIf
η	=	10.0	15.0	10.0	15.0
RESULTS (kcal/mole):					
A	=	-17.557574	-21.503549	-17.637866	-21.601886
B	=	5.984813	12.255828	6.035977	12.335283
Γ_T	=	20.207126	17.881666	20.105518	17.769966
E_C	=	8.634364	8.633945	8.503629	8.503363
$-\Delta$	=	-99.689427	-99.689427	-99.849724	-99.849724
E_C	=	-91.055063	-91.055482	-91.346095	-91.346361
RESULTS (eV/molecule):					
Cation Δ_2	=	2.204701	2.204701	2.204701	2.204701
Anion Δ_1	=	2.119207	2.119207	2.126160	2.126160
Δ	=	4.323908	4.323908	4.330861	4.330861
H	=	- 3.055664	- 3.055664	- 3.064104	- 3.064104
E_C	=	- 3.949403	- 3.949421	- 3.962026	- 3.962038
MADELUNG CONSTANT, ω	=	1.292486	1.292492	1.293046	1.293049

Data Col. No.	:	XIII-13	XIII-14
EWALD No.	:	ZZ12 (e = 7)	ZZ06 (e = 7)
Cation CAL	:	Ic'	Ic'
Anion CAL	:	VIIIg	VIIIg
η	=	10.0	15.0
RESULTS (kcal/mole):			
A	=	-18.808385	-23.035485
B	=	5.843242	12.001998
Γ_T	=	17.368411	15.435415
E_C	=	4.403958	4.401928
$-\Delta$	=	-94.448315	-94.448315
E_C	=	-90.045057	-90.046387
RESULTS (EV/molecule):			
Cation Δ_2	=	2.204701	2.204701
Anion Δ_1	=	1.891880	1.891880
Δ	=	4.096581	4.096581
H	=	- 3.024899	- 3.024899
E_C	=	- 3.905595	- 3.905653
MADELUNG CONSTANT, ω	=	1.291149	1.291168

TABLE XIV

Crystal Coulomb Energy of (1:1)-(N,N,N',N'-Tetramethyl-para-phenylenediamine: para-Chloranil)
(TMPD$^{\dot{+}}$ pChl$^{\dot{-}}$)

Crystal structure data of : S. C. Wallwork (91) (see Table XIX)
CELLMAP Run Identifier : D26
Space group : $\underline{C}2/\underline{m}$
Number of molecules per unit cell, Z = 2
Number of charged atoms per unit cell, M = 40
Cube root of unit cell volume, $V^{1/3}$ = 9.5742868 Å

INPUT PARAMETERS:

EWALD Run Identifier : ZZ05
Convergence parameter, η = 12.0
Initial sum limits to B term:
p,q,r = 3,3,3
Sum limits to Γ term:
t,u,v = 1,1,1
Charge assignments: see below for CAL (Charge Assignment Label)

CONVERGENCE ESTIMATES:

Final sum limits to B term:
p,q,r = 5,5,5
"Last" contribution to B term, for e = 1, (kcal/mole) = 0.0003658670
"Test" contribution to Γ term, Γ_{test} for e = 1, due to (d = t+1, f = 0, g = 0) cell (kcal/mole) = 1.0×10^{-10}

B-5500 COMPUTER RUN TIMES:

Compiler time = 69 seconds
Processor time = 7847 seconds
Input/Output time = 106 seconds

TABLE XIV--Continued

Data Col. No.	:	XIV-1	XIV-2	XIV-3	XIV-4
EWALD No.	:	ZZ05 (e = 7)	ZZ05 (e=12)	ZZ05 (e = 6)	ZZ05 (e = 5)
Cation CAL	:	Ia	Ia	Ia	Ia
Anion CAL	:	VIIa	VIIb	VIIc	VIId
η	=	12.0	12.0	12.0	12.0
RESULTS (kcal/mole):					
A	=	-32.339147	-26.782901	-25.750280	-24.227530
B	=	6.297833	7.083324	7.287370	7.710442
Γ_T	=	9.886424	15.196729	17.951436	19.750383
E_C	=	-16.154890	- 4.502847	- 0.511474	3.233295
$-\Delta$	=	-85.216636	-97.262210	-101.674288	-105.041229
E_C	=	-101.371526	-101.765057	-102.185762	-101.807934
RESULTS (eV/molecule):					
Cation Δ_2	=	1.821351	1.821351	1.821351	1.821351
Anion Δ_1	=	1.874817	2.397279	2.588648	2.734685
Δ	=	3.696168	4.218630	4.409999	4.556036
H	=	- 3.367022	- 3.392768	- 3.405868	- 3.402497
E_C	=	- 4.396867	- 4.413936	- 4.432183	- 4.415796
MADELUNG CONSTANT, ω	=	1.305862	1.300984	1.301337	1.297810

Data Col. No.	:	XIV-5	XIV-6	XIV-7	XIV-8
EWALD No.	:	ZZ05 (e = 8)	ZZ05 (e=10)	ZZ05 (e = 9)	ZZ05 (e-11)
Cation CAL	:	Ib	Ib	Ib	Ib
Anion CAL	:	VIIa	VIIb	VIIc	VIId
η	=	12.0	12.0	12.0	12.0
RESULTS (kcal/mole):					
A	=	-29.104392	-23.548146	-22.515525	-20.992775
B	=	6.499017	7.025759	7.193447	7.535748
Γ_T	=	15.214924	20.368214	23.087060	24.831212
E_C	=	- 7.390452	3.845827	7.764982	11.374185
$-\Delta$	=	-94.728734	-106.774309	-111.186387	-114.553328
E_C	=	-102.119186	-102.928482	-103.421405	-103.179143
RESULTS (eV/molecule):					
Cation Δ_2	=	2.233927	2.233927	2.233927	2.233927
Anion Δ_1	=	1.874817	2.397279	2.588648	2.734685
Δ	=	4.108744	4.631206	4.822575	4.968612
H	=	- 3.389885	- 3.423817	- 3.438371	- 3.437539
E_C	=	- 4.429296	- 4.464398	- 4.485778	- 4.475270
MADELUNG CONSTANT, ω	=	1.306621	1.303924	1.304623	1.301882

TABLE XIV--Continued

Data Col. No.	:	XIV-9	XIV-10	XIV-11	XIV-12
EWALD No.	:	ZZ05 (e = 2)	ZZ05 (e = 4)	ZZ05 (e = 3)	ZZ05 (e = 1)
Cation CAL	:	Ic'	Ic'	Ic'	Ic'
Anion CAL	:	VIIa	VIIb	VIIc	VIId
n	=	12.0	12.0	12.0	12.0
RESULTS (kcal/mole):					
A	=	-28.357338	-22.801091	-21.768470	-20.245720
B	=	6.449782	6.886061	7.050417	7.360370
Γ_T	=	14.500237	19.579168	22.301744	24.020214
E_C	=	- 7.407318	3.664138	7.583691	11.134863
$-\Delta$	=	-93.739057	-105.784631	-110.196709	-113.563649
E_C	=	-101.146375	-102.120493	-102.613018	-102.428786
RESULTS (eV/molecule):					
Cation Δ_2	=	2.191001	2.191001	2.191001	2.191001
Anion Δ_1	=	1.874817	2.397279	2.588648	2.734685
Δ	=	4.065818	4.588280	4.779649	4.925686
H	=	- 3.360216	- 3.397214	- 3.411660	- 3.412000
E_C	=	- 4.387101	- 4.429352	- 4.450715	- 4.442724
MADELUNG CONSTANT, ω	=	1.305601	1.303819	1.304560	1.302088

TABLE XV

Crystal Coulomb Energy of N-Methylphenazinium 7,7,8,8-Tetracyanoquinodimethanide
$(\mathrm{MPNZ}^{\dot{+}}\ \mathrm{TCNQ}^{\dot{-}})$

Crystal structure data of : C. J. Fritchie, Jr. (145)

CELLMAP Run Identifier : E3
Space group : $P\bar{1}$
Number of molecules per unit cell, Z = 1
Number of charged atoms per unit cell, M = 30
Cube root of unit cell volume, $V^{1/3}$ = 7.778924 Å

INPUT PARAMETERS			
EWALD Run Identifier	:	ZZ11	ZZ10
Convergence parameter,	=	6.0	9.0
Initial sum limits to B term: p,q,r	=	3,3,3	3,3,3
Sum limits to Γ term: t,u,v	=	1,1,1	1,1,1
Charge assignments: see below for CAL (Charge Assignment Label)			
CONVERGENCE ESTIMATES:			
Final sum limits to B term: p,q,r	=	4,4,4	5,5,5
"Last" contribution to B term, for e = 1, (kcal/mole)	=	0.0018434927	0.0002289059
"Test" contribution to Γ term, Γ_{test} for e = 1, due to (d = t+1, f = 0, g = 0) cell (kcal/mole)	=	0.0890061284	0.0184908437
B-5500 COMPUTER RUN TIMES:			
Compiler time	=	70 seconds	70 seconds
Processor time	=	2897 seconds	3481 seconds
Input/Output time	=	101 seconds	101 seconds

TABLE XV--Continued

Data Col. No.	:	XV-1	XV-2	XV-3	XV-4
EWALD No.	:	ZZ11 (e = 1)	ZZ10 (e = 1)	ZZ11 (e = 2)	ZZ10 (e = 2)
Cation CAL	:	IVa'	IVa	IVa	IVa
Anion CAL	:	VIIIa	VIIIa	VIIIb	VIIIb
η	=	6.0	9.0	6.0	9.0
RESULTS (kcal/mole):					
A	=	-13.123411	-16.127294	-13.672609	-16.745457
B	=	89.402120	104.951976	85.542947	100.263065
Γ_T	=	38.319964	26.282846	35.961677	24.572765
E_C	=	114.598673	115.107529	107.832017	108.090374
$-\Delta$	=	-106.892389	-107.104183	-103.832754	-103.832754
E_C	=	7.706284	8.003346	3.999262	4.257619
RESULTS (eV/molecule):					
Cation Δ_2	=	2.474001	2.483188	2.483188	2.483188
Anion Δ_1	=	2.162326	2.162326	2.020431	2.020431
Δ	=	4.636328	4.645514	4.503620	4.503620
H	=	- 1.679747	- 1.683031	- 1.688516	- 1.688516
E_C	=	0.334251	0.347135	0.173463	0.184669
MADELUNG CONSTANT, ω	=	- 0.198989	- 0.206256	- 0.102731	- 0.109368

Data Col. No.	:	XV-5	XV-6	XV-7	XV-8
EWALD No.	:	ZZ11 (e = 3)	ZZ10 (e = 3)	ZZ11 (e = 4)	ZZ10 (e = 4)
Cation CAL	:	IVa	IVa	IVa	IVa
Anion CAL	:	VIIIc'	VIIIc'	VIIId	VIIId
η	=	6.0	9.0	6.0	9.0
RESULTS (kcal/mole):					
A	=	-17.695692	-21.672708	-10.839688	-13.275853
B	=	82.154302	96.558240	80.933070	94.783479
Γ_T	=	29.898179	19.729060	36.587065	25.444840
E_C	=	94.356790	94.614592	106.680446	106.952466
$-\Delta$	=	-93.019725	-93.019725	-106.852818	-106.852818
E_C	=	1.337064	1.594867	- 0.172372	0.099647
RESULTS (eV/molecule):					
Cation Δ_2	=	2.483188	2.483188	2.483188	2.483188
Anion Δ_1	=	1.551429	1.551429	2.151423	2.151423
Δ	=	4.034618	4.034618	4.634611	4.634611
H	=	- 1.673553	- 1.673553	- 1.705926	- 1.705926
E_C	=	0.057994	0.069175	- 0.007476	0.004322
MADELUNG CONSTANT, ω	=	- 0.034653	- 0.041334	0.004383	- 0.002534

TABLE XV--Continued

Data Col. No.:	XV-9	XV-10	XV-11	XV-12
EWALD No. :	ZZ11 (e = 5)	ZZ10 (e = 5)	ZZ11 (e = 6)	ZZ10 (e = 6)
Cation CAL :	IVa	IVa	IVa	IVa
Anion CAL :	VIIIe	VIIIe	VIIIf	VIIIf
η =	6.0	9.0	6.0	9.0
RESULTS (kcal/mole):				
A =	-12.806113	-15.684221	-12.885025	-15.780868
B =	86.948334	101.833840	88.219014	103.273969
Γ_T =	37.495823	25.740102	37.675918	25.760821
E_C^T =	111.638044	111.889721	113.009907	113.253922
$-\Delta$ =	-106.163054	-106.163054	-106.330127	-106.330127
E_C =	5.474990	5.726666	6.679780	6.923795
RESULTS (eV/molecule):				
Cation Δ_2 =	2.483188	2.483188	2.483188	2.483188
Anion Δ_1 =	2.121505	2.121505	2.128752	2.128752
Δ =	4.604694	4.604694	4.611940	4.611940
H =	- 1.684208	- 1.684208	- 1.682904	- 1.682904
E_C =	0.237471	0.248387	0.289727	0.300311
MADELUNG CONSTANT, ω =	- 0.140999	- 0.147480	- 0.172159	- 0.178448

Data Col. No.:	XV-13	XV-14
EWALD No. :	ZZ11 (e = 7)	ZZ10 (e = 7)
Cation CAL :	IVa	IVa
Anion CAL :	VIIIg	VIIIg
η =	6.0	9.0
RESULTS (kcal/mole):		
A =	-14.035437	-17.189830
B =	82.969765	97.277693
Γ_T =	33.737643	22.841083
E_C^T =	102.671971	102.928946
$-\Delta$ =	-100.929501	-100.929501
E_C =	1.742469	1.999444
RESULTS (eV/molecule):		
Cation Δ_2 =	2.483188	2.483188
Anion Δ_1 =	1.894506	1.894506
Δ =	4.377695	4.377695
H =	- 1.694709	- 1.694709
E_C =	0.075577	0.086723
MADELUNG CONSTANT, ω =	- 0.044596	- 0.051173

TABLE XVI

Crystal Coulomb Energy of (1:1)-(Naphthalene:Tetracyanoethylene) $(\text{Naphth}^{\dot{+}}\ \text{TCNE}^{\dot{-}})$

Crystal structure data of : Williams & Wallwork (85)

CELLMAP Run Identifier : E1
Space group : $\underline{C}\ 2/\underline{m}$
Number of molecules per unit cell, Z = 2
Number of charged atoms per unit cell, M = 40
Cube root of unit cell volume, $V^{1/3}$ = 8.7166689 Å

INPUT PARAMETERS:

EWALD Run Identifier	:	ZZ07	ZZ13
Convergence parameter, η	=	10.0	15.0
Initial sum limits to B term: p,q,r	=	3,3,3	3,3,3
Sum limits to Γ term: t,u,v	=	1,1,1	1,1,1
Charge assignments: see below for CAL (Charge Assignment Label)			

CONVERGENCE ESTIMATES:

Final sum limits to B term: p,q,r	=	5,5,5	5,5,5
"Last" contribution to B term, for e = 1, (kcal/mole)	=	0.0000033382	0.0003552742
"Test" contribution to Γ term, Γ_{test} for e = 1, due to (d = t+1, f = 0, g = 0) cell (kcal/mole)	=	0.0000081735	0.0000000564

B-5500 COMPUTER RUN TIMES:

Compiler time	=	70 seconds	69 seconds
Processor time	=	5904 seconds	4992 seconds
Input/Output time	=	98 seconds	98 seconds

TABLE XVI--Continued

Data Col. No.	:	XVI-1	XVI-2
EWALD No.	:	ZZ07 (e = 1)	ZZ13 (e = 1)
Cation CAL	:	IIa	IIa
Anion CAL	:	Va	Va
η	=	10.0	15.0
RESULTS (kcal/mole):			
A	=	-32.224436	-39.466713
B	=	12.717601	22.745957
Γ_T	=	14.795215	12.009300
E_C	=	- 4.711620	- 4.711456
$-\Delta$	=	-94.557419	-94.557419
E_C	=	-99.269039	-99.268875
RESULTS (eV/molecule):			
Cation Δ_2	=	1.416489	1.416489
Anion Δ_1	=	2.684825	2.684825
Δ	=	4.101314	4.101314
H	=	- 3.357014	- 3.357014
E_C	=	- 4.305674	- 4.305667
MADELUNG CONSTANT, ω	=	1.285590	1.282588

TABLE XVII

Crystal Coulomb Energy of (1:1)-(Hexamethylbenzene: para-Chloranil) ($HMB^{\dot{+}}\ pChl^{\dot{-}}$)

Crystal structure data of : Harding, Wallwork, Jones, & Marsh (104)

CELLMAP Run Identifier : A15

Space group : $\underline{P}2_1/\underline{c}$

Number of molecules per unit cell, Z = 2

Number of charged atoms per unit cell, M = 36

Cube root of unit cell volume, $V^{1/3}$ = 9.7441567 Å

INPUT PARAMETERS:

EWALD Run Identifier	:	ZZ02	ZZ08
Convergence parameter, η	=	9.0	10.0
Initial sum limits to B term: p,q,r	=	3,3,3	3,3,3
Sum limits to Γ term: t,u,v	=	1,1,1	1,1,1
Charge assignments: see below for CAL (Charge Assignment Label)			

CONVERGENCE ESTIMATES:

Final sum limits to B term: p,q,r	=	4,4,4	4,4,4
"Last" contribution to B term, for e = 1, (kcal/mole)	=	0.0001671385	0.0004050352
"Test" contribution to Γ term, Γ_{test} for e = 1, due to (d = t+1, f = 0, g = 0) cell (kcal/mole)	=	0.0020085706	0.0010121726

B-5500 COMPUTER RUN TIMES:

Compiler time	=	71 seconds	70 seconds
Processor time	=	3385 seconds	3109 seconds
Input/Output time	=	101 seconds	96 seconds

TABLE XVII--Continued

Data Col. No.	:	XVII-1	XVII-2	XVII-3	XVII-4
EWALD No.	:	ZZ02 (e = 1)	ZZ08 (e = 1)	ZZ02 (e = 3)	ZZ08 (e = 3)
Cation CAL	:	IIIa	IIIa	IIIa	IIIa
Anion CAL	:	VIIa	VIIa	VIIb	VIIb
η	=	9.0	10.0	9.0	10.0
RESULTS (kcal/mole):					
A	=	-23.369768	-24.633898	-18.641803	-19.650186
B	=	7.467943	9.456233	6.939577	8.837323
Γ_T	=	32.828274	32.107089	37.631481	36.745106
E_C	=	16.926449	16.929423	25.929255	25.932242
$-\Delta$	=	-115.744441	-115.744441	-127.990478	-127.990478
E_C	=	-98.817992	-98.815018	-102.061223	-102.058236
RESULTS (eV/molecule):					
Cation Δ_2	=	3.146447	3.146447	3.146447	3.146447
Anion Δ_1	=	1.873828	1.873828	2.404985	2.404985
Δ	=	5.020275	5.020275	5.551432	5.551432
H	=	- 3.258340	- 3.258340	- 3.347024	- 3.347024
E_C	=	- 4.286111	- 4.285981	- 4.426782	- 4.426652
MADELUNG CONSTANT, ω	=	1.315428	1.315387	1.322602	1.322564

Data Col. No.	:	XVII-5	XVII-6	XVII-7	XVII-8
EWALD No.	:	ZZ02 (e = 4)	ZZ08 (e = 4)	ZZ02 (e = 2)	ZZ08 (e = 2)
Cation CAL	:	IIIa	IIIa	IIIa	IIIa
Anion CAL	:	VIIc	VIIc	VIId	VIId
η	=	9.0	10.0	9.0	10.0
RESULTS (kcal/mole):					
A	=	-17.763117	-18.723969	-16.467366	-17.358128
B	=	6.943905	8.854317	6.847847	8.741923
Γ_T	=	40.446760	39.500187	42.090231	41.089907
E_C	=	29.627548	29.630535	32.470712	32.473702
$-\Delta$	=	-132.378748	-132.378748	-135.882249	-135.882249
E_C	=	-102.751200	-102.748213	-103.411537	-103.408547
RESULTS (eV/molecule):					
Cation Δ_2	=	3.146447	3.146447	3.146447	3.146447
Anion Δ_1	=	2.595320	2.595320	2.747281	2.747281
Δ	=	5.741767	5.741767	5.893728	5.893728
H	=	- 3.364824	- 3.364824	- 3.385302	- 3.385302
E_C	=	- 4.456709	- 4.456579	- 4.485350	- 4.485220
MADELUNG CONSTANT, ω	=	1.324500	1.324461	1.324948	1.324910

TABLE XVIII

Unpublished Room-Temperature Crystal and Molecular Structure Data for WBP (from Turner and Albrecht (200))[*]

Space group:	Pn2n or, more likely, Pnmn
Unit cell axes:	$a = 5.98 \pm .01$ Å, $b = 10.21 \pm .01$ Å, $c = 10.23 \pm .015$ Å
Observed reflections:	46 out of 78 h0l, 64 out of 69 0kl
Unweighted Reliability factor:	0.118 for h0l data, 0.252 for 0kl data

Atomic parameters:	x/a:	y/b:	z/c:
Chlorine :	0.5	0.5	0.0
Oxygen 1 :	0.296	0.420	0.021
Oxygen 2 :	0.536	0.580	0.119
Carbon 1 :	-0.092	0.118	0.041
Carbon 2 :	-0.186	0.0	0.083
Nitrogen :	-0.370	0.0	0.166
Carbon 3 :	-0.466	0.125	0.209
Hydrogen 1:	-0.166	±0.210	0.073
Hydrogen 2:	-0.612	±0.106	0.270
Hydrogen 3:	-0.345	±0.181	0.261
Hydrogen 4:	-0.524	±0.181	0.121

[*] At this writing, new crystallographic work on WBP is reported in progress (cf. Ref. (201)).

TABLE XIX

Unpublished Crystal and Molecular Structure for TMPD$^{\dot{+}}$pChl$^{\dot{-}}$ (from Wallwork (91))*

Space group: C 2/m

Unit cell axes: a = 16.390±.015 Å, b = 6.505±.01 Å, c = 8.91±.01 Å, β = 112°30'±20'

Observed reflections: not specified

Reliability factor: not specified

Atomic parameters:	x/a:	y/b:	z/c:
Carbon 1 :	-0.030	0.0	0.128
Carbon 2 :	0.062	0.0	0.170
Carbon 3 :	0.090	0.0	0.030
Oxygen 1 :	0.121	0.0	0.311
Chlorine 1:	0.203	0.0	0.072
Chlorine 2:	-0.063	0.0	0.293
Carbon 4 :	-0.021	0.5	0.142
Carbon 5 :	0.067	0.5	0.160
Carbon 6 :	0.088	0.5	0.019
Carbon 7 :	0.112	0.5	0.459
Carbon 8 :	0.227	0.5	0.325
Nitrogen 1:	0.133	0.5	0.313

---

*After the work described here and in Table XIV was completed, a crystal and molecular structure study for TMPD$^{\dot{+}}$pChl$^{\dot{-}}$ was published by de Boer and Vos (18); see Proposition II for a discussion.

E. Discussion of Test Crystals

The EWALD results are reported in kcal/mole[*] and also in eV/molecule, and were obtained to four more significant figures than are recorded in Tables X to XVII.

EWALD was first tested for Sodium chloride, Table X. The value $\omega = 1.747564$[**] compares favorably with Madelung's original $\alpha = 1.743_8$ (176), the value $\alpha = 1.747558$ quoted by Sherman (202), and Sakamoto's ultra-precise value[***] $\alpha = 1.747564\ 594633\ 1822$ (203).

A further, and more sensitive, test of both CELLMAP and EWALD was the calculation of E_C^T for Yttrium chloride (Table XI), a monoclinic crystal for which we could not only check for independence of E_C^T from η, but also confirm our calculation against Johnson and Templeton's (198) recent calculation of E_C^T by Bertaut series. Johnson and Templeton define a Madelung-type constant, $A(R_o)$, based on R_o, the shortest anion-cation distance in the crystal, and for $R_o = 2.5845$ Å they get $A(R_o) = 8.313$; we get for $R_o = 2.5845506$ Å the best value $A(R_o) = 8.312522$. E_C, Δ_2, H and ω for YCl are discussed in Appendix I.

A final check on the applicability of EWALD for triclinic crystals was made by calculating E_C^T for $Mg_2(OH)_3Cl.4H_2O$ (space

---

[*] For DA complexes, a mole consists of $N_o D^+$ and $N_o A^-$ ions; for WBP a mole consists of N_o WBP monomers.

[**] Actually $\omega = 1.747563\ 9556$ (EWALD BZ87) and $\omega = 1.747563\ 9597$ (EWALD ZZ01).

[***] Obtained by Ewald's method.

group $P\bar{1}$) (204). A value of E_C^T of about -1200 kcal/mole was obtained, for $\eta = 6.0$ and $\eta = 9.0$, with negligible η-dependence.*

F. Discussion of Wurster's Blue Perchlorate

We now turn to the organic crystals. The first general trend that becomes obvious from a cursory glance at Tables XII to XVII is the remarkable insensitivity of E_C and H to the nontrivial changes in the assumed relative charge distributions. It could be argued that almost all the charge distributions chosen in Tables I to VIII are, on the whole, "chemically reasonable", and so no rude surprises in calculations of E_C should be expected. We feel, however, that this relative insensitivity of E_C and H to charge variations actually answers rather well the following objection to our whole approach: that to substitute classical point charges for diffuse charge clouds, and Ewald summations for quantum-mechanical integrations is too crude an approximation. Indeed, the variance of E_C and H would be expected to be much greater than observed if the point-charge approximation were an over-simplification. Another general conclusion is that small (< 1%) deviations from the electrical neutrality required by Eq. (216), which can be observed on closer inspection of some of the charge distributions in Tables I to VIII, do not seem to affect E_C drastically.

---

*The detailed results are not tabulated because a trivial error was made in the charge distribution assignment.

It was found, however, that large deviations from Eq. (216) do cause big changes in E_C.

The first organic crystal studied was Wurster's Blue Perchlorate. For an account of the known physical properties of this interesting salt, the reader is referred to a review by Nordio et al. (3) and to the references cited therein; more recent work is reported in Refs. (183, 191, 205, 206, 207, 208, 209, 210). The E_C data recorded in Table XII show satisfactory independence from η, and a remarkably consistent value $\omega = 1.48$ to 1.49.[*] WBP is hereby unequivocally shown to be an ionic crystal that is sufficiently stable under the influence of ordinary classical Coulomb forces, and there is no need to invoke quantum-mechanical exchange Coulomb interactions to explain its stability (167,168). There are two small trends in the data obtained; (i) for fixed perchlorate CAL, E_C becomes more negative by about 0.3 to 0.4 kcal/mole as the $TMPD^+$ charge assignment model is changed from Ib to Ic to Id: this trend parallels the increase of the charge on the benzene ring at the expense of the nitrogen atoms; (ii) for fixed $TMPD^+$ CAL, E_C becomes more negative, by about 0.45 to 0.67 kcal/mole, as the ClO_4^- charge assignment goes from either VIa or VIb to either VId or VIe; this trend follows the increase in charge on the oxygen atoms at the expense of the chlorine atom.

---

[*] Except in Columns XII-11 and XII-12, where we assume with Monkhorst and Kommandeur (191) that the chlorine atom charge is 3.0, which seems "unphysical" anyway.

One might like to discuss trend (ii) above in light of the well-known phase transition in WBP. Many inorganic perchlorates undergo a phase transition at relatively elevated temperature. It is well established that the high-temperature phase (II) exhibits freely rotating or statistically disordered perchlorate ions, and hence higher crystallographic symmetry, whereas the low-temperature phase (I) has perchlorate ions frozen into well-defined orientations, and the phase I crystal frequently exhibits twinning. At room temperature WBP is orthorhombic (phase II, space group Pn2n or more likely, Pnmn if perchlorates are disordered (201,212)); below a transition temperature $T_t = 186°K$ or 190°K (213) it is monoclinic, with alternating interionic distances along the $TMPD^+$ linear chains and a doubled primitive cell* (phase I, space group unspecified (212)). WBP is paramagnetic above T_t, and is an alternating Heisenberg antiferromagnet below T_t with a thermally accessible Frenkel triplet spin exciton state; the phase transition is of first order and exothermic; the experimental data** are $\Delta H \equiv H_{II} - H_I = 0.408 \pm 4.5$ kcal/mole of WBP monomer (213), $(dp/dT) = 0.1$ kbar/degree (214), whence $\Delta S \equiv S_{II} - S_I = 2.19 \pm 0.02$ cal/mole-deg, and $\Delta V \equiv V_{II} - V_I = 1.5 \pm 0.1$ Å^3/monomer. The $p\Delta V$ term amounts to only 2.19×10^{-6} kcal/mole, so we derive from experiment $\Delta H \cong \Delta E \equiv E_{II} - E_I = +0.41$ kcal/mole.

---

*This model is due to Hausser and Murrell (215) and McConnell (212)

**H_{II} is the enthalpy for the high-temperature phase II, H_I is the enthalpy for the low-temperature phase I.

The entropy change $\Delta S = 2.19$ e.u. may be partially accounted for (213) by: (i) statistical disorder of perchlorate ion orientations in phase II, which accounts for* $R \log_e 2 = 1.38$ e.u. (213); (ii) Chesnut's exciton condensation theory (216) which Hughes (214) has shown would contribute only $(1/2)R(\rho_{II}-\rho_I)\log_e 3 = (1/2)R$ $(0.15) \log_e 3 = 0.16$ e.u.; the remaining 0.64 e.u. (or 0.80 e.u. if Chesnut's theory is not correct) must be explained by other means. There is an entropy change due to the structural dissociation at T_t of the low-temperature "TMPD$^+$ dimer": above T_t we cannot tell whether two adjacent TMPD$^+$ ions had belonged to the same low-temperature dimer or to two adjacent low-temperature dimers: this contributes $(1/2)R \log_e 2 = 0.69$ e.u. Thus all or almost all of ΔS seems to be explained.

One might like to calculate ΔE. Let $E_C(II)$ be the Madelung energy of WBP just above T_t and let $E_C(I)$ be the Madelung energy just below T_t; then one might expect that the largest contribution to ΔE would be $E_C(II)-E_C(I)$. The exact evaluation of $E_C(II)-E_C(I)$ is impossible for two reasons: (i) the absence of reliable crystallographic data around T_t, (ii) the theoretical uncertainties in the charge distribution in the perchlorate ion, for which no experimental estimate is available. It is likely that the real charge distribution in the perchlorate ion is intermediate between CAL VIb (chlorine -1, oxygen 0) and CAL VIe

---

*See Ref. (217) pages 371-378.

(chlorine 0, oxygen -0.25); of course CAL VIb describes the freely rotating or statistically disordered perchlorate ion. One might therefore hope that the E_C calculated in Table XII with CAL VIb might approximate E_C(II), and that E_C calculated with CAL VId or CAL VIe will give some estimate of E_C(I). But subtracting for instance E_C (Column XII-7) from E_C (Column XII-3) gives -0.53 kcal/mole, which is close to ΔE in magnitude but has the wrong sign. This is true for all such attempted subtractions in Table XII: obviously the crystal-structure data used are unsuitable for the calculation of $E_C(II) - E_C(I)$.

Mention should be made here of the extensive efforts of Kommandeur *et al*. (183,191,207,208) to interpret the phase transition of WBP as due to a transition from a high-temperature lattice consisting of linear chains of equidistant $TMPD^+$ ions, to a low-temperature lattice consisting of linear chains of disproportionated pairs, with $TMPD^{++}$ and TMPD constituting the low-temperature dimer. The most important experimental evidence adduced by Kommandeur is the purported optical spectrum of solid phase I; however, Young has noticed (211) that Kommandeur's spectra are actually solution spectra, as is obvious from the spectra of Uemura *et al*. (206); moreover a recently published study by Anderson (210) of the low-temperature crystal polarized optical reflectance spectrum of WBP vindicates completely the earlier model discussed above.

G. Discussion of DA Crystals

The DA crystals will be discussed next. It was naively hoped that for holoionic DA crystals the Madelung energy E_C would be negative and greater in magnitude than the respective $I_{CT}-A_{CT}$, and that for nonionic crystals E_C would be either positive or, at any rate, smaller in magnitude than $I_{CT}-A_{CT}$. This would offer a relatively effortless "final" proof of the correctness of McConnell's classification of DA crystals.

The η-independence is satisfactory in Tables XIII, XVI, and XVII; the convergence of the results in Table XIV, for which only one EWALD run was made, is acceptable. The independence of E_C, H and ω in Tables XIII, XIV, XVI, and XVII from the details of the charge model is very reassuring. However, the comparison of the E_C with the relevant $I_{CT}-A_{CT}$ of Table I of Chapter I, and also the comparison of $E_S^{\perp}$ of Fig. II of Chapter I with H in Tables XVI and XVII show that the approximations $H \cong E_S^{\perp}$, $E_C \cong 2\epsilon_1$ (cf. Eq. (119)) are too crude. In other words, interactions other than direct Coulomb are very important in DA crystals.

Let us summarize the relevant results of Tables XIII, XIV, XVI, XVII, of Table I of Chapter I and Fig. II of Chapter I as follows:

(i) for ($TMPD^+TCNQ^-$) (space group C 2/m):

$E_C = -4.0$ eV, $H = -3.0$ eV, $\omega = 1.29$,

$I_{CT} - A_{CT} = 4.6_5$ eV, $e_S^H = 0.075$ eV;

(ii) for ($TMPD^+pChl^-$) (space group $\underset{\sim}{C}\ 2/\underline{m}$):

$E_C = -4.4$ eV, $H = -3.4$ eV, $\omega = 1.30$,

$I_{CT} - A_{CT} = 5.0$ eV, $e_S^H = 0.13$ eV or 0.16 eV;

(iii) for (HMB: pChl) (space group $P\ 2_1/c$):

$E_C = -4.5$ eV, $H = -3.4$ eV, $\omega = 1.32$,

$I_{CT} - A_{CT} = 6.6$ eV, $E_S^{\perp} = -5.0$ eV, $H_{01}^{\perp} = -0.5$ eV;

(iv) for (Naphth:TCNE) (space group $\underset{\sim}{C}\ 2/\underline{m}$):

$E_C = -4.3$ eV, $H = -3.4$ eV, $\omega = 1.28$,

$I_{CT} - A_{CT} = 6.5$ eV, $E_S^{\perp} = -4.9$ eV, $H_{01}^{\perp} = -0.5$ eV.

If all exchange Coulomb and multipole effects were negligible, then one would have to say that ($TMPD^+TCNQ^-$) misses being a holoionic crystal by $I_{CT} - A_{CT} + E_C = 0.6_5$ eV, ($TMPD^+pChl^-$) by 0.6 eV, and that (HMB:pChl) and (Naphth:TCNE) are nonionic by 2.1 eV and 2.2 eV/DA pair respectively. Such a statement is patently belied by experiment. The donor ionization potentials obtained from CT spectra have been verified by direct experiment to be fairly reliable, but the same cannot be said for the electron affinities of the acceptors, which are very difficult to measure directly: so we could say that increasing the popularly accepted values of A_A for all acceptors in Table I of Chapter I by about 1 eV would get us out of our difficulties. It is hard to believe, however, that such a huge error in A_A should have gone unnoticed in the correlations of Briegleb (4), and accordingly we shall accept the $I_{CT} - A_{CT}$ values and seek relief elsewhere.

By comparing our calculations with the relevant data presented in Chapter I we will show that if proper account is taken of exchange Coulomb effects, i.e. if a good estimate of E_x (Eq. (119)) is found, then McConnell's classification of DA crystals can be salvaged. The following approximations shall be invoked (cf. Fig. I to IV of Chapter I):

(i) because of the short range of multipole forces, the energies E_p, E_m, E_m' are considered comparable to $H_{00}^{\perp}$, and since $H_{00}^{\perp}$ is small (about 0.1 eV), therefore E_p, E_m, E_m' will be neglected altogether:

(279a) $$2\epsilon_1 \cong E_c + E_x ,$$

(279b) $$\epsilon_1' \cong H + E_x' ;$$

(ii) E_{corr} is neglected, whence:

(279c) $$2\epsilon_0 \cong I_{CT} - A_{CT} ;$$

(iii) ϵ_1' differs from $E_S^{\perp}$ only by small charge-induced dipole effects in the crystal, and similarly γ is not very different from $H_{01}^{\perp}$:

(279d) $$\epsilon_1' \cong E_S^{\perp} ,$$

(279e) $$\gamma \cong H_{01}^{\perp} ;$$

(iv) E_x differs from E_x' only if the exchange Coulomb interactions are not very short-ranged; a naive guess is that E_x may be bracketed by the following inequality:

(279f) $$\omega E_x' < E_x < E_x' < 0,$$

which expresses the fact that the exchange Coulomb forces are less long-ranged than direct Coulomb forces, yet more long-ranged than multipole forces.

Solution $E_S^{\perp}$ values are available for (HMB:pChl) and (Naphth:TCNE); from Eq. (279b) we obtain $E_X' \cong -1.6$ eV, $\omega E_X' \cong -2.1$ eV for (HMB:pChl) and $E_X' \cong -1.5$ eV, $\omega E_X' \cong -1.9$ eV for (Naphth:TCNE). If indeed E_X is anywhere between E_X' and $\omega E_X'$ as assumed by Eq. (279f), then we can still safely predict that (HMB:pChl) and (Naphth:TCNE) must be nonionic, since $\varepsilon_o + \varepsilon_1 = 0$ is reached only if $E_X < -2.1$ eV and $E_X < -2.2$ eV respectively.

A different approach is required for ($TMPD^+TCNQ^-$) and for ($TMPD^+pChl^-$) because solution $E_S^{\perp}$ are not available. We use the experimental activation energies for paramagnetism, $e_S^H = J$, a crude estimate of $H_{01}^{\perp}$, and the following expression obtained by combining Eqs. (129, 130, 279a, 279b, 279c, 279e):

(280) $$2E_x - E_x' = (2E_c - H) - (I_{CT} - A_{CT}) - \frac{(H_{01}^{\perp})^2}{e_S^H}.$$

For ($TMPD^+TCNQ^-$) this equation becomes:

(281a) $$2E_x - E_x' = -0.45 - \frac{(H_{01}^{\perp})^2}{0.075};$$

for ($TMPD^+pChl^-$) it yields either:

(282a) $$2E_x - E_x' = -0.4 - \frac{(H_{01}^{\perp})^2}{0.13}$$

or:

(282b) $$2E_x - E_x' \cong -0.4 - \frac{(H_{01}^{\perp})^2}{0.16}.$$

Since all we really need is $E_x < -0.65$ for $(\mathrm{TMPD}^+\mathrm{TCNQ}^-)$, $E_x < -0.6$ for $(\mathrm{TMPD}^+\mathrm{pChl}^-)$, therefore we can rewrite Eq. (280) to require that:

(281b) $$E_x \cong 0.5\,E_x' - 0.27 - 6.7(H_{01}^{\perp})^2 < -0.65$$

for the former, and either:

(282c) $$E_x \cong 0.5\,E_x' - 0.2 - 3.1(H_{01}^{\perp})^2 < -0.6$$

or:

(282d) $$E_x \cong 0.5\,E_x' - 0.2 - 3.8(H_{01}^{\perp})^2 < -0.6$$

for the latter. If $H_{01}^{\perp}$ is independent of $I_D - A_A$, then we could propose $H_{01}^{\perp} \cong -0.5$ eV for the TMPD complexes, whence the above conditions are easily satisfied, except for the very unlikely event $E_x' > 0$.* Thus we seem to be easily assured of enough additional binding energy E_x due to exchange Coulomb interactions to guarantee that $(\mathrm{TMPD}^+\mathrm{TCNQ}^-)$ and $(\mathrm{TMPD}^+\mathrm{pChl}^-)$ are holoionic crystals.

The need to obtain E_x theoretically in order to avoid the above "hand-waving" arguments is rather obvious. A formalism for such quantum-mechanical calculations is developed in Chapter III.

---

*Of course if $H_{01}^{\perp} \ll -0.5$ then things are even rosier.

An interesting side-product of the Madelung calculations is the remarkable constancy of ω not only with respect to variations in charge distributions for a given DA crystal, but also for different DA crystals belonging to the same space group.* The explanation probably lies in the fact that the charge distribution pattern within the unit cell is rather similar for all these complexes.

H can be evaluated trivially, and if ω is indeed so dependable, and known a priori, then one could get a value for E_C good to 3% for any monoclinic DA crystal belonging to the same space group with very little effort. This led us to wonder whether, e.g., inorganic salts that crystallize in the space group $\underline{C}\ 2/\underline{m}$ have the same ω as the DA crystals described in Tables XIII, XIV, and XVI. In Appendix I we show that things are not quite so simple.

A "small" trend noticeable in the data of Table XIII, XIV, XVII is that the SHMO spin densities produce consistently the smallest binding energies, apparently because in $TMPD^+$ and in $pChl^-$ they overrate the charge at atoms I-3, VII-3, but for $TCNQ^-$ such an interpretation fails. Runs were made for (Naphth:TCNE) with charge densities for $Naphth^+$ in place of the spin densities of CAL IIa, but because of small errors these runs were not recorded in Table XVI: they showed, however, that the

---

*Similar trends have been noticed by Templeton <u>et al</u>. for inorganic salts, cf. Ref. (198).

use of charge density models yields essentially the same E_C as the use of spin densities. Therefore it becomes evident that, to within 3%, the same E_C and H are obtained with SHMO spin densities as with the best available SCF charge or spin densities.

H. Results for $MPNZ^+$ $TCNQ^-$

In a curious afterthought, the Madelung energy E_C was also calculated for the triclinic ion-radical salt $MPNZ^+TCNQ^-$. The crystal structure of this salt consists of linear chains of $MPNZ^+$ ions with vertical interionic separations of 3.36 Å, and of linear chains of $TCNQ^-$ ions with interionic distances of 3.26 Å, which puts this salt in the same category as WBP or other TCNQ ion-radical salts; but the $MPNZ^+$ ions and $TCNQ^-$ ions are strongly slanted with respect to the stacking axis $\underset{\sim}{a}$, with almost equal angles of tilt, and one could argue for <u>some</u> charge-transfer overlap in a [101] projection: the difficulty is that although the $MPNZ^+$-to-$TCNQ^-$ vertical separation is 3.5 Å, the separation between molecular centers is 8.2 Å, and the overlap is rather small. The resistivity of single crystals is remarkably low, 0.001 Ω cm at room temperature (144), presumably along the $\underset{\sim}{a}$ axis; no other physical properties seem to have been reported for this interesting salt.

The E_C data collected in Table XV show that <u>direct Coulomb forces provide little or no binding energy for the crystal</u>. The binding energy must obviously be found in exchange Coulomb interactions; one wonders whether this situation has a strong bearing on the relatively very high electrical conductivity. This result reinforced the need to develop a method for calculating crystal binding energies due to exchange Coulomb forces, and spurred the research described in Chapter III.

I. Acknowledgments

I am most grateful to Prof. H. M. McConnell for suggesting the Wurster's Blue Calculation, to Prof. B. M. Hoffman for calling my attention to the Ewald method, to Dr. D. J. Silverman for helpful discussions, to Mr. J. C. Lennie for programming assistance, and to the Computation Center, Stanford University, in particular to Mr. A. Crosby, for financial support above and beyond the call of duty.

APPENDIX I

The total Coulomb energy E_C^T for Yttrium trifluoride and Bismuth trifluoride are tabulated in Tables XX and XXI. The constant $A(R_o) = 8.898887$ for YF_3 agrees with Johnson and Templeton's value 8.899 (198). The Coulomb binding energy of BiF_3 $E_C^T = -1306.68$ kcal/mole agrees well with Cubicciotti's experimental binding energy (218) $\Delta E = -1170$ kcal/mole, once the conventional 10% correction is applied to E_C^T for core repulsion forces.*

We now resume the discussion of ω , Eq. (205). One can readily define ω for binary inorganic salts such as NaCl and interpret ω as a measure of the additional Coulomb binding, over the single-molecule interionic attraction, which is provided by the crystal lattice. The interionic distance in a single alkali halide molecule in the gas phase is about 20% smaller than nearest-neighbor distances in the crystal (Ref. (190) Table 13-9 and Table 13-11); so H should really be calculated using gas phase data, if ω is to be a comparison between crystals and gas phases; we feel, however, that calculations of H for an equilibrium crystal interionic distance are not devoid of meaning, and thus we avoid questions of different ionic contributions to the ground state of the molecule in the two phases.

---

*Minor discrepancies may be due to inaccuracies in the published crystal structure of BiF_3 (219).

The calculation of H, E_C, and ω for polyanionic salts like YCl_3 presents more serious problems. Let us postulate that H is calculated to include the attractive interactions between those neighboring ions in the crystal which approximate most closely the geometrical shape of the ionic crystal in the gas phase, as determined by microwave spectroscopy. YCl_3, YF_3, and BiF_3 belong to a class of pyramidal molecules, the cation being at the vertex and the anions at the base vertices. H is calculated accordingly in Tables XI, XX, XXI. To get values of ω greater than 1, we decided ad hoc to correct E_C^T for Δ_2, the Coulomb repulsions between the three same anions which were considered for H; this gives the E_C and ω of Tables XI, XX, XXI.

Note that the three organic DA crystals belonging to space group C 2/m have $\omega = 1.29$ (Table XIII), 1.30 (Table XIV), 1.28 (Table XVI), whereas YCl_3 belonging to the same space group has $\omega = 1.17$ (Table XI), and note also that the isostructural YF_3 and BiF_3 have $\omega = 1.32$ and $\omega = 1.27$, respectively. This shows that the "Madelung constant ω", as defined by Eq. (205) and by the conventions above, is not as general as had been hoped, because the effect of atoms in general positions in the unit cell cannot be streamlined into an ω universally valid for all ionic crystals belonging to the same space group.

TABLE XX

Crystal Coulomb Energy of Yttrium(Tri)fluoride (YF_3)

Crystal structure data of : Zalkin & Templeton (220)

CELLMAP run identifier : F9 SRI
Space group : Pnma
Number of molecules per unit cell, Z = 4
Number of charged atoms per unit cell, M = 16
Cube root of unit cell volume, $V^{1/3}$ = 5.760722 Å
Shortest interionic distance = 2.162973 Å

INPUT PARAMETERS:

EWALD Run: ZZ19SRI
η = 12.0
Sum limits to B term (initial):
p,q,r = 5,5,5
Sum limits to Γ term:
t,u,v = 1,1,1

CONVERGENCE ESTIMATES:

Final sum limits to B:
p,q,r = 6,6,6
"Last" contrib. to B: (kcal/mole) = 6.4×10^{-10}
"Test" contrib. to Γ (kcal/mole) = -1.60×10^{-9}

B5500 COMPUTER RUN TIMES:

Compiler = 50 seconds
Processor = 712 seconds
I/O time = ?

INPUT CHARGE ASSIGNMENTS: Yttrium cation = 3, Fluoride anion = -1

TABLE XX--Continued

Data Col. No. : XX-1
EWALD No. : ZZ19SRI
Cation Charge : 3.0
Anion Charge : -1.0
η = 12.0

RESULTS
(kcal/mole):

A = -1351.525882
B = 136.376077
Γ = -150.655696
E_C^T = -1365.805501
$-\Delta$ = -324.037620
E_C = -1689.843121

RESULTS
(eV/molecule):

Cation Δ_2 = 0.0
Anion Δ_1 = 14.054739
Δ = 14.054739
H = -55.596701
E_C = -73.294895
MADELUNG CONSTANT, ω = 1.318332
Johnson-Templeton Constant, $A(R_o)$ = 8.898887

TABLE XXI

Crystal Coulomb Energy of Bismuth Trifluoride (BiF_3)

Crystal structure data of	:	Zalkin (220) Aurivillius (219)
CELLMAP run identifier	:	F6SRI
Space group	:	Pnma
Number of molecules per unit cell, Z	=	4
Number of charged atoms per unit cell, M	=	16
Cube root of unit cell volume, $V^{1/3}$	=	6.0646798 Å
Shortest interionic distance	=	2.2352095 Å

INPUT PARAMETERS:

EWALD Run	:	ZZ15SRI	ZZ16SRI	ZZ17SRI
η	=	4.0	10.0	12.0
Sum limits to B term (initial): p,q,r	=	3,3,3	3,3,3	3,3,3
Sum limits to Γ term: t,u,v	=	1,1,1	1,1,1	1,1,1

CONVERGENCE ESTIMATES:

Final sum limits to B: p,q,r	=	4,4,4	4,4,4	6,6,6
"Last" contrib. to B: (kcal/mole)	=	$< 1.0 \times 10^{-10}$	0.0003391974	0.0000000024
"Test" contrib. to Γ (kcal/mole)	=	-0.00592973121	-0.00000011011	-0.0000000030

B5500 COMPUTER RUN TIMES:

Compiler	=	31 seconds	67 seconds	?
Processor	=	125 seconds	279 seconds	721 seconds
I/O time	=	?	?	?

INPUT CHARGE ASSIGNMENTS: Bismuth cation = 3.0,
Fluoride anion = -1.0

TABLE XXI--Continued

Data Col. No.	:	XXI-1	XXI-2	XXI-3
EWALD No.	:	ZZ15SRI	ZZ16SRI	ZZ17SRI
Cation Charge	:	3.0	3.0	3.0
Anion Charge	:	-1.0	-1.0	-1.0
η	=	4.0	10.0	12.0
RESULTS (kcal/mole)	:			
A	=	- 741.195442	-1171.932894	-1283.788164
B	=	1.057724	75.119668	126.957136
Γ_T	=	- 565.933777	- 209.863018	- 149.846904
E_C	=	-1306.071496	-1306.676243	-1306.677932
$-\Delta$	=	- 321.890872	- 321.890872	- 321.890872
E_C	=	-1627.962368	-1628.567115	-1628.568804
RESULTS (eV/molecule)	:			
Cation Δ_2	=	0.0	0.0	0.0
Anion Δ_1	=	13.961626	13.961626	13.961626
Δ	=	13.961626	13.961626	13.961626
H	=	-55.738005	-55.738005	-55.738005
E_C	=	-70.610892	-70.637122	-70.637196
MADELUNG CONSTANT, ω	=	1.266836	1.267306	1.267308
Johnson-Templeton Constant, $A(R_o)$	=	8.793886	8.797958	8.797970

CHAPTER III

A RAPID-CONVERGENCE FORMALISM FOR QUANTUM-MECHANICAL CALCULATIONS OF THE ELECTRONIC BINDING ENERGY OF ORGANIC IONIC CRYSTALS

> E quindi uscimmo a riveder le stelle
> D. Alighieri, *Inf.* XXXIV 139

A. Introduction

The results of the classical calculations described above lead us to believe--and hope--that the stability of holoionic donor-acceptor lattices must be explained by quantum-mechanical calculations which include the short-range exchange Coulomb effects neglected by the classical treatment. Accordingly, a formalism for quantum-mechanical calculations of the ground state of non-ionic and holoionic crystals will be sketched below. The ultimate purpose is to use such formulas in digital computer calculations--if and when funds become available. The initial idea was to try to merge the classical results of Bertaut (169), obtained *via* the convolution theorem, with the Fourier methods recently developed by H. Silverstone (221,222,223,224,225) for the so-called one-, two-, three-, and four-center atomic integrals. Our intention is *not* to perform *ab initio* calculations for the whole crystal lattice, but to adapt the results of existing single-molecule calculations to the requirements of crystalline periodicity.

A few words about notation might be useful. The origin for the "direct-lattice coordinate system" $\{\vec{e}_a (\equiv \underset{\sim}{a}|\underset{\sim}{a}|^{-1}), \vec{e}_b, \vec{e}_c\}$ is located at some convenient spot in the "zeroth unit cell" (see p. 93) and is referred to as the "center of the crystal." Details about this and other local systems are discussed in Appendix I. The label ν identifies one of the M nuclei (or atomic cores) situated at $\underset{\sim}{r}_{\nu}^{0}$ within the zeroth unit cell; the label μ identifies one of the Λ electrons which on the average are in the zeroth unit cell, at instantaneous "positions" $\underset{\sim}{r}_{\mu}$; the label λ identifies molecular or crystal orbitals. There are N_0/Z unit cells, each of volume V and each containing Z molecules, in our crystal. If any of the above labels is construed as applicable to objects throughout the crystal, then it is underlined: thus if $\{\nu = 1, 2, \ldots, M\}$ then $\{\underline{\nu} = 1, 2, \ldots, MN_0/Z\}$. The single index $\{\underline{\delta} = 0, 1, 2, \ldots, N_0/Z - 1\}$ is restricted to direct-lattice vectors $\underset{\sim}{r}_{\underline{\delta}}$, previously defined as $\underset{\sim}{r}_{dfg}$ (see Eq. (265)):

$$\underset{\sim}{r}_{\underline{\delta}} \equiv \underset{\sim}{r}_{dfg} \equiv d\underset{\sim}{a} + f\underset{\sim}{b} + g\underset{\sim}{c}, \tag{301}$$

where $\underset{\sim}{a}$, $\underset{\sim}{b}$, and $\underset{\sim}{c}$ are direct-lattice translations and d, f, g are are integers. The restrictions on d, f, g in Eq. (301) are taken to be, without loss of generality:

$$-\frac{1}{2}\left[\left(\frac{N_0}{Z}\right)^{1/3} - 1\right] \leqslant d, f, g \leqslant \frac{1}{2}\left[\left(\frac{N_0}{Z}\right)^{1/3} - 1\right]. \tag{302}$$

We shall assume three-dimensional Born-von Kármán periodic boundary conditions on the crystal.

We want to evaluate the quantity

(303) $$\Delta E_{CT} \equiv E_{TX}^{D^+A^-} - E_{TX}^{DA},$$

where $E_{TX}^{D^+A^-}$ is the (electronic) internal energy of the holoionic lattice and E_{TX}^{DA} is the corresponding quantity for the neutral lattice. Both these quantities are for a mole's worth of donor-acceptor pairs. If $\Delta E_{CT} > 0$ then the lattice is predicted to be neutral at 0°K; if $\Delta E_{CT} < 0$ then it is expected to be holoionic at 0°K.

The Hamiltonian for the electrons in the whole crystal (within the limits of the Born-Oppenheimer approximation) is:

(304a) $$\hat{\mathcal{H}}_{TX} \equiv \hat{\mathcal{H}}_{TX}^{o} + \hat{\mathcal{H}}_{TX}^{int},$$

where we define:

(304b) $$\hat{\mathcal{H}}_{TX}^{o} \equiv \hat{\sum_{\mu=1}^{\frac{N_e}{2}}} \left(\hat{h}_{\mu}^{K.E.} + \hat{h}_{\mu}^{N.A.} \right),$$

(304c) $$\hat{\mathcal{H}}_{TX}^{int} \equiv \frac{|e|^2}{2} \hat{\sum_{\mu=1}^{\frac{N_e}{2}}} \hat{\sum_{\substack{\mu'=1 \\ \mu \neq \mu'}}^{\frac{N_e}{2}}} \frac{1}{|\underset{\sim}{r}_{\mu'} - \underset{\sim}{r}_{\mu}|},$$

and where in turn the one-electron kinetic energy and nuclear attraction Hamiltonians are given by:

$$(304\text{d})\quad \hat{h}^{\text{K.E.}}_{\underline{\mu}} \equiv -\frac{\hbar^2}{2m_e}\left[\frac{\partial^2}{\partial(r^x_{\underline{\mu}})^2}+\frac{\partial^2}{\partial(r^y_{\underline{\mu}})^2}+\frac{\partial^2}{\partial(r^z_{\underline{\mu}})^2}\right] \equiv -\frac{\hbar^2}{2m_e}\sum_{i=1}^{3}\frac{\partial^2}{\partial(r^i_{\underline{\mu}})^2},$$

$$(304\text{e})\quad \hat{h}^{\text{N.A.}}_{\mu} \equiv -|\epsilon|^2\sum_{\underline{\nu}=1}^{M\frac{N_0}{Z}}\frac{\zeta_{\underline{\nu}}}{|\underset{\sim}{r}_{\mu}-\underset{\sim}{r}^{\circ}_{\underline{\nu}}|}.$$

We will next invoke a series of well-known approximations in order to reduce the size of the calculations.

APPROXIMATION I: "The wavefunction for the whole crystal Ψ_{TX} is approximated by a single Slater determinant of orthonormalized one-electron 'crystal spin-orbitals'[*] $\Psi^{TX}_{\underline{\lambda}}(r_{\mu})$:

$$(305)\quad \Psi_{TX} = \left[\left(\Lambda\frac{N_0}{Z}\right)!\right]^{-1/2}\times$$
$$\times\left|\Psi^{TX}_{1}(\underset{\sim}{r}_1)\,\Psi^{TX}_{2}(\underset{\sim}{r}_2)\ldots\Psi^{TX}_{\underline{\lambda}}(\underset{\sim}{r}_{\underline{\mu}})\ldots\Psi^{TX}_{\Lambda\frac{N_0}{Z}-1}(\underset{\sim}{r}_{\Lambda\frac{N_0}{Z}-1})\,\Psi^{TX}_{\Lambda\frac{N_0}{Z}}(\underset{\sim}{r}_{\Lambda\frac{N_0}{Z}})\right|.$$

The spin-orbital $\Psi^{TX}_{\lambda}(r_{\mu})$ is assumed to be a linear combination of atomic orbitals (LCAO):

---

[*] The labelling is such that all "spin down" or "β spin function" crystal spin-orbitals can be denoted with " —— ", and have $\underline{\lambda}$ greater than the $\underline{\lambda}$ of the crystal spin-orbitals with "spin up" or "α spin projection": thus all $\Psi^{TX}_{\underline{\lambda}}$ $\{1 \leqslant \underline{\lambda} \leqslant \underline{\lambda}_0\}$ have "α spin" and all $\overline{\Psi^{TX}_{\underline{\lambda}}}$, $\{\underline{\lambda}_0 + 1 \leqslant \underline{\lambda}' \leqslant \Lambda(N_0/Z)\}$ have "β spin."

$$\Psi^{TX}_{\underline{\lambda}}(\underset{\sim}{r}_{\underline{\mu}}) \equiv \sum_{\underline{\nu}=1}^{M\frac{N_0}{Z}} d_{\underline{\nu}\underline{\lambda}} \psi_{\underline{\nu}\underline{\lambda}}(\underset{\sim}{r}_{\underline{\mu}} - \underset{\sim}{r}^{\circ}_{\underline{\nu}}) \equiv \tag{306a}$$

$$\equiv \sum_{\underline{\delta}=0}^{N_0/Z-1} \sum_{\nu=1}^{M} d_{\nu\underline{\delta}\underline{\lambda}} \psi_{\nu\underline{\delta}\underline{\lambda}}(\underset{\sim}{r}_{\underline{\mu}} - \underset{\sim}{r}^{\circ}_{\nu} - \underset{\sim}{r}_{\underline{\delta}}), \tag{306b}$$

$$\left\{\underline{\lambda}, \underline{\mu} = 1, 2, \ldots, \Lambda \frac{N_0}{Z}\right\}$$

where the $\psi_{\underline{\nu}\underline{\lambda}}(\underset{\sim}{r}_{\underline{\mu}} - \underset{\sim}{r}^{\circ}_{\underline{\nu}})$ are normalized atomic orbitals, possibly hybrid, centered about $\underset{\sim}{r}^{\circ}_{\underline{\nu}}$; and the $d_{\underline{\nu}\underline{\lambda}}$ are complex coefficients."

The ground-state energy E_{GS} (which will be either E^{DA}_{TX} or $E^{D^+A^-}_{TX}$ depending on which crystal spin-orbitals are used) is given by:

$$\begin{aligned} E_{GS} \equiv \sum_{\underline{\lambda}=1}^{\Lambda\frac{N_0}{Z}} \left\{ -\frac{\hbar^2}{2m_e} Q_{\underline{\lambda}} - |\epsilon|^2 [\underline{\lambda}|\underline{\lambda}] \right\} + |\epsilon|^2 \sum_{\underline{\lambda}=2}^{\Lambda\frac{N_0}{Z}} \sum_{\underline{\lambda}'=1}^{\underline{\lambda}-1} [\underline{\lambda}\underline{\lambda}|\underline{\lambda}'\underline{\lambda}'] - \\ -|\epsilon|^2 \left\{ \sum_{\underline{\lambda}=2}^{\underline{\lambda}_0} \sum_{\underline{\lambda}'=1}^{\underline{\lambda}-1} + \sum_{\underline{\lambda}=\underline{\lambda}_0+2}^{\Lambda\frac{N_0}{Z}} \sum_{\underline{\lambda}'=\underline{\lambda}_0+1}^{\underline{\lambda}-1} \right\} [\underline{\lambda}\underline{\lambda}'|\underline{\lambda}'\underline{\lambda}], \end{aligned} \tag{307}$$

where according to Slater's notation:

$Q_{\underline{\lambda}} \equiv$ Kinetic Energy Integral for Crystal Orbital $\underline{\lambda} \equiv$

$$\equiv \iiint_{\frac{N_0V}{Z}} d\omega(\underset{\sim}{r}_{\underline{\mu}}) \Psi^{TX*}_{\underline{\lambda}}(\underset{\sim}{r}_{\underline{\mu}}) \sum_{i=1}^{3} \frac{\partial^2}{\partial(r^i_{\underline{\mu}})^2} \Psi^{TX}_{\underline{\lambda}}(\underset{\sim}{r}_{\underline{\mu}}), \tag{308a}$$

$$\left\{\underline{\lambda} = 1, 2, \ldots, \Delta \frac{N_0}{Z}\right\}$$

$[\underline{\lambda}|\underline{\lambda}] \equiv$ Electron-Nucleus Attraction Integral for Crystal Orbital λ

$$\equiv \sum_{\nu=1}^{M} \zeta_{\nu} \sum_{\underline{\delta}=0}^{\frac{N_0}{Z}-1} \iiint_{\frac{N_0V}{Z}} d\omega(\underset{\sim}{r}_{\underline{\mu}}) \Psi^{TX*}_{\underline{\lambda}}(\underset{\sim}{r}_{\underline{\mu}}) \frac{1}{|\underset{\sim}{r}_{\underline{\mu}} - \underset{\sim}{r}^{\circ}_{\nu} - \underset{\sim}{r}_{\underline{\delta}}|} \Psi^{TX}_{\underline{\lambda}}(\underset{\sim}{r}_{\underline{\mu}}), \tag{308b}$$

$$\left\{\underline{\lambda} = 1, 2, \ldots, \Lambda \frac{N_0}{Z}\right\}$$

$[\underline{\lambda}\underline{\lambda}|\underline{\lambda}'\underline{\lambda}']$ ≡ Direct Coulomb Interelectronic Repulsion Integral for Crystal Orbitals $\underline{\lambda}, \underline{\lambda}'$ ≡

(308c) $$\equiv \iiint\limits_{\frac{N_0V}{Z}} dv(\underset{\sim}{r}_{\mu'}) \iiint\limits_{\frac{N_0V}{Z}} dv(\underset{\sim}{r}_{\mu}) \Psi^{TX^*}_{\underline{\lambda}}(\underset{\sim}{r}_{\mu}) \Psi^{TX^*}_{\underline{\lambda}'}(\underset{\sim}{r}_{\mu'}) \frac{1}{|\underset{\sim}{r}_{\mu}-\underset{\sim}{r}_{\mu'}|} \Psi^{TX}_{\underline{\lambda}}(\underset{\sim}{r}_{\mu}) \Psi^{TX}_{\underline{\lambda}'}(\underset{\sim}{r}_{\mu'}),$$

$$\left\{\underline{\lambda},\underline{\lambda}' = 1,2,\ldots,\Lambda\frac{N_0}{Z} \text{ but } \underline{\lambda} \neq \underline{\lambda}'\right\}$$

$[\underline{\lambda}\underline{\lambda}'|\underline{\lambda}'\underline{\lambda}]$ ≡ Exchange Coulomb Interelectronic Repulsion Integral for Crystal Orbitals $\underline{\lambda}, \underline{\lambda}'$ ≡

(308d) $$\equiv \iiint\limits_{\frac{N_0V}{Z}} dv(\underset{\sim}{r}_{\mu'}) \iiint\limits_{\frac{N_0V}{Z}} dv(\underset{\sim}{r}_{\mu}) \Psi^{TX^*}_{\underline{\lambda}}(\underset{\sim}{r}_{\mu}) \Psi^{TX^*}_{\underline{\lambda}'}(\underset{\sim}{r}_{\mu'}) \frac{1}{|\underset{\sim}{r}_{\mu}-\underset{\sim}{r}_{\mu'}|} \Psi^{TX}_{\underline{\lambda}'}(\underset{\sim}{r}_{\mu}) \Psi^{TX}_{\underline{\lambda}}(\underset{\sim}{r}_{\mu'}).$$

$$\left\{\begin{matrix}\underline{\lambda},\underline{\lambda}' = 1,2,\ldots,\Lambda\frac{N_0}{Z}, \\ \underline{\lambda} \neq \underline{\lambda}'\end{matrix} \text{ except for those pairs of } \lambda',\lambda' \text{ which have opposite spin projections}\right\}$$

B. Bloch's Theorem and Its Consequences

So far we have not invoked crystalline symmetry, and the problem remains formidably difficult, because every step of the calculation would involve Avogadro's number as a measure of the rank of matrices and of the number of independent electrons and orbitals that we would have to keep track of. Therefore, to simplify matters at least formally, we introduce Bloch's theorem (226) and the "tight-binding method" (227):

> RECIPE I: "Assume that, thanks to some isolated-molecule LCAO calculations (Hückel, Hartree-Fock, or other) we have obtained an orthonormal basis set of Λ "zeroth unit cell spin-orbitals" $\Psi^{c}_{\lambda}(\underset{\sim}{r}_{\mu})$ for the M atoms and the Λ electrons in the zeroth cell:

(309) $$\Psi^{c}_{\lambda}(\underset{\sim}{r}_{\mu}) \equiv \sum_{\nu=1}^{M} c_{\nu\lambda}\, \psi_{\nu\lambda}(\underset{\sim}{r}_{\mu} - \underset{\sim}{r}^{o}_{\nu})$$

$$\left\{ \mu, \lambda = 1, 2, \ldots, \Lambda \quad \begin{array}{l} \text{with } \alpha \text{ spin for } \lambda = 1, 2, \ldots, \lambda_0 \\ \text{and } \beta \text{ spin for } \lambda = \lambda_0 + 1, \ldots, \Lambda \end{array} \right\}$$

where the $c_{\nu\lambda}$ are complex coefficients and, as before, the $\psi_{\nu\lambda}$ are normalized atomic orbitals:

$$(310) \qquad \iiint\limits_{\frac{N_0 V}{Z}} dv(\underset{\sim}{r}_\mu)\, \psi^{*}_{\nu\lambda}(\underset{\sim}{r}_\mu - \underset{\sim}{r}^{\circ}_{\nu})\, \psi_{\nu\lambda}(\underset{\sim}{r}_\mu - \underset{\sim}{r}^{\circ}_{\nu}) = 1.$$

$$\{\nu = 1, 2, \ldots, M;\ \lambda = 1, 2, \ldots, \Lambda\}$$

The orthonormalization condition for the zeroth unit cell orbitals reads:

$$(311) \qquad \iiint\limits_{\frac{N_0 V}{Z}} dv(\underset{\sim}{r}_\mu)\, \Psi^{c*}_{\lambda}(\underset{\sim}{r}_\mu)\, \Psi^{c}_{\lambda'}(\underset{\sim}{r}_\mu) = \delta_{\lambda\lambda'}\ .$$

$$\{\lambda, \lambda' = 1, 2, \ldots, \Lambda\}$$

Let $E^{\text{cell}}_{\text{GS}}$, the ground-state energy of the unit cell, be:

$$(312) \qquad \begin{aligned} E^{\text{cell}}_{GS} \equiv {} & \sum_{\lambda=1}^{\Lambda} \left\{ -\frac{\hbar^2}{2m_e} Q_\lambda - |\epsilon|^2 [\lambda|\lambda] \right\} + |\epsilon|^2 \sum_{\lambda=2}^{\Lambda} \sum_{\lambda'=1}^{\lambda-1} [\lambda\lambda|\lambda'\lambda'] - \\ & - |\epsilon|^2 \left\{ \sum_{\lambda=2}^{\lambda_0} \sum_{\lambda'=1}^{\lambda-1} + \sum_{\lambda=\lambda_0+2}^{\Lambda} \sum_{\lambda'=\lambda_0+1}^{\lambda-1} \right\} [\lambda\lambda'|\lambda'\lambda]. \end{aligned}$$

Then crystal symmetry allows N_0/Z different wavevectors $\underset{\sim}{\not k}_{\omega}$, all lying within the first Brillouin zone, which we define as:*

---

*Do not confuse with $\underset{\sim}{\not d}_{hkl}$ (Eq. (214)):

$$\underset{\sim}{\not d}_{hkl} \equiv \frac{2\pi}{V} \left\{ h[\underset{\sim}{b} \wedge \underset{\sim}{c}] + k[\underset{\sim}{c} \wedge \underset{\sim}{a}] + \ell[\underset{\sim}{a} \wedge \underset{\sim}{b}] \right\}.$$

As in Chapter II, all quantities with an implicit factor of 2π bear a vertical slash. Thus $\underset{\sim}{\not k} \equiv 2\pi\, \underset{\sim}{k}$, etc.

$$(313) \qquad \underset{\sim}{k}_{\underline{\omega}} \equiv \underset{\sim}{k}_{hkl} \equiv \frac{2\pi}{V}\left(\frac{Z}{N_0}\right)^{1/3}\left\{h\left[\underset{\sim}{b}\wedge\underset{\sim}{c}\right]+k\left[\underset{\sim}{c}\wedge\underset{\sim}{a}\right]+l\left[\underset{\sim}{a}\wedge\underset{\sim}{b}\right]\right\}$$

$$\left\{\underline{\omega}=0,1,2,\ldots,\frac{N_0}{Z}-1\ ;\ h,k,l \text{ within first Brillouin zone}\right\}$$

such that the object:

$$(314) \qquad \Psi_{\lambda\underline{\omega}}\left(\underset{\sim}{r}_{\underline{\mu}}\right) \equiv \sqrt{\frac{Z}{N_0}}\sum_{\underline{\delta}=0}^{\frac{N_0}{Z}-1} \exp\left(i\,\underset{\sim}{k}_{\underline{\omega}}\cdot\underset{\sim}{r}_{\underline{\delta}}\right)\Psi_{\lambda}^{C}\left(\underset{\sim}{r}_{\underline{\mu}}-\underset{\sim}{r}_{\underline{\delta}}\right) \equiv$$

$$(315) \qquad \equiv \sqrt{\frac{Z}{N_0}}\sum_{\nu=1}^{M} c_{\nu\lambda}\sum_{\underline{\delta}=0}^{\frac{N_0}{Z}-1} \exp\left(i\,\underset{\sim}{k}_{\underline{\omega}}\cdot\underset{\sim}{r}_{\underline{\delta}}\right)\psi_{\nu\lambda}\left(\underset{\sim}{r}_{\underline{\mu}}-\underset{\sim}{r}_{\nu}^{\circ}-\underset{\sim}{r}_{\underline{\delta}}\right)$$

$$\left\{\lambda=1,2,\ldots,\Lambda\ ;\ \underline{\omega}=0,1,2,\ldots,\frac{N_0}{Z}-1;\ \underline{\mu}=1,2,\ldots,\Lambda\frac{N_0}{Z}\right\}$$

will provide the N_0/Z required crystal wavefunctions which we baptize 'Bloch-Symmetrized crystal wavefunctions'."

In order that we may write the crystal equivalent of Eq. (307) the $\Psi_{\lambda\underline{\omega}}$ would have to belong to an orthonormal basis. Unfortunately, the orthonormality properties of Ψ_{λ}^{C} do not extend <u>ipso facto</u> to orthonormality for the $\Psi_{\lambda\underline{\omega}}(\underset{\sim}{r}_{\underline{\mu}})$. We shall show that $\Psi_{\lambda\underline{\omega}}(\underset{\sim}{r}_{\underline{\mu}})$ is orthogonal to $\Psi_{\lambda\underline{\omega}'}(\underset{\sim}{r}_{\underline{\mu}})$ for $\underset{\sim}{k}_{\underline{\omega}} \neq \underset{\sim}{k}_{\underline{\omega}'}$, but will find that it is not automatically normalized and also that it is not orthogonal to $\Psi_{\lambda'\underline{\omega}}(\underset{\sim}{r}_{\underline{\mu}})$ when $\lambda' \neq \lambda$.

In fact, we write, for $\underset{\sim}{k}_{\underline{\omega}} \neq \underset{\sim}{k}_{\underline{\omega}'}$:

$$(316a) \qquad I_1 \equiv \iiint_{\frac{N_0 V}{Z}} dv(\underset{\sim}{r}_{\underline{\mu}})\,\Psi_{\lambda\underline{\omega}}^{*}(\underset{\sim}{r}_{\underline{\mu}})\,\Psi_{\lambda'\underline{\omega}'}(\underset{\sim}{r}_{\underline{\mu}}) =$$

$$(316b) \quad = \frac{Z}{N_0} \sum_{\underline{\delta}=0}^{\frac{N_0}{Z}-1} \sum_{\underline{\delta}'=0}^{\frac{N_0}{Z}-1} \exp\left(i \underset{\sim}{k}_{\underline{\omega}'} \cdot \underset{\sim}{r}_{\underline{\delta}'} - i \underset{\sim}{k}_{\underline{\omega}} \cdot \underset{\sim}{r}_{\underline{\delta}}\right) \iiint_{\frac{N_0 V}{Z}} dv(\underset{\sim}{r}_{\mu}) \Psi_{\lambda}^{c^*}\left(\underset{\sim}{r}_{\mu} - \underset{\sim}{r}_{\underline{\delta}}\right) \Psi_{\lambda'}^{c}\left(\underset{\sim}{r}_{\mu} - \underset{\sim}{r}_{\underline{\delta}'}\right),$$

and note that the integral is a function of the difference $\underset{\sim}{r}_{\underline{\delta}''} \equiv \underset{\sim}{r}_{\underline{\delta}'} - \underset{\sim}{r}_{\underline{\delta}}$, whence by a change in the dummy variable of integration from $\underset{\sim}{r}_{\mu}$ to $\underset{\sim}{r} \equiv \underset{\sim}{r}_{\mu} - \underset{\sim}{r}_{\underline{\delta}}$ we get:

$$(316c) \quad I_1 = \frac{Z}{N_0} \sum_{\underline{\delta}''=0}^{\frac{N_0}{Z}-1} \exp\left(i \underset{\sim}{k}_{\underline{\omega}} \cdot \underset{\sim}{r}_{\underline{\delta}''}\right) \iiint_{\frac{N_0 V}{Z}} dv(\underset{\sim}{r}) \Psi_{\lambda}^{c^*}(\underset{\sim}{r}) \Psi_{\lambda'}^{c}(\underset{\sim}{r} - \underset{\sim}{r}_{\underline{\delta}''}) \times \\ \times \sum_{\underline{\delta}'=0}^{\frac{N_0}{Z}-1} \exp\left[i\left(\underset{\sim}{k}_{\underline{\omega}'} - \underset{\sim}{k}_{\underline{\omega}}\right) \cdot \underset{\sim}{r}_{\underline{\delta}'}\right],$$

and the last factor equals $(N_0/Z)\, \delta_{\underline{\omega}\,\underline{\omega}'}$; whence $I_1 = 0$ as claimed, if $\underset{\sim}{k}_{\underline{\omega}} \neq \underset{\sim}{k}_{\underline{\omega}'}$. If $\underset{\sim}{k}_{\underline{\omega}} = \underset{\sim}{k}_{\underline{\omega}'}$, then:

$$(317a) \quad I_2 \equiv \iiint_{\frac{N_0 V}{Z}} dv(\underset{\sim}{r}_{\mu}) \Psi_{\lambda\underline{\omega}}^{*}(\underset{\sim}{r}_{\mu}) \Psi_{\lambda'\underline{\omega}}(\underset{\sim}{r}_{\mu}) =$$

$$(317b) \quad = \sum_{\underline{\delta}=0}^{\frac{N_0}{Z}-1} \exp\left(i \underset{\sim}{k}_{\underline{\omega}} \cdot \underset{\sim}{r}_{\underline{\delta}}\right) \iiint_{\frac{N_0 V}{Z}} dv(\underset{\sim}{r}_{\mu}) \Psi_{\lambda}^{c^*}(\underset{\sim}{r}_{\mu}) \Psi_{\lambda'}^{c}\left(\underset{\sim}{r}_{\mu} - \underset{\sim}{r}_{\underline{\delta}}\right),$$

which refuses to equal $\delta_{\lambda\lambda'}$ without further approximations.

> APPROXIMATION II: "Assume that the zeroth unit cell orbitals do not overlap with the unit cell orbitals of any other unit cell, i.e.:

$$(318) \quad \iiint_{\frac{N_0 V}{Z}} dv(\underset{\sim}{r}_{\mu}) \Psi_{\lambda}^{c^*}(\underset{\sim}{r}_{\mu}) \Psi_{\lambda'}^{c}(\underset{\sim}{r}_{\mu} - \underset{\sim}{r}_{\underline{\delta}}) = \delta_{\lambda\lambda'} \delta_{\underline{\delta}0} ."$$

This most obvious, if severe, approximation yields $I_2 = \delta_{\lambda\lambda'}$, and makes our $\{\Psi_{\lambda\underline{\omega}}(\underline{r}_\mu), \lambda = 1,2,\ldots,\Lambda ; \underline{\omega} = 0,1,2,\ldots, N_o/Z - 1\}$ into an acceptable orthonormal basis set of functions. This approximation is related to those of Pariser-Parr and Hückel theory, and is also rather routine in the treatment of metals, where it is supposed to be far less realistic than for the molecules in our molecular crystals.

Those who refuse to accept the crudity of Approximation II can always resort to a large-scale Gram-Schmidt orthonormalization procedure (228) for the set of functions $\{\Psi^c_\lambda(\underline{r}_\mu - \underline{r}_{\underline{\delta}}), \underline{\delta} = 0, 1,2,\ldots, N_o/Z - 1; \lambda = 1,2,\ldots,\Lambda\}$ but this seems somewhat cumbersome. Fortunately, however, Löwdin (229) has developed an elegant recipe for orthonormalization:

> RECIPE II: "We set up a gigantic hermitian overlap matrix with elements:
>
> $$(319a)\quad \mathcal{S}_{\lambda\underline{\delta},\lambda'\underline{\delta}'} \equiv \iiint_{\frac{N_oV}{Z}} d\tau(\underline{r}_\mu)\,\Psi^{c*}_\lambda(\underline{r}_\mu - \underline{r}_{\underline{\delta}})\,\Psi^{c}_{\lambda'}(\underline{r}_\mu - \underline{r}_{\underline{\delta}'}) - \delta_{\lambda\lambda'}\delta_{\underline{\delta}\underline{\delta}'}.$$
>
> This matrix $\underset{\sim}{\mathcal{S}}$ consists of $(N_o/Z)^2$ blocks of Λ^2 elements each; the general block is defined by:
>
> $$(319b)\quad \boxed{B_{\underline{\delta},\underline{\delta}'}} \equiv \begin{pmatrix} \mathcal{S}_{1\underline{\delta},1\underline{\delta}'} & \mathcal{S}_{1\underline{\delta},2\underline{\delta}'} & \cdots & \mathcal{S}_{1\underline{\delta},\Lambda\underline{\delta}'} \\ \mathcal{S}_{2\underline{\delta},1\underline{\delta}'} & \mathcal{S}_{2\underline{\delta},2\underline{\delta}'} & \cdots & \mathcal{S}_{2\underline{\delta},\Lambda\underline{\delta}'} \\ \vdots & & & \vdots \\ \mathcal{S}_{\Lambda\underline{\delta},1\underline{\delta}'} & \mathcal{S}_{\Lambda\underline{\delta},2\underline{\delta}'} & \cdots & \mathcal{S}_{\Lambda\underline{\delta},\Lambda\underline{\delta}'} \end{pmatrix},$$

and the blocks are arranged inside the $\underset{\approx}{S}$ matrix as follows:

$$(319c)\qquad \underset{\approx}{S} = \begin{pmatrix} \boxed{B_{0,0}} & \boxed{B_{0,1}} & \cdots & \cdots & \boxed{B_{0,\frac{N_0}{Z}-1}} \\ \boxed{B_{1,0}} & \boxed{B_{1,1}} & & & \vdots \\ \vdots & & & \ddots & \\ \boxed{B_{\frac{N_0}{Z}-1,0}} & & \cdots & & \boxed{B_{\frac{N_0}{Z}-1,\frac{N_0}{Z}-1}} \end{pmatrix}.$$

Therefore, the $\underset{\approx}{S}$ matrix will have zero elements *along* as well as close to the main diagonal ($\lambda = \lambda'$, $\underline{\delta} = \underline{\delta}'$), but non-zero elements further away which rapidly go to zero as the distance from the diagonal increases. The integrals:

$$(320)\qquad \iiint_{\frac{N_0V}{Z}} dv(\underset{\sim}{r}_\mu)\,\Psi^{c*}_{\lambda}(\underset{\sim}{r}_\mu - \underset{\sim}{r}_{\underline{\delta}})\,\Psi^{c}_{\lambda'}(\underset{\sim}{r}_\mu - \underset{\sim}{r}_{\underline{\delta}'}) =$$

$$= \sum_{\nu=1}^{M}\sum_{\nu'=1}^{M} c^*_{\nu\lambda}c_{\nu'\lambda'} \iiint_{\frac{N_0V}{Z}} dv(\underset{\sim}{r}_\mu)\,\psi^*_{\nu\lambda}(\underset{\sim}{r}_\mu - \underset{\sim}{r}^{\circ}_{\nu} - \underset{\sim}{r}_{\underline{\delta}})\,\psi_{\nu'\lambda'}(\underset{\sim}{r}_\mu - \underset{\sim}{r}^{\circ}_{\nu'} - \underset{\sim}{r}_{\underline{\delta}'})$$

must, alas, be obtained by some brute-force methods, but once ($\underset{\sim}{r}_{\underline{\delta}} - \underset{\sim}{r}_{\underline{\delta}'}$) exceeds, say, 20 Å, they can be set to zero without excessive danger. Let us replace the four-fold index $\lambda\underline{\delta}$ by a single index i coupled by the ordering procedure: i goes over all λ for each value of $\underline{\delta}$, then goes to the next value $\underline{\delta} + 1$, and again spans all λ, etc. Then Löwdin proves that the 'modified unit cell orbitals' defined by:

$$(321)\qquad \Psi^{NEW}_{i} \equiv \Psi^{c}_{i} - \frac{1}{2}\sum_{j} \Psi^{c}_{j} S_{ji} + \frac{3}{8}\sum_{j}\sum_{j'} \Psi^{c}_{j} S_{jj'} S_{j'i} - \ldots$$

are normalized and orthogonal. In theory, the sums over i go from 1 to $\Lambda N_0/Z$, i.e. over the whole crystal, but in practice they might be truncated if, say, $\underset{\sim}{r}_{\underline{\delta}} - \underset{\sim}{r}_{\underline{\delta}'}$ exceeds 20 Å."

Under the conditions of either Approximation II or Recipe II a simple form for the ground-state energy of the crystal can be written (we will use Approximation II):

(322)
$$E_{GS}=\sum_{\underline{\omega}=0}^{\frac{N_0}{2}-1}\sum_{\lambda=1}^{\Lambda}\left\{-\frac{\hbar^2}{2m_e}Q_{\lambda\underline{\omega}}-|\epsilon|^2[\lambda|\lambda]_{\underline{\omega}}\right\}+\frac{|\epsilon|^2}{2}\sum_{\underline{\omega}=0}^{\frac{N_0}{2}-1}\sum_{\underline{\omega}'=0}^{\frac{N_0}{2}-1}\sum_{\lambda=1}^{\Lambda}\sum_{\lambda'=1}^{\Lambda}[\lambda\lambda|\lambda'\lambda']_{\underline{\omega}\underline{\omega}'}-$$
$$-\frac{|\epsilon|^2}{2}\sum_{\underline{\omega}=0}^{\frac{N_0}{2}-1}\sum_{\underline{\omega}'=0}^{\frac{N_0}{2}-1}\left\{\sum_{\lambda=1}^{\lambda_0}\sum_{\lambda'=1}^{\lambda_0}+\sum_{\lambda=\lambda_0+1}^{\Lambda}\sum_{\lambda'=\lambda_0+1}^{\Lambda}\right\}[\lambda\lambda'|\lambda'\lambda]_{\underline{\omega}\underline{\omega}'}\,.$$

The contribution to the second and third terms of the right hand side of Eq. (322) due to the cases $\{\lambda = \lambda', \ \underline{\omega} = \underline{\omega}'\}$ cancel each other. If Recipe II were used, then the orbital labels λ, λ' in Eq. (322) and in what follows would refer to a new set of orbitals and orbital energies obtained from the original set Eq. (308a, 308b, 308c, 308d) by Löwdin's orthonormalization scheme, and the zeroth unit cell would be replaced by a somewhat larger non-primitive cell containing more molecules.

The crystal Slater integrals in Eq. (322) may be written as follows:

(323a)
$$Q_{\lambda\underline{\omega}}\equiv\iiint_{\frac{N_0V}{2}}dv(\underset{\sim}{r}_{\underline{\mu}})\,\Psi^{*}_{\lambda\underline{\omega}}(\underset{\sim}{r}_{\underline{\mu}})\sum_{i=1}^{3}\frac{\partial^2}{\partial(r^{i}_{\underline{\mu}})^2}\,\Psi_{\lambda\underline{\omega}}(\underset{\sim}{r}_{\underline{\mu}})\,,$$

(323b)
$$[\lambda|\lambda]_{\underline{\omega}}\equiv\sum_{\underline{\delta}=0}^{\frac{N_0}{2}-1}\sum_{\nu=1}^{M}\zeta_{\nu}\iiint_{\frac{N_0V}{2}}dv(\underset{\sim}{r}_{\underline{\mu}})\,\frac{\Psi^{*}_{\lambda\underline{\omega}}(\underset{\sim}{r}_{\underline{\mu}})\Psi_{\lambda\omega}(\underset{\sim}{r}_{\underline{\mu}})}{|\underset{\sim}{r}_{\underline{\mu}}-\underset{\sim}{r}^{0}_{\nu}-\underset{\sim}{r}_{\underline{\delta}}|}\,,$$

$$(323c)\quad [\lambda\lambda|\lambda'\lambda']_{\underline{\omega}\underline{\omega}'} \equiv \iiint_{\frac{N_0V}{2}} dv(\underset{\sim}{r}_{\mu'}) \iiint_{\frac{N_0V}{2}} dv(\underset{\sim}{r}_{\mu})\, \frac{\Psi^*_{\lambda\underline{\omega}}(\underset{\sim}{r}_{\mu})\Psi_{\lambda\underline{\omega}}(\underset{\sim}{r}_{\mu})\Psi^*_{\lambda'\underline{\omega}'}(\underset{\sim}{r}_{\mu'})\Psi_{\lambda'\underline{\omega}'}(\underset{\sim}{r}_{\mu'})}{|\underset{\sim}{r}_{\mu} - \underset{\sim}{r}_{\mu'}|},$$

$$(323d)\quad [\lambda\lambda'|\lambda'\lambda]_{\underline{\omega}\underline{\omega}'} \equiv \iiint_{\frac{N_0V}{2}} dv(\underset{\sim}{r}_{\mu'}) \iiint_{\frac{N_0V}{2}} dv(\underset{\sim}{r}_{\mu})\, \frac{\Psi^*_{\lambda\underline{\omega}}(\underset{\sim}{r}_{\mu})\Psi_{\lambda'\underline{\omega}'}(\underset{\sim}{r}_{\mu})\Psi^*_{\lambda'\underline{\omega}'}(\underset{\sim}{r}_{\mu'})\Psi_{\lambda\underline{\omega}}(\underset{\sim}{r}_{\mu'})}{|\underset{\sim}{r}_{\mu} - \underset{\sim}{r}_{\mu'}|}.$$

A formal simplification of Eq. (323b) will prove convenient: we define, as in Chapter II, Eq. (211), the nuclear charge density function:

$$(324)\qquad \rho^N(\underset{\sim}{r}) \equiv \sum_{\underline{\delta}=0}^{\frac{N_0}{2}-1} \sum_{\nu=1}^{M} Z_\nu\, \delta(\underset{\sim}{r} - \underset{\sim}{r}^\circ_\nu - \underset{\sim}{r}_{\underline{\delta}}),$$

whence we may write:

$$(325)\quad [\lambda|\lambda]_{\underline{\omega}} = \iiint_{\frac{N_0V}{2}} \frac{dv(\underset{\sim}{r})}{|\underset{\sim}{r}|} \iiint_{\frac{N_0V}{2}} dv(\underset{\sim}{r}_{\mu})\, \Psi^*_{\lambda\underline{\omega}}(\underset{\sim}{r}_{\mu})\Psi_{\lambda\underline{\omega}}(\underset{\sim}{r}_{\mu})\rho^N(\underset{\sim}{r}_{\mu} + \underset{\sim}{r}).$$

Note that, from Eq. (322), we may define the energy of the one-electron state associated with the wavevector $\underset{\sim}{k}_{\underline{\omega}}$ and the orbital λ as:

$$(326)\quad E_\lambda(\underset{\sim}{k}_{\underline{\omega}}) = \left\{ -\frac{\hbar^2}{2m_e} Q_{\lambda\underline{\omega}} - |\epsilon|^2[\lambda|\lambda]_{\underline{\omega}} \right\} + |\epsilon|^2 \sum_{\underline{\omega}'=0}^{\frac{N_0}{2}-1} \sum_{\lambda'=1}^{\Lambda} [\lambda\lambda|\lambda'\lambda']_{\underline{\omega}\underline{\omega}'} - \\ - |\epsilon|^2 \sum_{\underline{\omega}'=0}^{\frac{N_0}{2}-1} \left\{ \text{Either} \sum_{\lambda'=1}^{\lambda_0} \text{ or } \sum_{\lambda'=\lambda_0+1}^{\Lambda} \right\} [\lambda\lambda'|\lambda'\lambda]_{\underline{\omega}\underline{\omega}'}.$$

This energy $E_\lambda(\mathbf{k}_{\underline{\omega}})$ may prove useful in calculations seeking explanations for conductivity and other transport properties in donor-acceptor crystals; the formalism developed below can be applied almost trivially to the evaluation of $E_\lambda(\mathbf{k}_{\underline{\omega}})$ (see Appendix IV). Our main concern is, however, E_{GS}. We write:

(327)
$$E_{GS} = \sum_{\lambda=1}^{\Lambda}\left\{-\frac{\hbar^2}{2m_e}Q_\lambda^{XT} - |\epsilon|^2[\lambda|\lambda]^{XT}\right\} + \frac{|\epsilon|^2}{2}\sum_{\lambda=1}^{\Lambda}\sum_{\lambda'=1}^{\Lambda}[\lambda\lambda|\lambda'\lambda']^{XT} - \frac{|\epsilon|^2}{2}\left\{\sum_{\lambda=1}^{\lambda_0}\sum_{\lambda'=1}^{\lambda_0} + \sum_{\lambda=\lambda_0+1}^{\Lambda}\sum_{\lambda'=\lambda_0+1}^{\Lambda}\right\}[\lambda\lambda'|\lambda'\lambda]^{XT},$$

where the "total" kinetic energy, nuclear attraction, direct Coulomb and exchange Coulomb integrals for the crystal spin-orbitals are defined by:

(328a)
$$Q_\lambda^{XT} \equiv \sum_{\underline{\omega}=0}^{N_0/z-1} Q_{\lambda\underline{\omega}},$$

(328b)
$$[\lambda|\lambda]^{XT} \equiv \sum_{\underline{\omega}=0}^{N_0/z-1} [\lambda|\lambda]_{\underline{\omega}},$$

(328c)
$$[\lambda\lambda|\lambda'\lambda']^{XT} \equiv \sum_{\underline{\omega}=0}^{N_0/z-1}\sum_{\underline{\omega}'=0}^{N_0/z-1} [\lambda\lambda|\lambda'\lambda']_{\underline{\omega}\underline{\omega}'},$$

(328d)
$$[\lambda\lambda'|\lambda'\lambda]^{XT} \equiv \sum_{\underline{\omega}=0}^{N_0/z-1}\sum_{\underline{\omega}'=0}^{N_0/z-1} [\lambda\lambda'|\lambda'\lambda]_{\underline{\omega}\underline{\omega}'}^{XT}.$$

Great simplifications are made possible by use of the identity:

(329)
$$\sum_{\underline{\omega}=0}^{N_0/z-1} \exp(i\mathbf{k}_{\underline{\omega}}\cdot\mathbf{r}_{\underline{\delta}}) = \frac{N_0}{z}\delta_{\underline{\delta}0},$$

and of sundry symmetry arguments and "neglect of crystal end effects." In fact, we obtain:

(330a) $$Q_{\lambda}^{XT} = \iiint\limits_{\frac{N_0 V}{Z}} dv(\mathbf{r}_{\mu}) \sum_{\underline{\delta}=0}^{\frac{N_0}{Z}-1} \Psi_{\lambda}^{c*}(\mathbf{r}_{\mu}-\mathbf{r}_{\underline{\delta}}) \sum_{i=1}^{3} \frac{\partial^2}{\partial (r_{\mu}^{i})^2} \Psi_{\lambda}^{c}(\mathbf{r}_{\mu}-\mathbf{r}_{\underline{\delta}}) =$$

(330b) $$= \frac{N_0}{Z} \iiint\limits_{\frac{N_0 V}{Z}} dv(\mathbf{r}_{\mu}) \Psi_{\lambda}^{c*}(\mathbf{r}_{\mu}) \sum_{i=1}^{3} \frac{\partial^2}{\partial (r_{\mu}^{i})^2} \Psi_{\lambda}^{c}(\mathbf{r}_{\mu}) =$$

(330c) $$= \frac{N_0}{Z} Q_{\lambda};$$

(331a) $$[\lambda|\lambda]^{XT} = \iiint\limits_{\frac{N_0 V}{Z}} \frac{dv(\mathbf{r})}{|\mathbf{r}|} \iiint\limits_{\frac{N_0 V}{Z}} dv(\mathbf{r}_{\mu}) \sum_{\underline{\delta}=0}^{\frac{N_0}{Z}-1} \left|\Psi_{\lambda}^{c}(\mathbf{r}_{\mu}-\mathbf{r}_{\underline{\delta}})\right|^2 \rho^{N}(\mathbf{r}_{\mu}+\mathbf{r}) =$$

(331b) $$= \frac{N_0}{Z} \sum_{\nu=1}^{\frac{N_0}{Z}-1} \zeta_{\nu} \sum_{\underline{\delta}=0}^{\frac{N_0}{Z}-1} \iiint\limits_{\frac{N_0 V}{Z}} \frac{dv(\mathbf{r}_{\mu})}{|\mathbf{r}_{\mu}-\mathbf{r}_{\nu}^{0}-\mathbf{r}_{\underline{\delta}}|} \left|\Psi_{\lambda}^{c}(\mathbf{r}_{\mu})\right|^2;$$

(332a) $$[\lambda\lambda|\lambda'\lambda']^{XT} = \iiint\limits_{\frac{N_0 V}{Z}} \frac{dv(\mathbf{r})}{|\mathbf{r}|} \iiint\limits_{\frac{N_0 V}{Z}} dv(\mathbf{r}_{\mu}) \sum_{\underline{\delta}=0}^{\frac{N_0}{Z}-1} \left|\Psi_{\lambda}^{c}(\mathbf{r}_{\mu}-\mathbf{r}_{\underline{\delta}})\right|^2 \sum_{\underline{\delta}'=0}^{\frac{N_0}{Z}-1} \left|\Psi_{\lambda'}^{c}(\mathbf{r}_{\mu}+\mathbf{r}-\mathbf{r}_{\underline{\delta}'})\right|^2 =$$

(332b) $$= \frac{N_0}{Z} \iiint\limits_{\frac{N_0 V}{Z}} \frac{dv(\mathbf{r})}{|\mathbf{r}|} \iiint\limits_{\frac{N_0 V}{Z}} dv(\mathbf{r}_{\mu}) \left|\Psi_{\lambda}^{c}(\mathbf{r}_{\mu})\right|^2 \sum_{\underline{\delta}=0}^{\frac{N_0}{Z}-1} \left|\Psi_{\lambda'}^{c}(\mathbf{r}_{\mu}+\mathbf{r}-\mathbf{r}_{\underline{\delta}})\right|^2;$$

(333a) $$[\lambda\lambda'|\lambda'\lambda]^{XT} = \iiint\limits_{\frac{N_0 V}{Z}} \frac{dv(\mathbf{r})}{|\mathbf{r}|} \iiint\limits_{\frac{N_0 V}{Z}} dv(\mathbf{r}_{\mu}) \sum_{\underline{\delta}=0}^{\frac{N_0}{Z}-1} \Psi_{\lambda}^{c*}(\mathbf{r}_{\mu}-\mathbf{r}_{\underline{\delta}}) \Psi_{\lambda}^{c}(\mathbf{r}_{\mu}+\mathbf{r}-\mathbf{r}_{\underline{\delta}}) \times$$
$$\times \sum_{\underline{\delta}'=0}^{\frac{N_0}{Z}-1} \Psi_{\lambda'}^{c*}(\mathbf{r}_{\mu}+\mathbf{r}-\mathbf{r}_{\underline{\delta}'}) \Psi_{\lambda'}^{c}(\mathbf{r}_{\mu}-\mathbf{r}_{\underline{\delta}'}) =$$

(333b) $$= \frac{N_0}{Z} \iiint\limits_{\frac{N_0 V}{Z}} \frac{dv(\mathbf{r})}{|\mathbf{r}|} \iiint\limits_{\frac{N_0 V}{Z}} dv(\mathbf{r}_{\mu}) \Psi_{\lambda}^{c*}(\mathbf{r}_{\mu}) \Psi_{\lambda}^{c}(\mathbf{r}_{\mu}+\mathbf{r}) \times$$
$$\times \sum_{\underline{\delta}=0}^{\frac{N_0}{Z}-1} \Psi_{\lambda'}^{c*}(\mathbf{r}_{\mu}+\mathbf{r}-\mathbf{r}_{\underline{\delta}}) \Psi_{\lambda'}^{c}(\mathbf{r}_{\mu}-\mathbf{r}_{\underline{\delta}}).$$

The total kinetic energy integral Q_λ^{XT} is thus simply N_o/Z times the kinetic energy integral for the electron in the λ-th orbital in the isolated zeroth unit cell, Q_λ, and should present no computational difficulties. Accordingly, we shall not consider Q_λ^{XT} any further.

If vast digital computing funds were available, then the total integrals $[\lambda|\lambda]^{XT}$, $[\lambda\lambda|\lambda'\lambda']^{XT}$, and $[\lambda\lambda'|\lambda'\lambda]^{XT}$ could be evaluated naively by "brute-force" techniques in direct space by expanding Eqs. (331b, 332b, 333b) in terms of atomic one-, two-, three-, and four-center integrals, to wit:

$$\begin{aligned}[\lambda|\lambda]^{XT} &= \frac{N_o}{Z}\sum_{\nu=1}^{M}\zeta_\nu\sum_{\nu'=1}^{M}\sum_{\nu''=1}^{M}c^*_{\nu'\lambda}c_{\nu''\lambda}\sum_{\underline{\delta}=0}^{\frac{N_o}{Z}-1}\times \\ &\times\iiint_{\frac{N_o v}{Z}}\frac{dv(\mathbf{r}_\mu)}{|\mathbf{r}_\mu-\mathbf{r}^\circ_\nu-\mathbf{r}_{\underline{\delta}}|}\psi^*_{\nu'\lambda}(\mathbf{r}_\mu-\mathbf{r}^\circ_{\nu'})\psi_{\nu''\lambda}(\mathbf{r}_\mu-\mathbf{r}^\circ_{\nu''}),\end{aligned} \tag{334}$$

$$\begin{aligned}[\lambda\lambda|\lambda'\lambda']^{XT} &= \frac{N_o}{Z}\sum_{\nu=1}^{M}\sum_{\nu'=1}^{M}\sum_{\nu''=1}^{M}\sum_{\nu'''=1}^{M}c^*_{\nu\lambda}c_{\nu'\lambda}c^*_{\nu''\lambda'}c_{\nu'''\lambda'}\times \\ &\times\sum_{\underline{\delta}=0}^{\frac{N_o}{Z}-1}\iiint_{\frac{N_o v}{Z}}\frac{dv(\mathbf{r})}{|\mathbf{r}|}\iiint_{\frac{N_o v}{Z}}dv(\mathbf{r}_\mu)\,\psi^*_{\nu\lambda}(\mathbf{r}_\mu-\mathbf{r}^\circ_\nu)\psi_{\nu'\lambda}(\mathbf{r}_\mu-\mathbf{r}^\circ_{\nu'})\times \\ &\times\psi^*_{\nu''\lambda'}(\mathbf{r}_\mu+\mathbf{r}-\mathbf{r}^\circ_{\nu''}-\mathbf{r}_{\underline{\delta}})\psi_{\nu'''\lambda}(\mathbf{r}_\mu+\mathbf{r}-\mathbf{r}^\circ_{\nu'''}-\mathbf{r}_\delta),\end{aligned} \tag{335}$$

$$[\lambda\lambda'|\lambda'\lambda]^{XT} = \frac{N_o}{Z}\sum_{\nu=1}^{M}\sum_{\nu'=1}^{M}\sum_{\nu''=1}^{M}\sum_{\nu'''=1}^{M}c^*_{\nu\lambda}c_{\nu'\lambda}c^*_{\nu''\lambda'}c_{\nu'''\lambda'}\times \tag{336}$$

$$\times \sum_{\boldsymbol{\delta}=0}^{\frac{N_c}{2}-1} \iiint_{\frac{N_cV}{2}} \frac{dv(\mathbf{r})}{|\mathbf{r}|} \iiint_{\frac{N_cV}{2}} dv(\mathbf{r}_\mu)\, \psi^*_{\nu\lambda}(\mathbf{r}_\mu - \mathbf{r}^\circ_\nu)\, \psi_{\nu'\lambda}(\mathbf{r}_\mu + \mathbf{r} - \mathbf{r}^\circ_{\nu'}) \times$$
$$\times\, \psi^*_{\nu''\lambda'}(\mathbf{r}_\mu + \mathbf{r} - \mathbf{r}^\circ_{\nu''} - \mathbf{r}_{\boldsymbol{\delta}})\, \psi_{\nu'''\lambda'}(\mathbf{r}_\mu - \mathbf{r}^\circ_{\nu'''} - \mathbf{r}_{\boldsymbol{\delta}}).$$

C. Evaluation of Integrals in Fourier Transform Space

The feasibility of the brute-force approach depends on the rates of convergence of the sums over $\boldsymbol{\delta}$ in Eqs. (334, 335, 336). Physical arguments lead us to believe that $[\lambda\lambda'|\lambda'\lambda]^{XT}$ might converge with reasonable rapidity, so that early truncation of the sum over $\boldsymbol{\delta}$ is feasible, but the long-range nature of the Coulomb interaction will probably cause slow convergence of Eqs. (334 and 335).

The main purpose of this chapter is, however, to utilize Fourier techniques and the crystal translational symmetry in a new scheme for the evaluation of $[\lambda|\lambda]^{XT}$, $[\lambda\lambda|\lambda'\lambda']^{XT}$, and $[\lambda\lambda'|\lambda'\lambda]^{XT}$. We shall concern ourselves with the integrands of Eqs. (331a, 332a, 333a). Both $\rho^N(\mathbf{r})$ and

$$\sum_{\boldsymbol{\delta}=0}^{\frac{N_c}{2}-1} \left|\Psi^c_\lambda(\mathbf{r}_\mu - \mathbf{r}_{\boldsymbol{\delta}})\right|^2$$

enjoy the translational periodicity of the direct crystal lattice, and hence may be expanded in the Fourier series:

$$\rho^N(\mathbf{r}) = \frac{1}{V} \sum_{h=-\infty}^{\infty} \sum_{k=-\infty}^{\infty} \sum_{l=-\infty}^{\infty} P(\mathbf{d}_{hkl}) \exp(i\,\mathbf{d}_{hkl}\cdot\mathbf{r}), \tag{337}$$

$$(338)\quad \sum_{\underline{\delta}=0}^{\frac{N_0}{Z}-1} \left|\Psi^{c}_{\lambda}\left(\underset{\sim}{r}_{\mu}-\underset{\sim}{r}_{\underline{\delta}}\right)\right|^{2} = \frac{1}{V}\sum_{h=-\infty}^{\infty}\sum_{k=-\infty}^{\infty}\sum_{l=-\infty}^{\infty} W_{\lambda}\left(\underset{\sim}{\text{đ}}_{hkl}\right)\exp\left(i\underset{\sim}{\text{đ}}_{hkl}\cdot\underset{\sim}{r}_{\mu}\right).$$

The Fourier coefficient P($\underset{\sim}{\text{đ}}_{hkl}$) was evaluated in Chapter II, Eq. (215) and is given by:

$$(339)\quad P\left(\underset{\sim}{\text{đ}}_{hkl}\right) = \sum_{\nu=1}^{M} Z_{\nu}\exp\left(-i\underset{\sim}{\text{đ}}_{hkl}\cdot\underset{\sim}{r}^{\circ}_{\nu}\right);$$

the Fourier coefficient W_λ($\underset{\sim}{\text{đ}}_{hkl}$) is obtained as follows:

$$(340a)\quad W_{\lambda}\left(\underset{\sim}{\text{đ}}_{hkl}\right) \equiv \iiint\limits_{V} dv\left(\underset{\sim}{r}_{\mu}\right)\exp\left(-i\underset{\sim}{\text{đ}}_{hkl}\cdot\underset{\sim}{r}_{\mu}\right)\sum_{\underline{\delta}=0}^{\frac{N_0}{Z}-1}\left|\Psi^{c}_{\lambda}\left(\underset{\sim}{r}_{\mu}-\underset{\sim}{r}_{\underline{\delta}}\right)\right|^{2} =$$

$$(340b)\quad = \frac{Z}{N_0}\sum_{\nu=1}^{M}\sum_{\nu'=1}^{M} c^{*}_{\nu\lambda}c_{\nu'\lambda}\sum_{\underline{\delta}=0}^{\frac{N_0}{Z}-1}\iiint\limits_{\frac{N_0 V}{Z}} dv\left(\underset{\sim}{r}_{\mu}\right)\exp\left(-i\underset{\sim}{\text{đ}}_{hkl}\cdot\underset{\sim}{r}_{\mu}\right)\times$$

$$\times\,\psi^{*}_{\nu\lambda}\left(\underset{\sim}{r}_{\mu}-\underset{\sim}{r}^{\circ}_{\nu}-\underset{\sim}{r}_{\underline{\delta}}\right)\psi_{\nu'\lambda}\left(\underset{\sim}{r}_{\mu}-\underset{\sim}{r}^{\circ}_{\nu'}-\underset{\sim}{r}_{\underline{\delta}}\right) =$$

$$(340c)\quad = \frac{Z}{N_0}\sum_{\underline{\delta}=0}^{\frac{N_0}{Z}-1}\exp\left(-i\underset{\sim}{\text{đ}}_{hkl}\cdot\underset{\sim}{r}_{\underline{\delta}}\right)\sum_{\nu=1}^{M}\sum_{\nu'=1}^{M} c^{*}_{\nu\lambda}c_{\nu'\lambda}\exp\left(-i\underset{\sim}{\text{đ}}_{hkl}\cdot\underset{\sim}{r}^{\circ}_{\nu}\right)\times$$

$$\times\iiint\limits_{\frac{N_0 V}{Z}} dv\left(\underset{\sim}{r}\right)\exp\left(-i\underset{\sim}{\text{đ}}_{hkl}\cdot\underset{\sim}{r}\right)\psi^{*}_{\nu\lambda}\left(\underset{\sim}{r}\right)\psi_{\nu'\lambda}\left(\underset{\sim}{r}-\underset{\sim}{r}^{\circ}_{\nu'}+\underset{\sim}{r}^{\circ}_{\nu}\right) =$$

$$(340d)\quad = \sum_{\nu=1}^{M}\sum_{\nu'=1}^{M} c^{*}_{\nu\lambda}c_{\nu'\lambda}\exp\left(-i\underset{\sim}{\text{đ}}_{hkl}\cdot\underset{\sim}{r}^{\circ}_{\nu}\right)I^{(0)}_{\nu\lambda,\nu'\lambda}\left(\underset{\sim}{\text{đ}}_{hkl}\right),$$

where:

$$\text{(340e)}\quad I^{(\underline{\delta})}_{\nu\lambda,\nu'\lambda'}(\mathbf{đ}_{hkl}) \equiv \iiint_{\frac{N_0V}{Z}} dv(\mathbf{r}_{\underline{\mu}}) \exp\left(-i\,\mathbf{đ}_{hkl}\cdot\mathbf{r}_{\underline{\mu}}\right) \psi^{*}_{\nu\lambda}(\mathbf{r}_{\underline{\mu}})\, \psi_{\nu'\lambda'}(\mathbf{r}_{\underline{\mu}}-\mathbf{r}^{\circ}_{\nu'}+\mathbf{r}^{\circ}_{\nu}-\mathbf{r}_{\underline{\delta}})$$

is a two-center integral which is evaluated analytically for Slater-type orbitals $\psi^{\mathrm{STO}}_{\nu\lambda}$ in Appendix II.

We would like to avoid the term h = k = l = 0 in the Fourier expansion for $\sum_{\underline{\delta}=0}^{N_0/Z-1} \left|\Psi^{C}_{\lambda}(\mathbf{r}_{\underline{\mu}}-\mathbf{r}_{\underline{\delta}})\right|^2$:

$$\text{(341)}\quad W_{\lambda}(0) = \frac{Z}{N_0} \iiint_{\frac{N_0V}{Z}} dv(\mathbf{r}_{\underline{\mu}}) \sum_{\underline{\delta}=0}^{\frac{N_0}{Z}-1} \left|\Psi^{C}_{\lambda}(\mathbf{r}_{\underline{\mu}}-\mathbf{r}_{\underline{\delta}})\right|^2 = 1;$$

otherwise nasty singularities will appear below in our results for the total nuclear attraction integral $[\lambda|\lambda]^{XT}$ and for the total direct Coulomb integral $[\lambda\lambda|\lambda'\lambda']^{XT}$. We can do this by remembering that the overall charge of the crystal is zero. In fact, we had not mentioned the crystal nucleus-nucleus (or atomic core-atomic core) Coulomb repulsion energy E_{nucl} which, thanks to the Born-Oppenheimer approximation, can be treated classically:

$$\text{(342)}\quad E_{\mathrm{nucl}} \equiv \frac{|e|^2}{2} \sum_{\underline{\delta}=0}^{\frac{N_0}{Z}-1} \sum_{\underline{\delta}'=0}^{\frac{N_0}{Z}-1} \sum_{\nu=1}^{M} \sum_{\nu'=1}^{M} \frac{\zeta_{\nu}\zeta_{\nu'}}{|\mathbf{r}^{\circ}_{\nu}+\mathbf{r}_{\underline{\delta}}-\mathbf{r}^{\circ}_{\nu'}-\mathbf{r}_{\underline{\delta}'}|};$$

The reason for our neglect was that normally E_{nucl} would not appear in the calculation of quantities such as ΔE_{CT} (see Eq. (303)). Now, the problem with the $W_\lambda(0)$ for the electrons has its complement in the Ewald treatment for the nuclei: the Ewald method, applied to the nuclei, would require electrical neutrality in each unit cell (see Eq. (216)); this can be satisfied if the electrons are included in the bookkeeping even when they are not included in the Ewald calculation; likewise, in the present calculation for the electrons we need to assume the presence of the nuclei, and from the electrical neutrality condition:

$$-|\epsilon| \sum_{\lambda=1}^{\Lambda} W_\lambda(0) + |\epsilon| \sum_{\nu=1}^{M} \zeta_\nu = 0 \tag{343}$$

we argue that the $h = k = l = 0$ term in Eq. (337) and Eq. (338) can be formally ignored.[*] This result will be signified by a single prime on the summation over h,k,l whenever Eq. (337) and (338) are used.

We now can attack $[\lambda|\lambda]^{XT}$ and $[\lambda\lambda|\lambda'\lambda']^{XT}$ (Eqs. (331a, 332a)) by the convolution theorem (cf. Chapter II, page 84); the Fourier transform of:

$$\iiint_{\frac{N_0 V}{Z}} dv(\underset{\sim}{r}_{\underline{\mu}}) \sum_{\underline{\delta}=0}^{\frac{N_0}{Z}-1} \left|\Psi_\lambda^C(\underset{\sim}{r}_{\underline{\mu}} - \underset{\sim}{r}_{\underline{\delta}})\right|^2 \rho^N(\underset{\sim}{r}_{\underline{\mu}} + \underset{\sim}{r})$$

---

[*] See also footnote on page 187.

is $(N_0/Z)P(\underset{\sim}{\mathfrak{h}}_{hkl})W_\lambda^*(\underset{\sim}{\mathfrak{h}}_{hkl})$, whence, following Bertaut (169) we get:

$$[\lambda|\lambda]^{XT} = \frac{N_0}{VZ}\iiint\limits_{\frac{N_0V}{Z}} \frac{dv(\underset{\sim}{r})}{|\underset{\sim}{r}|} \sum_{h=-\infty}^{\infty}\sum_{k=-\infty}^{\infty}{\sum_{l=-\infty}^{\infty}}' P(\underset{\sim}{\mathfrak{h}}_{hkl})W_\lambda^*(\underset{\sim}{\mathfrak{h}}_{hkl}) \times \exp(i\underset{\sim}{\mathfrak{h}}_{hkl}\cdot\underset{\sim}{r}) = \tag{344a}$$

$$= \frac{4\pi N_0}{VZ}\sum_{h=-\infty}^{\infty}\sum_{k=-\infty}^{\infty}{\sum_{l=-\infty}^{\infty}}' \frac{P(\underset{\sim}{\mathfrak{h}}_{hkl})W_\lambda^*(\underset{\sim}{\mathfrak{h}}_{hkl})}{|\underset{\sim}{\mathfrak{h}}_{hkl}|^2} = \tag{344b}$$

$$= \frac{4\pi N_0}{VZ}\sum_{h=-\infty}^{\infty}\sum_{k=-\infty}^{\infty}{\sum_{l=-\infty}^{\infty}}' \frac{W_\lambda^*(\underset{\sim}{\mathfrak{h}}_{hkl})}{|\underset{\sim}{\mathfrak{h}}_{hkl}|^2}\sum_{\nu=1}^{M} Z_\nu \exp(-i\underset{\sim}{\mathfrak{h}}_{hkl}\cdot\underset{\sim}{r}_\nu^0). \tag{344c}$$

Similarly, the Fourier transform of

$$\iiint\limits_{\frac{N_0V}{Z}} dv(\underset{\sim}{r}_\mu)\sum_{\underline{\delta}=0}^{\frac{N_0}{Z}-1}\left|\Psi_\lambda^c(\underset{\sim}{r}_\mu-\underset{\sim}{r}_{\underline{\delta}})\right|^2 \sum_{\underline{\delta}'=0}^{\frac{N_0}{Z}-1}\left|\Psi_{\lambda'}^c(\underset{\sim}{r}_\mu+\underset{\sim}{r}-\underset{\sim}{r}_{\underline{\delta}'})\right|^2$$

is $(N_0/Z)W_\lambda^*(\underset{\sim}{\mathfrak{h}}_{hkl})W_{\lambda'}(\underset{\sim}{\mathfrak{h}}_{hkl})$, whence:

$$[\lambda\lambda|\lambda'\lambda']^{XT} = \frac{N_0}{VZ}\iiint\limits_{\frac{N_0V}{Z}} \frac{dv(\underset{\sim}{r})}{|\underset{\sim}{r}|} \sum_{h=-\infty}^{\infty}\sum_{k=-\infty}^{\infty}{\sum_{l=-\infty}^{\infty}}' W_\lambda^*(\underset{\sim}{\mathfrak{h}}_{hkl})W_{\lambda'}(\underset{\sim}{\mathfrak{h}}_{hkl}) \times \exp(i\underset{\sim}{\mathfrak{h}}_{hkl}\cdot\underset{\sim}{r}) = \tag{345a}$$

(345b)
$$= \frac{4\pi N_0}{VZ} \sum_{h=-\infty}^{\infty} \sum_{k=-\infty}^{\infty} \sum_{l=-\infty}^{\infty}{}' \frac{W_\lambda^*(\underset{\sim}{\mathfrak{k}}_{hkl})\, W_{\lambda'}(\underset{\sim}{\mathfrak{k}}_{hkl})}{|\underset{\sim}{\mathfrak{k}}_{hkl}|^2} .$$

The total exchange Coulomb integral $[\lambda\lambda'|\lambda'\lambda]$ (Eq. (333a)) presents some complications. Let us define:

(346a,b)
$$K(\underset{\sim}{r}) \equiv \sum_{\underline{\delta}=0}^{\frac{N_0}{Z}-1} \sum_{\underline{\delta}'=0}^{\frac{N_0}{Z}-1} K_{\underline{\delta}\underline{\delta}'}(\underset{\sim}{r}) \equiv \iiint_{\frac{N_0V}{Z}} dv(\underset{\sim}{r}_{\underline{\mu}})\, J(\underset{\sim}{r}, \underset{\sim}{r}_{\underline{\mu}}) \equiv$$

(346c)
$$\equiv \iiint_{\frac{N_0V}{Z}} dv(\underset{\sim}{r}_{\underline{\mu}}) \sum_{\underline{\delta}=0}^{N_0/Z-1} \sum_{\underline{\delta}'=0}^{N_0/Z-1} J_{\underline{\delta}\underline{\delta}'}(\underset{\sim}{r}, \underset{\sim}{r}_{\underline{\mu}}) \equiv \iiint_{\frac{N_0V}{Z}} dv(\underset{\sim}{r}_{\underline{\mu}}) \sum_{\underline{\delta}=0}^{\frac{N_0}{Z}-1} \sum_{\underline{\delta}'=0}^{\frac{N_0}{Z}-1} \times$$

(346d)
$$\times\, \Psi_\lambda^{c*}(\underset{\sim}{r}_{\underline{\mu}} - \underset{\sim}{r}_{\underline{\delta}})\, \Psi_{\lambda'}^{c}(\underset{\sim}{r}_{\underline{\mu}} - \underset{\sim}{r}_{\underline{\delta}})\, \Psi_{\lambda'}^{c*}(\underset{\sim}{r}_{\underline{\mu}} + \underset{\sim}{r} - \underset{\sim}{r}_{\underline{\delta}'})\, \Psi_\lambda^{c}(\underset{\sim}{r}_{\underline{\mu}} + \underset{\sim}{r} - \underset{\sim}{r}_{\underline{\delta}}) .$$

Now $J(\underset{\sim}{r}, \underset{\sim}{r}_{\underline{\mu}})$ is periodic in $\underset{\sim}{r}_{\underline{\mu}}$ but it is not obviously periodic in $\underset{\sim}{r}$; moreover, in contrast with the situation in Eqs. (331a, 332a), $J(\underset{\sim}{r}, \underset{\sim}{r}_{\underline{\mu}})$ as written cannot be decomposed into a product of two functions, one periodic only in $\underset{\sim}{r}_{\underline{\mu}}$, the other periodic in both $\underset{\sim}{r}_{\underline{\mu}}$ and $\underset{\sim}{r}$. A procedure of uncertain legality, in view of the factor $1/|\underset{\sim}{r}|$ in Eq. (333a), is to: (i) use $\underset{\sim}{r}_{\underline{\mu}} + \underset{\sim}{r} \equiv \underset{\sim}{r}_{\underline{\mu}'}$ in Eq. (346d), (ii) pull the two sums over $\underline{\delta}$ and $\underline{\delta}'$ and the two factors $\Psi_{\lambda'}^{C*}(\underset{\sim}{r}_{\underline{\mu}'} - \underset{\sim}{r}_{\underline{\delta}'})$ and $\Psi_{\lambda}^{C}(\underset{\sim}{r}_{\underline{\mu}'} - \underset{\sim}{r}_{\underline{\delta}})$ out of the integral over $\underset{\sim}{r}_{\underline{\mu}}$, (iii) use Eq. (318) on the remaining integral over $\underset{\sim}{r}_{\underline{\mu}}$, and (iv) obtain:

(346e)
$$K(\underset{\sim}{r}) \equiv \iiint_{\frac{N_0V}{Z}} dv(\underset{\sim}{r}_{\underline{\mu}}) \sum_{\underline{\delta}=0}^{\frac{N_0}{Z}-1} \Psi_\lambda^{c*}(\underset{\sim}{r}_{\underline{\mu}} - \underset{\sim}{r}_{\underline{\delta}})\, \Psi_{\lambda'}^{c}(\underset{\sim}{r}_{\underline{\mu}} - \underset{\sim}{r}_{\underline{\delta}}) \sum_{\underline{\delta}'=0}^{\frac{N_0}{Z}-1} \times$$
$$\times\, \Psi_{\lambda'}^{c*}(\underset{\sim}{r}_{\underline{\mu}} + \underset{\sim}{r} - \underset{\sim}{r}_{\underline{\delta}'})\, \Psi_\lambda^{c}(\underset{\sim}{r}_{\underline{\mu}} + \underset{\sim}{r} - \underset{\sim}{r}_{\underline{\delta}'}),$$

whence $J(\underset{\sim}{r},\underset{\sim}{r}_{\underline{\mu}})$ and $K(\underset{\sim}{r})$ become periodic. Instead of relying on this "proof" of periodicity, we proceed in a more roundabout fashion. We first evaluate the aperiodic Fourier transform of $\Psi^{C*}_{\lambda'}(\underset{\sim}{r}_{\underline{\mu}}-\underset{\sim}{r}_{\underline{\delta}'})\Psi^{C}_{\lambda}(\underset{\sim}{r}_{\underline{\mu}}-\underset{\sim}{r}_{\underline{\delta}})$:

$$\text{(347a)}\quad U_{\lambda'\underline{\delta}'\lambda\underline{\delta}}(\underset{\sim}{k}) \equiv \iiint\limits_{\frac{N_0V}{Z}} dv(\underset{\sim}{r}_{\underline{\mu}}) \exp(-i\underset{\sim}{k}\cdot\underset{\sim}{r}_{\underline{\mu}})\, \Psi^{C*}_{\lambda'}(\underset{\sim}{r}_{\underline{\mu}}-\underset{\sim}{r}_{\underline{\delta}'})\Psi^{C}_{\lambda}(\underset{\sim}{r}_{\underline{\mu}}-\underset{\sim}{r}_{\underline{\delta}}) =$$

$$\text{(347b)}\quad = \exp(-i\underset{\sim}{k}\cdot\underset{\sim}{r}_{\underline{\delta}'}) \sum_{\nu=1}^{M}\sum_{\nu'=1}^{M} c^*_{\nu'\lambda'}c_{\nu\lambda} \exp(-i\underset{\sim}{k}\cdot\underset{\sim}{r}^{\circ}_{\nu'})\, I^{(\underline{\delta}-\underline{\delta}')}_{\nu'\lambda',\nu\lambda}(\underset{\sim}{k}),$$

where again we need the two-center integral of Appendix II:

$$\text{(347c)}\quad I^{(\underline{\delta}-\underline{\delta}')}_{\nu'\lambda',\nu\lambda}(\underset{\sim}{k}) \equiv \iiint\limits_{\frac{N_0V}{Z}} dv(\underset{\sim}{r}) \exp(-i\underset{\sim}{k}\cdot\underset{\sim}{r})\, \psi^*_{\nu'\lambda'}(\underset{\sim}{r})\, \psi_{\nu\lambda}(\underset{\sim}{r}-\underset{\sim}{r}^{\circ}_{\nu}+\underset{\sim}{r}^{\circ}_{\nu'}-\underset{\sim}{r}_{\underline{\delta}}+\underset{\sim}{r}_{\underline{\delta}'}).$$

The rapid decay of atomic wavefunctions will probably make $I^{(\underline{\delta}-\underline{\delta}')}_{\nu'\lambda',\nu\lambda}(\underset{\sim}{k})$ negligibly small if $\underset{\sim}{r}_{\underline{\delta}} - r_{\underline{\delta}'}$ exceeds, say, 20 Å. By the convolution theorem the Fourier transform of $K_{\underline{\delta}\underline{\delta}'}(\underset{\sim}{r})$ (Eqs. (346a, 346d)) is $|U_{\lambda'\underline{\delta}'\lambda\underline{\delta}}(\underset{\sim}{k})|^2$. But the sums over $\underline{\delta}$ and $\underline{\delta}'$ happen to introduce the desired periodicity into the two integrands involved in the application of the convolution theorem to $K(r)$:

$$\iiint\limits_{\frac{N_0V}{Z}} dv(\underset{\sim}{r}) \exp(-i\underset{\sim}{k}\cdot\underset{\sim}{r}) K(\underset{\sim}{r}) = \sum_{\underline{\delta}=0}^{\frac{N_0}{Z}-1}\sum_{\underline{\delta}'=0}^{\frac{N_0}{Z}-1} \iiint\limits_{\frac{N_0V}{Z}} dv(\underset{\sim}{r}_{\mu}) \exp(i\underset{\sim}{k}\cdot\underset{\sim}{r}_{\mu}) \times$$

$$\text{(348)}\quad \times\, \Psi^{C*}_{\lambda}(\underset{\sim}{r}_{\mu}-\underset{\sim}{r}_{\underline{\delta}})\Psi^{C}_{\lambda'}(\underset{\sim}{r}_{\mu}-\underset{\sim}{r}_{\underline{\delta}'}) \iiint\limits_{\frac{N_0V}{Z}} dv(\underset{\sim}{t}) \exp(-i\underset{\sim}{k}\cdot\underset{\sim}{t}) \times$$

$$\times\, \Psi^{C*}_{\lambda'}(\underset{\sim}{t}-\underset{\sim}{r}_{\underline{\delta}'})\, \Psi^{C}_{\lambda}(\underset{\sim}{t}-\underset{\sim}{r}_{\underline{\delta}})$$

whence the Fourier transform of $K(\underset{\sim}{r})$ must be:

$$(349a)\quad \sum_{\underline{\delta}=0}^{\frac{N_0}{Z}-1}\sum_{\underline{\delta}'=0}^{\frac{N_0}{Z}-1}\left|U_{\lambda'\underline{\delta}'\lambda\underline{\delta}}(\underset{\sim}{\mathbf{d}}_{hkl})\right|^2 = \frac{N_0}{Z}\sum_{\underline{\delta}=0}^{\frac{N_0}{Z}-1}\left|U_{\lambda'0\lambda\underline{\delta}}(\underset{\sim}{\mathbf{d}}_{hkl})\right|^2,$$

where:

$$(349b)\quad U_{\lambda'0\lambda\underline{\delta}}(\underset{\sim}{\mathbf{d}}_{hkl}) = \sum_{\nu=1}^{M}\sum_{\nu'=1}^{M} c^{*}_{\nu'\lambda'}\, c_{\nu\lambda}\, \exp(-i\underset{\sim}{\mathbf{d}}_{hkl}\cdot\underset{\sim}{r}^{\circ}_{\nu'})\, I^{(\underline{\delta})}_{\nu'\lambda',\nu\lambda}(\underset{\sim}{\mathbf{d}}_{hkl}).$$

As before, we wish to neglect the Fourier coefficient for $h = k = l = 0$. From Eqs. (318, 347a, 349a) we get:

$$(350)\quad \frac{N_0}{Z}\sum_{\underline{\delta}=0}^{\frac{N_0}{Z}-1}\left|U_{\lambda'0\lambda\underline{\delta}}(0)\right|^2 = \frac{N_0}{Z}\sum_{\underline{\delta}=0}^{\frac{N_0}{Z}-1}\delta_{\lambda\lambda'}$$

and since the exchange Coulomb integral cancels the contribution $\lambda = \lambda'$ made by the direct Coulomb integral to E_{GS} (Eq. (322)); therefore we can safely neglect the $h = k = l = 0$ term, and denote this fact by a double prime[*]:

---

[*] If the above conclusion that $K(\underset{\sim}{r})$ is periodic proves to be incorrect, then the final expression for the total exchange Coulomb integral obtained below (Eq. (352b)) must be changed, and a rather painful integration over $\underset{\sim}{\mathbf{k}}$ must replace the summations over h, k, l:

$$[\lambda\lambda'|\lambda'\lambda] = \left(\frac{1}{2\pi}\right)^4 \iiint_{\frac{N_0V}{Z}} \frac{dv(\underset{\sim}{\mathbf{k}})}{|\underset{\sim}{\mathbf{k}}|^2}\exp(i\underset{\sim}{\mathbf{k}}\cdot\underset{\sim}{r})\sum_{\underline{\delta}=0}^{\frac{N_0}{Z}-1}\sum_{\underline{\delta}'=0}^{\frac{N_0}{Z}-1}\left|U_{\lambda'\underline{\delta}'\lambda\underline{\delta}}(\underset{\sim}{\mathbf{k}})\right|^2.$$

(351) $$K(\underset{\sim}{r}) = \frac{N_0}{VZ} \sum_{h=-\infty}^{\infty} \sum_{k=-\infty}^{\infty} {\sum_{l=-\infty}^{\infty}}'' \sum_{\underline{\delta}=0}^{\frac{N_0}{Z}-1} \left| U_{\lambda' 0 \lambda \underline{\delta}} (\underset{\sim}{d}_{hkl}) \right|^2 \times$$
$$\times \exp(i \underset{\sim}{d}_{hkl} \cdot \underset{\sim}{r}).$$

A quick integration yields the total exchange Coulomb integral:

(352a) $$[\lambda\lambda'|\lambda'\lambda] = \frac{N_0}{VZ} \sum_{h=-\infty}^{\infty} \sum_{k=-\infty}^{\infty} {\sum_{l=-\infty}^{\infty}}'' \sum_{\underline{\delta}=0}^{\frac{N_0}{Z}-1} \left| U_{\lambda' 0 \lambda \underline{\delta}} (\underset{\sim}{d}_{hkl}) \right|^2 \times$$
$$\times \iiint_{\frac{N_0 V}{Z}} \frac{dv(\underset{\sim}{r})}{|\underset{\sim}{r}|} \exp(i \underset{\sim}{d}_{hkl} \cdot \underset{\sim}{r}) =$$

(352b) $$= \frac{4\pi N_0}{VZ} \sum_{h=-\infty}^{\infty} \sum_{k=-\infty}^{\infty} {\sum_{l=-\infty}^{\infty}}'' \sum_{\underline{\delta}=0}^{\frac{N_0}{Z}-1} \frac{\left| U_{\lambda' 0 \lambda \underline{\delta}} (\underset{\sim}{d}_{hkl}) \right|^2}{d_{hkl}^2}.$$

The sum over $\underline{\delta}$ can be truncated after a very few terms in Eq. (352b).

The expressions (344c, 345b, 352b) are Fourier transforms of finite expressions and therefore must converge.* Of course, no guarantees can be made here about the rates of convergence. General arguments show that whereas early truncation in $\underline{\delta}$ for the direct-space "brute-force" integrals, Eqs. (334, 335, 336),

---

*R. H. Young has shown (230) that the h = k = l = 0 terms in Eqs. (337, 338), if included in the Fourier expansions with due precautions in the interchanges of sums and integrals, contribute "finite quantities that are related to the self-energy of a cube of uniform charge density" and that hence can be safely disregarded.

will give a faithful representation of the "short-range" trend of Slater's integrals $[\lambda|\lambda]^{XT}$, $[\lambda\lambda|\lambda'\lambda']^{XT}$, $[\lambda\lambda'|\lambda'\lambda]^{XT}$, on the other hand, early truncation in h, k, l in the reciprocal-lattice sums, Eqs. (344c, 345b, 352b), will account for the long-range behavior of Slater's integrals but fail to describe their short-range, "non-smooth" portions.

D. Fast Convergence

Of course, the whole idea behind the Ewald technique in classical physics is to exploit these mutually compensating trends in direct and reciprocal space. Accordingly, we next sketch an approach which is conceptually simple, and may simultaneously give reasonable rates of convergence in both direct and reciprocal space. The idea is inspired by Shockley's interpretation of the Ewald technique (see Chapter II, pages 70-93) and consists of adding and then subtracting integrals involving a set of atomic orbitals each multiplied by a Gaussian "convergence acceleration factor."

We must ask the reader to bear with some further definitions. We define a "Gauss-modified, Bloch-symmetrized crystal wavefunction":

$$\Psi^{G}_{\lambda\underline{\omega}}(\underset{\sim}{r}_{\underline{\mu}}) \equiv \sqrt{\frac{Z}{N_0}} \sum_{\nu=1}^{M} c_{\nu\lambda} \sum_{\underline{\delta}=0}^{\frac{N_0}{Z}-1} \exp(i\,\underset{\sim}{k}_{\underline{\omega}}\cdot\underset{\sim}{r}_{\underline{\delta}}) \times \tag{353}$$

$$\times\, \psi_{\nu\lambda}(\underset{\sim}{r}_{\underline{\mu}} - \underset{\sim}{r}^{\circ}_{\nu} - \underset{\sim}{r}_{\underline{\delta}}) \exp\left(-\frac{\eta}{V^{2/3}}\left|\underset{\sim}{r}_{\underline{\mu}} - \underset{\sim}{r}^{\circ}_{\nu} - \underset{\sim}{r}_{\underline{\delta}}\right|^{2}\right);$$

as in Chapter II, η is a convenient dimensionless positive definite convergence parameter. Correspondingly, we define a "Gauss-modified zeroth unit cell spin-orbital" by:

$$(354)\quad \Psi^{CG}_{\lambda}(\underset{\sim}{r}_{\mu}) \equiv \sum_{\nu=1}^{M} c_{\nu\lambda}\,\psi_{\nu\lambda}(\underset{\sim}{r}_{\mu}-\underset{\sim}{r}^{0}_{\nu})\exp\left(-\frac{\eta}{V^{2/3}}|\underset{\sim}{r}_{\mu}-\underset{\sim}{r}^{0}_{\nu}|^{2}\right).$$

Note that if $\psi_{\nu\lambda}$ is a Slater-type orbital (STO) $\psi^{STO}_{\nu\lambda}(\underset{\sim}{r}_{\mu})$ then the extra convergence factor $\exp\left(-\frac{\eta}{V^{2/3}}|\underset{\sim}{r}_{\mu}|^{2}\right)$ transforms it into a "Gaussian-type orbital" (GTO) with a "displaced radial origin", and if $\psi_{\nu\lambda}$ is a GTO $\psi^{GTO}_{\nu\lambda}(\underset{\sim}{r}_{\mu})$ then this factor will merely change the constant factor in the radial exponent.

The "Gauss-modified total Slater integrals" $[\lambda_{G}|\lambda_{G}]^{XT}$, $[\lambda_{G}\lambda_{G}|\lambda'_{G}\lambda'_{G}]^{XT}$, and $[\lambda_{G}\lambda'_{G}|\lambda'_{G}\lambda_{G}]^{XT}$ have definitions similar to Eqs. (331a, 332a, 333a) with $\Psi^{CG}_{\lambda}(\underset{\sim}{r}_{\mu})$ and $\Psi^{CG}_{\lambda'}(\underset{\sim}{r}_{\mu'})$ replacing $\Psi^{C}_{\lambda}(\underset{\sim}{r}_{\mu})$ and $\Psi^{C}_{\lambda'}(\underset{\sim}{r}_{\mu'})$ respectively. The equivalents of the direct-space brute-force expansions Eqs. (334, 335, 336) for $\Psi^{CG}_{\lambda}(\underset{\sim}{r}_{\mu})$ have, trivially, extra Gaussian factors for each atomic orbital; this should make the direct-space integrations analytically feasible and numerically easier than for the customary STO.

The Fourier expansions, Eqs. (344c, 345b, 352b) can be obtained anew for the $\Psi^{CG}_{\lambda}(\underset{\sim}{r}_{\mu})$ by defining the suitable Fourier coefficients which parallel Eqs. (340a, 349b) namely:

$$(355a)\quad W^{G}_{\lambda}(\underset{\sim}{H}_{hkl}) \equiv \iiint_{V} dv(\underset{\sim}{r}_{\mu})\exp(-i\underset{\sim}{H}_{hkl}\cdot\underset{\sim}{r}_{\mu})\sum_{\underset{\sim}{\delta}=0}^{\frac{N_e}{2}-1}\left|\Psi^{CG}_{\lambda}(\underset{\sim}{r}_{\mu}-\underset{\sim}{r}_{\delta})\right|^{2}$$

(355b) $$= \sum_{\nu=1}^{M} \sum_{\nu'=1}^{M} c^{*}_{\nu\lambda} c_{\nu'\lambda} \exp(-i \underset{\sim}{d}_{hkl} \cdot \underset{\sim}{r}^{\circ}_{\nu}) \, J^{(0)}_{\nu\lambda,\nu'\lambda}(\underset{\sim}{d}_{hkl}),$$

(356a) $$U^{G}_{\lambda' 0 \lambda \underline{\delta}}(\underset{\sim}{d}_{hkl}) \equiv \iiint_{\frac{N_0 V}{Z}} dv(\underset{\sim}{r}) \exp(-i \underset{\sim}{d}_{hkl} \cdot \underset{\sim}{r}) \, \Psi^{CG^{*}}_{\lambda'}(\underset{\sim}{r}) \, \Psi^{CG}_{\lambda}(\underset{\sim}{r} - \underset{\sim}{r}_{\underline{\delta}}) =$$

(356b) $$= \sum_{\nu=1}^{M} \sum_{\nu'=1}^{M} c^{*}_{\nu'\lambda'} c_{\nu\lambda} \exp(-i \underset{\sim}{d}_{hkl} \cdot \underset{\sim}{r}^{\circ}_{\nu'}) \, J^{(\underline{\delta})}_{\nu'\lambda',\nu\lambda}(\underset{\sim}{d}_{hkl});$$

here the two-center atomic integral:

(357) $$J^{(\underline{\delta})}_{\nu\lambda,\nu'\lambda'}(\underset{\sim}{d}_{hkl}) \equiv \iiint_{\frac{N_0 V}{Z}} dv(\underset{\sim}{r}) \exp\left(-i \underset{\sim}{d}_{hkl} \cdot \underset{\sim}{r} - \eta V^{-2/3} |\underset{\sim}{r}|^{2}\right) \psi^{*}_{\nu\lambda}(\underset{\sim}{r}) \times \\ \times \, \psi_{\nu'\lambda'}(\underset{\sim}{r} - \underset{\sim}{r}^{\circ}_{\nu'} + \underset{\sim}{r}^{\circ}_{\nu} - \underset{\sim}{r}_{\underline{\delta}}) \exp\left(-\eta \frac{|\underset{\sim}{r} - \underset{\sim}{r}^{\circ}_{\nu'} + \underset{\sim}{r}^{\circ}_{\nu} - \underset{\sim}{r}_{\underline{\delta}}|^{2}}{V^{2/3}}\right)$$

differs from $I^{(\underline{\delta})}_{\nu\lambda,\nu'\lambda'}$ (Eq. (347c)) by trivial constant factors if $\psi_{\nu\lambda} = \psi^{GTO}_{\nu\lambda}$; however if $\psi_{\nu\lambda} = \psi^{STO}_{\nu\lambda}$ then the difference between $I^{(\underline{\delta})}_{\nu\lambda,\nu'\lambda'}$ and $J^{(\underline{\delta})}_{\nu\lambda,\nu'\lambda'}$ is considerable. Indeed, in the case $\psi_{\nu\lambda} = \psi^{STO}_{\nu\lambda}$ numerical integration procedures may be advisable;* another, analytical, approach would be to start from the Fourier transform:

---

*S. A. Hagstrom (231) has developed a very efficient computer program for molecular SCF-MO calculations, using Silverstone's transform techniques. Hagstrom evaluates $I^{(\underline{\delta})}_{\nu\lambda,\nu'\lambda'}(\underset{\sim}{k}_{\nu})$ numerically for his three- and four-center integrals.

$$(358)\quad F^{G}_{\nu\lambda}(\mathbf{k}_{\nu}) \equiv \iiint\limits_{\frac{N_0 V}{Z}} dv(\mathbf{r}_{\nu\mu})\, \exp\left(-i\mathbf{k}_{\nu}\cdot\mathbf{r}_{\nu\mu} - \eta V^{-2/3}|\mathbf{r}_{\nu\mu}|^{2}\right) \psi^{STO}_{\nu\lambda}(\mathbf{r}_{\nu\mu})$$

evaluated in Appendix III, and follow Silverstone's convolution scheme to obtain the expansion coefficients $v^{(n'\zeta')}_{l_1 l_2 l'}$ (cf. Eq. (A18), and Ref. (224)) suitable for Gauss-modified STO, after which the $J^{(\boldsymbol{\delta})}_{\nu\lambda,\nu'\lambda'}$ could be obtained trivially. (For the sake of comparison the Fourier transform of $\psi^{STO}_{\nu\lambda}$:

$$(359)\quad F_{\nu\lambda}(\mathbf{k}_{\nu}) \equiv \iiint\limits_{\frac{N_0 V}{Z}} dv(\mathbf{r}_{\nu\mu})\, \exp\left(-i\mathbf{k}_{\nu}\cdot\mathbf{r}_{\nu\mu}\right) \psi^{STO}_{\nu\lambda}(\mathbf{r}_{\nu\mu})$$

is given in Appendix II).

The dependence of the integrals $[\lambda_G|\lambda_G]^{XT}$, $[\lambda_G\lambda_G|\lambda'_G\lambda'_G]^{XT}$, and $[\lambda_G\lambda'_G|\lambda'_G\lambda_G]^{XT}$ on the arbitrary convergence parameter η deserves a few comments. If η is large enough to be "dominant" then the direct-space integrals will depend on η as $\exp(-\eta r^2)$, and their Fourier transforms will depend on η as $\exp\left(-\mathbf{d}^{2}_{hkl}/\eta\right)$. We wish to exploit these mutually compensating trends in a method for the evaluation of $[\lambda|\lambda]^{XT}$, $[\lambda\lambda|\lambda'\lambda']^{XT}$, and $[\lambda\lambda'|\lambda'\lambda]^{XT}$. If we follow a scheme suggested by Shockley's derivation of Ewald's technique, we write:

$$(360a)\quad [\lambda|\lambda]^{XT} = \left\{[\lambda|\lambda]^{XT} - [\lambda_G|\lambda_G]^{XT}\right\} + \frac{4\pi N_0}{VZ} \sum_{h=-\infty}^{\infty}\sum_{k=-\infty}^{\infty}\sum_{l=-\infty}^{\infty}{}' \frac{P(\mathbf{d}_{hkl})\, W^{G}_{\lambda}(\mathbf{d}_{hkl})}{\mathbf{d}^{2}_{hkl}},$$

$$(360b)\quad [\lambda\lambda|\lambda'\lambda']^{XT} = \left\{[\lambda\lambda|\lambda'\lambda']^{XT} - [\lambda_G\lambda_G|\lambda'_G\lambda'_G]^{XT}\right\} + \frac{4\pi N_0}{VZ}\sum_{h=-\infty}^{\infty}\sum_{k=-\infty}^{\infty}{\sum_{l=-\infty}^{\infty}}' \frac{W_{\lambda}^{G^*}(\underset{\sim}{\mathfrak{d}}_{hkl})\,W_{\lambda'}^{G}(\underset{\sim}{\mathfrak{d}}_{hkl})}{\mathfrak{d}_{hkl}^{2}},$$

$$(360c)\quad [\lambda\lambda'|\lambda'\lambda]^{XT} = \left\{[\lambda\lambda'|\lambda'\lambda]^{XT} - [\lambda_G\lambda'_G|\lambda'_G\lambda_G]^{XT}\right\} + \frac{4\pi N_0}{VZ}\sum_{h=-\infty}^{\infty}\sum_{k=-\infty}^{\infty}{\sum_{l=-\infty}^{\infty}}''\sum_{\underline{\delta}=0}^{\frac{N_0}{Z}-1} \frac{\left|U^{G}_{\lambda'0\lambda\underline{\delta}}(\underset{\sim}{\mathfrak{d}}_{hkl})\right|^{2}}{\mathfrak{d}_{hkl}^{2}}.$$

The left-hand side of Eqs. (360a, 360b, 360c) is obtained by choosing a reasonable value of η, evaluating the quantity in braces by direct-space integration procedures (cf. Eqs. (334, 335, 336)) and carrying out the summation over the Fourier transforms: if η was chosen wisely, rapid convergence is obtained both for the direct-space calculations (few terms needed in $\underline{\delta}$-sums of Eqs. (334, 335, 336) and their analogs for Gauss-modified orbitals) and for the reciprocal-lattice sums (few values of $\underset{\sim}{\mathfrak{d}}_{hkl}$ required). The result should, of course, be independent of η. An alternate scheme is however suggested by some comments of Nijboer and de Wette (232): if a direct-lattice sum:

$$\sum_{\underline{\delta}=0}^{\frac{N_0}{Z}-1} c(\underset{\sim}{r}_{\underline{\delta}})$$

is conditionally and/or slowly convergent, they suggest introducing a "convergence acceleration factor" $f(\underset{\sim}{r})$, summing:

$$\sum_{\underline{\delta}=0}^{\frac{N_0}{Z}-1} c(\underset{\sim}{r}_{\underline{\delta}})\, f(\underset{\sim}{r})$$

in direct space and adding to this result the summation over the reciprocal lattice of the Fourier transform of $\sum_{\underline{\delta}=0}^{N_0/Z-1} c(\underset{\sim}{r}_{\underline{\delta}})\left[1-f(\underset{\sim}{r})\right]$, the idea being that the "flatter" the function $c(\underset{\sim}{r}_{\delta})[1 - f(\underset{\sim}{r})]$ is, the better its Fourier transform will converge. Thus we are led to write:

$$[\lambda|\lambda]^{XT} = \left\{[\lambda_G|\lambda_G]^{XT}\right\} + \frac{4\pi N_0}{VZ}\sum_{h=-\infty}^{\infty}\sum_{k=-\infty}^{\infty}{\sum_{l=-\infty}^{\infty}}' \frac{P(\underset{\sim}{\mathfrak{h}}_{hkl})\left[W_\lambda^{*}(\underset{\sim}{\mathfrak{h}}_{hkl}) - W_\lambda^{G*}(\underset{\sim}{\mathfrak{h}}_{hkl})\right]}{\mathfrak{h}_{hkl}^2}, \tag{361a}$$

$$\begin{aligned}[\lambda\lambda|\lambda'\lambda']^{XT} &= \left\{[\lambda_G\lambda_G|\lambda'_G\lambda'_G]\right\} + \\ &+ \frac{4\pi N_0}{VZ}\sum_{h=-\infty}^{\infty}\sum_{k=-\infty}^{\infty}{\sum_{l=-\infty}^{\infty}}' \frac{W_\lambda^{*}(\underset{\sim}{\mathfrak{h}}_{hkl})W_{\lambda'}(\underset{\sim}{\mathfrak{h}}_{hkl}) - W_\lambda^{G*}(\underset{\sim}{\mathfrak{h}}_{hkl})W_{\lambda'}^{G}(\underset{\sim}{\mathfrak{h}}_{hkl})}{\mathfrak{h}_{hkl}^2},\end{aligned} \tag{361b}$$

$$\begin{aligned}[\lambda\lambda'|\lambda'\lambda]^{XT} &= \left\{[\lambda_G\lambda'_G|\lambda'_G\lambda_G]\right\} + \\ &+ \frac{4\pi N_0}{VZ}\sum_{h=-\infty}^{\infty}\sum_{k=-\infty}^{\infty}{\sum_{l=-\infty}^{\infty}}''\sum_{\delta=0}^{\frac{N_0}{Z}-1} \frac{|U_{\lambda'0\lambda\delta}(\underset{\sim}{\mathfrak{h}}_{hkl})|^2 - |U^G_{\lambda'0\lambda\delta}(\underset{\sim}{\mathfrak{h}}_{hkl})|^2}{\mathfrak{h}_{hkl}^2},\end{aligned} \tag{361c}$$

where again we must evaluate in direct space the integrals enclosed in braces. An a priori choice between Eq. (360) and Eq. (361) seems difficult to the writer at the present time, and will be left to a future empirical test: it is probable that Eq. (360) and (361) differ only in the values of η which sundrily yield optimal convergence.

E. Application to Donor-Acceptor Crystals

We now return to consider ΔE_{CT} (Eq. (303)). The addition or withdrawal of even a single electron from an isolated neutral molecule disturbs the system sufficiently to justify separate quantum-mechanical calculations for the neutral molecule, for its anion, and for its cation. This consideration is reflected in the reminimization procedures of Hoyland and Goodman (180) and in the effects of formal charge on the internuclear distances observed in X-ray diffraction studies of holoionic donor-acceptor crystals.

In practice, however, most published organic MO calculations have avoided such fully independent reminizations, and have been satisfied with accepting:

> APPROXIMATION III: "a molecular orbital description of the ground state of the radical cation (radical anion) of an aromatic molecule can be obtained from the MO description of the neutral molecule by withdrawing (adding) an electron from the highest occupied (to the lowest unoccupied) pi MO of the neutral molecule."

This approximation is discussed by Salem (Ref. (30), pages 152-158); in Pariser-Parr-Pople SCF theory it gives so-called "vertical" estimates of the adiabatic (experimental) ionization potential of donors that can be about 30% too high, and estimates for the electron affinity of acceptor molecules which can be twice as large as the rather unreliable (but popular) value obtained indirectly from experiment (185). Thus it is fair to guess that if these errors compensate sufficiently, then by accepting Approximation III and the concomitant simplifications in the evaluation of ΔE_{CT}, one may get a value of ΔE_{CT} which differs by 20-30% from the value calculated by using four separate MO calculations (one for the neutral donor, one for its cation, and for the neutral acceptor, and one for its anion).

For the curious, we derive an equation for ΔE_{CT} that incorporates the consequences of Approximation III. Assume, for simplicity, that $Z = 1$, and that upon ionization to the holoionic lattice an electron from λ_D, the top-most filled orbital of the donor molecule, is transferred to λ_A, the lowest unoccupied orbital of the acceptor molecule, in each unit cell.* Then we obtain from Eq. (303) and (327):

$$\begin{aligned}\Delta E_{CT} = & -\frac{\hbar^2}{2m_e}\left\{Q^{XT}_{\lambda_A} - Q^{XT}_{\lambda_D}\right\} - |\epsilon|^2\left\{[\lambda_A|\lambda_A]^{XT} - [\lambda_D|\lambda_D]^{XT}\right\} + \\ & + |\epsilon|^2\left\{\sum_{\substack{\lambda'=1\\ \lambda'\neq\lambda_D}}^{\Lambda}\left([\lambda_A\lambda_A|\lambda'\lambda']^{XT} - [\lambda_D\lambda_D|\lambda'\lambda']^{XT}\right) - \right. \\ & \left. - \sum_{\substack{\lambda'=1\\ \lambda'\neq\lambda_D}}^{\lambda_o}\left([\lambda_A\lambda'|\lambda'\lambda_A]^{XT} - [\lambda_D\lambda'|\lambda'\lambda_D]^{XT}\right)\right\}.\end{aligned} \tag{362}$$

F. Acknowledgments

Without the helpful suggestions and painstaking critique of Dr. R. H. Young this chapter could not have been written: his assistance with the earlier drafts will not be easily forgotten. I am most grateful to Prof. H. J. Silverstone for helpful

---

*Without loss of generality assume $1 \leqslant \lambda_D \leqslant \lambda_o$, whence if the total spin remains zero the λ_A spin-orbital $\Psi_{\lambda_A \underline{\omega}}$ must also have α spin.

discussions and correspondence, and to Profs. H. M. McConnell and P. G. Simpson for their patience and forbearance while this chapter was being written.

APPENDIX I

We had worried about coordinate systems in Chapter II, pages 93-96: the same headaches, compounded with some new ones, return in the present chapter. On page 164 we defined the "direct lattice coordinate system" $\{\vec{e}_a \equiv \underset{\sim}{a}|\underset{\sim}{a}|^{-1}, \vec{e}_b \equiv \underset{\sim}{b}|\underset{\sim}{b}|^{-1}, \vec{e}_c \equiv \underset{\sim}{c}|\underset{\sim}{c}|^{-1}\}$ as the obvious and natural coordinate system (c.s.), with origin at the "center of the crystal" somewhere inside the zeroth unit cell.

We further define the orthogonal "crystal Cartesian c.s." $\{\vec{e}_x, \vec{e}_y, \vec{e}_z\}$ as described by Eq.(262) of Chapter II; the discrete direct lattice vectors ($\underset{\sim}{r}_{\underline{\delta}}$ or $\underset{\sim}{r}_{dfg}$) and all other continuous vectors in direct space have Cartesian components as in Eq.(266). The "crystal spherical polar c.s." $\{\vec{e}_r, \vec{e}_\vartheta, \vec{e}_\varphi\}$ is defined in the usual fashion from the crystal Cartesian c.s. Thus, the vector $\underset{\sim}{r}^{o}_{\nu}$ has components ($x^{o}_{\nu}, y^{o}_{\nu}, z^{o}_{\nu}$) in crystal Cartesian coordinates and ($r^{o}_{\nu}, \vartheta^{o}_{\nu}, \varphi^{o}_{\nu}$) in crystal spherical polar coordinates, where:

(A1a) $$x^{o}_{\nu} = (r^{o}_{\nu}) \sin(\vartheta^{o}_{\nu}) \cos(\varphi^{o}_{\nu}),$$

(A1b) $$y^{o}_{\nu} = (r^{o}_{\nu}) \sin(\vartheta^{o}_{\nu}) \sin(\varphi^{o}_{\nu}),$$

(A1c) $$z^{o}_{\nu} = (r^{o}_{\nu}) \cos(\vartheta^{o}_{\nu});$$

in these crystal c.s. the general vector $\underset{\sim}{r}$ will have components (x, y, z) and (r, ϑ, φ), respectively.

The LCAO technique assumes tacitly that the "local" Cartesian axes of quantization within the zeroth unit cell are all parallel to the crystal Cartesian axes, but this does not usually happen, since in the various single-molecule calculations the axes of quantization are usually chosen to utilize as much as possible the internal symmetry of each molecule, and the molecules usually differ in orientation from the crystal Cartesian axes. Assume that either by our own choice or by the whim of others each nucleus in the zeroth unit cell is the origin for a "local Cartesian c.s." $\{(\vec{e}^{\,\nu x}, \vec{e}^{\,\nu y}, \vec{e}^{\,\nu z}),\ \nu = 1, 2, \ldots, M\}$ and for a "local spherical polar c.s." $\{(\vec{e}^{\,\nu r}, \vec{e}^{\,\nu\vartheta}, \vec{e}^{\,\nu\varphi}),\ \nu = 1, 2, \ldots, M\}$: then typical vectors from the ν-th nucleus to "the μ-th electron," $r_{\nu\mu} \equiv \underset{\sim}{r}_{\mu} - \underset{\sim}{r}^{0}_{\nu}$ would have components $(r^{\nu x}_{\mu}, r^{\nu y}_{\mu}, r^{\nu z}_{\mu})$ and $(r^{\nu}_{\mu}, \vartheta^{\nu}_{\mu}, \varphi^{\nu}_{\mu})$, respectively.

We may then define a new set of M "local reoriented Cartesian c.s." $\{(\vec{e}^{\,\nu}_{x}, \vec{e}^{\,\nu}_{y}, \vec{e}^{\,\nu}_{z}),\ \nu = 1, 2, \ldots, M\}$ which have axes parallel to those of the crystal Cartesian c.s., and M "local reoriented spherical polar c.s." $\{(\vec{e}^{\,\nu}_{r}, \vec{e}^{\,\nu}_{\vartheta}, \vec{e}^{\,\nu}_{\varphi}),\ \nu = 1, 2, \ldots, M\}$. In these reoriented frames, $\underset{\sim}{r}_{\nu\mu}$ has components $(r^{x}_{\nu\mu}, r^{y}_{\nu\mu}, r^{z}_{\nu\mu})$ and $(r_{\nu\mu}, \vartheta_{\nu\mu}, \varphi_{\nu\mu})$, respectively. Of course $r_{\nu\mu} = r^{\nu}_{\mu}$.

In general, we find at each nucleus ν an atomic orbital $\psi_{\nu\lambda}(\underset{\sim}{r}_{\nu\mu})$ consisting of the product of a radial part and an angular part; if the atomic orbital is hybrid, then we find instead a linear combination of a few such products. We will assume here that these atomic orbitals are normalized Slater-type orbitals (STO): for the atomic orbital centered about the ν-th nucleus and used in the λ-th zeroth unit cell orbital, call n_ν^λ the principal quantum number, l_ν^λ the orbital angular momentum quantum number, m_ν^λ the quantum number for the $\vec{e}^{\,\nu}{}_z$-projection of the orbital angular momentum and ζ_ν^λ the effective nuclear charge: the following notations may be used interchangeably, as convenience dictates:

$$\psi^{STO}_{\nu\lambda}(\underset{\sim}{r}_{\nu\mu}) \equiv \psi_{n_\nu^\lambda, \ell_\nu^\lambda, m_\nu^\lambda, \zeta_\nu^\lambda}(\underset{\sim}{r}_{\nu\mu}) \equiv \psi^{n\ell m\zeta}_{\nu\lambda}(\underset{\sim}{r}_{\nu\mu}) = \tag{A2a,b}$$

$$= R^{n\zeta}_{\nu\lambda}(r^\nu_\mu) Y^m_{\ell(\nu\lambda)}(\vartheta^\nu_\mu, \varphi^\nu_\mu) = R^{n\zeta}_{\nu\lambda}(r_{\nu\mu}) Y^m_\ell(\vartheta^\nu_\mu, \varphi^\nu_\mu). \tag{A2c,d}$$

The radial function is defined by:

$$R^{n\zeta}_{\nu\lambda}(r_{\nu\mu}) = \frac{(2\zeta)^{n+\frac{1}{2}}}{(2n)!} (r_{\nu\mu})^{n-1} \exp(-\zeta r_{\nu\mu}), \tag{A3}$$

and the angular part is a spherical harmonic function defined according to the conventions of Condon and Shortley (Ref. (233), p. 52) as:

$$m>0: \quad Y^m_\ell(\vartheta,\varphi) \equiv (-1)^m \exp(im\varphi) \left[\frac{2\ell+1}{4\pi} \frac{(\ell-m)!}{(\ell+m)!}\right]^{1/2} \sin^m\vartheta \frac{d^m}{d(\cos\vartheta)^m} P_\ell(\cos\vartheta), \tag{A4a}$$

$$m>0: \quad Y^{-m}_\ell(\vartheta,\varphi) \equiv (-1)^m \left[Y^m_\ell(\vartheta,\varphi)\right]^*, \tag{A4b}$$

$$m=0: \quad Y^0_\ell(\vartheta,\varphi) = \left[\frac{2\ell+1}{4\pi}\right]^{1/2} P_\ell(\cos\vartheta), \tag{A4c}$$

where the Legendre polynomial may be defined by Rodriguez' formula:

$$\text{(A4d)} \qquad P_\ell(\cos\vartheta) \equiv \frac{1}{2^\ell \ell!}\,\frac{d^\ell}{d(\cos\vartheta)^\ell}\,(\cos^2\vartheta - 1)^\ell$$

the radial functions are normalized; the spherical harmonics are orthonormalized:

$$\text{(A5)} \qquad \int_0^{2\pi} d\varphi \int_0^{\pi} d\vartheta \sin\vartheta\; Y_\ell^{m*}(\vartheta,\varphi)\, Y_{\ell'}^{m'}(\vartheta,\varphi) = \delta_{\ell\ell'}\,\delta_{mm'}$$

We shall also need the Condon-Shortley coefficients (Ref. (233), pages 175-176):

$$\text{(A6a)} \qquad c^\lambda(L,M;\ell,m) \equiv \sqrt{\frac{4\pi}{2\lambda+1}} \int_0^{2\pi} d\varphi \int_0^{\pi} d\vartheta \sin\vartheta\; Y_\ell^{m*}(\vartheta,\varphi)\, Y_\lambda^{M-m*}(\vartheta,\varphi)\, Y_L^{M}(\vartheta,\varphi) =$$

$$\text{(A6b)} \qquad = \sqrt{\frac{4\pi}{2\lambda+1}} \int_0^{2\pi} d\varphi \int_0^{\pi} d\vartheta \sin\vartheta\; Y_\ell^{m}(\vartheta,\varphi)\, Y_\lambda^{M-m}(\vartheta,\varphi)\, Y_L^{M*}(\vartheta,\varphi),$$

where $|\ell - L| \leqslant \lambda \leqslant \ell + L$, and $\ell + \lambda + L$ = even positive integer.

Now, to go from the local Cartesian c.s. $\{\vec{e}^{\,\nu x}, \vec{e}^{\,\nu y}, \vec{e}^{\,\nu z}\}$ to the local reoriented Cartesian c.s. we follow Messiah (234) and define a set of three Eulerian rotation angles (α_ν, β_ν, γ_ν) and a unitary orthogonal rotation matrix $\underset{\sim}{\mathbb{R}}^{(\ell)}$ of rank $2\ell + 1$ by its elements:

(A7) $$\mathbb{R}^{(\ell)}_{m\,m'}(\alpha_\nu\,\beta_\nu\,\gamma_\nu) \equiv \left\langle \ell m \middle| \exp\left(-i\alpha_\nu \hat{L}_z - i\beta_\nu \hat{L}_y - i\gamma_\nu \hat{L}_x\right) \middle| \ell m \right\rangle$$

where the ket $|\ell m'\rangle$ is a simultaneous eigenket of the square of the orbital angular momentum operator, $\hat{L}^2$, with eigenvalue $\hbar\ell(\ell + 1)$, and of the z-component of this operator, $\hat{L}_z$, with eigenvalue $\hbar m'$. Then we may write:

(A8) $$Y_\ell^m(\vartheta_{\nu\mu},\varphi_{\nu\mu}) = \sum_{m'=-\ell}^{\ell} \mathbb{R}^{(\ell)}_{m'm}(\alpha_\nu\,\beta_\nu\,\gamma_\nu)\, Y_\ell^{m'}(\vartheta^\nu_\mu,\varphi^\nu_\mu),$$

and the "old" in terms of a sum over the "new" is:

(A9) $$Y_\ell^{m'}(\vartheta^\nu_\mu,\varphi^\nu_\mu) = \sum_{m=-\ell}^{\ell} \mathbb{R}^{(\ell)*}_{m'm}(\alpha_\nu\,\beta_\nu\,\gamma_\nu)\, Y_\ell^{m}(\vartheta_{\nu\mu},\varphi_{\nu\mu}).$$

Thus we can "realign" $\Psi_{\nu\lambda}(\underset{\sim}{r}_{\nu\mu})$ so that in the local reoriented spherical polar c.s. $\{\vec{e}^{\,\nu}_r, \vec{e}^{\,\nu}_\vartheta, \vec{e}^{\,\nu}_\varphi\}$ Eq. (A2d) becomes:

(A10) $$\Psi^{n\ell m\zeta}_{\nu\lambda}(\underset{\sim}{r}_{\nu\mu}) = R^{n\ell\zeta}_{\nu\lambda}(r_{\nu\mu}) \sum_{m''=-\ell}^{\ell} Y_\ell^{m''}(\vartheta_{\nu\mu},\varphi_{\nu\mu})\, \mathbb{R}^{(\ell)*}_{mm''}(\alpha_\nu\,\beta_\nu\,\gamma_\nu)$$

The reciprocal lattice vector $\underset{\sim}{\mathfrak{d}}_{hkl}$ and the reciprocal space vector $\underset{\sim}{\mathfrak{k}}_{\underline{\omega}}$ both have origin at the center of the crystal and are adequately described by Eq. (214) and Eq. (313), respectively. The components of these vectors along crystal direct lattice Cartesian axes $\{\vec{e}_x, \vec{e}_y, \vec{e}_z\}$ are given by Eq. (263) and

(264). The components of $\underset{\sim}{d}_{hkl}$ in the direct-space crystal spherical polar c.s. $\{\vec{e}_r, \vec{e}_\vartheta, \vec{e}_\varphi\}$ are $(d_{hkl}, \vartheta_{hkl}, \varphi_{hkl})$. The local continuous reciprocal space vector $\{\underset{\sim}{\Bbbk}_\nu, \nu = 1, 2, \ldots, M\}$ used in Eq. (358) has origin at $\underset{\sim}{r}^{o}_{\nu}$ and is defined with respect to the local reoriented spherical polar c.s. $\{\vec{e}^{\,\nu}_r, \vec{e}^{\,\nu}_\vartheta, \vec{e}^{\,\nu}_\varphi\}$ of direct space as having components $(\Bbbk_\nu, \vartheta^\nu_{\Bbbk}, \varphi^\nu_{\Bbbk})$.

APPENDIX II

We must now worry about the Fourier transform $F_{\nu\lambda}(\underset{\sim}{\mathbb{k}}_\nu)$ of the atomic orbital $\psi_{\nu\lambda}$ (Eq. (359)) and about the two-center integral $I^{(\delta)}_{\nu\lambda,\nu'\lambda'}(\underset{\sim}{\mathbb{d}}_{hkl})$ (Eq. (340e)).

Given a general form of $\psi_{\nu\lambda}$, numerical integration schemes may prove to be the most convenient approach, but, for the STO defined in Appendix I:

$$\psi^{n\ell m\zeta}_{\nu\lambda}(\underset{\sim}{r}_{\nu\mu}) = \frac{(2\zeta)^{n+\frac{1}{2}}}{(2n)!}(r_{\nu\mu})^{n-1}\exp(-\zeta r_{\nu\mu}) \times \tag{A11}$$
$$\times \sum_{m_1=-\ell}^{\ell} \mathcal{R}^{(\ell)*}_{mm_1}(\alpha_\nu\beta_\nu\gamma_\nu) Y^{m_1}_\ell(\vartheta_{\nu\mu},\varphi_{\nu\mu}).$$

Silverstone (221,225) has already obtained explicit and elegant expressions for both $F_{\nu\lambda}$ and $I^{(\delta)}_{\nu\lambda,\nu'\lambda'}$, and for the sake of completeness we quote his results here.

Indeed $F_{\nu\lambda}$ is given by Eq. (12,13) of Ref. (221):

$$F^{n\ell m\zeta}_{\nu\lambda}(\underset{\sim}{\mathbb{k}}_\nu) \equiv \underset{\text{all space}}{\iiint} dv(\underset{\sim}{r}_{\nu\mu})\exp(-i\underset{\sim}{\mathbb{k}}_\nu\cdot\underset{\sim}{r}_{\nu\mu})\,\psi^{n\ell m\zeta}_{\nu\lambda}(\underset{\sim}{r}_{\nu\mu}) =$$
$$= \frac{(2\zeta)^{n+\frac{1}{2}}}{(2n)!}\sum_{m_1=-\ell}^{\ell}\mathcal{R}^{(\ell)*}_{mm_1}(\alpha_\nu\beta_\nu\gamma_\nu)Y^{m_1}_\ell(\vartheta^\nu_{\mathbb{k}},\varphi^\nu_{\mathbb{k}}) \times \tag{A12}$$
$$\times\, 4\pi i^\ell\,\Gamma(n-\ell+1)\,\mathbb{k}^\ell_\nu\left[\frac{1}{\mathbb{k}_\nu}\frac{d}{d\mathbb{k}_\nu}\right]^\ell \frac{(\zeta-i\mathbb{k}_\nu)^{\ell-n-1}-(\zeta+i\mathbb{k}_\nu)^{\ell-n-1}}{2i\mathbb{k}_\nu},$$

where $\Gamma(z)$ is the Eulerian gamma-function:

$$\Gamma(z) \equiv \int_0^\infty dt\, t^{z-1} \exp(-t), \qquad \mathcal{R}e(z) > 0, \tag{A12c}$$

and the following identity (Eq. (14) in Ref. (222)) may be helpful:

$$\left[\frac{1}{x}\frac{d}{dx}\right]^{\ell} \frac{f(x)}{x} = \sum_{j=0}^{\ell} \frac{(\ell+j)!\,(-1)^j}{(\ell-j)!\,j!\,2^j}\, x^{-\ell-j-1} \left(\frac{d}{dx}\right)^{\ell-j} f(x). \tag{A13}$$

To use Eq. (A12b) in Eq. (359) we blithely replace the components of $\underset{\sim}{\mathbb{k}}_{\nu}$ in the local reoriented spherical polar c.s. by the components of $\underset{\sim}{\mathbb{d}}_{hkl}$ in the crystal spherical polar c.s. $\{\vec{e}_r, \vec{e}_\vartheta, \vec{e}_\varphi\}$.

To obtain the integral $I^{(\delta)}_{\nu\lambda,\nu'\lambda'}(\underset{\sim}{\mathbb{d}}_{hkl})$ we first need the expansion (235) of $\exp(-i\,\underset{\sim}{\mathbb{d}}_{hkl}\cdot\underset{\sim}{r})$ in spherical harmonic functions:

$$\exp(-i\,\underset{\sim}{\mathbb{d}}_{hkl}\cdot\underset{\sim}{r}) =$$

$$= \sum_{p=0}^{\infty} \sum_{m_2=-p}^{p} 4\pi(-i)^p j_p(\mathbb{d}_{hkl} r)\, Y_p^{m_2 *}(\vartheta,\varphi)\, Y_p^{m_2}(\vartheta_{hkl},\varphi_{hkl}) = \tag{A14a}$$

$$= \sum_{p=0}^{\infty} \sum_{m_2=-p}^{p} 4\pi(-i)^p j_p(\mathbb{d}_{hkl} r)\, Y_p^{m_2}(\vartheta,\varphi)\, Y_p^{m_2 *}(\vartheta_{hkl},\varphi_{hkl}), \tag{A14b}$$

where the spherical Bessel function of the first kind $j_l(xy)$ may be represented by its Rayleigh formula:

(A15) $$j_\ell(xy) = (-x)^\ell \left[\frac{1}{x}\frac{d}{dx}\right]^\ell \frac{\sin(xy)}{x y^{\ell+1}}.$$

The atomic orbital $[\psi^{n\ell m\zeta}_{\nu\lambda}(\underset{\sim}{r})]^*$ is the complex conjugate of Eq. (A11) with (r, ϑ, φ) replacing ($r_{\nu\mu}$, $\vartheta_{\nu\mu}$, $\varphi_{\nu\mu}$). The atomic orbital $\psi^{n'\ell'm'\zeta'}_{\nu'\lambda'}\left(\underset{\sim}{r}-(\underset{\sim}{r}^0_\nu + \underset{\sim}{r}_{\underline{\delta}} - \underset{\sim}{r}^0_{\nu'})\right)$ is centered about the point:

(A16) $$\underset{\sim}{R}_{\nu\underline{\delta}\nu'} \equiv \underset{\sim}{r}^0_\nu + \underset{\sim}{r}_{\underline{\delta}} - \underset{\sim}{r}^0_{\nu'} ;$$

in the local realigned spherical c.s. centered about this same point the vector $\underset{\sim}{r} - \underset{\sim}{R}_{\nu\underline{\delta}\nu'}$ has components $(|\underset{\sim}{r} - \underset{\sim}{R}_{\nu\underline{\delta}\nu'}|, \vartheta^{(r)}_{\nu\underline{\delta}\nu'}, \varphi^{(r)}_{\nu\underline{\delta}\nu'})$; the Eulerian angles required by Eq. (A11) are ($\alpha_{\nu'}$, $\beta_{\nu'}$, $\gamma_{\nu'}$), as is readily seen from Eq. (340c); in the crystal spherical polar c.s. the vector $\underset{\sim}{R}_{\nu\underline{\delta}\nu'}$ has components ($R_{\nu\underline{\delta}\nu'}$, $\vartheta^0_{\nu\underline{\delta}\nu'}$, $\varphi^0_{\nu\underline{\delta}\nu'}$), so we can finally write:

$$\psi^{n'\ell'm'\zeta'}_{\nu'\lambda'}\left(\underset{\sim}{r} - (\underset{\sim}{r}^0_\nu + \underset{\sim}{r}_{\underline{\delta}} - \underset{\sim}{r}^0_{\nu'})\right) =$$

(A17) $$= \frac{(2\zeta')^{n'+\frac{1}{2}}}{(2n')!} \sum_{m_3=-\ell'}^{\ell'} \mathcal{R}^{(\ell')*}_{m'm_3}(\alpha_{\nu'}, \beta_{\nu'}, \gamma_{\nu'}) \times$$

$$\times Y^{m_3}_{\ell'}\left(\vartheta^{(r)}_{\nu\underline{\delta}\nu'}, \varphi^{(r)}_{\nu\underline{\delta}\nu'}\right) |\underset{\sim}{r} - \underset{\sim}{R}_{\nu\underline{\delta}\nu'}|^{n'-1} \exp\left(-\zeta|\underset{\sim}{r} - \underset{\sim}{R}_{\nu\underline{\delta}\nu'}|\right).$$

Silverstone (224) has shown how Eq. (A17) can be rewritten in terms of spherical harmonics whose coordinates (ϑ, φ) are those of the vector $\underset{\sim}{r}$, measured from the center of the crystal; another spherical harmonic function with arguments $\vartheta^{0}_{\nu\underline{\delta}\nu'}$ and $\varphi_{\nu\underline{\delta}\nu'}$ will also appear. In fact he obtains:

$$\psi^{n'\ell'm'\zeta'}_{\nu'\lambda'}\left(\underset{\sim}{r}-\underset{\sim}{R}_{\nu\underline{\delta}\nu'}\right)=\frac{(2\zeta')^{n'+\frac{1}{2}}}{(2n')!}\sum_{m_3=-\ell'}^{\ell'}\mathcal{R}^{(\ell')*}_{m'm_3}(\alpha_{\nu'}\beta_{\nu'}\gamma_{\nu'})\times$$

$$\text{(A18a)}\qquad \times\sum_{\ell_1=0}^{\infty}\sum_{\ell_2=|\ell'-\ell_1|}^{\ell'+\ell_1}v^{(n'\zeta')}_{\ell_1,\ell_2,\ell'}\left(r,R_{\nu\underline{\delta}\nu'}\right)\sum_{m_4=-\ell_1}^{\ell_1}\left(\frac{2\ell_2+1}{4\pi}\right)^{1/2}\times$$

$$\times\frac{2}{\pi}i^{\ell_2-\ell_1}c^{\ell_2}(\ell',m_3;\ell_1,m_4)Y^{m_3-m_4}_{\ell_2}\left(\vartheta^{0}_{\nu\underline{\delta}\nu'},\varphi_{\nu\underline{\delta}\nu'}\right)Y^{m_4}_{\ell_1}(\vartheta,\varphi),$$

where if $r < R_{\nu\underline{\delta}\nu'}$ then:

$$v^{(n'\zeta')}_{\ell_1,\ell_2,\ell'}\left(r,R_{\nu\underline{\delta}\nu'}\right)=4\pi(-1)^{n'-\ell'}\left(\frac{d}{d\zeta'}\right)^{n'-\ell'}\left[\frac{1}{\zeta'}\frac{d}{d\zeta'}\right]^{\ell'}(\zeta')^{\ell'+1}\times$$

$$\text{(A18b)}\qquad \times\mathcal{K}_{\ell_2}\left(\zeta'R_{\nu\underline{\delta}\nu'}\right)\mathcal{J}_{\ell_1}(\zeta'r),$$

and if $r > R_{\nu\underline{\delta}\nu'}$ then:

$$v^{(n'\zeta')}_{\ell_1,\ell_2,\ell'}\left(r,R_{\nu\underline{\delta}\nu'}\right)=4\pi(-1)^{n'}\left(\frac{d}{d\zeta'}\right)^{n'-\ell'}\left[\frac{1}{\zeta'}\frac{d}{d\zeta'}\right]^{\ell'}(\zeta')^{\ell'+1}\times$$

$$\text{(A18c)}\qquad \times\mathcal{J}_{\ell_2}\left(\zeta'R_{\nu\underline{\delta}\nu'}\right)\mathcal{K}_{\ell_1}(\zeta'r).$$

$\mathcal{J}_\ell$ and $\mathcal{K}_\ell$ are modified spherical Bessel functions of the third kind, whose Rayleigh representations are:

$$\mathcal{J}_\ell(xy) = y^{-\ell-1}x^\ell\left[\frac{1}{x}\frac{d}{dx}\right]^\ell\frac{\sinh(xy)}{x}, \tag{A19}$$

$$\mathcal{K}_\ell(xy) = y^{-\ell-1}(-x)^\ell\left[\frac{1}{x}\frac{d}{dx}\right]^\ell\frac{\exp(-xy)}{x}. \tag{A20}$$

Substituting Eq. (A11, A14b, A18) in Eq. (340d) we obtain with Silverstone the following:

$$\begin{aligned}
I^{(\underline{\delta})}_{\nu\lambda,\nu'\lambda'}\left(\underset{\sim}{\text{đ}}_{hk\ell}\right) = {} & \frac{(2\zeta)^{n+\frac{1}{2}}}{(2n)!}\,\frac{(2\zeta')^{n'+\frac{1}{2}}}{(2n')!}\sum_{m_1=-\ell}^{\ell} R^{(\ell)}_{mm_1}(\alpha_\nu\beta_\nu\gamma_\nu)\times \\
& \times\sum_{m_3=-\ell'}^{\ell'} R^{(\ell')*}_{m'm_3}(\alpha_{\nu'},\beta_{\nu'},\gamma_{\nu'})\sum_{p=0}^{\infty}\sum_{m_2=-p}^{p}4\pi(-i)^p Y_p^{m_2*}(\vartheta_{hk\ell},\varphi_{hk\ell})\times \\
& \times(-\text{đ}_{hk\ell})^p\left[\frac{1}{\text{đ}_{hk\ell}}\frac{d}{d\text{đ}_{hk\ell}}\right]^p\frac{1}{\text{đ}_{hk\ell}}\sum_{\ell_1=0}^{\infty}\sum_{\ell_2=|\ell'-\ell_1|}^{\ell'+\ell_1}\sum_{m_4=-\ell_1}^{\ell_1}\sqrt{\frac{2\ell_2+1}{4\pi}}\times \\
& \times\frac{2}{\pi}i^{\ell_2-\ell_1}c^{\ell_2}(\ell',m_3;\ell_1,m_4)Y_{\ell_2}^{m_3-m_4}\left(\vartheta^{\circ}_{\nu\underline{\delta}\nu'},\varphi^{\circ}_{\nu\underline{\delta}\nu'}\right)4\pi\times \\
& \times(-1)^{n'}\left(\frac{d}{d\zeta'}\right)^{n'-\ell'}\left[\frac{1}{\zeta'}\frac{d}{d\zeta'}\right]^{\ell'}(\zeta')^{\ell'+1}\left\{\mathcal{K}_{\ell_2}(\zeta' R_{\nu\underline{\delta}\nu'})(\zeta')^{\ell_1}\times\right. \\
& \times\left[\frac{1}{\zeta'}\frac{d}{d\zeta'}\right]^{\ell_1}\frac{1}{\zeta'}\int_0^{R_{\nu\underline{\delta}\nu'}}dr\left[r^2 r^{-p-1}\sin(\text{đ}_{hk\ell}r)\,r^{-\ell_1-1}\sinh(\zeta' r)\times\right. \\
& \left.\times\, r^{n-1}\exp(-\zeta r)\right] + (-1)^{\ell'}\mathcal{J}_{\ell_2}(\zeta' R_{\nu\underline{\delta}\nu'})(-\zeta')^{\ell_1}\left[\frac{1}{\zeta'}\frac{d}{d\zeta'}\right]^{\ell_1}\frac{1}{\zeta'}\times
\end{aligned} \tag{A21a}$$

$$\times \int_{R_{\nu\underline{\delta}\nu'}}^{\infty} dr \left[r^{2} r^{-p-1} \sin(\mathbb{k}_{hkl} r)\, r^{-\ell_1-1} \exp(-\zeta' r)\, r^{n-1} \exp(-\zeta r) \right] \Big\} \times$$

$$\times \int_{0}^{2\pi} d\varphi \int_{0}^{\pi} d\vartheta \sin\vartheta\, Y_{\ell}^{m_1 *}(\vartheta,\varphi)\, Y_{\ell_1}^{m_4}(\vartheta,\varphi)\, Y_{p}^{m_2}(\vartheta,\varphi),$$

where each differential operator differentiates everything to its right. This expression can be simplified by using Condon-Shortley coefficients, Eq. (A6b), which will restrict m_4 to $m_4 = m_2 - m_1$, and the sum over ℓ_1 to $|\ell - p| \leqslant \ell_1 \leqslant \ell + p$. The integrations over r may be simplified by a change of variable to $t \equiv r(R_{\nu\underline{\delta}\nu'})^{-1}$. We get:

$$I^{(\underline{\delta})}_{\nu\lambda,\nu'\lambda'}(\underset{\sim}{\mathbb{k}}_{hkl}) = \frac{(2\zeta)^{n+\frac{1}{2}}\,(2\zeta')^{n'+\frac{1}{2}}}{(2n)!\,(2n')!} \sum_{m_1=-\ell}^{\ell} R^{(\ell)}_{mm_1}(\alpha_\nu \beta_\nu \gamma_\nu) \times$$

$$\times \sum_{m_3=-\ell'}^{\ell'} R^{(\ell')*}_{m'm_3}(\alpha_{\nu'} \beta_{\nu'} \gamma_{\nu'}) \sum_{p=0}^{\infty} \sum_{m_2=-p}^{p} 4\pi(-i)^{p}\, Y_{p}^{m_2 *}(\vartheta_{hkl}, \varphi_{hkl}) \times$$

$$\times \sum_{\ell_1=|\ell-p|}^{\ell+p} \sqrt{\frac{2\ell_1+1}{4\pi}}\, c^{\ell_1}(\ell, m_1; p, m_2) \sum_{\ell_2=|\ell'-\ell_1|}^{\ell'+\ell_1} \sqrt{\frac{2\ell_2+1}{4\pi}}\, \frac{2}{\pi}\, i^{\ell_2-\ell_1} \times \qquad \text{(A21b)}$$

$$\times c^{\ell_2}(\ell', m_3; \ell_1, m_2-m_1)\, Y_{\ell_2}^{m_3-m_2+m_1}(\vartheta^{\circ}_{\nu\underline{\delta}\nu'}, \varphi^{\circ}_{\nu\underline{\delta}\nu'})\, (R_{\nu\underline{\delta}\nu'})^{n-p-\ell_2} \times$$

$$\times (-\mathbb{k}_{hkl})^{p} \left[\frac{1}{\mathbb{k}_{hkl}} \frac{d}{d\mathbb{k}_{hkl}} \right]^{p} \frac{1}{\mathbb{k}_{hkl}}\, 4\pi (-1)^{n'} \left(\frac{d}{d\zeta'} \right)^{n'-\ell'} \left[\frac{1}{\zeta'} \frac{d}{d\zeta'} \right]^{\ell'} (\zeta')^{\ell'+1} \times$$

$$\times \left\{ \mathcal{K}_{\ell_2}(\zeta' R_{\nu\underline{\delta}\nu'})(\zeta')^{\ell_1}\left[\frac{1}{\zeta'}\frac{d}{d\zeta'}\right]^{\ell_1}\frac{1}{\zeta'}\,\frac{1}{4i}\int_0^1 dt\, t^{n-p-\ell_1-1} \times\right.$$

$$\times \left\{ \exp\left[-(\zeta-\zeta'-i\eth_{hk\ell})R_{\nu\delta\nu'}\,t\right] - \exp\left[-(\zeta+\zeta'-i\eth_{hk\ell})R_{\nu\underline{\delta}\nu'}\,t\right] - \right.$$

$$\left. - \exp\left[-(\zeta-\zeta'+i\eth_{hk\ell})R_{\nu\underline{\delta}\nu'}\,t\right] + \exp\left[-(\zeta+\zeta'+i\eth_{hk\ell})R_{\nu\delta\nu'}\,t\right]\right\} +$$

$$+ (-1)^{\ell'}\mathcal{J}_{\ell_2}(\zeta' R_{\nu\underline{\delta}\nu'})(-\zeta')^{\ell_1}\left[\frac{1}{\zeta'}\frac{d}{d\zeta'}\right]^{\ell_1}\frac{1}{\zeta'}\,\frac{1}{2i}\int_1^\infty dt\, t^{n-p-\ell_1-1} \times$$

$$\times \left\{ \exp\left[-(\zeta+\zeta'+i\eth_{hk\ell})R_{\nu\underline{\delta}\nu'}\,t\right] - \exp\left[-(\zeta+\zeta'-i\eth_{hk\ell})\times\right.\right.$$

$$\left.\left.\left.\times R_{\nu\underline{\delta}\nu'}\,t\right]\right\}\right\}.$$

The two terms of the second integral are, very simply, generalized exponential integrals:

$$\text{(A22)} \qquad E_q(z) \equiv \int_1^\infty dt\, t^{-q} \exp(-zt); \qquad \{q=0,1,2,\ldots\}$$

these functions satisfy the very useful recursion relation (236):

$$\text{(A23)} \qquad \frac{dE_q(z)}{dz} = -E_{q-1}(z).$$

The four terms of the first integral, taken severally out of Eq. (A21), look like:

$$\int_0^1 dt\, t^{-q} \exp(-zt),$$

which for positive q diverges at t = 0. However,[*] if we perform the explicit differentiations with respect to ζ' and $\mathcal{A}_{hkl}$ indicated in Eq. (A20), then the <u>sum</u> of these four terms in Eq. (A21) does not diverge. In fact, as $r \rightarrow 0$,

$$\left[\frac{1}{\mathcal{A}_{hkl}}\frac{d}{d\mathcal{A}_{hkl}}\right]^{p}\frac{\sin(\mathcal{A}_{hkl}r)}{\mathcal{A}_{hkl}} = r^{2p+1}\left[\frac{1}{x}\frac{d}{dx}\right]^{p}\frac{\sin x}{x} \propto r^{2p+1},$$

$$\left[\frac{1}{\zeta'}\frac{d}{d\zeta'}\right]^{\ell_1}\frac{\sinh(\zeta' r)}{\zeta'} = r^{2\ell_1+1}\left[\frac{1}{x}\frac{d}{dx}\right]^{\ell_1}\frac{\sinh x}{x} \propto r^{2\ell_1+1},$$

and all negative powers of t vanish from the first integrand in Eq. (A21), and the first integral is non-singular when differentiated properly with respect to ζ' and $\mathcal{A}_{hkl}$. We need, therefore, a non-singular representation for each of the four terms of the first integral; this is provided by:

$$\text{(A24a)} \qquad \tilde{E}_q(z) \equiv - \sum_{\substack{m=0 \\ [m \neq q-1]}}^{\infty} \frac{(-z)^m}{m!\,(m-q+1)} =$$

$$\text{(A24b)} \qquad = -\int_0^1 dt\, t^{-q}\left[\exp(-zt) - \sum_{m=0}^{q-1}\frac{(-zt)^m}{m!}\right] - \sum_{m=0}^{q-2}\frac{(-z)^m}{m!\,(m-q+1)}.$$

In fact, the differentiations with respect to ζ' and $\mathcal{A}_{hkl}$ of Eq. (A21) will kill all but the integral in Eq. (A24b). Furthermore $E_q(z)$ also satisfies the useful relation:

---

[*] I am very much indebted to H. J. Silverstone for helpful correspondence (251) clarifying this point.

$$\frac{d\tilde{E}_q(z)}{dz} = -\tilde{E}_{q-1}(z). \qquad \text{(A24c)}$$

APPENDIX III

We evaluate here the Fourier transform of the STO defined in Appendix I and modified by the Gaussian convergence parameter η (and hence unnormalized):

$$\begin{aligned}\psi^{n\ell m\zeta}_{\nu\lambda\eta}(\underset{\sim}{r}_{\nu\mu}) \equiv {}& \frac{(2\zeta)^{n+\frac{1}{2}}}{(2n)!}(r_{\nu\mu})^{n-1}\exp\left[-\zeta r_{\nu\mu}-\eta V^{-2/3}(r_{\nu\mu})^{2}\right]\times \\ & \times\sum_{m_1=-\ell}^{\ell}\mathbb{R}^{(\ell)*}_{m m_1}(\alpha_\nu\beta_\nu\gamma_\nu)\,Y^{m_1}_{\ell}(\vartheta_{\nu\mu},\varphi_{\nu\mu}).\end{aligned} \tag{A25}$$

The Fourier transform is defined as:

$$F^{G}_{\nu\lambda}(\underset{\sim}{\mathbb{k}}_\nu) \equiv \iiint_{\frac{N_0V}{2}} dv(\underset{\sim}{r}_{\nu\mu})\exp(-i\,\underset{\sim}{\mathbb{k}}_\nu\cdot\underset{\sim}{r}_{\nu\mu})\,\psi^{n\ell m\zeta}_{\nu\lambda\eta}(\underset{\sim}{r}_{\nu\mu}). \tag{A26}$$

By using the expansion of $\exp(-i\,\underset{\sim}{\mathbb{k}}_\nu\cdot\underset{\sim}{r}_{\nu\mu})$ in spherical Bessel functions:

$$\begin{aligned}\exp(-i\,\underset{\sim}{\mathbb{k}}_\nu\cdot\underset{\sim}{r}_{\nu\mu}) = {}& \sum_{p=0}^{\infty}\sum_{m_2=-p}^{p}4\pi(-i)^{p}j_p(\mathbb{k}_\nu r_{\nu\mu})\,Y^{m_2 *}_{p}(\vartheta_{\nu\mu},\varphi_{\nu\mu})\times \\ & \times Y^{m_2}_{p}(\vartheta^{\nu}_{\mathbb{k}},\varphi^{\nu}_{\mathbb{k}}),\end{aligned} \tag{A27}$$

we get after using the orthonormality properties of the spherical harmonic functions in the angular integration:

(A28)
$$F^{G}_{\nu\lambda}(\mathbb{k}_\nu) = 4\pi(-i)^{\ell}\,\frac{(2\zeta)^{n+\frac{1}{2}}}{(2n)!}\sum_{m_1=-\ell}^{\ell}\mathcal{R}^{(\ell)*}_{mm_1}(\alpha_\nu\beta_\nu\gamma_\nu)\times$$
$$\times Y^{m_1}_{\ell}(\vartheta^{\nu}_{\mathbb{k}},\varphi^{\nu}_{\mathbb{k}})\,K^{n\ell\zeta}_{\nu\lambda},$$

where the radial integral, defined by:

(A29)
$$K^{n\ell\zeta}_{\nu\lambda} \equiv \int_0^\infty dr\; r^{n+1} j_\ell(\mathbb{k}_\nu r)\exp\left[-\eta V^{-2/3} r^2 - \zeta r\right]$$

can be solved by the technique used by Silverstone (221); from Eq. (A15) we get:

(A30)
$$K^{n\ell\zeta}_{\nu\lambda} = \frac{1}{2i}(-\mathbb{k}_\nu)^{\ell}\left[\frac{1}{\mathbb{k}_\nu}\,\frac{d}{d\mathbb{k}_\nu}\right]^{\ell}\frac{1}{\mathbb{k}_\nu}\int_0^\infty dr\; r^{n-\ell}\times$$
$$\times\left\{\exp\left[-\eta V^{-2/3} r^2 - \zeta r + i\mathbb{k}_\nu r\right] - \exp\left[-\eta V^{-2/3} r^2 - \zeta r - i\mathbb{k}_\nu r\right]\right\}.$$

The integrals can be solved in terms of Weber's parabolic cylinder functions or of confluent hypergeometric functions (237):

(A31a)
$$K^{n\ell\zeta}_{\nu\lambda} = \frac{1}{2i}(-\mathbb{k}_\nu)^{\ell}\left[\frac{1}{\mathbb{k}_\nu}\,\frac{d}{d\mathbb{k}_\nu}\right]^{\ell}\frac{1}{\mathbb{k}_\nu}\,\Gamma(n-\ell+1)\left(\frac{V^{2/3}}{2\eta}\right)^{\frac{n-\ell+1}{2}}\times$$
$$\times\left\{\exp\left[\frac{V^{2/3}}{8\eta}(\zeta - i\mathbb{k}_\nu)^2\right]D_{-(n-\ell+1)}\left(\frac{(\zeta - i\mathbb{k}_\nu)V^{1/3}}{\sqrt{2\eta}}\right)-\right.$$
$$\left.-\exp\left[\frac{V^{2/3}}{8\eta}(\zeta + i\mathbb{k}_\nu)^2\right]D_{-(n-\ell+1)}\left(\frac{(\zeta + i\mathbb{k}_\nu)V^{1/3}}{\sqrt{2\eta}}\right)\right\} =$$

$$(\text{A31b})\quad \begin{aligned} &= \left(\frac{V^{2/3}}{\eta}\right)^{\frac{n-\ell+1}{2}} \frac{\sqrt{\pi}\,\Gamma(n-\ell+1)}{2i} (-\mathbb{k}_\nu)^\ell \left[\frac{1}{\mathbb{k}_\nu}\frac{d}{d\mathbb{k}_\nu}\right]^\ell \frac{1}{\mathbb{k}_\nu} \times \\ &\times\left\{\frac{1}{\Gamma\left(\frac{n-\ell+2}{2}\right)}\left[{}_1F_1\left(\frac{n-\ell+1}{2}, \frac{1}{2}; \frac{V^{2/3}(\zeta-i\mathbb{k}_\nu)^2}{4\eta}\right)-\right.\right. \\ &\left.-{}_1F_1\left(\frac{n-\ell+1}{2}, \frac{1}{2}; \frac{V^{2/3}(\zeta+i\mathbb{k}_\nu)^2}{4\eta}\right)\right] - \frac{\sqrt{2}}{\Gamma\left(\frac{n-\ell+1}{2}\right)} \frac{V^{1/3}}{\sqrt{\eta}} \times \\ &\times\left[(\zeta-i\mathbb{k}_\nu)\,{}_1F_1\left(\frac{n-\ell+2}{2}, \frac{3}{2}; \frac{V^{2/3}(\zeta-i\mathbb{k}_\nu)^2}{4\eta}\right)-\right. \\ &\left.\left.-(\zeta+i\mathbb{k}_\nu)\,{}_1F_1\left(\frac{n-\ell+2}{2}, \frac{3}{2}; \frac{V^{2/3}(\zeta+i\mathbb{k}_\nu)^2}{4\eta}\right)\right]\right\}. \end{aligned}$$

The confluent hypergeometric functions are defined by (238):

$$(\text{A32})\quad {}_1F_1(\alpha, \beta; z) \equiv \sum_{n=0}^{\infty} \frac{z^n}{n!} \frac{\alpha(\alpha-1)\ldots(\alpha-n+1)}{\beta(\beta-1)\ldots(\beta-n+1)},$$

and so we obtain more simply:

$$(\text{A33})\quad \begin{aligned} \mathbb{K}^{n\ell\zeta}_{\nu\lambda} &= \sqrt{\pi}\,\Gamma(n-\ell+1)\left(\frac{V^{2/3}}{\eta}\right)^{\frac{n-\ell+1}{2}} (-\mathbb{k}_\nu)^\ell \left[\frac{1}{\mathbb{k}_\nu}\frac{d}{d\mathbb{k}_\nu}\right]^\ell \frac{1}{\mathbb{k}_\nu} \times \\ &\times \left\{ \frac{V^{1/3}}{\sqrt{\eta}} \frac{\sqrt{2}}{\Gamma\left(\frac{n-\ell+1}{2}\right)} \operatorname{Im}\left[(\zeta+i\mathbb{k}_\nu)\,{}_1F_1\left(\frac{n-\ell+2}{2}, \frac{3}{2}; \frac{V^{\frac{2}{3}}}{4\eta}\times\right.\right.\right. \\ &\left.\left.\left.\times(\zeta+i\mathbb{k}_\nu)^2\right)\right] - \frac{1}{\Gamma\left(\frac{n-\ell+2}{2}\right)} \operatorname{Im}\left[{}_1F_1\left(\frac{n-\ell+1}{2}, \frac{1}{2}; \frac{V^{2/3}}{4\eta}(\zeta-i\mathbb{k}_\nu)^2\right)\right]\right\}. \end{aligned}$$

Some further research is obviously advisable to ensure that the optimal form, amenable to rapid and precise computation, is found.

APPENDIX IV

For the purpose of reference we give here the Fourier series of $Q_{\lambda\underline{\omega}}$, $[\lambda|\lambda]_{\underline{\omega}}$, $[\lambda\lambda|\lambda'\lambda']_{\underline{\omega}\,\underline{\omega}'}$, and $[\lambda\lambda'|\lambda'\lambda]_{\underline{\omega}\,\underline{\omega}'}$. We use the Fourier series for the periodic functions:

$$\Phi_{\lambda\underline{\omega}}(\underset{\sim}{r}_{\mu}) \equiv \exp(-i\,\underset{\sim}{\mathfrak{k}}_{\underline{\omega}}\cdot\underset{\sim}{r}_{\mu})\,\Psi_{\lambda\underline{\omega}}(\underset{\sim}{r}_{\mu}), \tag{A34}$$

and $\Phi^{*}_{\lambda\underline{\omega}}(\underset{\sim}{r}_{\mu})\ \Phi_{\lambda'\underline{\omega}'}(\underset{\sim}{r}_{\mu})$:

$$\Phi_{\lambda\underline{\omega}}(\underset{\sim}{r}_{\mu}) = \frac{1}{V}\sum_{h=-\infty}^{\infty}\sum_{k=-\infty}^{\infty}\sum_{l=-\infty}^{\infty} C_{\lambda\underline{\omega}}(\underset{\sim}{\mathfrak{b}}_{hkl})\exp(i\,\underset{\sim}{\mathfrak{b}}_{hkl}\cdot\underset{\sim}{r}_{\mu}), \tag{A35}$$

$$\Phi^{*}_{\lambda\underline{\omega}}(\underset{\sim}{r}_{\mu})\,\Phi_{\lambda'\underline{\omega}'}(\underset{\sim}{r}_{\mu}) = \frac{1}{V}\sum_{h=-\infty}^{\infty}\sum_{k=-\infty}^{\infty}\sum_{l=-\infty}^{\infty} D_{\lambda\underline{\omega}\lambda'\underline{\omega}'}(\underset{\sim}{\mathfrak{b}}_{hkl})\exp(i\,\underset{\sim}{\mathfrak{b}}_{hkl}\cdot\underset{\sim}{r}_{\mu}). \tag{A36}$$

It can be shown that:

$$C_{\lambda\underline{\omega}}(\underset{\sim}{\mathfrak{b}}_{hkl}) \equiv \iiint\limits_{V} dv(\underset{\sim}{r}_{\mu})\exp\left[-i(\underset{\sim}{\mathfrak{b}}_{hkl}+\underset{\sim}{\mathfrak{k}}_{\underline{\omega}})\cdot\underset{\sim}{r}_{\mu}\right]\Psi_{\lambda\underline{\omega}}(\underset{\sim}{r}_{\mu}) = \tag{A37a}$$

$$= \sqrt{\frac{Z}{N_0}}\sum_{\nu=1}^{M} c_{\nu\lambda}\exp\left[-i(\underset{\sim}{\mathfrak{b}}_{hkl}+\underset{\sim}{\mathfrak{k}}_{\underline{\omega}})\cdot\underset{\sim}{r}^{\circ}_{\nu}\right]F_{\nu\lambda}(\underset{\sim}{\mathfrak{k}}_{\underline{\omega}}+\underset{\sim}{\mathfrak{b}}_{hkl}), \tag{A37b}$$

where $F_{\nu\lambda}$ is given by Eqs. (359, A25). Also:

$$D_{\lambda\underline{\omega}\lambda'\underline{\omega}'}(\underset{\sim}{\mathfrak{b}}_{hkl}) \equiv \iiint\limits_{V} dv(\underset{\sim}{r}_{\mu})\exp\left[-i(\underset{\sim}{\mathfrak{b}}_{hkl}-\underset{\sim}{\mathfrak{k}}_{\underline{\omega}}+\underset{\sim}{\mathfrak{k}}_{\underline{\omega}'})\cdot\underset{\sim}{r}_{\mu}\right]\Psi^{*}_{\lambda\underline{\omega}}(\underset{\sim}{r}_{\mu})\,\Psi_{\lambda'\underline{\omega}'}(\underset{\sim}{r}_{\mu}) = \tag{A38a}$$

(A38b)
$$= \frac{Z}{N_0}\sum_{\nu=1}^{M}\sum_{\nu'=1}^{M} c^*_{\nu\lambda}\, c_{\nu'\lambda'} \exp\left[-i\left(\underset{\sim}{d}^*_{hk\ell} - \underset{\sim}{k}_{\underline{\omega}} + \underset{\sim}{k}_{\underline{\omega}'}\right)\cdot \underset{\sim}{r}^{0}_{\nu}\right] \times$$
$$\times \sum_{\underline{\delta}=0}^{N_0/Z-1} \exp\left(i\underset{\sim}{k}_{\underline{\omega}'}\cdot \underset{\sim}{r}_{\underline{\delta}}\right) I^{(\delta)}_{\nu\lambda,\nu'\lambda'}\left(\underset{\sim}{d}^*_{hk\ell} - \underset{\sim}{k}_{\underline{\omega}} + \underset{\sim}{k}_{\underline{\omega}'}\right),$$

where $I^{(\delta)}_{\nu\lambda,\nu'\lambda'}$ is given by Eq. (340e). Alternately, the multiplication of two Fourier series for $\Phi^*_{\lambda\underline{\omega}}(\underset{\sim}{r}_\mu)$ and $\Phi_{\lambda'\underline{\omega}'}(\underset{\sim}{r}_\mu)$ yields:

(A39)
$$D_{\lambda\underline{\omega}\,\lambda'\underline{\omega}'}(\underset{\sim}{d}^*_{hk\ell}) = \frac{1}{V}\sum_{h'=-\infty}^{\infty}\sum_{k'=-\infty}^{\infty}\sum_{\ell'=-\infty}^{\infty} G^*_{\lambda\underline{\omega}}\left(\underset{\sim}{d}^*_{h'-h,\,k'-k,\,\ell'-\ell}\right) \times$$
$$\times\, G_{\lambda'\underline{\omega}'}\left(\underset{\sim}{d}^*_{h'+h,\,k'+k,\,\ell'+\ell}\right).$$

Then it can be further shown that:

(A40a)
$$Q_{\lambda\underline{\omega}} = -\frac{N_0}{VZ}\sum_{h=-\infty}^{\infty}\sum_{k=-\infty}^{\infty}\sum_{\ell=-\infty}^{\infty}\left|G_{\lambda\underline{\omega}}(\underset{\sim}{d}^*_{hk\ell})\right|^2\left|\underset{\sim}{d}^*_{hk\ell} + \underset{\sim}{k}_{\underline{\omega}}\right|^2,$$

(A40b)
$$[\lambda|\lambda]_{\underline{\omega}} = \frac{4\pi N_0}{VZ}\sum_{h=-\infty}^{\infty}\sum_{k=-\infty}^{\infty}{\sum_{\ell=-\infty}^{\infty}}' \frac{P(\underset{\sim}{d}^*_{hk\ell})\, D^*_{\lambda\underline{\omega}\,\lambda\underline{\omega}}(\underset{\sim}{d}^*_{hk\ell})}{d^{*2}_{hk\ell}},$$

(A40c)
$$[\lambda\lambda|\lambda'\lambda']_{\underline{\omega}\,\underline{\omega}'} = \frac{4\pi N_0}{VZ}\sum_{h=-\infty}^{\infty}\sum_{k=-\infty}^{\infty}{\sum_{\ell=-\infty}^{\infty}}' \frac{D^*_{\lambda\underline{\omega}\,\lambda\underline{\omega}}(\underset{\sim}{d}^*_{hk\ell})\, D_{\lambda'\underline{\omega}'\,\lambda'\underline{\omega}'}(\underset{\sim}{d}^*_{hk\ell})}{d^{*2}_{hk\ell}},$$

(A40d)
$$[\lambda\lambda'|\lambda'\lambda]_{\underline{\omega}\,\underline{\omega}'} = \frac{4\pi N_0}{VZ}\sum_{h=-\infty}^{\infty}\sum_{k=-\infty}^{\infty}{\sum_{\ell=-\infty}^{\infty}}'' \frac{\left|D_{\lambda'\underline{\omega}'\,\lambda\underline{\omega}}(\underset{\sim}{d}^*_{hk\ell})\right|^2}{\left|\underset{\sim}{d}^*_{hk\ell} + \underset{\sim}{k}_{\underline{\omega}} - \underset{\sim}{k}_{\underline{\omega}'}\right|^2}.$$

Similar expressions can be written for the $\Psi^{G}_{\lambda\underline{\omega}}(\underset{\sim}{r}_\mu)$.

REFERENCES

(1) R. S. Mulliken, J. Chim. Phys., 61, 20-38 (1964); R. S. Mulliken and W. B. Person, Ann. Rev. Phys. Chem., 13, 107-126 (1962).

(2) H. M. McConnell, "Magnetic Excitations in Molecular Crystals" in "Molecular Biophysics", M. Weissbluth, Ed. (Academic Press, Inc., New York, 1965), pp. 311-324.

(3) P.-L. Nordio, Z. G. Soos, and H. M. McConnell, Ann. Rev. Phys. Chem., 17, 237-260 (1966).

(4) G. Briegleb, "Elektronen-Donator-Acceptor-Komplexe" (Springer-Verlag, Berlin, 1961).

(5) L. J. Andrews and R. M. Keefer, "Molecular Complexes in Organic Chemistry" (Holden-Day, San Francisco, 1964).

(6) J. Kommandeur, "Conductivity" in "Physics and Chemistry of Organic Solid State", Vol. 2, D. Fox, M. M. Labes, and A. Weissberger, Eds. (Interscience, Inc., New York, 1965), pp. 1-66, especially pp. 48-56.

(7) O. H. LeBlanc, Jr., "Conductivity", in "Physics and Chemistry of the Organic Solid State", Vol. 3, D. Fox, M. M. Labes, and A. Weissberger, Eds. (Interscience, Inc., New York, 1967), pp. 133-198.

(8) G. Briegleb and J. Czekalla, Z. Elektrochem., 63, 6-12 (1959).

(9) G. Briegleb, Angew. Chem. (Intern. Ed. Engl.), 3, 617-632 (1964).

(10) J. Weiss, J. Chem. Soc., 1942, 245-252.

(11) R. S. Mulliken, J. Am. Chem. Soc., 72, 600-608 (1950); ibid., 72, 4493-4503 (1950); ibid., 74, 811-824 (1952); J. Phys. Chem., 56, 801-822 (1952); J. Chem. Phys., 19, 514-515 (1951); J. Chim. Phys., 51, 341-344 (1954).

(12) M. J. S. Dewar and A. R. Lepley, J. Am. Chem. Soc., 83, 4560-4563 (1961).

(13) H. M. McConnell, B. M. Hoffman, and R. M. Metzger, Proc. Natl. Acad. Sci. U.S., 53, 46-50 (1965).

(14) J. Krugler, C. G. Montgomery, and H. M. McConnell, J. Chem. Phys., 41, 2421-2428 (1964).

(15) J. Kommandeur and G. T. Pott, Mol. Phys., 11, 93-95 (1966).

(16) G. T. Pott and J. Kommandeur, Mol. Phys., 13, 373-390 (1967).

(17) T. Amano, H. Kuroda, and H. Akamatu, Bull. Chem. Soc. Japan, 41, 83-87 (1968).

(18) J. L. deBoer and A. Vos, Acta Cryst., B24, 720-725 (1968).

(19) G. Scheibe, Chimia (Aarau), 15, 10-20 (1961).

(20) U. H. Kollaard and J. P. Colpa, Mol. Phys., 8, 295-297 (1964).

(21) J. C. A. Boeyens, J. Phys. Chem., 71, 2969-2974 (1967).

(22) M. Hanna, J. Am. Chem. Soc., 90, 285-291 (1968).

(23) R. Foster and T. J. Thomson, Trans. Faraday Soc., 58, 860-868 (1962).

(24) R. Foster and P. Hanson, Biochim. Biophys. Acta, 112, 482-489 (1966).

(25) R. Foster and T. J. Thomson, Trans. Faraday Soc., 59, 1059-1063 (1963).

(26) R. M. Metzger, unpublished results (1967).

(27) R. M. Metzger, unpublished results (1964).

(28) D. C. Douglass, J. Chem. Phys., 32, 1882-1883 (1960).

(29) H. O. Hooper, J. Chem. Phys., 41, 599-601 (1964).

(30) L. Salem, "The Molecular Orbital Theory of Conjugated Systems" (W. A. Benjamin, Inc., New York, 1966).

(31) R. C. Hughes, unpublished results (1964).

(32) T. Sakurai, Acta Cryst., 19, 320-330 (1965).

(33) Y. Ohashi, H. Iwasaki, and Y. Sato, Bull. Chem. Soc. Japan, 40, 1789-1796 (1967).

(34) P. L. Kronick, H. Scott, and M. M. Labes, J. Chem. Phys., 40, 890-894 (1964).

(35) Y. Matsunaga, J. Chem. Phys., 41, 1609-1613 (1964).

(36) T. J. Schaafsma and J. Kommandeur, J. Chem. Phys., 42, 438-439 (1965).

(37) Z. G. Soos, J. Chem. Phys., 46, 4284-4288 (1967).

(38) R. C. Hughes and Z. G. Soos, J. Chem. Phys., 48, 1066-1076 (1968).

(39) Z. G. Soos, "Theory of Temperature-Dependent g-Tensor Splittings in p-Phenylenediamine-Chloranil" (to be published, 1968).

(40) W. H. Bentley and H. G. Drickamer, J. Chem. Phys., 42, 1573-1587 (1965).

(41) A. Ottenberg, private communication (1965).

(42) R. H. Boyd, J. Chem. Phys., 38, 2529-2535 (1963).

(43) A. L. Farragher and F. M. Page, Trans. Faraday Soc., 62, 3072-3080 (1966).

(44) K. Watanabe, J. Chem. Phys., 22, 1565-1570 (1954); ibid., 26, 542-547 (1957); K. Watanabe and J. R. Mottl, J. Chem. Phys., 26, 1773-1774 (1957).

(45) A. D. Baker, D. P. May, and D. W. Turner, J. Chem. Soc., 1968, B22-B34.

(46) L. E. Lyons and J. C. Mackie, Proc. Chem. Soc., 1962, 71.

(47) L. E. Lyons and J. C. Mackie, Nature, 197, 589 (1963).

(48) S. Iwata, H. Tsubomura, and S. Nagakura, Bull. Chem. Soc. Japan, 37, 1506-1508 (1964).

(49) M. Kinoshita, Bull. Chem. Soc. Japan, 35, 1609-1611 (1962).

(50) M. E. Wacks and V. H. Dibeler, J. Chem. Phys., 31, 1557-1562 (1959).

(51) A. J. Yencha and M. A. El-Sayed, J. Chem. Phys., 48, 3469-3475 (1968).

(52) R. S. Becker and W. E. Wentworth, J. Am. Chem. Soc., 85, 2210-2214 (1963).

(53) M. Batley and L. E. Lyons, Mol. Cryst., 3, 357-374 (1968).

(54) D. Kearns and M. Calvin, J. Chem. Phys., 34, 2026-2030 (1961).

(55) D. Feil, M. H. Linck, and J. J. McDowell, Nature, 207, 285-286 (1965).

(56) R. G. Wood, C. H. McCale, and G. Williams, Phil. Mag., 31, 71-80 (1941).

(57) B. G. Anex and L. J. Parkhurst, J. Am. Chem. Soc., 85, 3301-3302 (1963).

(58) H. W. Offen and M. S. F. A. Abidi, J. Chem. Phys., 44, 4642-4643 (1965).

(59) H. Böhme and W. Schürhoff, Chem. Ber., 84, 28-47 (1950) page 42.

(60) J. W. Eastman, G. Engelsma, and M. Calvin, J. Am. Chem. Soc., 84, 1339-1345 (1962).

(61) American Institute of Physics Handbook, D. E. Gray, Coord. Ed., Second Edition (McGraw-Hill Book Co., New York, 1963) pp. 5-121 to 5-134.

(62) R. D. Srivastava and G. Prasad, Spectrochim. Acta, 22, 1869-1875 (1966).

(63) H. M. Rosenberg, E. Eimutis, and D. Hale, Can. J. Chem., 44, 2405-2407 (1966).

(64) R. E. Merrifield and W. D. Phillips, J. Am. Chem. Soc., 80, 2778-2782 (1958).

(65) E. M. Voigt and C. Reid, J. Am. Chem. Soc., 86, 3930-3934 (1964).

(66) M. J. S. Dewar and H. Rogers, J. Am. Chem. Soc., 84, 395-398 (1962).

(67) G. Briegleb, J. Czekalla, and G. Reuss, Z. Physik. Chem. (Frankfurt), 30, 333-348 (1961); ibid., 316-332.

(68) W. L. Peticolas, J. Chem. Phys., 26, 429-430 (1957).

(69) J. N. Murrell, J. Am. Chem. Soc., 81, 5037-5043 (1959).

(70) R. Foster, D. L. Hammick, and B. N. Parsons, J. Chem. Soc., 1956, 555-558.

(71) R. Foster, Nature, 181, 337-338 (1958).

(72) G. Briegleb and J. Czekalla, Z. Elektrochem., 59, 184-202 (1955).

(73) J. Czekalla, G. Briegleb, W. Herre, and R. Glier, Z. Elektrochem., 61, 537-546 (1957).

(74) J. Czekalla, G. Briegleb, and W. Herre, Z. Elektrochem., 63, 712-715 (1959).

(75) A. Bier, Rec. trav. chim., 75, 866-870 (1956).

(76) C. C. Thompson, Jr., and P. A. D. de Maine, J. Phys. Chem., 69, 2766-2771 (1965).

(77) D. M. G. Lawrey and H. M. McConnell, J. Am. Chem. Soc., 74, 6175-6177 (1952).

(78) S. C. Wallwork, J. Chem. Soc., 1961, 494-499.

(79) R. Beukers and A. Szent-Györgyi, Rec. trav. chim., 81, 255-268 (1962).

(80) H. Kuroda, M. Kobayashi, M. Kinoshita, and S. Takemoto, J. Chem. Phys., 36, 457-462 (1962).

(81) H. Kuroda, T. Amano, I. Ikemoto, and H. Akamatu, J. Am. Chem. Soc., 89, 6056-6063 (1967).

(82) A. H. Kadhim and H. W. Offen, Mol. Cryst., 3, 311-323 (1968).

(83) H. W. Offen and A. H. Kadhim, J. Chem. Phys., 45, 269-274 (1966).

(84) R. Foster and T. J. Thomson, Trans. Faraday Soc., 59, 296-300 (1963).

(85) R. M. Williams and S. C. Wallwork, Acta Cryst., 22, 899-906 (1967).

(86) J. C. A. Boeyens and F. H. Herbstein, J. Phys. Chem., 69, 2153-2159 (1965).

(87) S. K. Chakrabarti and S. Basu, Trans. Faraday Soc., 60, 465-475 (1964).

(88) R. E. Miller and W. F. K. Wynne-Jones, J. Chem. Soc., 1959, 2375-2384.

(89) C. C. Thompson, Jr., and P. A. D. de Maine, J. Am. Chem. Soc., 85, 3096-3101 (1963).

(90) L. Van Duuren and C. E. Bardi, Anal. Chem., 35, 2198-2202 (1963).

(91) S. C. Wallwork, private communication (13 July 1965).

(92) D. D. Thomas, A. W. Merkl, A. F. Hildebrandt, and H. M. McConnell, J. Chem. Phys., 40, 2588-2594 (1964).

(93) J. Czekalla, Z. Elektrochem., 63, 1157-1163 (1959).

(94) J. Stanley, D. Smith, B. Latimer, and J. P. Devlin, J. Phys. Chem., 70, 2011-2016 (1966).

(95) M. M. Labes, R. Sehr, and M. Bose, J. Chem. Phys., 33, 868-872 (1960).

(96) B. Hall and J. P. Devlin, J. Phys. Chem., 71, 465-466 (1967).

(97) R. Foster, D. L. Hammick, and P. J. Placito, J. Chem. Soc., 1956, 3881-3887.

(98) H. Offen and T. T. Nakashima, J. Chem. Phys., 47, 4446-4450 (1967).

(99) H. Kainer and W. Otting, Chem. Ber., 88, 1921-1931 (1955).

(100) K. M. C. Davis and M. C. R. Symons, J. Chem. Soc., 1965, 2079-2083.

(101) K. Nakamoto, J. Am. Chem. Soc., 74, 1739-1742 (1952).

(102) D. R. Stephens and H. G. Drickamer, J. Chem. Phys., 30, 1518-1520 (1959).

(103) T. T. Harding and S. C. Wallwork, Acta Cryst., 8, 787-794 (1955).

(104) N. D. Jones and R. E. Marsh, Acta Cryst., 15, 809-810 (1962).

(105) S. C. Wallwork and T. T. Harding, Acta Cryst., 15, 810 (1962).

(106) R. Foster, J. Chem. Soc., 1960, 1075-1077.

(107) D. D. Eley, H. Inokuchi, and M. R. Willis, Discussions Faraday Soc., 28, 54-63 (1959).

(108) D. C. Mukherjee and A. K. Chandra, J. Phys. Chem., 68, 477-480 (1964).

(109) H. Kuroda, K. Yoshihara, and H. Akamatu, Bull. Chem. Soc. Japan, 35, 1604-1608 (1962).

(110) R. Foster and D. L. Hammick, J. Chem. Soc., 1954, 2685-2692.

(111) R. Foster and I. Horman, J. Chem. Soc. (B), 1966, 171-173.

(112) M. Peover, Trans. Faraday Soc., 58, 1656-1660 (1962).

(113) A. Ottenberg, R. L. Brandon, and M. E. Browne, Nature, 201, 1119-1120 (1964).

(114) D. S. Acker, R. J. Harder, W. R. Hertler, W. Mahler, L. R. Melby, R. E. Benson, and W. E. Mochel, J. Am. Chem. Soc., 82, 6408-6409 (1960).

(115) L. R. Melby, R. J. Harder, W. R. Hertler, W. Mahler, R. E. Benson, and W. E. Mochel, J. Am. Chem. Soc., 84, 3374-3387 (1962).

(116) D. S. Acker and D. C. Blomstrom, U. S. Patent No. 3,162,641 (1964).

(117) H. Kuroda, I. Ikemoto, and H. Akamatu, Bull. Chem. Soc. Japan, 39, 1842-1849 (1966).

(118) H. Kuroda, T. Kunii, S. Hiroma, and H. Akamatu, J. Mol. Spectry., 22, 60-75 (1967).

(119) H. Kuroda and H. Akamatu, J. Chem. Phys., 40, 3748-3749 (1964).

(120) H. Akamatu and H. Kuroda, J. Chem. Phys., 39, 3364-3368 (1963).

(121) H. Kuroda, I. Ikemoto, and H. Akamatu, Bull. Chem. Soc. Japan, 39, 547-551 (1966).

(122) S. C. Chu, G. A. Jeffrey, and (in part) T. Sakurai, Acta Cryst., 15, 661-671 (1962).

(123) V. A. Benderskii, L. A. Blyumenfeld, I. B. Shevchenko, and T. S. Altshuler, Sov. Physics-Solid State (English Transl.), 6, 1206-1208 (1964).

(124) A. Szent-Györgyi, "Introduction to a Submolecular Biology" (Academic Press, Inc., New York, 1960).

(125) Y. Matsunaga, Nature, 205, 72-73 (1965)

(126) G. Kortüm and W. Braun, Z. Physik. Chem. (Frankfurt), 18, 242-254 (1958).

(127) R. M. Williams and S. C. Wallwork, Acta Cryst., B24, 168-174 (1968).

(128) S. K. Lower, R. M. Hochstrasser, and C. Reid, Mol. Phys., 4, 161-168 (1961).

(129) K. Nakamoto, Bull. Chem. Soc. Japan, 26, 70-72 (1953).

(130) H. W. Offen, J. Chem. Phys., 42, 430-434 (1965).

(131) D. S. Brown, S. C. Wallwork, and (in part) A. Wilson, Acta Cryst., 17, 168-176 (1964).

(132) H. Inokuchi, K. Ikeda, and H. Akamatu, Bull. Chem. Soc. Japan, 33, 1622-1624 (1960).

(133) G. Briegleb and J. Czekalla, Z. Elektrochem., 58, 249-263 (1954).

(134) J. M. Corkill, R. Foster, and D. L. Hammick, J. Chem. Soc., 1955, 1202-1208.

(135) J. J. André and G. Weill, Compt. Rend., 262, 1413-1416 (1966).

(136) J. W. Eastman, G. M. Androes, and M. Calvin, J. Chem. Phys., 36, 1197-1208 (1962).

(137) M. Schwartz, H. W. Davies, and B. J. Dobriansky, J. Chem. Phys., 40, 3257-3259 (1964).

(138) M. M. Labes, R. A. Sehr, and M. Bose, Proc. Intern. Conf. Semicond. Phys. (Prague, 1960), pp. 850-853.

(139) R. M. Metzger, unpublished results (1966).

(140) C. J. Fritchie, Jr., Proc. Amer. Cryst. Assoc. Meeting, Atlanta, Ga., January, 1967, page 50.

(141) H. Scott, P. L. Kronick, P. Chairge, and M. M. Labes, J. Phys. Chem., 69, 1740-1742 (1965).

(142) Y. Matsunaga, Nature, 211, 183-184 (1966).

(143) P. L. Kronick and M. M. Labes, J. Chem. Phys., 40, 890-894 (1961).

(144) L. R. Melby, Can. J. Chem., 43, 1448-1453 (1965).

(145) C. J. Fritchie, Jr., Acta Cryst., 20, 892-898 (1966).

(146) H. Kusakawa and S.-I. Nishizaki, Bull. Chem. Soc. Japan, 38, 2201-2202 (1965).

(147) J. Osiecki, Nature, 198, 85-86 (1963).

(148) D. Bijl, H. Kainer, and A. C. Rose-Innes, J. Chem. Phys., 30, 765-770 (1959).

(149) H. Kainer, D. Bijl, and A. C. Rose-Innes, Naturwissenschaften, 41, 303-304 (1954).

(150) A. Ottenberg, C. J. Hoffman, and J. Osiecki, J. Chem. Phys., 38, 1898-1906 (1963)

(151) V. A. Benderskii, I. B. Shevchenko, and L. A. Blyumenfeld, Opt. Spectry. USSR (Engl. Transl.), 16, 254-258 (1964).

(152) M. M. Labes, R. Sehr, and M. Bose, J. Chem. Phys., 32, 1570-1572 (1960).

(153) Y. Matsunaga and C. A. McDowell, Nature, 185, 916-917 (1960).

(154) M. Bose and M. M. Labes, J. Am. Chem. Soc., 83, 4505-4508 (1964).

(155) M. E. Browne, A. Ottenberg, and R. L. Brandon, J. Chem. Phys., 41, 3265-3266 (1964).

(156) P. Ackermann, J.-P. Faucher, and H. Robert, Compt. rend. 263B, 272-275 (1966).

(157) R. C. Hughes, private communication (Feb. 1967).

(158) H. Kainer and A. Ueberle, Chem. Ber., 88, 1147-1157 (1955).

(159) M. Kinoshita and H. Akamatu, Nature, 207, 291-292 (1965).

(160) A. W. Hanson, Acta Cryst., 19, 610-613 (1965).

(161) A. Redoch, private communication to I. C. Smith (1966).

(162) A. W. Hanson, Acta Cryst., B24, 768-778 (1968).

(163) Ref. (4), page 50, footnote 7: the work in question apparently was never published.

(164) B. G. Anex and E. B. Hill, J. Am. Chem. Soc., 88, 3648-3650 (1966).

(165) R. Foster and T. J. Thomson, Trans. Faraday Soc., 59, 2287-2295 (1963).

(166) S. Iwata, H. Tsubomura, and S. Nagakura, Bull. Chem. Soc. Japan, 37, 1506-1508 (1964).

(167) Z. G. Soos and H. M. McConnell, J. Chem. Phys., 43, 3780-3794 (1965).

(168) H. M. McConnell and Z. G. Soos, J. Chem. Phys., 40, 586-588 (1964).

(169) F. Bertaut, J. Phys. Radium, 13, 499-503 (1952).

(170) G. Leibfried, "Mechanische und thermische Eigenschaften der Kristalle", Ziff. 26, pages 132-138 in S. Flügge, Ed., "Handbuch der Physik", 2nd Ed., Volume VII, Part I (Springer-Verlag, Berlin, 1955).

(171) C. Kittel, "Introduction to Solid-State Physics", 2nd Edition (J. Wiley & Sons, Inc., New York, 1956), pp. 571-574.

(172) M. Born and K. Huang, "Dynamical Theory of Crystal Lattices" (Oxford University Press, Oxford, 1954), p. 3 and pp. 385-387.

(173) J. M. Ziman, "Principles of the Theory of Solids", (Cambridge University Press, Cambridge, 1964), pp. 39-41.

(174) "International Tables for X-ray Crystallography", N. F. M. Henry and K. Lonsdale, Editors (Kynoch Press, Birmingham, 1952).

(175) "Real Error Function", Stanford University Computation Center Library Program No. 4, ALGOL REAL PROCEDURE, Certified by L. Teijelo and revised 14 October 1966 by B. Davis; implemented from M. Crawford and R. Techo, Comm. Assoc. Computing Machinery, 5, 483 (1962).

(176) E. Madelung, Physik. Z., 19, 524-535 (1918).

(177) H. M. Evjen, Phys. Rev., 39, 675-687 (1932).

(178) R. E. Jones and D. H. Templeton, J. Chem. Phys., 25, 1062-1063 (1956).

(179) P. P. Ewald, Ann. der Physik, 64, 253-287 (1921).

(180) J. R. Hoyland and L. Goodman, J. Chem. Phys., 34, 1446-1447 (1961).

(181) T. Amos and L. C. Snyder, J. Chem. Phys., 41, 1773-1783 (1964).

(182) A. D. McLachlan, Mol. Phys., 1, 233-240 (1958).

(183) H. J. Monkhorst and J. Kommandeur, J. Chem. Phys., 47, 391-395 (1967).

(184) J. Bolton, A. Carrington, and J. dos Santos-Veiga, Mol. Phys., 5, 615-619 (1962).

(185) G. Giacometti, P. L. Nordio, and G. Rigatti, Nuovo Cimento, 23, 433-439 (1962).

(186) M. T. Melchior and A. H. Maki, J. Chem. Phys., 34, 471-476 (1961).

(187) J. R. Hoyland and L. Goodman, J. Chem. Phys., 36, 12-20 (1962).

(188) J. R. Bolton, A. Carrington, and J. dos Santos-Veiga, Mol. Phys., 5, 465-473 (1962).

(189) P. H. Rieger and G. K. Fraenkel, J. Chem. Phys., 37, 2795-2810 (1962).

(190) L. Pauling, "The Nature of the Chemical Bond", 3rd Edition (Cornell University Press, Ithaca, N. Y., 1960), pp. 321-322.

(191) H. J. Monkhorst, G. T. Pott, and J. Kommandeur, J. Chem. Phys., 47, 401-407 (1967).

(192) M. Broze, Z. Luz, and B. L. Silver, J. Chem. Phys., 46, 4891-4902 (1967).

(193) D. A. Lowitz, J. Chem. Phys., 46, 4698-4717 (1967).

(194) E. Menefee and Y.-H. Pao, J. Chem. Phys., 36, 3472-3481 (1962).

(195) R. C. West, Editor-in-Chief, "Handbook of Chemistry and Physics", 47th Edition, 1966-67, page F138; source: National Bureau of Standards Technical News Bulletin, October, 1963.

(196) T. Batuecas, Nature, 173, 345-346 (1954).

(197) Sir L. Bragg and G. F. Claringbull, "Crystal Structures of Minerals" (Vol. IV of "The Crystalline State", Sir L. Bragg, Ed.) (Cornell University Press, Ithaca, N. Y., 1965), p. 38.

(198) Q. C. Johnson and D. H. Templeton, J. Chem. Phys., 34, 2004-2007 (1961).

(199) D. H. Templeton and G. F. Carter, J. Phys. Chem., 58, 940-944 (1954).

(200) J. D. Turner and A. C. Albrecht, "The Crystal Structure of Wurster's Blue Perchlorate" (unpublished, September, 1954).

(201) J. L. de Boer, A. Vos, and K. Huml, Acta Cryst., B24, 542-549 (1968).

(202) J. Sherman, Chem. Rev., 11, 93-170 (1932).

(203) Y. Sakamoto, J. Chem. Phys., 28, 164-165 (1958).

(204) P. M. de Wolff and L. Walter-Lévy, Acta Cryst., 6, 40-44 (1953).

(205) A. Kawamori, A. Honda, N. Joo, K. Suzuki, and Y. Ooshika, J. Chem. Phys., 44, 4363 (1966).

(206) K. Uemura, S. Nakayama, Y. Seo, K. Suzuki, and Y. Ooshika, Bull. Chem. Soc. Japan, 39, 1348 (1966).

(207) G. T. Pott and J. Kommandeur, J. Chem. Phys., 47, 395-401 (1967).

(208) G. T. Pott, C. F. van Bruggen, and J. Kommandeur, J. Chem. Phys., 47, 408-413 (1967).

(209) Z. G. Soos and R. C. Hughes, J. Chem. Phys., 46, 253-259 (1967).

(210) G. R. Anderson, J. Chem. Phys., 47, 3853-3860 (1967).

(211) R. H. Young, private communication (September, 1967)

(212) D. D. Thomas, H. Keller, and H. M. McConnell, J. Chem. Phys., 39, 2321-2329 (1963).

(213) H. Chihara, M. Nakamura, and S. Seki, Bull. Chem. Soc. Japan, 38, 1776-1778 (1965).

(214) R. C. Hughes, A. W. Merkl, and H. M. McConnell, J. Chem. Phys., 44, 1720-1721 (1966).

(215) K. H. Hausser and J. N. Murrell, J. Chem. Phys., 27, 500-504 (1957).

(216) D. B. Chesnut, J. Chem. Phys., 40, 405-411 (1964).

(217) N. Davidson, "Statistical Mechanics" (McGraw-Hill Book Co., New York, 1962).

(218) D. Cubicciotti, to be published (March, 1968).

(219) B. Aurivillius, Acta Chem. Scand., 9, 1206-1208 (1955).

(220) A. Zalkin and D. H. Templeton, J. Am. Chem. Soc., 75, 2453-2458 (1953).

(221) H. J. Silverstone, J. Chem. Phys., 45, 4337-4341 (1966).

(222) H. J. Silverstone, J. Chem. Phys., 46, 4368-4376 (1967).

(223) H. J. Silverstone, J. Chem. Phys., 46, 4377-4380 (1967).

(224) H. J. Silverstone, J. Chem. Phys., 47, 537-540 (1967).

(225) H. J. Silverstone, Proc. Natl. Acad. Sci. U.S., 58, 34-36 (1967).

(226) F. Bloch, Z. Physik, 52, 555-600 (1928).

(227) cf. e.g. Ref. (171), pp. 586-587; Ref. (173), pp. 80-85; J. M. Ziman, "Electrons and Phonons", (Oxford University Press, Oxford, 1960), pp. 82-85.

(228) cf. e.g. E. P. Wigner, "Group Theory and Its Applications to the Quantum Mechanics of Atomic Spectra" (Academic Press, New York, 1959), p. 28.

(229) P.-O. Löwdin, J. Chem. Phys., 18, 365-375 (1950).

(230) R. H. Young, private communication (May, 1968).

(231) S. A. Hagstrom, private communication (May, 1968).

(232) R. A. Nijboer and F. W. de Wette, Physica, 23, 309-321 (1957).

(233) E. U. Condon and G. H. Shortley, "The Theory of Atomic Spectra", (Cambridge University Press, Cambridge, 1963).

(234) A. Messiah, "Quantum Mechanics", Vol. II (North-Holland Publishing Co., Amsterdam, 1962), pp. 1068-1075.

(235) A. Messiah, "Quantum Mechanics", Vol. I (North-Holland Publishing Co., Amsterdam, 1961), p. 497.

(236) "Handbook of Mathematical Functions", M. Abramowitz and I. Stegun, Editors (National Bureau of Standards, Appl. Math. Ser. No. 55, Washington, 1964), p. 230, Eq. (5.1.26).

(237) I. S. Gradshteyn and I. M. Ryzhik, "Tables of Integrals, Series, and Products", (Engl. Transl.) (Academic Press, N. Y., 1965), p. 337, Eq. (3.462-1); p. 1064, Eq. (9.240); see also p. 496, Eq. (3.953-1).

(238) Ref. (236), p. 504, Eq. (13.1.2).

(239) J. Czekalla, A. Schmillen, and K. J. Mager, Z. Elektrochem., 63, 623-626 (1959).

(240) B. R. Hamilton and D. L. Hammick, J. Chem. Soc., 1938, 1350-1352.

(241) J. R. Gott and W. G. Maisch, J. Chem. Phys., 39, 2229-2235 (1963).

(242) M. E. Peover, Trans. Faraday Soc., 60, 479-483 (1964).

(243) M. E. Peover and J. D. Davies, Trans. Faraday Soc., 60, 476-478 (1964).

(244) R. A. Bennett and H. O. Hooper, J. Chem. Phys., 47, 4855-4856 (1967).

(245) R. Foster, Tetrahedron, 10, 96-101 (1960).

(246) P. R. Hammond, J. Chem. Soc., 1963, 3113-3118.

(247) R. M. Hochstrasser, S. K. Lower, and C. Reid, J. Mol. Spectry., 15, 257-263 (1965).

(248) R. M. Hochstrasser, S. K. Lower, and C. Reid, J. Chem. Phys., 41, 1073-1078 (1964).

(249) J. Tanaka and K. Yoshihara, Bull. Chem. Soc. Japan, 38, 739-745 (1965).

(250) B. Chakrabarti and S. Basu, J. Chim. Phys., 65, 1006-1008 (1968).

(251) H. J. Silverstone, private communication (20 August 1968).

ABSTRACT OF PROPOSITIONS

PROPOSITION I - LATTICE SUMS FOR CLASSICAL MULTIPOLE INTERACTIONS, AND APPLICATIONS TO ORGANIC DONOR-ACCEPTOR CRYSTALS

The Ewald technique for calculating Coulomb interactions between electrical charges in crystals can be extended by explicit differentiations to calculate multipole interactions in crystals (Ewald-Kornfeld method). Explicit computer calculations are suggested to test Kommandeur and Pott's molionic lattice model for (1:1)-(Tetramethyl-para-phenylenediamine:para-Chloranil).

PROPOSITION II - X-RAY CRYSTALLOGRAPHY OF DONOR-ACCEPTOR CRYSTALS

Four crystallographic problems related to McConnell's classification of organic donor-acceptor (DA) crystals are discussed: (i) a reinterpretation or redetermination of de Boer and Vos' structure for (1:1)-(N,N,N',N'-Tetramethyl-para-phenylenediamine:para-Chloranil); (ii) the formal fractional charge on the atoms of a DA crystal, and its possible effect on the calculated structure factors; (iii) current work on (1:1)-(Chlorpromazine: 7,7,8,8-Tetracyanoquinodimethan); (iv) a possible phase transition in (1:1)-(para-Phenylenediamine:para-Chloranil).

PROPOSITION III - THE PHASE TRANSITION AND CHANGES IN THE FINE-STRUCTURE SPLITTINGS OF A FRENKEL TRIPLET SPIN EXCITON CRYSTAL: A HIGH-PRESSURE, LOW-TEMPERATURE, HIGH-FIELD ELECTRON PARAMAGNETIC RESONANCE STUDY OF THE ION-RADICAL SALT TRIPHENYLMETHYLARSONIUM $(TCNQ)_2^-$

An abortive attempt was made to measure the changes in the D and E splittings in Triphenylmethylarsonium $(TCNQ)_2^-$ at 130°K and 144°K across the phase transition, using a high-pressure bomb with a hybrid helix resonator in place of the EPR resonant cavity. The changes in D,E could help describe the nature of the transition and the changes in the spin system. Improvements in the experiment are suggested.

PROPOSITION IV - SEARCH FOR QUARKS IN SEA-WATER: THE USE OF ION-EXCHANGE COLUMNS

High-energy physicists have been searching in vain for the quarks, three hypothetical massive long-lived elementary particles carrying a fraction of the electronic charge. Their search for quarks in sea-water could be made more efficient by the use of ion-exchange chromatography.

PROPOSITION V - SOLUTION DIMERS OF ORGANIC DONOR CATIONS AND OF ACCEPTOR ANIONS. THE BENZIDINE REARRANGEMENT REVISITED

The cations of the donors, para-Phenylenediamine, N,N-Dimethyl-para-phenylenediamine, N,N,N',N'-Tetramethyl-para-phenylenediamine, Diaminodurene, and the anion of the acceptor: 7,7,8,8-Tetracyanoquinodimethan, are known to dimerize in polar solutions. A theoretical calculation for these exchange-bound dimers is suggested to explain their stability and their correlation with the crystalline ion-radical salts. The caged-radical transition state theory for the benzidine rearrangement is closely related to these dimers, but lacks experimental proof; EPR experiments on the rearrangements of specially selected hydrazobenzenes may help determine the plausibility of this theory.

PROPOSITION I

LATTICE SUMS FOR CLASSICAL MULTIPOLE INTERACTIONS, AND APPLICATIONS TO ORGANIC DONOR-ACCEPTOR CRYSTALS

A. Introduction

A complete classical calculation of the Coulomb binding energy of a crystal would have to include not only the Madelung energy due to monopole-monopole interactions between point charges, but also the lattice energy due to all the multipole interactions between the diffuse charge distributions.

Multipole interaction energies involve higher powers of the reciprocal interatomic distance, and hence their calculation for a crystal will converge more rapidly than the Madelung energy. It is of some formal interest, however, to show how the Ewald fast-convergence scheme utilized in this Thesis can be adapted to multipole calculations. The mathematical sketch developed below can make no claim to originality, and is given only for didactic completeness. It is the object of this proposition to suggest that thanks to digital computers such multipole calculations can be performed to obtain "better" values for the binding energies of organic donor-acceptor crystals insofar as that is possible within a classical framework (i.e. neglecting overlap and exchange); in particular, we propose that a rigorous test be performed of Kommandeur and Pott's assertion (1) that the interactions due to the induced electric dipoles are very important in "molionic" lattices of organic donor-acceptor (DA) crystals.

As mentioned in Chapter I, Kommandeur and Pott suggested that, because of multipole effects, organic DA complexes may crystallize in molionic lattices, i.e. lattices of mixed ionic and neutral species. This suggestion is in direct opposition to the predictions of McConnell et al. (2), which, however, are based on monopole-monopole interactions. A schematic calculation was performed by Kommandeur and Pott, presumably by the Evjen method (3), for a highly idealized cubic lattice consisting of two interpenetrating sublattices: sublattice A contains an ordinary array of sodium ions and chloride ions, at twice the ordinary interionic separations; sublattice B is a molecular array of neutral sodium atoms and chlorine atoms. The DA crystals are presumed by Kommandeur and Pott to consist of similar, if random, alternations of neutral and ionic species. In a later experimental effort Pott and Kommandeur (4) presented evidence that (1:1)-(N,N,N',N'-Tetramethyl-para-phenylenediamine:para-Chloranil) (TMPD:pChl) is a molionic crystal, with statistical disproportionation into $TMPD^{++}$, $pChl^{--}$, TMPD, and pChl; exact disproportionation was not claimed either by Pott and Kommandeur or in the later crystallographic study by deBoer and Vos (5); the spectroscopic evidence for such a classification has been dismissed in Chapter I; the crystallographic evidence is discussed in Proposition II. A thoroughgoing numerical calculation on a molionic lattice model of (TMPD:pChl) would settle Kommandeur and Pott's claims conclusively.

The Evjen method is obviously unsuitable for Coulomb calculations in organic crystals, but we shall show that the same reasons that made the Ewald method so convenient for the calculations of monopole interactions described in Chapter II will make the Ewald-Kornfeld method ideal for calculations of multipole interactions in organic crystals.

B. Multipole Expansion of the Classical Coulomb Binding Energy

We review briefly the derivation of the multipole expansion of the molar crystal Coulomb energy due to Coulomb interactions between arbitrary non-overlapping charge distributions. As in Chapter II, assume that there are M atoms per crystallographic unit cell, and N_o/Z unit cells per mole (where N_o is Avogadro's number). After setting an arbitrary origin for a Cartesian coordinate system $\{\vec{e}_x, \vec{e}_y, \vec{e}_z\}$ (see Eq. (262) of Chapter II) somewhere in the zeroth unit cell, assume that $\underset{\sim}{r}_i^o \equiv x_{i1}\vec{e}_x + x_{i2}\vec{e}_y + x_{i3}\vec{e}_z$ denotes the i-th atomic position ($i = 1, 2, \ldots, M\,N_o/Z$), which is the center for a charge distribution ρ_i; the elements of charge $\Delta\rho_i$ can be described by a (source) vector $\underset{\sim}{\xi} \equiv x_1'\vec{e}_x + x_2'\vec{e}_y + x_3'\vec{e}_z$. Let $\underset{\sim}{r}_j^o \equiv x_{j1}\vec{e}_x + x_{j2}\vec{e}_y + x_{j3}\vec{e}_z$ denote the center for a different distribution ρ_j; the charge element $\Delta\rho_j$ can be described by the (field) vector $\underset{\sim}{R} \equiv x_1\vec{e}_x + x_2\vec{e}_y + x_3\vec{e}_z$. The vectors $\underset{\sim}{\xi}_i \equiv \underset{\sim}{\xi} - \underset{\sim}{r}_i^o$, $\underset{\sim}{R}_j \equiv \underset{\sim}{R} - \underset{\sim}{r}_j^o$, and $\underset{\sim}{r}_{ij}^o \equiv \underset{\sim}{r}_j^o - \underset{\sim}{r}_i^o$

have Cartesian components $y'_{i\alpha}$, $y_{j\alpha}$, and x^{ij}_{α} ($\alpha = 1, 2, 3$) respectively. Let us adopt the Einstein summation convention: repeated Greek subscripts in any term imply summation over those subscripts (in our case, always from 1 to 3). The electrostatic energy due to the Coulomb interactions between ρ_i and ρ_j is given by:

$$\text{(I-1a)} \qquad W_{ij} \equiv \iiint dv(\underset{\sim}{R})\rho_j(\underset{\sim}{R}) \iiint dv(\underset{\sim}{\xi})\rho_i(\underset{\sim}{\xi}) \left|\underset{\sim}{R} - \underset{\sim}{\xi}\right|^{-1} =$$

$$\text{(I-1b)} \qquad = \iiint dv(\underset{\sim}{R}_j)\rho_j(\underset{\sim}{R}_j) \iiint dv(\underset{\sim}{\xi}_i)\rho_i(\underset{\sim}{\xi}_i) \left|\underset{\sim}{R}_j - \underset{\sim}{\xi}_i + \underset{\sim}{r}^{\circ}_{ij}\right|^{-1};$$

where the domains of integration are the whole crystal and the zero of energy is assumed to be for infinite distance between ρ_i and ρ_j. The integral over $\underset{\sim}{\xi}_i$ is the scalar potential $\varphi_i(\underset{\sim}{R}_j + \underset{\sim}{r}^{\circ}_{ij})$ due to ρ_i. Let a be the limiting dimension of the bounded distribution of ρ_i: if $\underset{\sim}{R}_j$ is so large that $a/\left|\underset{\sim}{R}_j - \underset{\sim}{\xi}_i + \underset{\sim}{r}^{\circ}_{ij}\right| \ll 1$, then we can expand $\left|\underset{\sim}{R}_j - \underset{\sim}{\xi}_i + \underset{\sim}{r}^{\circ}_{ij}\right|^{-1}$ as a Taylor series about $\underset{\sim}{r}^{\circ}_{i}$:

$$\text{(I-2)} \qquad \begin{aligned} \frac{1}{\left|\underset{\sim}{R}_j - \underset{\sim}{\xi}_i + \underset{\sim}{r}^{\circ}_{ij}\right|} &= \frac{1}{\left|\underset{\sim}{R}_j + \underset{\sim}{r}^{\circ}_{ij}\right|} + \frac{y'_{i\alpha}}{1!}\left[\frac{\partial}{\partial y'_{i\alpha}}\frac{1}{|\underset{\sim}{r}|}\right]_{\underset{\sim}{r} = \underset{\sim}{R}_j + \underset{\sim}{r}^{\circ}_{ij}} + \\ &+ \frac{y'_{i\alpha}y'_{i\beta}}{2!}\left[\frac{\partial^2}{\partial y'_{i\alpha}\partial y'_{i\beta}}\frac{1}{|\underset{\sim}{r}|}\right]_{\underset{\sim}{r} = \underset{\sim}{R}_j + \underset{\sim}{r}^{\circ}_{ij}} + \dots + \\ &+ \frac{1}{p!}\, y'_{i\alpha}y'_{i\beta}\cdots y'_{i\pi}\left[\frac{\partial^p}{\partial y'_{i\alpha}\partial y'_{i\beta}\cdots\partial y'_{i\pi}}\frac{1}{|\underset{\sim}{r}|}\right]_{\underset{\sim}{r} = \underset{\sim}{R}_j + \underset{\sim}{r}^{\circ}_{ij}} + \dots \end{aligned}$$

Let us define the 2^p-pole (multipole of order p) of the charge distribution ρ_i as a symmetric tensor of rank p and dimension 3, by writing its general Cartesian component:

$$\text{(I-3a)} \quad M^p_{i\alpha\beta\ldots\pi} \equiv \iiint dv(\underset{\sim}{\xi})\, x'_\alpha x'_\beta \ldots x'_\pi \rho_i(\underset{\sim}{\xi}) =$$

$$\text{(I-3b)} \quad = \iiint dv(\underset{\sim}{\xi}_i)\, y'_{i\alpha} y'_{i\beta} \cdots y'_{i\pi} \rho_i(\underset{\sim}{\xi}_i),$$

where there are p Greek subscripts. If p = 0 then $M^0_i \equiv Z_i$ is the charge or monopole moment; if p = 1 then $M^1_{i\alpha} \equiv D_{i\alpha}$ is the dipole moment; if p = 2 then $M^2_{i\alpha\beta} \equiv Q_{i\alpha\beta}$ is the quadrupole moment; if p = 3 then $M^3_{i\alpha\beta\gamma} \equiv \emptyset_{i\alpha\beta\gamma}$ is the octupole moment; if p = 4 then $M^4_{i\alpha\beta\gamma\epsilon} \equiv H_{i\alpha\beta\gamma\epsilon}$ is the sedecupole (hexakaidecupole?) moment. For any function $g(|\underset{\sim}{R}_j - \underset{\sim}{\xi}_i + \underset{\sim}{r}^0_{ij}|)$ it can be shown that:

$$\text{(I-4)} \quad \frac{\partial g}{\partial y'_{i\alpha}} = -\frac{\partial g}{\partial y_{j\alpha}}.$$

Using Eqs. (I-1b, I-2, I-3b, I-4) we obtain for the potential:

$$\text{(I-5)} \quad \varphi_i(\underset{\sim}{R}_j + \underset{\sim}{r}^0_{ij}) = \sum_{p=0}^{\infty} \frac{(-1)^p}{p!} M^p_{i\alpha\beta\ldots\pi} \left[\frac{\partial^p}{\partial y_{j\alpha} \partial y_{j\beta} \ldots \partial y_{j\pi}} \frac{1}{|\underset{\sim}{r}|} \right]_{\underset{\sim}{r} = \underset{\sim}{R}_j + \underset{\sim}{r}^0_{ij}} .$$

If $\varphi_i(\underset{\sim}{R}_j + \underset{\sim}{r}^o_{ij})$ is a slowly varying function over the region where $\rho_j(\underset{\sim}{R}_j)$ is non-negligible, then we may expand it in a Taylor series around $\underset{\sim}{r}^o_j$, the center of ρ_j:

$$\text{(I-6)}\quad \varphi_i\left(\underset{\sim}{R}_j + \underset{\sim}{r}^o_{ij}\right) = \sum_{q=0}^{\infty} \frac{1}{q!} y_{j\alpha} y_{j\beta} \cdots y_{j\sigma} \left[\frac{\partial^q}{\partial y_{j\alpha} \partial y_{j\beta} \cdots \partial y_{j\sigma}} \phi_i\left(\underset{\sim}{R}\right)\right]_{\underset{\sim}{R}=\underset{\sim}{r}^o_j} .$$

If we also define multipole moments for ρ_j by:

$$\text{(I-7)}\qquad M^{q}_{j\alpha\beta\ldots\sigma} \equiv \iiint d\tau\left(\underset{\sim}{R}_j\right) y_{j\alpha} y_{j\beta} \cdots y_{j\sigma} \rho_j\left(\underset{\sim}{R}_j\right),$$

then we obtain finally:

$$\text{(I-8)}\quad \begin{aligned} W_{ij} \equiv \sum_{p=0}^{\infty} W^p_{ij} &= \sum_{p=0}^{\infty} (-1)^p \sum_{q=0}^{p} \frac{(-1)^q}{q!\,(p-q)!} M^{p-q}_{i\alpha\beta\ldots\lambda} \times \\ &\times M^{q}_{j\mu\nu\ldots\pi} \left[\frac{\partial^p}{\partial y_{j\alpha} \partial y_{j\beta} \cdots \partial y_{j\lambda} \partial y_{j\mu} \partial y_{j\nu} \cdots \partial y_{j\pi}} \frac{1}{|\underset{\sim}{r}|}\right]_{\underset{\sim}{r}=\underset{\sim}{r}^o_{ij}} , \end{aligned}$$

or in greater detail:

$$\text{(I-9)}\quad \begin{aligned} W_{ij} = \frac{Z_i Z_j}{|\underset{\sim}{r}^o_{ij}|} &+ \left\{Z_i D_{j\alpha} - Z_j D_{i\alpha}\right\}\left[-\frac{x^{ij}_\alpha}{|\underset{\sim}{r}^o_{ij}|^3}\right] + \\ &+ \left\{\frac{1}{2}\left(Z_i Q_{j\alpha\beta} - Q_{i\alpha\beta} Z_j\right) - D_{i\alpha} D_{j\beta}\right\}\left[-\frac{\delta_{\alpha\beta}}{|\underset{\sim}{r}^o_{ij}|^3} + \frac{3 x^{ij}_\alpha x^{ij}_\beta}{|\underset{\sim}{r}^o_{ij}|^5}\right] + \end{aligned}$$

$$+\left\{\frac{1}{6}\left(Z_i\,\phi_{j\alpha\beta\gamma}-\phi_{i\alpha\beta\gamma}\,Z_j\right)-\frac{1}{2}\left(D_{i\alpha}\,Q_{j\beta\gamma}-Q_{i\alpha\beta}\,D_{j\gamma}\right)\right\}\times$$

$$\times\left[\frac{3}{|\underset{\sim}{r}^{\circ}_{ij}|^5}\left(\delta_{\alpha\beta}x^{ij}_{\gamma}+\delta_{\beta\gamma}x^{ij}_{\alpha}+\delta_{\gamma\alpha}x^{ij}_{\beta}\right)-\frac{15}{|\underset{\sim}{r}^{\circ}_{ij}|^7}\,x^{ij}_{\alpha}x^{ij}_{\beta}x^{ij}_{\gamma}\right]+$$

$$+\left\{\frac{1}{24}\left(Z_i\,H_{j\alpha\beta\gamma\epsilon}+H_{i\alpha\beta\gamma\epsilon}\,Z_j\right)-\frac{1}{6}\left(D_{i\alpha}\,\phi_{j\beta\gamma\epsilon}+\phi_{i\alpha\beta\gamma}\,D_{j\epsilon}\right)+\right.$$

$$\left.+\frac{1}{4}Q_{i\alpha\beta}\,Q_{j\gamma\epsilon}\right\}\left[\frac{3}{|\underset{\sim}{r}^{\circ}_{ij}|^5}\left(\delta_{\alpha\beta}\delta_{\gamma\epsilon}+\delta_{\beta\gamma}\delta_{\epsilon\alpha}+\delta_{\gamma\alpha}\delta_{\beta\epsilon}\right)-\right.$$

$$-\frac{15}{|\underset{\sim}{r}^{\circ}_{ij}|^7}\left(\delta_{\epsilon\alpha}x^{ij}_{\beta}x^{ij}_{\gamma}+\delta_{\beta\epsilon}x^{ij}_{\alpha}x^{ij}_{\gamma}+\delta_{\gamma\epsilon}x^{ij}_{\alpha}x^{ij}_{\beta}+\delta_{\alpha\beta}x^{ij}_{\gamma}x^{ij}_{\epsilon}+\right.$$

$$\left.\left.+\delta_{\beta\gamma}x^{ij}_{\alpha}x^{ij}_{\epsilon}+\delta_{\gamma\alpha}x^{ij}_{\beta}x^{ij}_{\epsilon}\right)+\frac{105}{|\underset{\sim}{r}^{\circ}_{ij}|^9}\,x^{ij}_{\alpha}x^{ij}_{\beta}x^{ij}_{\gamma}x^{ij}_{\epsilon}\right]+\dots$$

where e.g. $\delta_{\alpha\beta}$ is a Kronecker delta. The total molar Coulomb interaction energy, after we invoke the periodicity of the lattice (or three-dimensional Born-von Kármán periodic boundaries on a unimolar crystal) becomes:

(I-10)
$$W_{TOT}=\frac{N_0}{2Z}\sum_{m=1}^{M}\sum_{\substack{j=1\\ m\neq j}}^{M\frac{N_0}{Z}}W_{mj}$$

and by using the lattice translation:

$$\underset{\sim}{r}_{\underline{\delta}} \equiv \underset{\sim}{r}_{dfg} \equiv d\underset{\sim}{a} + f\underset{\sim}{b} + g\underset{\sim}{c} \quad \left\{ \underline{\delta} = 0,1,2,\ldots,\tfrac{N_0}{Z}-1;\ -\tfrac{1}{2}\left[\left(\tfrac{N_0}{Z}\right)^{1/3}-1\right] \leq d,f,g \leq \tfrac{1}{2}\left[\left(\tfrac{N_0}{Z}\right)^{1/3}-1\right] \right\}$$

given by Eqs. (265, 266) of Chapter II, we obtain:

(I-11)

$$W_{TOT} = \frac{N_0}{2Z} \underbrace{\sum_{m=1}^{M} \sum_{n=1}^{M}}_{\boxed{\text{if } \underline{\delta}=0 \text{ then } m \neq n}} \sum_{p=0}^{\infty} \sum_{q=0}^{p} \frac{(-1)^{p+q}}{q!\,(p-q)!} M^{p-q}_{m\alpha\beta\ldots\lambda} \times$$

$$\times M^{q}_{n\mu\nu\ldots\pi} \sum_{\underline{\delta}=0}^{N_0/Z-1} \left[\frac{\partial^p}{\partial x_\alpha \partial x_\beta \ldots \partial x_\pi} \frac{1}{|\underset{\sim}{r}|} \right]_{\underset{\sim}{r} = \underset{\sim}{r}^0_n - \underset{\sim}{r}^0_m + \underset{\sim}{r}_{\underline{\delta}}} .$$

C. Convergence of Lattice Sums

The crucial problem in the evaluation of W_{TOT} to any particular order p is the convergence of the lattice sum:

(I-12)

$$\sum_{\underline{\delta}=0}^{\frac{N_0}{Z}-1} \left[\frac{\partial^p}{\partial x_\alpha \partial x_\beta \cdots \partial x_\pi} \frac{1}{|\underset{\sim}{r}|} \right]_{\underset{\sim}{r} = \underset{\sim}{r}^0_n - \underset{\sim}{r}^0_m + \underset{\sim}{r}_{\underline{\delta}}}$$

By the integral test one can show that this sum converges absolutely if $p > 3$. Therefore lattice sums of the monopole-monopole, monopole-dipole, monopole-quadrupole, and dipole-dipole interactions converge only conditionally, or, in other words, their convergence is dependent on the shape of the crystal, i.e., for any truncated summation scheme the true value of the sum can only be approached if the order of summation has been chosen wisely.

D. Fast-Convergence Schemes

All the popular fast-convergence schemes for evaluating lattice sums can be considered as inspired by the work of Epstein (6,7). They rely on the periodicity of the lattice, which justifies the use of Fourier transform (FT) techniques, and either on wise choices on the order of summation (OS) or on some integral transform (IT) which allows calculations in direct space of short-range effects and in reciprocal space of quasi-periodic long-range effects; they include Madelung's method (8) (multipole order p = 1, OS and FT), Bertaut's method (9) (p = 1, FT), Ewald's method (10) (p = 1, IT and FT), the Ewald-Kornfeld technique (11) (p > 1, IT and FT), Nijboer and de Wette's method (12) (p > 1, IT and FT), and its close relative, the technique of Erdélyi, Born, Misra, and Bradburn (13) (p > 4, IT and FT). Another OS technique is that of Evjen ((3), p = 1).

For our organic crystals neither Madelung's nor Evjen's methods are helpful. The transform used by Ewald, namely:

$$\frac{1}{r} = \frac{2}{\sqrt{\pi}} \int_0^\infty dt \, \exp(-r^2 t^2)$$

cannot be applied directly for r^{-p}, $p > 1$; hence Nijboer, de Wette, Erdelyi, Born, Misra, and Bradburn use instead:

$$\frac{1}{r^p} = \frac{1}{\Gamma(\frac{p}{2})} \int_0^\infty dt \, t^{\frac{1}{2}p-1} \exp(-r^2 t), \quad p>0 \tag{I-13}$$

where $\Gamma(n)$ is Euler's gamma function:

$$\Gamma(n) = \int_0^\infty dt\, t^{n-1} \exp(-t). \qquad n>0 \tag{I-14}$$

By techniques very similar to those described in Chapter II for the Ewald method, Nijboer and de Wette obtain for the lattice sum, valid for p > 3:

$$\begin{aligned}\sum_{\underset{\sim}{\delta}=0}^{\frac{N_a}{2}-1} \frac{1}{|\underset{\sim}{r}-\underset{\sim}{r}_{\underset{\sim}{\delta}}|^p} = \frac{1}{\Gamma\left(\frac{p}{2}\right)} \Bigg\{ & \frac{2\pi^{3/2}}{V^{\frac{p+3}{6}}} \frac{\eta^{\frac{p-3}{2}}}{p-3} + \\ & + \frac{\pi^{3/2}}{V} \sum_{h=-\infty}^{\infty} \sum_{k=-\infty}^{\infty} {\sum_{l=-\infty}^{\infty}}' \exp(i\, \underset{\sim}{\mathfrak{h}}_{hkl} \cdot \underset{\sim}{r}) \frac{\Gamma\left(\frac{3-p}{2}, \frac{\pi^2 \mathfrak{h}_{hkl}^2 V^{2/3}}{\eta}\right)}{(\pi |\underset{\sim}{\mathfrak{h}}_{hkl}|)^{3-p}} + \\ & + \sum_{\underset{\sim}{\delta}=0}^{\frac{N_a}{2}-1} \frac{\Gamma\left(\frac{p}{2}, \frac{\eta}{V^{2/3}} |\underset{\sim}{r}-\underset{\sim}{r}_{\underset{\sim}{\delta}}|^2\right)}{|\underset{\sim}{r}-\underset{\sim}{r}_{\underset{\sim}{\delta}}|^p} \Bigg\},\end{aligned} \tag{I-15}$$

where all symbols have been already defined in Chapter II except for the incomplete gamma function:

$$\Gamma(\nu, x) \equiv \int_x^\infty dt\, t^{\nu-1} \exp(-t)$$

If $\underset{\sim}{r}_{\underset{\sim}{\delta}} = 0$ must be excluded then the term $-\frac{2}{p}\left(\frac{\eta}{V^{p/6}}\right)^{p/2}$ should be added inside the curly brackets of Eq. (I-15). Because of the conditional convergence, special precautions must be followed if p < 4 (12b). Unfortunately, the methods of Nijboer and de Wette and of Born, Erdélyi <u>et al</u>. require the use of the exponential integral as well as of the error function. Kornfeld's elegant adaptation of the Ewald method, however, does not need the exponential integral, and is conceptually very straightforward; accordingly, it is considered in greater detail below. Kornfeld's recipe is disarmingly simple: to obtain the desired crystal multipole potentials, electric fields, or binding energies, perform explicitly all the partial differentiations on the Ewald series for the monopole-monopole interactions (see Chapter II), that may be required by Eq. (I-5) or (I-10). As p increases, the expressions rapidly become rather lengthy, but their evaluation presents no problem for a digital computer, once a good program is available for the p = 1 case.

There is, however, one important difficulty, related to that encountered in Chapter III: whereas in all crystals the zero unit cell must be electrically neutral, $\sum_{m=1}^{M} Z_m = 0$, the multipole moments do not necessarily add up to zero:

$$\sum_{m=1}^{M} M^{p}_{m\alpha\beta\dots\pi} \neq 0 \, ; \qquad \left\{ \begin{matrix} \alpha, \beta, \dots, \pi = 1,2,3 \\ p \geq 2 \end{matrix} \right\} \tag{I-17}$$

this is especially true in ferroelectric crystals or for crystals placed in a polarizing external field. If p > 4 this presents no problem since the relevant lattice sums converge absolutely, but the cases p = 2, 3 are a headache. As in Chapter II, Eq. (217), the left-hand side of (I-17) is the h = 0, k = 0, l = 0 term in the Fourier expansion of the periodic multipole distribution; both in the Ewald-Kornfeld method and in the Nijboer-de Wette method the sum over reciprocal space involves a fraction, whose numerator does not vanish if $\underset{\sim}{\mathfrak{h}}_{hkl} = 0$, but whose denominator is $\left|\underset{\sim}{\mathfrak{h}}_{hkl}\right|^2$. This singularity has been discussed often (14): it seems to arise from an infinite but meaningless self-energy which is customarily ignored by avoiding pari passu the summation term h = 0, k = 0, l = 0 even when inequality (I-17) holds. Some writers superimpose a fictitious "neutralizing" uniform background which supposedly legalizes everything, but probably gives an erroneous macroscopic external field (14b).

E. Effects of Induced Dipole Moments

Assume, with Kommandeur and Pott, that an arbitrary holoionic DA crystal, say (TMPD:pChl), is molionic: sublattice A is ionic, with M charged atoms per unit cell; sublattice B is neutral with M' atoms of finite scalar polarizability $\alpha_{i'}$ (i' = 1, 2,..., M' N_o/Z) (primed subscripts will refer to atoms in sublattice B). The induced dipoles $D^{ind}_{i'} \vec{e}_x + D^{ind}_{i'2} \vec{e}_y + D^{ind}_{i'3} \vec{e}_z$ in sublattice B are due to the electric field $\underset{\sim}{E}$ created by the charges Z_i (i = 1, 2,..., M N_o/Z) in sublattice A. These induced dipoles are described by:

$$\text{(I-18)} \qquad D^{ind}_{i'\beta} \equiv \alpha_{i'} \sum_{i=1}^{M\frac{N_o}{Z}} Z_i \left[-\frac{\partial}{\partial x_\beta} \frac{1}{|\underset{\sim}{r}|} \right]_{\underset{\sim}{r} = \underset{\sim}{r}^o_i - \underset{\sim}{r}^o_{i'}} \equiv \alpha_{i'} E_\beta(\underset{\sim}{r}^o_{i'}).$$

They interact with each other and with all other multipoles in both sublattices just as if they were the permanent dipoles $D_{i\beta}$ of Eq. (I-9). The interaction energy between the $D^{\text{ind}}_{i'\beta}$ and $\underset{\sim}{E}$ is given by:

$$W^{1,\text{ind}} = -\frac{1}{2}\sum_{i'=1}^{M'\frac{N_0}{Z}} \alpha_{i'}\, E_\beta(\underset{\sim}{r}^{\circ}_{i'})\, E_\beta(\underset{\sim}{r}^{\circ}_{i'}) = \tag{I-19a}$$

$$= -\frac{N_0}{2Z}\sum_{m'=1}^{M'} \alpha_{m'}\, E_\beta(\underset{\sim}{r}^{\circ}_{m'})\, E_\beta(\underset{\sim}{r}^{\circ}_{m'}). \tag{I-19b}$$

The electric field is obtained by a straightforward differentiation of Ewald's series for the electrical potential ψ(r) (Eq. (229) of Chapter II):

$$E_\beta(\underset{\sim}{r}_{i'}) = |\epsilon|\sum_{m=1}^{M} Z_m \sum_{\underline{\delta}=0}^{\frac{N_0}{Z}-1}\left[-\frac{\partial}{\partial x_\beta}\,\frac{1}{|\underset{\sim}{r}|}\right]_{\underset{\sim}{r}=\underset{\sim}{r}^{\circ}_{m}+\underset{\sim}{r}_{\underline{\delta}}-\underset{\sim}{r}^{\circ}_{i'}} = \tag{I-20a}$$

$$= -\left[\frac{\partial}{\partial x_\beta}\psi(\underset{\sim}{r})\right]_{\underset{\sim}{r}=\underset{\sim}{r}^{\circ}_{i'}} = \tag{I-20b}$$

$$= -\frac{4\pi i|\epsilon|}{V}\sum_{h=-\infty}^{\infty}\sum_{k=-\infty}^{\infty}\sum_{l=-\infty}^{\infty}{}' \mathfrak{d}^{\beta}_{hkl}\,\mathfrak{d}^{-2}_{hkl} \times \tag{I-20c}$$

$$\times \exp\left(-\frac{\mathfrak{d}^{2}_{hkl}V^{2/3}}{4\eta}\right)\sum_{m=1}^{M} \zeta_m \exp\left[i\underset{\sim}{\mathfrak{d}}_{hkl}\cdot(\underset{\sim}{r}^{\circ}_{i'}-\underset{\sim}{r}^{\circ}_{m})\right] +$$

$$+|\epsilon| \sum_{d=-\frac{1}{2}\left[\left(\frac{N_0}{2}\right)^{1/3}-1\right]}^{\frac{1}{2}\left[\left(\frac{N_0}{2}\right)^{1/3}-1\right]} \sum_{f=-\frac{1}{2}\left[\left(\frac{N_0}{2}\right)^{1/3}-1\right]}^{\frac{1}{2}\left[\left(\frac{N_0}{2}\right)^{1/3}-1\right]} \sum_{g=-\frac{1}{2}\left[\left(\frac{N_0}{2}\right)^{1/3}-1\right]}^{\frac{1}{2}\left[\left(\frac{N_0}{2}\right)^{1/3}-1\right]} \times$$

$$\times \sum_{m=1} \frac{Z_m\left(r_{i'\beta}-r_{m\beta}-r_{dfg\beta}\right)}{\left|\underset{\sim}{r}^{o}_{i'}-\underset{\sim}{r}^{o}_{m}-\underset{\sim}{r}_{dfg}\right|^{3}}\left\{1-\mathrm{erf}\left(\frac{\sqrt{\eta}}{V^{1/3}}\times\right.\right.$$

$$\left.\times\left|\underset{\sim}{r}^{o}_{i'}-\underset{\sim}{r}^{o}_{m}-\underset{\sim}{r}_{dfg}\right|\right)+\frac{2\sqrt{\eta}}{\sqrt{\pi}\,V^{1/3}}\left|\underset{\sim}{r}^{o}_{i'}-\underset{\sim}{r}^{o}_{m}-\underset{\sim}{r}_{dfg}\right|\times$$

$$\left.\times\exp\left(-\frac{\eta}{V^{2/3}}\left|\underset{\sim}{r}^{o}_{i'}-\underset{\sim}{r}^{o}_{m}-\underset{\sim}{r}_{dfg}\right|^{2}\right)\right\}, \qquad \{\beta=1,2,3\}$$

where

$$Z_m,\ \Phi^{\beta}_{hk\ell}\ (\beta=1,2,3),\ r_{m\beta}\ (\beta=1,2,3),\ r_{dfg\beta}\ (\beta=1,2,3)$$

replace

$$\zeta_m,\ \Phi^{x}_{hk\ell},\ \Phi^{y}_{hk\ell},\ \Phi^{z}_{hk\ell},\ r^{x}_{m},\ r^{y}_{m},\ r^{z}_{m},\ r^{x}_{dfg},\ r^{y}_{dfg},\ r^{z}_{dfg}$$

of Eqs. (201, 264, 267, 266), respectively.

The computer program EWALD described in Chapter II was modified to calculate $E_\beta(r^{O}_{i'})$; this modification, nicknamed FIELD, was not completely debugged when computer funds ran out.

REFERENCES

(1) J. Kommandeur and G. T. Pott, Mol. Phys., 11, 93-95 (1966).

(2) H. M. McConnell, B. M. Hoffman, and R. M. Metzger, Proc. Natl. Acad. Sci. (U.S.), 53, 46-50 (1965).

(3) (a) H. M. Evjen, Phys. Rev., 39, 675-687 (1932);
(b) C. Kittel, "Introduction to Solid-State Physics", 2nd Edition (J. Wiley & Sons, Inc., New York, 1956), pp. 74-76.

(4) G. T. Pott and J. Kommandeur, Mol. Phys., 13, 373-390 (1967).

(5) J. L. deBoer and A. Vos, Acta Cryst., B24, 720-725 (1968).

(6) P. Epstein, Math. Ann., 56, 615 (1903); Math. Ann., 63, 205 (1907).

(7) Cf. review on lattice sums by M. P. Tosi, "Cohesion of Ionic Solids in the Born Model" in Vol. 16 of "Solid State Physics--Advances in Research and Applications", F. Seitz and D. Turnbull, Editors (Academic Press, New York, 1964) pp. 1-120.

(8) (a) E. Madelung, Physik. Z., 19, 524-535 (1918).
(b) L. S. Ornstein and F. Zernike, Proc. kon. Acad. Wetensch. Amsterdam, 21, 911 (1918).

(9) (a) F. Bertaut, J. Phys. Radium, 13, 499-503 (1952);
(b) D. H. Templeton, J. Chem. Phys., 23, 1629-1630 (1955);
(c) R. E. Jones and D. H. Templeton, J. Chem. Phys., 25, 1062-1063 (1956);
(d) Q. C. Johnson and D. H. Templeton, J. Chem. Phys., 34, 2004-2007 (1961).

(10) P. P. Ewald, Ann. Phys., 64, 253-287 (1921).

(11) (a) H. Kornfeld, Z. Physik, 22, 27-43 (1924);
(b) J. Bouman, Archiv. néerland. sci., 13, 1-28 (1930);
(c) Ref. (3b), pp. 574-575;
(d) M. Born and K. Huang, "Dynamical Theory of Crystal Lattices" (Oxford University Press, Oxford, 1954), pp. 248-255;
(e) J. M. Ziman, "Principles of the Theory of Solids," (Cambridge, 1964), pp. 41-42.

(12) (a) B. R. A. Nijboer and F. W. deWette, Physica, 23, 309-321 (1957);
(b) B. R. A. Nijboer and F. W. deWette, Physica, 24, 422-432 (1958);
(c) F. W. deWette and B. R. A. Nijboer, Physica, 24, 1105-1118 (1958);
(d) F. W. deWette, Phys. Rev., 123, 103-112 (1961);
(e) F. W. deWette and G. E. Schacher, Phys. Rev., 137, A78-A91 (1965);
(f) F. W. deWette and G. E. Schacher, Phys. Rev., 137, A92-A94 (1965).

(13) (a) R. D. Misra, Proc. Camb. Phil. Soc., 36, 173 (1940);
(b) M. Born and M. Bradburn, Proc. Camb. Phil. Soc., 39, 104 (1942);
(c) Ref. (11d), Appendix III, pp. 388-390.

(14) (a) Ref. (11b), page 12;
(b) Ref. (11d), pp. 252-253;
(c) Ref. (12b), p. 427;
(d) Ref. (12c), p. 1111;
(e) R. H. Young, see footnote on page 187 of this Thesis.

PROPOSITION II

X-RAY CRYSTALLOGRAPHY OF DONOR-ACCEPTOR CRYSTALS

A. Introduction

Crystallographic evidence is discussed here with reference to the classification of McConnell et al. (1) of organic donor-acceptor (DA) crystals into the holoionic $|D^+A^-\rangle$ and the non-ionic $|DA\rangle$ categories. In particular: (i) we review the bond-length data on the holoionic crystals studied to date, and suggest a reinterpretation or a redetermination of the molecular structure of (1:1)-(N,N,N',N'-Tetramethyl-para-phenylenediamine:p-Chloranil)(TMPD:pChl); (ii) we discuss the feasibility of detecting the effect of complete charge transfer, $|DA\rangle \rightarrow |D^+A^-\rangle$, on the calculated X-ray structure; (iii) we describe current experiments on systems for which the molecular symmetry of the D^+ ion must be sufficiently different from the symmetry of the D molecule to lead to an unequivocal distinction between a $|D^+A^-\rangle$ structure and a $|DA\rangle$ structure; (iv) we discuss a possible phase transition in (1:1)-(para-Phenylenediamine:para-Chloranil).

B. The Bond-Length Argument and the Structure of (1:1)-(TMPD:pChl)

In the recent room-temperature crystal and molecular structure determination of (1:1)-(TMPD:pChl), de Boer and Vos (2) conclude that the crystal consists of neutral TMPD and pChl molecules, but admit that a small fraction (< 20%) of doubly charged species $TMPD^{++}$ and $pChl^{--}$ cannot be excluded. Their conclusions do agree with the statements of Pott and Kommandeur (3) but we have shown in this Thesis that the spin resonance and optical absorption data of Pott and Kommandeur should be reinterpreted to show that the crystal is indeed holoionic, and consists mainly of $TMPD^{+}$ and $pChl^{-}$ ions and maybe some 10% or less back-charge transfer TMPD and pChl molecules.

Accordingly, we propose that the crystal and molecular structure of (1:1)-(TMPD:pChl) be redetermined with a larger set of observed diffraction intensities, or, alternately, we argue that a more extensive comparison of de Boer and Vos' interatomic distances with published data for closely related crystals suggests (but does not prove) that de Boer and Vos in fact may have studied a holoionic crystal consisting mostly of $TMPD^{+}$ and $pChl^{-}$. Tables I, II give bond-lengths for $TMPD^{+}$, pChl, and $pChl^{-}$ in various crystals. For the sake of comparison, data for 7,7,8,8-Tetracyanoquinodimethan (TCNQ) and $TCNQ^{-}$ are given in Table III. The atom designations are given in the diagram below (p. 256).

The bond-length argument used by de Boer and Vos and by many other authors runs as follows: the bond-lengths are "benzenoid" for TMPD, $pChl^{-}$, and $TCNQ^{-}$, and "quinonoid" for $TMPD^{+}$, TCNQ, pChl; in a benzenoid structure, bond 2-3 is relatively long, and bonds 1-1' and 1-2 tend to be equal in length; in a quinonoid structure bond 2-3 is relatively short and bond 1-1'

TABLE I

Interatomic Distances in Å for $TMPD^+$, with (Standard Deviations)

Atoms	(a)	(b)	(c)*	(d)*	(e)*	(f)*
1-1'	1.384 (10)	1.361 (8)	1.374 (10)	1.367 (3)	1.374 (10)	1.435 (?)
1-2	1.397 (50)	1.422 (5)	1.416 (7)	1.418 (3)	1.400 (10),	1.389 (?),
					1.405 (10)	1.424 (?)
2-3	1.390 (10)	1.344 (6)	1.365 (7)	1.373 (3)	1.357 (10)	1.378 (?)
3-4	1.47 (5)	1.454 (5)	1.474 (7)	1.458 (15)	1.459 (10),	1.467 (?)
					1.470 (10)	1.503 (?)

* In DA crystals.

(a) In $TMPD^+ClO_4^-$, see Ref. (4)

(b) In $TMPD^+I^-$, see Ref. (5).

(c) In (1:1)-(TMPD:TCNQ), see Ref. (6).

(d) In (1:2)-(TMPD:TCNQ), see Ref. (7).

(e) In (1:1)-(TMPD:pChl), see de Boer and Vos (2).

(f) In preliminary data on (1:1)-(TMPD:pChl), see Wallwork (8).

TABLE II

Interatomic Distances in Å for pChl and pChl$^-$, with (Standard Deviations)

Atoms	pChl (a)	pChl (b)*	pChl$^-$ (c)*	pChl$^-$ (d)*
1-1'	1.342 (11)	1.343 (85)	1.350 (10)	1.375 (?)
1-2	1.477 (11)	1.400 (85),	1.459 (10),	1.408 (?),
		1.435 (85)	1.466 (10)	1.485 (?)
2-3	1.195 (11)	1.326 (85)	1.230 (10)	1.258 (?)
1-6	1.714 (8)	1.705 (65),	1.713 (7),	1.743 (?),
		1.829 (65)	1.718 (7)	1.750 (?)

* In DA crystals.

(a) In pChl, see Ref. (9).

(b) In (1:1)-(HMB:pChl), see Ref. (10).

(c) In (1:1)-(TMPD:pChl), see de Boer and Vos, Ref. (2).

(d) In (1:1)-(TMPD:pChl), see Wallwork, Ref. (8).

TABLE III

Interatomic Distances in Å for TCNQ and $TCNQ^-$, with (Standard Deviations)

Atoms	TCNQ (a)	TCNQ (b)	TCNQ (c)*	TCNQ (d)*	$TCNQ^-$ (e)	$TCNQ^-$ (f)	$TCNQ^-$ (g)	$TCNQ^-$ (h)*
1-1'	1.346(3)	1.341(5)	1.365(8)	1.355(15)	1.37(1)	1.341(7)	1.355(4)	1.373(9)
1-2	1.448(3)	1.444(4)	1.438(8)	1.460(8)	1.42(1)	1.434(5)	1.427(3)	1.414(6)
2-3	1.374(3)	1.371(5)	1.375(8)	1.370(14)	1.40(1)	1.388(7)	1.410(4)	1.406(8)
3-4	1.440(3)	1.428(4)	1.432(8)	1.430(9)	1.41(1)	1.420(5)	1.419(3)	1.412(6)
4-5	1.138(2)	1.140(4)	1.141(8)	1.135(10)	1.13(1)	1.156(5)	1.152(3)	1.160(7)

* In DA crystals.

(a) In TCNQ, see Ref. (11).

(b) "Centric" TCNQ species in $(Cs^+)_2(TCNQ^-)_2(TCNQ)$, see Ref. (12).

(c) In (1:1)-(Bis-(8-hydroxyquinolato)copperII:TCNQ), see Ref. (13).

(d) In (1:1)-(Anthracene:TCNQ), see Ref. (14).

(e) In K^+TCNQ^-, see Ref. (12,15).

(f) In N-Methylphenazinium$^+$$TCNQ^-$, see Ref. (16).

(g) "Non-centric" $TCNQ^-$ in $(Cs^+)_2(TCNQ^-)_2(TCNQ)$, see Ref. (12).

(h) In (1:1)-(TMPD:TCNQ), see Ref. (6).

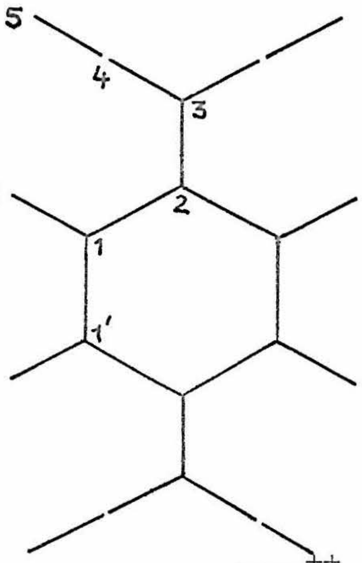

is much shorter than bond 1-2. For TMPD^{++} a quinonoid structure and for pChl^{--} a benzenoid structure are predicted.

The data for TCNQ and TCNQ^{-} in Table III confirm this trend, but the bonds 1-1' and 1-2 do not become equal in TCNQ^{-}: their difference, however, is significantly smaller in TCNQ^{-} than in TCNQ; the 2-3 bond distance is significantly longer in TCNQ^{-} than in TCNQ.

The data for pChl and pChl^{-} in Table II are so imprecise that we wish to follow de Boer and Vos in ignoring them. The data listed in Table I for TMPD^{+} in crystals other than DA crystals are not <u>significantly</u> different from the data for DA crystals, including those of de Boer and Vos. Accordingly, to within 2 standard deviations in de Boer and Vos' bond distances, (1:1)-(TMPD:pChl) along with (1:1)-(TMPD:TCNQ) is a holoionic crystal. One might hope that a more extensive set of X-ray data on (1:1)-(TMPD:pChl) would ultimately reduce the uncertainty in bond lengths and reinforce our conclusion.

C. The Effects of Charge Transfer on the Calculated Electron Density

If in a DA crystal the organic donor molecule is ionized D → D^+, or if the acceptor molecule A is ionized A → A^-, then the fractional positive or negative net charge density at the various atoms might be detectable in an electron density map obtained from X-ray diffraction data. Or, the calculated structure might refine better if account were taken of charge transfer by adjusting slightly the atomic scattering form factors to allow for fractional net atomic changes.

A similar problem in boron hydride chemistry was resolved by Simpson and Lipscomb (17) who showed that "stripping" electrons off B_9H_{15} worsened the reliability factor of its calculated crystal structure sufficiently to prove that no more than a 5% B_9 hydride impurity could have been present.

The usual atomic form factors tabulated for crystallographers do not even account for bonding delocalized electrons, because the quality of X-ray diffraction data has been too low to allow for realistic detection of bonding effects. Typically, a 3% long-term variation in X-ray source intensity and a 3-5% uncertainty in the visually estimated diffraction intensities are to be expected in manual X-ray techniques.

Recently, current and voltage-regulated X-ray generators with a 1% power output stability have been manufactured for use with four-circle automatic diffractometers. Careful spot shape analysis and integration techniques may lower significantly the uncertainties in the diffracted intensities. Indeed, Hartmann and Hirschfeld (18) and Steward (19) have observed reasonable electron densities between atoms, and the day may have already come when the effect of charge transfer in organic crystals is observable by X-ray diffraction analysis (35).

D. A Holoionic DA Crystal for which D^+ and D Have Measurably Different Molecular Symmetries[*]

On the basis of intercalation experiments (20) of chlorpromazine radical cation (I:CPZ^+) with deoxyribonucleic acid,

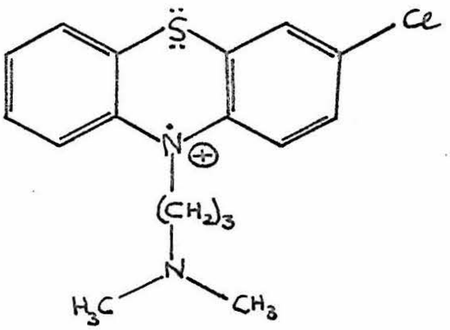

I

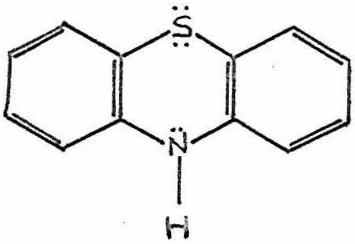

II

McConnell has proposed (21) that, while neutral phenothiazine (II:PTZ) is known to be a non-planar, butterfly-shaped molecule (22), the radical cation $PTZ^{+\cdot}$ is planar.[**] McConnell suggested

---

[*] For the sake of completeness, we report here on current research, which had originally been scheduled as part of the thesis requirement, and comment on recent results obtained by Fritchie.

[**] This prediction disagrees with the calculation of Malrieu and Pullman (23).

further that a DA complex of PTZ or its derivatives with strong electron acceptors would yield a holoionic crystal in which X-ray diffraction techniques could identify a planar $PTZ^{\dot{+}}$ nucleus and thereby prove complete charge-transfer (except for the predicted small amount of back charge-transfer).

With 7,7,8,8-Tetracyanoquinodimethan (TCNQ) as the acceptor, beautiful crystals of (1:1)-(PTZ:TCNQ) and of (1:1)-(5-MethylPTZ:TCNQ) were obtained (24), but partial disorder (25) prevented further X-ray studies. No acceptable crystals were obtained for PTZ or 5-MethylPTZ with the acceptors Tetracyanoethylene, para-Chloranil, para-Bromanil, or Pyromellitic Dianhydride. Crystals of (1:1)-(CPZ:TCNQ) have been obtained in very low yield, and are under study in collaboration with P. G. Simpson (26).

Fritchie has obtained good crystals of (1:1)-(PTZ:sym-Trinitrobenzene) ((PTZ:sTNB)) (27) and of (1:1)-(PTZ:2,4-Dinitrotoluene) (28). The former contains either planar PTZ species or a statistically disordered mixture of non-planar PTZ molecules (29),[*] while in the latter the PTZ molecules are definitely non-planar.

The scanty experimental data presented in Chapter II for (1:1)-(PTZ:sTNB) seem to classify it as a nonionic crystal, but

---

[*] I understand that the (1:1)-(PTZ:sTNB) structure determination has been submitted for publication, but do not know how the ambiguity has been resolved.

it is remotely possible that, even though $I_D - A_A = 6.6$ eV is 0.6 eV higher than our guessed threshold for complete charge transfer, exchange effects may suffice to make (1:1)-(PTZ:sTNB) into a holoionic crystal.

E. Phase Transition in (1:1)-(pPD:pChl)?

Recently Hughes and Soos (30) studied the electron paramagnetic resonance (EPR) spectrum of single crystals of (1:1)-(para-Phenylenediamine:para-Chloranil) (pPD:pChl) obtained by co-sublimation. Below about 315°K three EPR signals are observed: they are due to Wannier spin excitons severally delocalized on the three magnetically inequivalent linear chains allowed by the room-temperature space group $P\bar{3}m1$ or $P3m1$. The other crystallographic data at ~ 295°K are (31): $\underset{\sim}{a} = 14.83$ Å, $\underset{\sim}{c} = 6.62$ Å, $Z = 3$, $\rho_{obs} = 1.630 \pm 0.005$ gcm^{-3}, $\rho_{calc} = 1.4$. Above 315°K only one EPR signal is detectable, even though the linewidth decreases continuously with increasing temperature. Two mutually exclusive interpretations are possible (30): (i) there is a relatively sluggish phase transition at or about 315°K, whereby the linear chains become magnetically equivalent; (ii) the Wannier spin exciton, which is a one-dimensional spin wave below 315°K, becomes three-dimensional or is very strongly affected by magnetic dipole interactions between different linear chains above 315°K.

The latter interpretation has been reformulated in theoretical language by Soos (32), but the former has not yet been disproved by X-ray techniques. Hughes (33) has suggested that a determination of the space group and unit cell parameters of (pPD:pChl) at 320°K would settle the ambiguity. In preliminary work (34) the data of Graeber (31) have been verified at 295°K.

F. Acknowledgments

Professors H. M. McConnell, R. E. Marsh, P. G. Simpson, D. H. Templeton, and S. C. Wallwork, Dr. J. C. A. Boeyens, Dr. R. C. Hughes, and Dr. A. W. Hanson have been most helpful with their advice, encouragement, and willingness to share their preliminary results: it is a pleasure to express here my gratitude to all of them.

REFERENCES

(1) H. M. McConnell, B. M. Hoffman, and R. M. Metzger, Proc. Natl. Acad. Sci. U.S., 53, 46-50 (1965)

(2) J. L. de Boer and A. Vos, Acta Cryst., B24, 720-725 (1968): final R = 0.076; N = 12 atoms in asymmetric unit (excluding hydrogen); n = 708 reflections observed, s = 944 reflections accessible.

(3) G. T. Pott and J. Kommandeur, Mol. Phys., 13, 373-390 (1967).

(4) J. D. Turner and A. C. Albrecht, "The Crystal Structure of Wurster's Blue Perchlorate" (Sept., 1954, unpublished): R = 0.118 for h0l data, 0.252 for 0kl data; N = 7; n = 76, b = 78 for h0l; n = 64, s = 69 for 0kl.

(5) J. L. de Boer, A. Vos, and K. Huml, Acta Cryst., B24, 542-549 (1968); R = 0.027; N = 5; n = 823, s = 1381.

(6) A. W. Hanson, Acta Cryst., 19, 610-613 (1965): R = 0.083; N = 9; n = 588, s = 1122.

(7) A. W. Hanson, Acta Cryst., B24, 768-778 (1968): R = 0.049; N = 22; n = 2595, s = 3279.

(8) S. C. Wallwork, private communication (July, 1965).

(9) S. C. Chu, G. A. Jeffrey, and (in part) T. Sakurai, Acta Cryst., 15, 661-671 (1962): R = 0.111; N = 6; n = 620, s = 828.

(10) N. D. Jones and R. E. Marsh, Acta Cryst., 15, 809-810 (1963) and references quoted therein: R = 0.14; N = 12, n = 185, s = ?.

(11) R. E. Long, R. A. Sparks, and K. N. Trueblood, Acta Cryst., 18, 932-939 (1965): R = 0.081; N = 8; n = 976, s = 1120.

(12) C. J. Fritchie, Jr., and P. Arthur, Jr., Acta Cryst., 21, 139-145 (1966): R = 0.039; N = 25; n = 2749, s = 3845.

(13) R. M. Williams and S. C. Wallwork, Acta Cryst., 23, 448-455 (1967); R = 0.068; N = 20; n = 2651, s = 4300.

(14) R. M. Williams and S. C. Wallwork, Acta Cryst., B24, 168-174 (1968); R = 0.111; N = 9; n = 469, s = 1800.

(15) G. R. Anderson and C. J. Fritchie, Jr., Second National Meeting, Society for Applied Spectroscopy, San Diego, Oct. 14-18, 1963, Paper 111.

(16) C. J. Fritchie, Jr., Acta Cryst., 20, 892-898 (1966); R = 0.098; N = 16; n = 865, s = 1919.

(17) P. G. Simpson and W. N. Lipscomb, J. Chem. Phys., 35, 1340-1343 (1961).

(18) A. Hartmann and F. L. Hirschfeld, Acta Cryst., 20, 80-82 (1966).

(19) R. F. Stewart, J. Chem. Phys., 48, 4882-4889 (1968).

(20) S. Ohnishi and H. M. McConnell, J. Am. Chem. Soc., 87, 2293 (1965).

(21) H. M. McConnell, private communication (January, 1966).

(22) R. G. Wood, C. H. McCale, and G. Williams, Phil. Mag. 31, 71-80 (1941).

(23) J. P. Malrieu and B. Pullman, Theoret. Chim. Acta, 2, 293-301 (1964).

(24) R. M. Metzger, unpublished results (1966).

(25) D. H. Templeton, private communication (August, 1966).

(26) R. M. Metzger, unpublished results (1967).

(27) C. J. Fritchie, Jr., American Crystall. Assoc. Meeting, (Atlanta, Ga.), January, 1967, p. 50, paper F10.

(28) C. J. Fritchie, Jr., American Crystall. Assoc. Meeting, (Buffalo, N. Y.), August, 1968.

(29) C. J. Fritchie, private communication to P. G. Simpson (January, 1967).

(30) R. C. Hughes and Z. G. Soos, J. Chem. Phys., 48, 1066-1076 (1968).

(31) E. J. Graeber, unpublished results quoted in Ref. (30,33).

(32) Z. G. Soos, "Theory of Temperature-Dependent g-Tensor Splittings in p-Phenylenediamine-Chloranil" (to be published, 1968).

(33) R. C. Hughes, private communication (March, 1967).

(34) R. M. Metzger, unpublished results (April, 1967).

(35) Note added in proof: R. Brill discusses in great detail the state-of-the-art in "Determination of Electron Distribution in Crystals by Means of X-Rays", pp. 1-35 of Vol. 20 of "Solid-State Physics--Advances in Research and Applications", F. Seitz, D. Turnbull, and H. Ehrenreich, Eds. (Academic Press, New York, 1967).

PROPOSITION III

THE PHASE TRANSITION AND CHANGES IN THE FINE-STRUCTURE SPLITTINGS OF A FRENKEL TRIPLET SPIN EXCITON CRYSTAL: A HIGH-PRESSURE, LOW-TEMPERATURE, HIGH-FIELD ELECTRON PARAMAGNETIC RESONANCE STUDY OF THE ION-RADICAL SALT TRIPHENYLMETHYLARSONIUM $(TCNQ)_2^-$

A. Introduction

We report here an experimental measurement of the fine-structure splitting parameters D, E in the electron paramagnetic resonance (EPR) powder spectrum of the thermally accessible Frenkel triplet spin excitons in the ion-radical salt Triphenylmethylarsonium $(TCNQ)_2^-$ ("arsonium salt") at 144°K as a function of applied pressure, across the phase transition.

B. The Phase Transition

Merkl *et al*. (1) investigated the phase transitions in the arsonium salt and Triphenylmethylphosphonium $(TCNQ)_2^-$ ("the phosphonium salt") by high-pressure EPR techniques at about 170 MHz and about 60 gauss in the temperature range 220°K to 362°K and the pressure range 1 bar to 9 kbar. They determined for both salts that the transition is of first order and that the shape of the p-T phase separation curves can be accounted for very simply by the phenomenological equation:

$$p = p_o + \frac{kT}{\Delta V^o} \log_e \left(\frac{1-\rho_I}{1-\rho_{II}} \right). \tag{III-1}$$

ρ_I is the concentration of Frenkel triplet spin excitons in phase I, which is the thermodynamically stable phase at 0°K and 1 bar; ρ_{II} is the corresponding concentration for phase II, which the data show to be attainable at 0°K and pressures p_o of 3.26 kbar for the arsonium salt and ~ 4.5 kbar for the phosphonium salt (2); $\Delta V^o \equiv V_{II} - V_I$ is the difference in volumes between the two phases at the transition point: this difference seems to be independent of temperature and pressure; for one pair of arsonium molecules $\Delta V^o = -11.7$ Å^3, for one pair of phosphonium molecules $\Delta V^o \cong -2$ Å^3. Furthermore, ρ_I is given by corrected boltzon statistics (3):

$$\rho_I = \frac{3\exp(-J_I/kT)}{1 + 3\exp(-J_I/kT)}, \tag{III-2}$$

where $J_I > 0$ is the singlet-triplet energy gap in phase I, ($J_I = 0.05$ eV at 295°K and 1 bar for the arsonium salt); a corresponding expression can be written for ρ_{II} and J_{II}. As p increases, J increases almost linearly, except for a large and sudden decrease across the phase transition. The volume change is very small: Arthur (4) finds V = 1630 Å^3 for two molecules of the arsonium salt at room temperature whence $\Delta V/V = -0.0072$; Goll and Phillips (5) measure a change $\Delta b/b = -0.007$ along the crystallographic $\underset{\sim}{b}$

axis, which Arthur had measured to be 9.06 Å (4). So most of the volume change is along the b-axis. Previous findings that the transition for the phosphonium salt is endothermic for increasing temperature at 1 bar and reversible (5-10) were confirmed and extended to the arsonium salt. The enthalpy of transition is given by $\Delta H \equiv H_{II} - H_{I} = (p - p_{o})\Delta V^{o} > 0$. Iida et al. (7) found that as the temperature is increased the conductivity of a single crystal of the phosphonium salt increases anisotropically by a factor of about six across the phase transition.

For the arsonium salt at constant temperature and for both phases the exciton concentration ρ decreases (and the singlet-triplet gap J and the EPR linewidth increase) with increasing pressure; at constant temperature at the transition pressure, as we go from phase I to phase II, ρ and the EPR linewidth increase discontinuously (and J decreases discontinuously). Kepler (8) had found for both the arsonium and the phosphonium salts that at 1 bar J decreases continuously and linearly with increasing temperature; for the arsonium salt alone J has no discontinuity at 1 bar, whereas the phosphonium salt at 1 bar exhibits a large drop in J at the phase transition. The decrease in J with increasing temperature can be attributed to a decreasing intermolecular overlap due to the thermal expansion of the lattice; similarly, the increase of J with increasing pressure can be due to an increased overlap at high pressures: these arguments have been presented in a review by Nordio et al. (11). But the effect $(dJ/dT) < 0$ need not depend entirely on lattice thermal expansion: indeed for the strongly alternating Frenkel spin exciton salts Wurster's Blue Perchlorate (WBP) and triethylammonium $(TCNQ)_2^-$ Soos and Hughes (12) performed a very satisfactory two-parameter curve fitting to Kepler's data (8) of Soos' (13,14) theoretical pseudo-spin expression for the paramagnetic susceptibility as a function of the temperature (with J at T = 0°K and the lattice alternation parameter δ as the two parameters): thus $dJ/dT < 0$ can be a many-body effect; for the arsonium salt, however, the fit obtained by Soos and Hughes was poor, presumably because lattice expansion effects are not negligible for the arsonium salt. But none of these explanations allows for the sudden small $\Delta V^o < 0$ and the large $\Delta J < 0$ at the phase transition. It is furthermore obvious that the exciton-exciton interactions mentioned by Chesnut (15) cannot be responsible, since it has been deduced experimentally that both phases may exist at 0°K (1). Merkl *et al*. (1) have obtained the limited result that the shape of the phase separation curve can be accounted for by some simple theory that allows for a large decrease in J accompanied by a small decrease in V, i.e. by some change in the spin system. Hughes (2) and Goll and Phillips (5) proposed that the small changes in molecular orientation reflected in ΔV^o may account for ΔJ; Itzkowitz (16) had observed in calculations of J for WBP that J was rather sensitive to the distance between adjacent Wurster's Blue cations. However, the experimental decrease in J for the arsonium salt at 295°K is $\Delta J =$

-192 cm^{-1}, whilst Itzkowitz calculates that for Wurster's Blue cations J decreases from 500 cm^{-1} to 300 cm^{-1} if the interionic distance increases from 2.94 Å to 3.11 Å, which would correspond to a positive ΔV^o, i.e. the wrong effect. Of course, it is possible that sideway slippage of the $TCNQ^-$ ions in the $(TCNQ)_2$-$(TCNQ^-)_2$ tetramer, with a very slight compression, may lead to acceptable $\Delta V^o < 0$ and $\Delta J < 0$, but this cannot yet be calculated, since the molecular structure of the salt has not been completely determined (4). The temperature-dependent X-ray study of typical diffraction intensities for the phosphonium salt, done by Maréchal and McConnell (17), shows no sudden intensity change at the transition temperature: accordingly the structural differences between the phases are very slight (5); definite X-ray evidence thereof has been noted by Iida et al. (7).

C. Soos' Proposal

Soos (18) has suggested that the fine-structure splitting in the EPR spectrum of the Frenkel triplet spin excitons in the arsonium salt be followed experimentally across the phase line: this would give some idea of the change in the intermolecular configuration in the $(TCNQ)_2$ $(TCNQ^-)_2$ tetramer, and maybe also give some clue as to the reason for the change in J. We shall next review briefly the theoretical EPR fine-structure Hamiltonian, and the pertinent experimental information.

D. The Fine-Structure Splitting

The electron spin-electron spin interaction Hamiltonian:

$$\text{(III-3)} \qquad \hat{\mathcal{D}} \equiv g^2\beta^2 \sum_{\mu <} \sum_{\nu} \left\{ \frac{\underset{\sim}{\hat{S}}_\mu \cdot \underset{\sim}{\hat{S}}_\nu}{|\underset{\sim}{r}_{\mu\nu}|^3} - \frac{3\,\underset{\sim}{\hat{S}}_\mu \cdot \underset{\sim}{r}_{\mu\nu}\,\underset{\sim}{\hat{S}}_\nu \cdot \underset{\sim}{r}_{\mu\nu}}{|\underset{\sim}{r}_{\mu\nu}|^5} \right\}$$

can be transformed (19-24) into the experimentally convenient principal-axis representation:

$$\text{(III-4)} \qquad \hat{\mathcal{H}}_{fs} = D\hat{S}_z^2 + E(\hat{S}_x^2 - \hat{S}_y^2)$$

where $(\vec{e}_x, \vec{e}_y, \vec{e}_z)$ is a unique coordinate system, fixed in the crystal or the molecule, D is a real number which gives the "magnitude" of the fine-structure interaction energy, and E is a real number which represents the "deviation from spherical symmetry" of the interaction.

For triplet states in zero external magnetic fields (24) the experimental EPR transitions occur at $|D+E|$, $|D-E|$, and $2|E|$; these transitions are allowed if the RF magnetic field vector is polarized in the $\vec{e}_x$, $\vec{e}_y$, and $\vec{e}_z$ directions, respectively. In relatively high external DC magnetic fields $\underset{\sim}{H}$ (say 3 kiloGauss) the Zeeman coupling $\beta\,\underset{\sim}{S}\cdot\underset{\approx}{g}\,\underset{\sim}{H}$ is usually much larger than $\hat{\mathcal{H}}_{fs}$; accordingly, the fine-structure splitting is treated as a perturbation, and for a constant microwave frequency $\nu_{\mu\lambda}$ and variable DC magnetic field intensity $\underset{\sim}{H}$, the EPR spectrum of a single crystal containing triplets consists of two lines symmetrically placed about the "g-field" $H_c = h\nu_{\mu\lambda}/g\beta$; the splitting between these two lines depends on the mutual orientation of $\underset{\sim}{H}$ and $(\vec{e}_x, \vec{e}_y, \vec{e}_z)$, and their intensity depends on the mutual orientation of the microwave magnetic field $\underset{\sim}{H}_{\mu\lambda}$, $\underset{\sim}{H}$, and $(\vec{e}_x, \vec{e}_y, \vec{e}_z)$. If $\underset{\sim}{H}$ is parallel to $\vec{e}_x$, then the splitting for a $\Delta m = 1$ transition is $|D-3E|$; if $\underset{\sim}{H} \parallel \vec{e}_y$ then it is $|D+3E|$; if $\underset{\sim}{H} \parallel \vec{e}_z$ then it is $2|D|$; these fields can be called "axial fields" (24). In general, if $\underset{\sim}{H}$ has direction cosines l, m, n with respect to $(\vec{e}_x, \vec{e}_y, \vec{e}_z)$:

$$\text{(III-5)} \qquad \underset{\sim}{H} = |\underset{\sim}{H}|(\ell\vec{e}_x + m\vec{e}_y + n\vec{e}_z),$$

then the "resonance DC magnetic fields at constant $\nu_{\mu\lambda}$" for the $\Delta m = 1$ transitions are given by:

$$\text{(III-6)} \qquad H_r \equiv H_c \pm \left[\frac{D-3E}{2}\ell^2 + \frac{D+3E}{2}m^2 + Dn^2\right].$$

Wasserman et al. (24) point out that one can observe simultaneously the six EPR lines due to all the axial field absorptions in a "powder" spectrum of randomly oriented molecules. In fact, since all the values of $\ell = \cos\alpha$, $m = \cos\beta$, $n = \cos\gamma$ are equally probable if the orientation of each molecule is perfectly random, therefore the fraction of the molecules which absorbs microwave radiation $\nu_{\mu\lambda}$ at a DC magnetic field between

H and dH is given (25) by:

$$g(H)\,dH \propto d\vartheta \equiv \sqrt{(dl)^2 + (dm)^2 + (dn)^2} = \tag{III-7a}$$

$$= dH\sqrt{\frac{\sin^2\alpha}{\left(\frac{dH}{d\alpha}\right)^2} + \frac{\sin^2\beta}{\left(\frac{dH}{d\beta}\right)^2} + \frac{\sin^2\gamma}{\left(\frac{dH}{d\gamma}\right)^2}} = \tag{III-7b}$$

$$= dH\sqrt{\frac{1}{l^2(D-3E)^2} + \frac{1}{m^2(D+3E)^2} + \frac{1}{n^2(2D)^2}}. \tag{III-7c}$$

Thus for signals of vanishing linewidth, "infinite" signals are obtained for $dH/d\alpha = 0$, $dH/d\beta = 0$, $dH/d\gamma = 0$ at the same axial fields as for single crystals, superposed on a background that is white in the short range, but whose long-range trend will tend to influence strongly the lineshapes of the axial EPR transitions (24).

E. Known Fine-Structure Splittings for TCNQ Salts

For single crystals of the arsonium salt (where the Frenkel triplet exciton state is localized on a tetramer $(TCNQ)_2(TCNQ^-)_2$) Chesnut and Phillips (9) obtained in a high-field EPR experiment $D = \pm 66.0$ gauss, $E = \mp 10.5$ gauss, $D/E = -6.3$ at 123°K. In a temperature-dependent zero-field experiment at atmospheric pressure Thomas <u>et al.</u> (26) obtained at 123°K $D = \pm 69.1$ gauss, $E = \mp 10.9$ gauss, $(D/E) = -6.35$; at 144°K their data extrapolate to $D = \pm 67.3$ gauss, $E = \mp 10.6$ gauss, $(D/E) = -6.35$.

For single crystals of morpholinium$^+$TCNQ$^-$ (where the triplet exciton is localized on a dimer $(TCNQ^-)_2$) Halford and McConnell (27) obtained at room temperature and atmospheric pressure $|D| = 191$ gauss, $|E| = 19.2$ gauss, $D/E = 8.4$; in a theoretical calculation Maréchal and McConnell and Itzkowitz (16,28) obtained $D = -166$ gauss, $E = 15.7$ gauss, $D/E = -10.6$. There has been some doubt as to the charge distribution in the $(TCNQ)_2(TCNQ^-)_2$ tetramer: recent crystallographic work (29) for the salt tetraphenylphosphonium $(TCNQ)_2^-$ cannot resolve the ambiguity between statistical disorder of TCNQ$^-$ species with respect to TCNQ species, and redistribution of half on electronic charge among four TCNQ molecules to give $(TCNQ^{1/2-})_4$.

Preliminary crystallographic evidence (15,28) would have the TCNQ$^-$ ions overlap exactly in morpholinium$^+$TCNQ$^-$, and partially in an arsonium salt: this would explain the difference in the observed $|D|$. The theoretical calculation of D,E cited above lends more credence to the "statistical disorder theory" for the arsonium salt, with perhaps the requirement that in the triplet state the TCNQ$^-$ species be adjacent. This could be confirmed by actual calculation once the crystal and molecular structure of the arsonium salt are determined.

In a high-pressure room-temperature EPR experiment using a hybrid helix resonator in place of a conventional cavity, Halford and McConnell (27) determined that for morpholinium$^+$TCNQ$^-$ $|D|$ and $|E|$ increase by 1.1% and 1.6% per kbar in the range 1 bar-680 bar, which is consistent with the compressibilities of 1% to

2% per kbar determined by Bridgman (30), and the assumption that D,E are proportional, in these salts, to intermolecular overlap between $TCNQ^-$ ions.

F. Experimental

Soos' proposal was put to test in an experiment devised by A. W. Merkl, carried out by Merkl and the present writer in 1966.

The EPR equipment was a Varian V-4502-15 EPR spectrometer modified as follows: the microwave cavity was replaced by a special length of RG-52/U rectangular waveguide bearing the high-pressure bomb and terminated in a sliding slotted microwave shorting plug; to accommodate the microwave bomb in its low-pressure dewar, the detachable pole pieces of the rotating 12" electromagnet were removed, and the Fieldial Hall-effect probe was reapplied to one of the bare pole faces. The pressurization equipment consisted of a Pine hydraulic pump, which delivered a maximum pressure of 0.7 kbar; the pump was connected to a Harwood Engineering Company Model A2.5J pressure intensifier (intensification ratio 14.5); output pressures of up to 10 kbar could be delivered to the high-pressure bomb by 1/8" O.D. stainless steel high-pressure tubing (also supplied by the Harwood Co.). The pressurizing fluid was a 50-50 mixture of n-pentane and isopentane. Pressures were monitored by balancing a home-built Wheatstone bridge, the unknown resistance being that of a pressure-sensitive manganin wire coil pre-calibrated by the

Harwood Co. This pressure equipment has been described previously (2). A sample temperature of 144°K was obtained by heating electrically liquid nitrogen in a Carboy-type dewar and directing the resulting gas to the high-pressure bomb enclosed in a cylindrical styrofoam dewar. The temperature was monitored with a copper-constantan thermocouple; the reference junction was kept at 0°C and the thermoelectric voltage measured with a Leeds and Northrup K-2 potentiometer. A section of the waveguide above the high-pressure bomb was kept at room temperature by a stream of nitrogen gas. This kept water from condensing in the microwave bridge, but did not prevent some frosting inside the waveguide section which carried the high pressure bomb: in especially long runs this became a nuisance, as the microwave bridge balance started to drift and the crystal detector current increased.

The heart of the experiment was the high-pressure bomb originally designed by Halford (27,31). A preliminary version, of brass, was used by Halford and McConnell (27) up to 0.7 kbar. Later models were machined of Berylco-25, a non-magnetic beryllium-copper alloy, and hardened by heat-treating for 3 hours at 320°C. The bomb consists of (1) a male part connected to the high-pressure line and partially drilled out to form a small high-pressure sample chamber, (2) six sturdy bolts; (3) a female part about 2" wide and 1" thick electrically coupled to the microwave waveguide and also (in the original design) to the magnetic field modulation source, (4) a high-pressure mating seal.

The male part is clearance-drilled to accept the six radially disposed bolts; the female part is tapped for the same purpose. The male part is drilled out in its center to half its thickness, to form a cylindrical pressure chamber of 1/4" radius and 1/4" depth, on the side facing the female part; a small ridge was added by Merkl to "bite into" a copper washer which, when compressed against the flat surface of the female part, formed the high pressure mating seal. The tip of the 1/8" stainless steel high-pressure line is threaded, mated and silver-soldered to the other side of the male part and opens into the high-pressure chamber.

The female part is fastened by a clutch-plate to the flat side of a RG-52/U waveguide: if the clutch plate is loose the bomb can rotate about an axis perpendicular to the flat side of the waveguide. Along this axis a 0.052" hole is drilled through the female part to accept a coaxial wire of 0.012" diameter phosphor bronze. A matching 0.070" hole pierces the center of the flat side of the waveguide. The coaxial wire protruding halfway into the waveguide acts as an antenna parallel to the microwave electric field vector in the $TE_{1,0}$ waveguide mode (32) and as a coaxial path for microwaves into the high-pressure region of the bomb. The wire terminates in a small helix of four or five turns, which protrudes from the flat surface of the female part but fits inside the small pressure chamber when the bomb is assembled. The single crystal to be studied is inserted into the helix. The helix alone is a narrow-band slow-wave microwave resonator that resembles a low quality-factor cavity but can have a very high filling factor. The antenna-coaxial line-helix system constitutes a wide-band slow-wave hybrid resonator. Through two other holes drilled into the female part Halford inserted two more coaxial wires ending in a loop inside the high-pressure chamber: by connecting these wires to the output of the Varian V-4560 100 kHz oscillator-phase-sensitive-detector, Halford introduced 100 kHz magnetic field modification.

By rotating the bomb around its axis and the 12" magnet around its base Halford could determine $|D|$, $|E|$ in single crystals. At pressures above 1 kbar, however, Merkl found that Halford's epoxy-packed coaxial lines leaked. Accordingly, Merkl redesigned the bomb somewhat. The wire-loop modulation scheme was discarded for sake of simplicity; this implied that an external 400 Hz modulation scheme would have to be used with an attendant sixteen-fold loss of sensitivity because of the increased 1/f noise in the microwave diode mixer crystals. A Berylco-25 cone pressure seal (height 0.15", base diameter 0.25") was made to replace a section of the coaxial wire; the helix was soldered to flat base of the cone and the coaxial wire soldered to its vertex. The seal seat in the female part was filled with epoxy resin, cured and then drilled out to a small residual thickness with a countersink bore. This metallic seal introduces a regrettable power mismatch on the coaxial line.

Merkl decided to study the arsonium salt at a temperature for which (i) the exciton line-widths were not exchange-broadened, (ii) the fine-structure splittings were not exchange-narrowed, (iii) the exciton concentration ρ was reasonably high. The conditions are met (26) in the temperature range 120-150°K. Merkl decided to avoid the technical difficulties involved in crystal orientation studies at low temperatures and opted for studying a microcrystalline powder of the arsonium salt at the cost of impaired sensitivity. It was confirmed that the arsonium salt was insoluble in the pressurizing fluid. To keep the powder sample from drifting out of the high-pressure chamber into the high-pressure plumbing, a teflon cup was constructed to line the chamber, with its lip pressing against the female part of the bomb when the bomb was assembled. A pinhole in the bottom of the cup allowed the pressurizing fluid to reach the sample.

The microwave system consisting of the Varian V-4500-41A Microwave Bridge with its slide-screw tuner, the hybrid helix resonator, and the sliding short proved to be rather difficult to operate. The metallic sliding short is a reflective termination so that the whole waveguide section from the magnetic to the short becomes a very low-Q cavity. Under ideal conditions for maximum power transfer to the helix, the sliding short is adjusted to be $\lambda/4$ wavelengths away from the antenna. If the klystron wavelength has been so chosen that the distance from the magic T to the sliding short is an integer number of half wavelengths, then the reflected wave is in phase with the primary wave and we expect a purely absorptive EPR signal from the sample in the helix. λ is typically 4.36 cm for $\nu_{\mu\lambda}$= 9.5 GHz (Ref. (32), pp. 113-123). For one reason or another many difficulties were encountered with the behavior of the helix, since for most frequencies it seemed to produce arbitrary mixtures of the absorptive and the dispersive EPR signals ("mixed coupling"). We were relieved in discovering that Webb (33) had similarly noticed that this helix would give pure absorptive EPR signals over only one-tenth of the helix bandwidth (1.6 GHz), and we proceeded empirically to locate in room-temperature experiments klystron frequencies for which pure absorption was obtained ("absorptive coupling"). At these frequencies compromises had to be made in the microwave power coupling to the helix.

When a klystron frequency was empirically found, for which a reasonable fraction of the power was coupled into the helix by adjustment of the sliding short, and for which the EPR signal was only slightly (< 30%) dispersive, then the final elimination of the dispersive component was achieved by (i) using the spectrometer's klystron mode display to select a klystron reflector voltage V_R for which the klystron power output was a *symmetrical* maximum of the klystron mode sweep; (ii) introducing the micrometer slide screw tuner of the V-4500-41A bridge into the waveguide until a reasonable ("cavity-like") dip due to absorption by the tuning stub was recorded; (iii) adjusting the position of this tuner on the waveguide until the tuner absorption power dip was at V_R, and the mode display was symmetrical about V_R; (iv) locking the klystron automatic frequency control (AFC) circuit onto the tuner power dip. AFC was found to be necessary despite Halford's claims to the contrary. 400 Hz external magnetic field modulation was achieved by driving two large Helmholtz coils installed on the bare pole faces of the 12" electromagnet.

G. Results, and a New Experimental Design

Two runs were made--one at 130°K in the pressure range 1 bar to 3.86 kbar and one at 144°K for pressures ranging from 1 bar to 5.08 kbar. At 144°K a transition pressure of 2.95 kbar is predicted by graphical extrapolation (1). For reasons explained below the data obtained were very poor, so poor that they are not recorded here. A safe conclusion we can draw from them is that changes in D,E at the transition point did not exceed 5%. But the scatter of the results was so great that the 1% to 1.6% increase per kbar observed for D and E by Halford could not be verified.

We present here the reasons for which our experiments failed, and suggestions for improvements:

(1) By crushing our sample we introduced a large "impurity signal," presumably due to free radicals at the end of the TCNQ linear chains. This $g = 2$ signal at H_c followed Curie's law, and was so large and so

broad that the signals at $H_c \pm D, H_c \pm (D - 3E)$, and especially $H_c \pm (D + 3E)$, appeared as small bell-shaped shoulders on the H_c signal. Theoretically, $2|D|_{obs} - |D - 3E|_{obs}$ should equal $|D + 3E|_{obs}$; we found, by reading the peaks of the exciton signals, that $|D + 3E|_{obs}$ exceeded $2|D|_{obs} - |D - 3E|_{obs}$ by 6 to 10%. Theoretically, the center of gravity of the three signals should coincide; we found them to differ by as much as 3% of the smallest splitting ($|D + 3E|_{obs}$). The effects were reproducible and were not due to malfunctions of the Varian Fieldial unit. Such discrepancies are intolerable. Two remedies are possible:

(a) Computer simulation of the powder spectra in a scheme similar to that of Wasserman et al. (24). This would aid the identification of the correct axial fields, which are then measured with a NMR gauss-meter.

(b) Abandonment of the powder technique. The study of a single crystal of the arsonium salt will require rotation of the Halford-Merkl bomb on its axis <u>at low temperature</u>.

(2) The substitution of 400 Hz external modulation for 100 kHz internal loop-modulation had almost fatal effects on the signal-to-noise level. We therefore

propose that, at the cost of two more cone seals in an enlarged high-pressure chamber, Halford's loop modulation at 100 kHz be restored.

(3) The accumulation of moisture in the cold waveguide section bearing the high-pressure bomb proved embarrassing, since the EPR signals changed from absorptive to dispersive during the course of the experiment. This can be avoided by keeping the waveguide at room temperature by blowing nitrogen gas through it, and keeping the bomb alone at low temperature. The price which has to be paid is a steep temperature gradient along the axial bearing shaft of the bomb.

The redesigned bomb and dewar are shown to scale in horizontal cross-section in Fig. I. They are designed to fit within the cylinder of diameter 5.35" described by the pole gap of the rotating Varian V-3603 12" electromagnet. W is a horizontal cross-section of the RG-52/U copper waveguide, T is a brass brace that surrounds the waveguide and bears the bomb. Nitrogen gas at room temperature is introduced into the waveguide through ports (not shown) and also into the brace T to heat locally part of the bomb shaft and ease the rotation of the bomb about the horizontal axis AA'. PT is the non-magnetic stainless steel high-pressure tubing, wrapped loosely six or seven times around the dewar to allow rotation of: (i) the male part MB and the female part FB of the Berylco-25 bomb, (ii) the hemispherical styrofoam dewar DW,

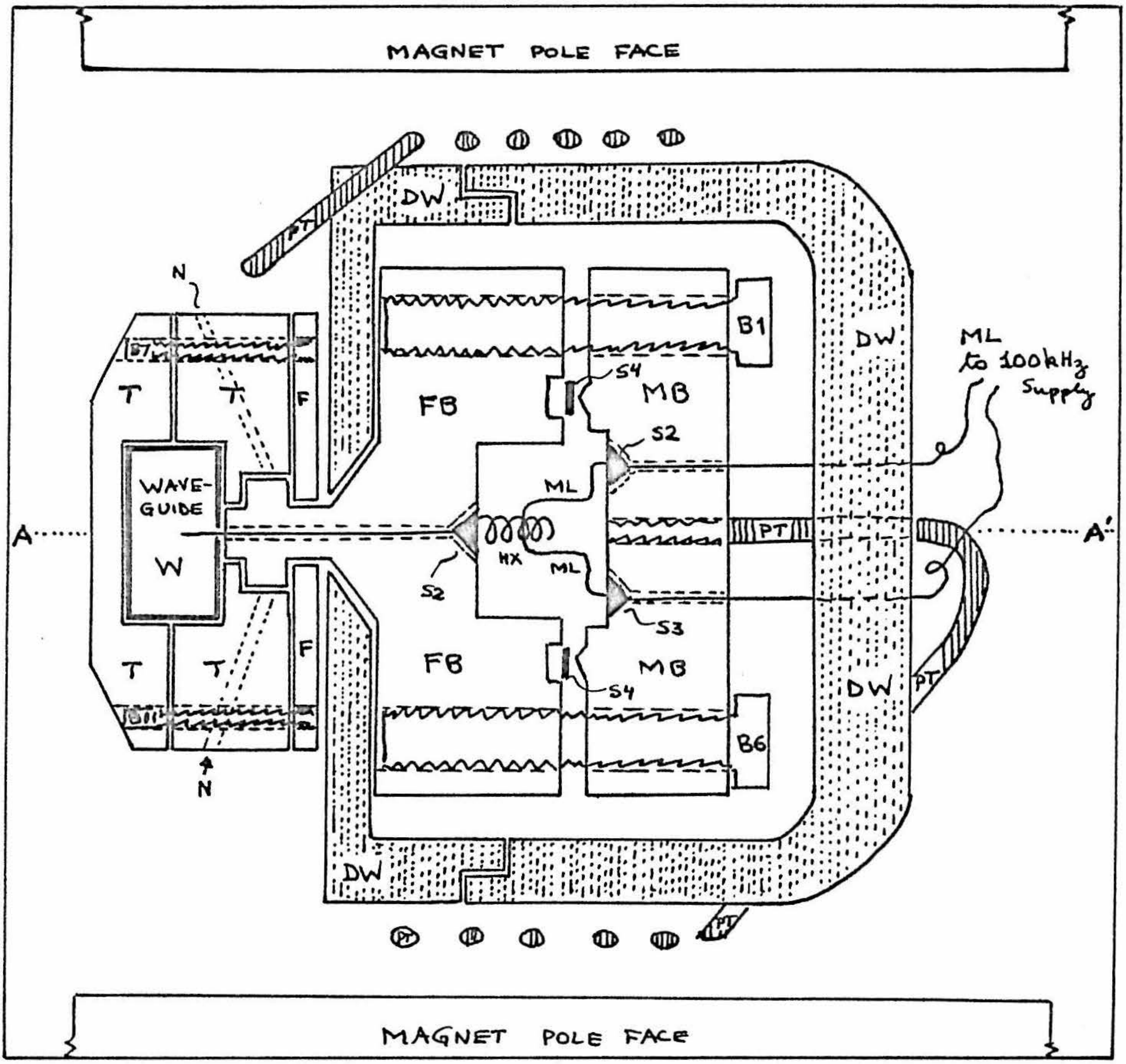

Figure I

Redesigned Halford High-Pressure EPR Bomb, in Varian V-3603 magnet pole gap. Horizontal cross-section, approximate scale 1:1.

and (iii) the brass index dial D. AA' is the axis of cylindrical symmetry for D, FB, MB, DW, the brass clutch-flange F, and the copper high-pressure seal S4, except that: (i) F bears 4 tapped holes for the clutch flange fastening screws B7 to B11, (ii) FB and MB bear six holes, tapped in FB and clearance in MB, for six 3/8"-24 Berylco-25 bolts; (iii) FB has two epoxied conical seats for the modulation loop ML cone seals S2, S3, plus the tapped and silver-soldered hole PH which receives the tapped end of PT. S2, S3, and PH are all symmetrically 0.5" apart at the vertices of an equilateral triangle centered about AA'.

H. Acknowledgments

I am most indebted to Dr. A. W. Merkl for his collaboration and guidance, to Prof. McConnell for permission to use the instrumentation, to Dr. D. Halford for many discussions and friendly assistance, and to Prof. W. O. Hamilton for an informative discussion.

REFERENCES

(1) A. W. Merkl, R. C. Hughes, L. J. Berliner and H. M. McConnell, J. Chem. Phys., 43, 953-957 (1965).

(2) R. C. Hughes, Ph.D. Thesis, Stanford University, 1966.

(3) N. R. Davidson, "Statistical Mechanics", McGraw-Hill Book Co., New York, 1962, p. 78.

(4) P. Arthur, Jr., unpublished X-ray data (1962).

(5) R. J. Goll and W. D. Phillips, J. Chem. Phys., 43, 1076-1077 (1965).

(6) Y. Iida, M. Kinoshita, A. Kawamori, and K. Suzuki, Bull. Chem. Soc. Japan, 37, 764 (1964).

(7) Y. Iida, M. Kinoshita, M. Sano, and H. Akamatu, Bull. Chem. Soc. Japan, 37, 428-429 (1964).

(8) R. G. Kepler, J. Chem. Phys. 39, 3528-3532 (1963).

(9) D. B. Chesnut and W. D. Phillips, J. Chem. Phys., 35, 1002-1012 (1961).

(10) M. T. Jones and D. B. Chesnut, J. Chem. Phys., 38, 1311-1317 (1963).

(11) P. L. Nordio, Z. G. Soos, and H. M. McConnell, Ann. Rev. Phys. Chem., 17, 237-260 (1966).

(12) Z. G. Soos and R. C. Hughes, J. Chem. Phys., 46, 253-259 (1967).

(13) Z. G. Soos, J. Chem. Phys. 43, 1121-1140 (1965).

(14) Z. G. Soos, Phys. Rev., 149, 330-342 (1966).

(15) D. B. Chesnut, J. Chem. Phys., 40, 405-411 (1964).

(16) M. S. Itzkowitz, Ph.D. Thesis, California Institute of Technology, 1967.

(17) Y. Maréchal and H. M. McConnell, J. Chem. Phys., 43, 4126-4129 (1965).

(18) Z. G. Soos, private communication (1965).

(19) A. D. McLachlan, Mol. Phys., 5, 441-444 (1963).

(20) K. W. H. Stevens, Proc. Roy. Soc. (London), A214, 237-246 (1952).

(21) H. J. Silverstone, Ph.D. Thesis, California Institute of Technology, 1964.

(22) H. A. Kramers, "Quantum Mechanics," (Dover, Inc., New York, 1964), p. 343.

(23) C. A. Hutchison and B. W. Mangum, J. Chem. Phys., 34, 908-922 (1961).

(24) E. Wasserman, L. C. Snyder, and W. A. Yager, J. Chem. Phys., 41, 1763-1772 (1964).

(25) A. Abragam, "The Principles of Nuclear Magnetism" (Oxford Univ. Press, 1961), pp. 205, 219.

(26) D. D. Thomas, A. W. Merkl, A. F. Hildebrandt, and H. M. McConnell, J. Chem. Phys., 40, 2588-2594 (1964).

(27) D. Halford and H. M. McConnell, J. Chem. Phys., 41, 898-899 (1964).

(28) M.-A. Maréchal and H. M. McConnell, J. Chem. Phys., 43, 497-498 (1965).

(29) P. Goldstein, K. Seff and K. N. Trueblood, Acta Cryst., B24, 778-791 (1968).

(30) P. W. Bridgman, Proc. Am. Acad. Arts Sci., 77, 129-146, 187-234 (1949).

(31) D. Halford, unpublished results (1964).

(32) T. Moreno, Microwave Transmission Design Data (Dover, Inc., New York, 1958), pp. 114, 127.

(33) R. H. Webb, Rev. Sci. Instr., 33, 732-737 (1962). We are indebted to Prof. W. O. Hamilton for this reference.

PROPOSITION IV

SEARCH FOR QUARKS IN SEA-WATER: THE USE OF ION-EXCHANGE COLUMNS

A. Introduction

Despite many partial insights, great confusion reigned for almost three decades (1932-1961) in the physics of hadrons (strongly interacting elementary particles), be they baryons (proton, neutron, Σ and Ξ hyperons, etc.) or mesons (pions, kaons, etc.). In 1961 Gell-Mann and Ne'eman helped systematize the field by discovering the physicists' analog to Buddha's "Eightfold Way" to virtue.

These systematics, when coupled to all previous efforts, do not yield a description of the interaction potential in the classical or semi-classical sense, but do allow for empirical conservation theorems for a set of new "quantum numbers", and for correlations of a vast amount of experimental data. There is an obvious analogy to Mendele'ev's achievement in classifying the chemical elements. This writer does not feel confident with the group-theoretical language or competent in the field of high-energy theoretical physics to present here an authoritative review, but refers the reader to books by Gell-Mann and Ne'eman (1) and Hamermesh (2).

Very roughly, Gell-Mann and Ne'eman found that hadrons can be classified by (i) parity, (ii) spin s, (iii) isotopic spin T, (iv) the z-component of T, T_z, (v) hypercharge $Y \equiv B + S$, where B is the baryon number, which is 0 for mesons and 1 for baryons, and where S is the strangeness, a quantum number defined semi-empirically by Gell-Mann and Nishijima in 1955 to classify the sundry hadron half-lines and decay schemes.

Consider three linearly independent vectors $\underset{\sim}{V}_1$, $\underset{\sim}{V}_2$, $\underset{\sim}{V}_3$ that span a three-dimensional complex vector space $\underset{\sim}{3}$. The direct (outer) product space $\underset{\sim}{3} \times \underset{\sim}{3} \times \underset{\sim}{3}$, of dimension 27, can be decomposed into the direct sum of four invariant subspaces, $\underset{\sim}{1}$, $\underset{\sim}{8}$, $\underset{\sim}{8}$, and $\underset{\sim}{10}$ of dimensions 1, 8, 8, and 10, respectively. Correspondingly, baryons can be organized in a set of 8 (the spin-1/2, parity + baryons) and of 10 (the spin-3/2, parity + baryons). A similar classification of mesons into two sets of 8 (the spin-0 and the spin-1 mesons) "corresponds" to the dimensionality 1, 8 of the invariant subspaces $\underset{\sim}{1}$, $\underset{\sim}{8}$ which constitute the direct product space $\underset{\sim}{3} \times \underset{\sim}{\overline{3}}$, where $\underset{\sim}{\overline{3}}$ is the vector space conjugate or dual to $\underset{\sim}{3}$. This classification of mesons and baryons is not trivial: it can be used to predict and confirm rest mass differences, magnetic moment ratios, and so forth. The intriguing possibility exists that the three vectors V_1, V_2, V_3 are not mathematical curiosities but might correspond to three real, if hitherto unobserved, particles, which Gell-Mann baptized the p-quark, the n-quark and the λ-quark.

The classification predicts for the p-quark (q_p): B = 1/3, T = 1/2, T_z = 1/2, S = 0, spin s = 1/2, and electrical charge 2/3; for the n-quark (q_n): B = 1/2, T = 1/2, T_z = -1/2, S = 0, spin s = 1/2, and electrical charge -1/3; for the λ-quark (q_λ): B = 1/3, T = 0, T_z = 0, S = -1, spin s = 1/2 and electrical charge -1/3. The antiparticles to the quarks, if they exist, $\overline{q_p}$, $\overline{q_n}$, $\overline{q_\lambda}$, would have charges -2/3, +1/3, and +1/3 and B = -1/3. A proton would consist of q_p, q_p, and q_n, a neutron would consist of q_p, q_n, and q_n; a π^+ meson would consist of q_p and $\overline{q_n}$. All nuclei of baryon number A would consist of 3A quarks. Moreover the quarks would react only with other quarks to form mesons or baryons; left to themselves or as extra "hangers-on" to other hadrons or nuclei, quarks would undergo only weak or electromagnetic interactions. It is guessed that the more massive quarks (the λ quark according to some, the p quark according to others) can undergo β-decay into the lighter quark, but the "fractionality" of this change would be conserved, i.e., fractional changes would essentially "live forever."

B. Search for Quarks: A Review

These intriguing predictions led to very extensive experimental efforts to detect and isolate quarks. Accelerator experiments have yielded no trace of fractionally changed particles with rest masses below about 5 GeV/c^2, the upper center-of-mass limit for quark-antiquark pair production in the more powerful accelerators (3-10); cosmic-ray experiments (11-24) have set typical upper limits for quark fluxes of 10^{-10} cm^{-2} sec^{-1} $steradian^{-1}$, at 90% confidence levels, as compared to typical total secondary cosmic-ray fluxes of 1 cm^{-2} sec^{-1} $steradian^{-1}$ and to typical Z = 1 primary cosmic-ray fluxes of 4 cm^{-2} sec^{-1} $steradian^{-1}$ (25). Millikan oil-drop experiments (26-29) have also been fruitless. Lines in the far ultraviolet solar emission spectrum have been calculated and could be assigned to "quarked atoms" if they could be measured to better than 0.04 Å (30,31); mass-spectrometric investigations on random samples of meteorites, air, dust, and sea water (29) have failed to yield quarks as have those on pre-concentrated samples of sea water (32); in a concerted attack on two present-day conundrums, the proposal has been made (33) to reassign quasar spectra to quarked-atom transitions.

All these experiments to date have been fruitless, and quarks seem to be destined to the role of mathematical curiosities. One big question that comes from the negative accelerator experiments is how three quarks, each with rest mass greater than 5 GeV/c^2 can combine to give a proton with a rest mass of only 0.9 GeV/c^2.

The chemical and geological consequences of the possible quark-atoms and quark-molecules have been sketched by Ritson (3), Chupka et al. (29), McDowell and Hasted (34) and Nir (35).

What the p-quark (or the λ-anti-quark or the n anti-quark) with its positive charge would do is a bit hard to predict; it may act like a bare proton and create a hydrogen-like "atom" with its one electron and net charge -1/3; with ordinary nuclei the p-quark would interact electrostatically: the nucleus-p-quark-plus-electrons system would probably be unstable.

The n- and λ-quarks (and p anti-quark) would interact with nuclei and electrons like a negative muon: if captured by an atom, it would go into the K-level; and the p-quarked atom would resemble a pi-mesic atom. The Bohr radius in fermi for a quark of rest mass M_q, and electrical charge $Q\,|\epsilon|$ in the K level, and a nucleus of rest-mass M_n and charge $Z\,|\epsilon|$ is, if M_p is the proton rest-mass:

$$a_q = \frac{28.8}{ZQ}\left(\frac{M_p}{M_n} + \frac{M_p}{M_q}\right)$$

and the nuclear radius in fermi is, very crudely:

$$R_o \cong 1.3\left(\frac{M_n}{M_p}\right)^{1/3}$$

Therefore for a proton-plus-λ-quark atom the quark Bohr radius would be just outside the nucleus, but for heavy nuclides it would lie inside the nucleus. Already for $_{14}^{7}N$ and for a λ-quark with $M_q \sim 5$ BeV/c^2, $R_o = 3.1$ fm and $a_q = 3.2$ fm. If quarks are present in primary cosmic rays, albeit in low concentrations, then apart from a fraction of thermalized secondary quark particles tied down or recycled into high-altitude plasmas (34), the quarks will either arrive on the surface of the earth as high-energy secondary particles or as ions solvated in rain drops. Ultimately, preferential solvation of the quark atoms (quark-N_2, quark-D_2, quark-A, or quark-H_2O) will tend to make the oceans into repositories of quark atoms and molecules, within a geological time span of 5 x 10^9 years (3,29). Ritson and Padmore (32) obtained samples of bittern, a 100-fold concentrate of sea water, from the Leslie Salt Co. salt evaporators, crystallized much of the salts by further evaporation, and analyzed the remaining liquid, and some of crystallized residue in a mass spectrometer. No quarks were found.

C. Ion-Exchange Purification of Sea-Water

We suggest that during evaporation of the bittern, the quarks in sea water could easily co-crystallize with the ordinary salts in lattice defects, and propose that large-scale ion-exchange chromatography be used instead of evaporation to deionize sea water or bittern samples. Since the selective adsorption on anionic or cationic resin columns is a function of ionic charge, therefore fractionally charged quark species will tend to reside on the columns between the bands due to ions differing by one whole electronic charge.

Careful identification of band edges, by isotopic labelling if necessary, and sampling of the interband eluates, should make a systematic search for quarks almost fool-proof. The intraband eluates could then be analyzed by mass spectrometry.

Primack (36) has suggested that n-quark-HD or n-quark-D_2 molecules would exhibit properties similar to those observed by Alvarez (37) for μ-mesic HD molecules: the muon catalyzes fission reactions:

$$^{1}_{1}H + ^{2}_{1}D \longrightarrow ^{3}_{2}He + \text{energy}$$

Thus, bubble chambers filled with D_2 could be used to detect quark-induced fission reactions and help confirm the presence of quark in injected samples.

D. Acknowledgments

I am indebted to Dr. D. Lundquist, Prof. D. Ritson, Dr. R. H. Young, Mr. T. Padmore, and Mr. J. Primack for discussions.

REFERENCES

(1) M. Gell-Mann and Y. Ne'eman, "The Eightfold Way", (W. A. Benjamin, Inc., New York, 1964).

(2) M. Hamermesh, "Group Theory and Its Application to Physical Problems" (Addison-Wesley Publ. Co., Inc., Reading, Mass., 1962).

(3) D. Ritson, unpublished notes (April, 1966).

(4) D. R. O. Morrison, Phys. Lett., 9, 199- (1964).

(5) H. H. Bingham, M. Dickinson, R. Diebold, W. Koch, D. W. G. Leith, M. Nikolič, R. Ronne, R. Huson, P. Musset, and J. J Veillet, Phys. Lett., 9, 201- (1964).

(6) V. Hagopian, W. Selove, R. Erlich, E. Leboy, R. Lanza, D. Rahm, and M. Webster, Phys. Rev. Letters, 13, 280-281 (1964).

(7) W. Blum, S. Brandt, V. T. Cocconi, O. Czyzewski, J. Dany, M. Jobes, C. Kellner, D. Miller, D. R. O. Morrison, W. Neal, and J. G. Rushbrooke, Phys. Rev. Letters, 13, 353a-355a (1964).

(8) P. Franzini, B. Leontič, D. Rahm, N. Samios, and M. Schwartz, Phys. Rev. Letters, 14, 196-197 (1965).

(9) L. B. Leipuner, W. T. Chu, R. C. Larsen, and R. K. Adair Phys. Rev. Letters, 12, 423-425 (1964).

(10) D. E. Dorfan, J. Eades, L. M. Lederman, W. Lee, and C. N. Ting, Phys. Rev. Letters, 14, 999-1003 (1965).

(11) T. Massam, T. Muller, and A. Zichichi, Nuovo Cimento, 40A, 589-596 (1965).

(12) A. W. Sunyar, A. Z. Schwarzschild, and P. I. Connors, Phys. Rev., 136, B1157-B1159 (1964).

(13) T. Bowen, D. A. DeLise, R. M. Kalbach, and L. B. Mortara, Phys. Rev. Letters, 13, 728-731 (1964).

(14) D. A. DeLise and T. Bowen, Phys. Rev., 140, B458-B462 (1966).

(15) J. C. Barton and C. T. Stockel, Phys. Lett., 21, 360- (1966).

(16) H. Kasha, L. B. Leipuner, and R. K. Adair, Phys. Rev., 150, 1140-1147 (1966).

(17) R. C. Lamb, R. A. Lundy, T. B. Novey, and D. D. Yovanovitch, Phys. Rev. Letters, 17, 1068-1070 (1966).

(18) A. Buhler-Broglin, G. Fortunato, T. Massam, T. Muller, and A. Zichichi, Nuovo Cimento, 45A, 520-526 (1966).

(19) A. Buhler-Broglin, G. Fortunato, T. Massam and A. Zichichi, Nuovo Cimento, 49A, 209-212 (1967).

(20) A. Buhler-Broglin, P. Dalpiaz, T. Massam, and A. Zichichi, Nuovo Cimento, 51A, 837-845 (1967).

(21) H. Kasha, R. C. Larsen, L. B. Leipuner, and R. K. Adair, Phys. Rev. Letters, 20, 217-219 (1968).

(22) R. Gomez, H. Kobrak, A. Moline, J. Mullins, C. Orth, J. Van Putten, and G. Zweig, Phys. Rev. Letters, 18, 1022-1024 (1967).

(23) H. Kasha, L. B. Leipuner, T. P. Wangler, J. Alspector, and R. K. Adair, Phys. Rev., 154, 1263-1264 (1967).

(24) D. A. De Lise and T. Bowen, Phys. Rev., 140, B458-B462 (1965).

(25) R. B. Leighton, "Principles of Modern Physics" (McGraw-Hill Book Company, Inc., New York, 1959).

(26) C. Becchi, G. Gallinaro, and G. Morpurgo, Nuovo Cimento, 39, 409-412 (1965).

(27) V. B. Braginskii, JETP Letters (Engl. Transl.), 3, 43- (1966).

(28) G. Gallinaro and G. Morpurgo, Phys. Lett., 23, 609-613 (1966).

(29) W. A. Chupka, J. P. Schiffer, and C. M. Stevens, Phys. Rev. Letters, 17, 60-65 (1966).

(30) O. Sinanoğlu, B. Skutnik, and R. Tousey, Phys. Rev. Letters, 17, 785-788 (1966).

(31) W. R. Bennett, Jr., Phys. Rev. Letters, 17, 1196-1198 (1966).

(32) D. Ritson and T. Padmore, unpublished results (1966).

(33) J. C. Huang and T. W. Edwards, Phys. Rev., 171, 1331-1334 (1968).

(34) M. R. C. McDowell and J. B. Hasted, Nature, 214, 235-237 (1967).

(35) A. Nir, Phys. Rev. Letters, 19, 336-339 (1967).

(36) J. Primack, private communication (September, 1968).

(37) L. Alvarez, H. Bradner, F. S. Crawford, Jr., J. A. Crawford, P. Falk-Vairant, M. L. Good, J. D. Gow, A. H. Rosenfeld, F. Solmitz, M. L. Stevenson, H. K. Ticho, and R. D. Tripp, Phys. Rev., 105, 1127-1128 (1957).

PROPOSITION V

SOLUTION DIMERS OF ORGANIC DONOR CATIONS AND OF ACCEPTOR ANIONS. THE BENZIDINE REARRANGEMENT REVISITED

A. Calculations on Solution Dimers

The strong organic donors (D):para-Phenylenediamine (pPD), N,N-Dimethyl-para-phenylenediamine (DMPD), N,N,N',N'-Tetramethyl-para-phenylenediamine (TMPD), Diaminodurene (DAD), and the strong acceptor (A):7,7,8,8-Tetracyanoquinodimethan (TCNQ), when they are respectively oxidized to their long-lived radical cations D^+, (reduced to the radical anion A^-) and are dissolved in a polar solvent, tend to form weakly bound cationic (anionic) dimers D^+D^+ (A^-A^-) (1,2,3,4). These dimers are formed in spite of the strong direct Coulomb repulsion between like ions; they are diamagnetic, i.e., spin-paired (2); their optical absorption spectra display all the transitions of the free monomeric ion, somewhat attenuated and blue-shifted (< 0.5 eV) (1), plus a charge-transfer band and some new unexplained transitions. The heats of dimerization ΔH in aqueous solution are: $(pPD^+)_2$ 8 kcal/mole of monomer (1); $(DMPD^+)_2$ 10 kcal/mole (1), $(TMPD^+)_2$ either 5 or 8 kcal/mole (1,2); $(TCNQ^-)_2$ 5.2 kcal/mole of monomer (3). The solution *dimers* resemble very closely the dimers observed in the low-temperature phase of $TMPD^+$ perchlorate (Wurster's Blue Perchlorate or WBP) crystals (5), and in the other $TCNQ^-$ Frenkel spin exciton salts (6,7).

It has been suggested that these dimers are bound by exchange Coulomb forces (8). Nordio has suggested (9) that the overlap between the two ions is staggered so that the polar 1,4-substituents interact strongly with the polarizable benzene ring. We propose here that a thorough pi-electron calculation be performed for these dimers, using the interplanar separation and the degree of staggering between the parallel planar ions as two free parameters, in an attempt to discover minima of the interionic potential with respect to these parameters, and hence the equilibrium interionic configuration(s). In a semi-empirical scheme, the electronic spectra (1) and the heats of dimerization (1,2,3) could be used to obtain the "best" ionic wavefunctions.

If solvent effects are neglected, then such a calculation would not only provide a rationalization for the solution dimers, but also allow us to estimate the effect of the crystalline electric field in changing the equilibrium solution configurations to the crystal configurations. There is some likelihood that these may differ: in fact, the experimental heats of transition for WBP are in the crystal $\Delta H = 0.408$ kcal/mole of WBP monomer (10), and in solution either 5 kcal/mole (1) or 8 kcal/mole (2) of WBP monomer; the difference, of course, cannot reside in the $p\Delta V$ term, but may be due either to some subtle difference in molecular configurations or to crystal-field effects.

Two related dimer calculations have already been performed: the calculation by Monkhorst, Pott and Kommandeur (11) on the

$(TMPD^+)_2$ dimer was biased a priori in favor of a disproportionation in the solid state at low temperatures, and may be discounted; a calculation by Fritchie, Chesnut, and Simmons on the $(TCNQ^-)_2$ dimer has been mentioned twice (12,13) but has not been published so far: it apparently obtained the desired result that the $(TCNQ^-)_2$ dimer has the lowest energy when the molecules are in parallel planes but in a staggered overlap configuration.

B. The Benzidine Rearrangement

If the excited electronic states can be included meaningfully in the dimer calculation suggested above, then this calculation may also become useful in the famous controversy over the mechanism of the acid-catalyzed benzidine rearrangement.

This reaction has occupied the attention of organic chemists for over a century, but the reaction pathway has never been completely explained. After a very brief sketch of the problem and its connection with the radical dimer discussions above, we shall suggest some electron paramagnetic resonance (EPR) experiments which might help to clarify the situation.

In acid solutions hydrazobenzene and substituted hydrazobenzenes (I) can rearrange to as many as eight different products (II to IX), all of which are never obtained in any given reaction:

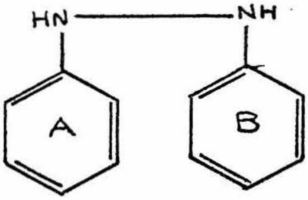

I

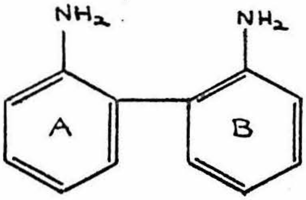

II

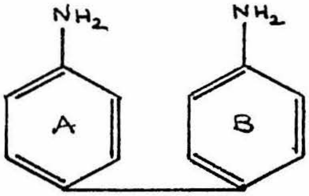

III

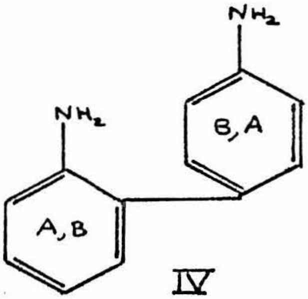

IV

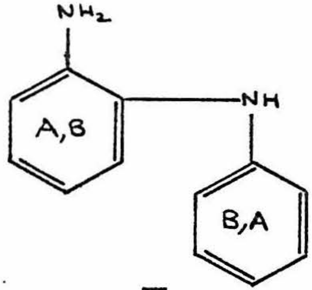

V

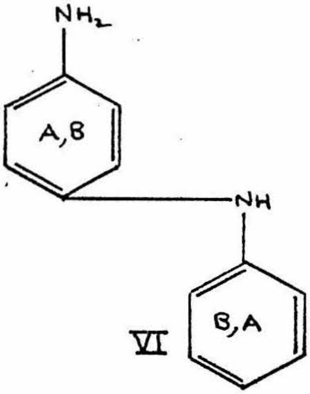

VI

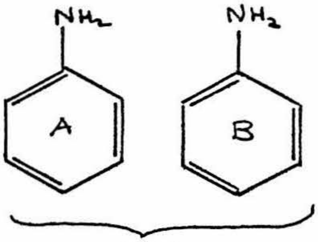

VII

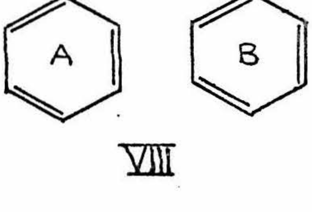

VIII

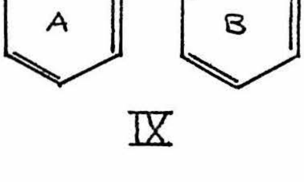

IX

I is Hydrazobenzene or 1,2-Diphenylhydrazine, and may bear substituents, as indicated by the labels A, B, or else the phenyl ring itself may be replaced by naphthyl, etc.; II is ortho-Benzidine or 2,2'-Diaminobiphenyl; III is (para)-Benzidine or 4,4'-Diaminobiphenyl; IV is Diphenyline or 2,4--Diaminobiphenyl; V is ortho-Semidine; VI is para-Semidine; VIII is Azobenzene and IX is Carbazole.

The literature to 1922 is reviewed by Jacobson (14); the work of the London group (Hughes, Banthorpe and Ingold) to 1964 is reviewed in Refs. (15, 16); the literature to about 1964 is reviewed by Shine (17) and by Dewar and Marchand (18). More recent work is reported by Hammond et al. (19), by Shine et al. (20), and most recently by the London group (21).

It is now firmly established that the acid-catalyzed benzidine rearrangement is intramolecular, "specific acid-catalyzed [i.e. the proton addition is not rate-determining], is of first order in hydrazo compound, and may be either separately or simultaneously first- and second-order in acid" (17). Things are not quite that well-established for the transition state; in fact, there are at present three competing models: the polar-transition-state (PTS) theory of the London group (16), the pi-complex theory of Dewar (18), and the caged-free radical pair theory (22). The first two involve a heterolytic scission of the N-N bond, whereas the last predicts a homolytic scission. The PTS theory assumes that a concerted mechanism breaks the

N-N bond and forms the C-N or C-C bonds in the same step, e.g.:

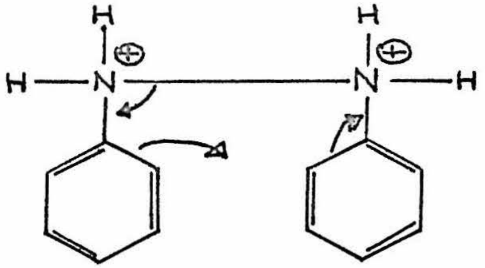

This theory explains substituent effects on reaction rates, but fails to account for the para-semidine VI and the disproportionation products VII, VIII. The pi-complex theory involves a transition state of the type:

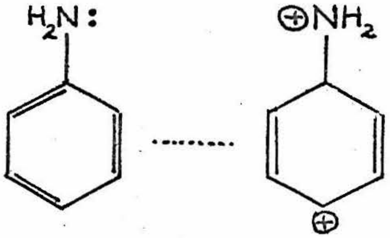

The caged-radical dimer theory postulates a transition state which for the first-order acid-catalyzed rearrangement is:

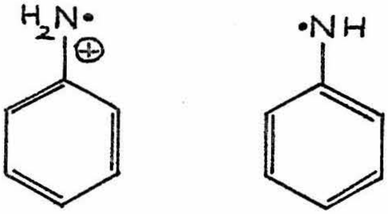

and for the second-order acid-catalyzed rearrangement is:

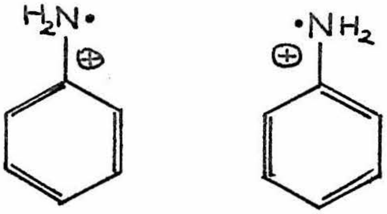

Both dimers would be bound inside a "cage" of solvent molecules. The difficulty is that one might expect the radicals to interact either with dissolved oxygen or with the solvent whenever they "leave the cage", whereas no evidence has been found of the products of such side-reactions; also, the attempts made so far to detect free radicals by EPR techniques (19d, 20b, 23) have been fruitless. It could be argued that in the reactions followed by EPR techniques the free radicals were too short-lived for detection when they left the solvent cage, since EPR at 10^{10} Hz cannot detect a radical whose lifetime is shorter than about 10^{-10} seconds. This writer does not know whether the cation radical of, say, aniline has been observed by EPR, but wishes to propose that the choice of a properly substituted hydrazobenzene could yield a transition state in which a free radical, if formed, would be relatively stable even <u>outside</u> the solvent cage and hence detectable by EPR: pPD^+, $DMPD^+$, and $TMPD^+$ would be such radicals. Jacobson's tabulation (14) provides six examples of substituted hydrazobenzenes which might be suitable: they are listed below with the indices showing the known reaction products (14) as schematized on page 300.

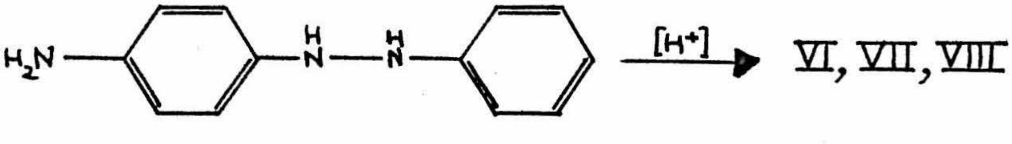

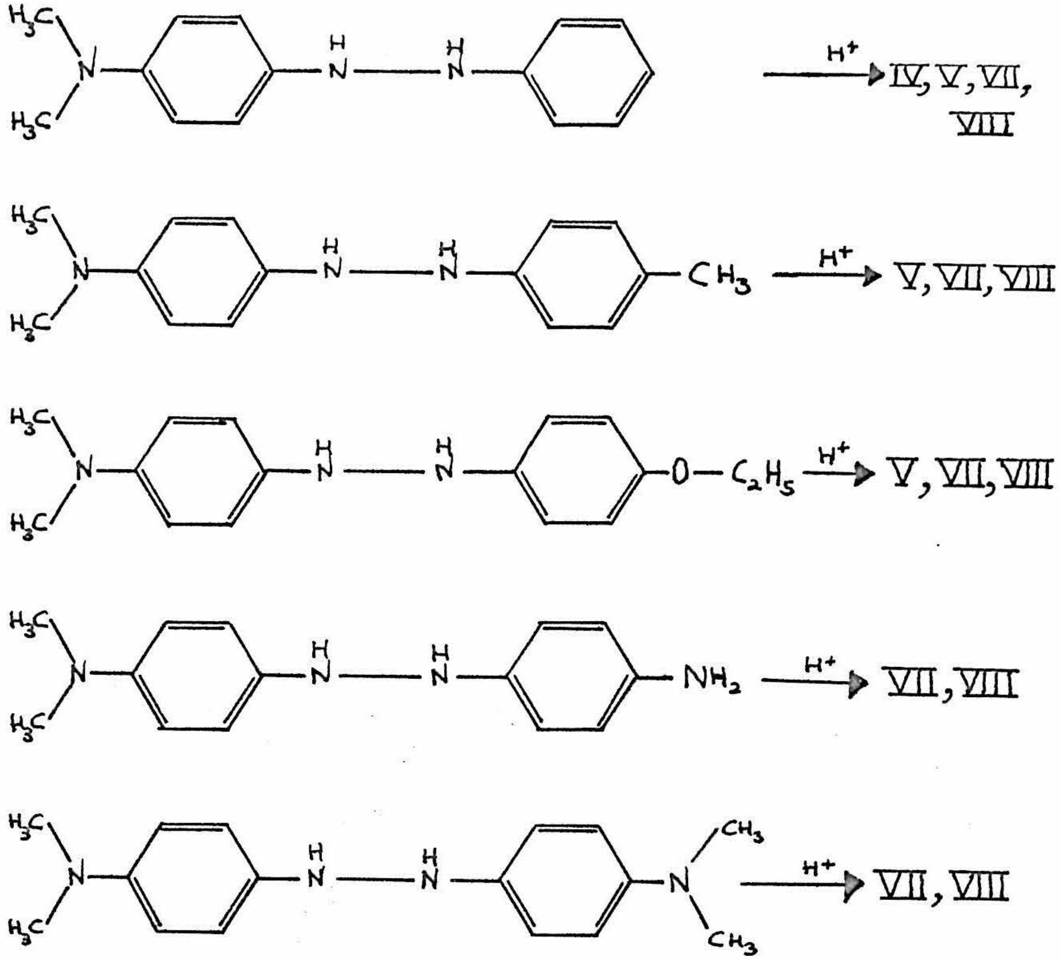

A thorough monitoring of the benzidine rearrangement reactions of the above compounds by EPR could either provide direct evidence of radical intermediates or send the caged-radical theory to final oblivion.

REFERENCES

(1) K. Uemura, S. Nakayama, Y. Seo, K. Suzuki, and Y. Ooshika, Bull. Chem. Soc. Japan, 39, 1348 (1966) and references therein.

(2) A. Kawamori, A. Honda, N. Joo, K. Suzuki, and Y. Ooshika, J. Chem. Phys., 44, 4363 (1966).

(3) R. H. Boyd and W. D. Phillips, J. Chem. Phys., 43, 2927-2929 (1965).

(4) L. R. Melby, R. J. Harder, W. R. Hertler, W. Mahler, R. E. Benson, and W. E. Mochel, J. Am. Chem. Soc., 84, 3374-3387 (1962), footnote 19.

(5) D. D. Thomas, H. Keller, and H. M. McConnell, J. Chem. Phys., 39, 2321-2329 (1963).

(6) Cf. review by P. L. Nordio, Z. G. Soos, and H. M. McConnell, Ann. Rev. Phys. Chem., 17, 237-260 (1966).

(7) Z. G. Soos, J. Chem. Phys., 46, 4284-4288 (1967).

(8) Z. G. Soos and H. M. McConnell, J. Chem. Phys., 43, 3780-3794 (1965).

(9) P. L. Nordio, private communication (1965).

(10) H. Chihara, M. Nakamura, and S. Seki, Bull. Chem. Soc. Japan, 38, 1776-1778 (1965).

(11) H. J. Monkhorst, G. T. Pott, and J. Kommandeur, J. Chem. Phys., 47, 401-407 (1967).

(12) C. J. Fritchie, Jr., Acta Cryst., 20, 892-898 (1966).

(13) C. J. Fritchie, Jr., and P. Arthur, Jr., Acta Cryst., 21, 139-145 (1966).

(14) P. Jacobson, Ann., 428, 76-121 (1922).

(15) C. K. Ingold, "Structures of Some Transition States" in "The Transition State," Chem. Soc. (London) Special Publication No. 16 (1962), pp. 118-139.

(16) D. V. Banthorpe, E. D. Hughes, and C. K. Ingold, J. Chem. Soc., 1964, 2864-2900.

(17) H. J. Shine, "Aromatic Rearrangements" (Elsevier Publishing Co., Amsterdam, 1967), pp. 124-171.

(18) M. J. S. Dewar and A. P. Marchand, Ann. Rev. Phys. Chem., 16, 321-346 (1965).

(19) (a) G. S. Hammond, B. Seidel, and R. E. Pincock, J. Org. Chem., 28, 3275-3279 (1963);

(b) B. Seidel and G. S. Hammond, ibid., 3280-3283;

(c) G. S. Hammond and J. S. Clovis, ibid., 3283-3290;

(d) J. S. Clovis and G. S. Hammond, ibid., 3290-3297.

(20) (a) H. J. Shine and J. T. Chamness, J. Org. Chem., 32, 901-905 (1967).

(b) H. J. Shine and J. P. Stanley, ibid., 905-910.

(21) (a) D. V. Banthorpe, C. K. Ingold, and J. Roy, J. Chem. Soc. (B), 1968, 64-66;

(b) D. V. Banthorpe and A. Cooper, ibid., 605-609;

(c) D. V. Banthorpe, A. Cooper, and C. K. Ingold, ibid., 609-614;

(d) D. V. Banthorpe and M. O'Sullivan, ibid., 615-617;

(e) D. V. Banthorpe and A. Cooper, ibid., 618-623;

(f) D. V. Banthorpe, C. K. Ingold, and M. O'Sullivan, ibid., 624-627;

(g) D. V. Banthorpe and M. O'Sullivan, ibid., 627-630.

(22) (a) J. Murrell, comment on page 139 of Ref. (15);

(b) Ref. (19d).

(23) D. V. Banthorpe, R. Bramley, and J. A. Thomas, J. Chem. Soc., 1964, 2900-2901.